PREPARATION AND STUDY OF SOME OXIDE AND SULPHIDE THIN FILMS DEPOSITED BY DIP AND CHEMICAL VAPOUR DEPOSITION TECHNIQUES

A thesis submitted to the
University of North Bengal, Raja Rammohunpur,
Siliguri, Darjeeling, India
for the award of the degree of

Doctor of Philosophy in Science

By

SEKHAR CHANDRA RAY

Department of Physics
University of North Bengal
Raja Rammohunpur, Siliguri, Darjeeling - 734430, India

July 1998

Dedicated to

The Service of Mankind

UNIVERSITY OF NORTH BENGAL

RAJA RAMMOHUNPUR, SILIGURI, DARJEELING, INDIA.

Certificate

This is to certify that the thesis entitled **"PREPARATION AND STUDY OF SOME OXIDE AND SULPHIDE THIN FILMS DEPOSITED BY DIP AND CHEMICAL VAPOUR DEPOSITION TECHNIQUES"** *submitted by Mr. Pekhar Chandra Ray, to the University of North Bengal, Siliguri, Darjeeling for the award of the degree of Doctor of Philosophy in Science, is a record of bonafide research work conducted by him under our supervision. The results embodied in this thesis have not been submitted for the award of any other degree or diploma.*

Malay K. Karanjai 08/07/98
Malay K. Karanjai
Department of Physics
Siliguri College, Siliguri.

Dhruba Dasgupta 8.7.98
Dhruba DasGupta
Department of Physics
North Bengal University

July 1998.

LIST OF PUBLICATIONS

1. Sekhar C. Ray, Malay K. Karanjai and D. DasGupta "Preparation and study of doped and Undoped tin dioxide films by the Open Air Chemical Vapour Deposition technique" 1997 ***Thin Solid Films*** Vol. 307 Page 221-227.

2. Sekhar C. Ray, Malay K. Karanjai and D. DasGupta "Tin dioxide based transparent semiconducting films deposited by the dip-coating technique" 1998 ***Surface and coating technology*** Vol. 102 Page 73-80.

3. Sekhar C. Ray, Malay K. Karanjai and D. DasGupta "Deposition and characterization of $Zn_xCd_{1-x}S$ thin films prepared by the dip technique" 1998 ***Thin Solid Films*** Vol. 322/1-2 Page 117-122.

4. Sekhar C. Ray and Malay K. Karanjai "Preparation and study of MoS_2 thin films deposited by the dip technique" (Abstract) ____ Proceedings of the Fifth West Bengal State Science Congress, University of North Bengal, March 21-23, 1998, Page 140.

5. Sekhar C. Ray, Malay K. Karanjai and D. DasGupta "Structure and photoconductive properties of dip deposited SnS and SnS_2 thin films and their conversion to tin dioxide by annealing in air" _____ Communicated in the "Thin Solid Films" July 1998.

ACKNOWLEDGEMENT

The author expresses his sincere gratitute to the academic supervisors, Dr. Dhruba DasGupta, Prof., Department of Physics, University of North Bengal and Dr. Malay K. Karanjai, Sr. Lecturer, Physics Department, Siliguri College, Siliguri for their inspiration, encouragement, supervision and good understanding during the research programme. He has received a patient guidance and continuous enthusiasm from them for which he is highly grateful. The support and encouragement of all faculty members and staff of the Department of Physics is gratefully acknowledged.

Research is rarely the product of a single person and completion of this work is due to the immense and sincere efforts of many individuals. The author would like to convey his gratitute to Sri A. K. Bhadra, Scientist, Central Glass & Ceramic Research Institute, Jadavpur for XRD measurements, Dr. Srikantha Chakraborty, USIC, Burdwan University for SEM measurements, Dr. S. K. Saha, Chemistry Department, University of North Bengal for helping in the optical absorption/Transmission measurements and Sri P. S. Tamang for his technical help.

Finally, the author expresses his deepest respect and a special debt of gratitude towards his beloved parents, parents in law, brothers and sister for their sacrifices, patience and understanding. The author wishes to express his warm thanks to his wife Smt. Susmita Ray, whose heartiest inspiration and help were a strong impetus towards the completion of the work. He would also like to thank Arunabha, Sajal, Basabdatta & Sanaul,

Physics Department, N.B.U. and Mr. Gutam Dutta, Army School, Bengdubi for their encouragement and moral support.

8th July 1998

Sekhar Chandra Ray

SEKHAR CHANDRA RAY

University of North Bengal

CONTENTS

Page number

CHAPTER - 2

Page number

CHAPTER - 3

KEY WORDS

Deposition technique

Dip technique

Open Air Chemical Vapour Deposition (OACVD) technique

SnO_2 transparent conducting oxide (TCO)

SnO_2-based transparent semiconducting oxide (TSCO)

Deposition process

Thickness

X-ray diffractometric study (XRD)

Scanning electron microscopy study (SEM)

Optical transmission (O.T)

Optical density (O.D)

Figure of merit

Lattice parameter

Spectral response of photoconductivity

Figure of merit

Bowing parameter

LIST OF FIGURES

LIST OF TABLES

ABSTRACT

During the past decade there has been a large amount of research activity in the field of thin film technology for its different practical and commercial applications. Realising its importance in technology, academic institutions, national laboratories and industries have entered this activity. The interests are varied and encompass both fundmental amd applied aspects for use in space, defence, industry and other areas. Many organisations have installed automatic as well as manually operated deposition systems.

In this work, a number of oxide and sulphide thin solid films have been prepared and their properties have been studied in relation to their practical and commercial applications. These films were prepared by (1) Dip technique and (2) Open air chemical vapour deposition technique (OACVD). The first has been used for deposition of oxide (SnO_2, CuO) and sulphide ($Zn_xCd_{1-x}S$, SnS, SnS_2, MoS_2 & Cu_2S) films, while the second, for transparent conducting tin oxide (SnO_2) films only.

In the first chapter, an introduction to thin film technology, its different applications in science and technology and a brief review of different techniques for deposition of thin films have been discussed.

In chapter two, details of the DIP TECHNIQUE are given and preparation of oxide (SnO_2 & CuO) films using this technique and their characterization have been discussed. In the dip technique as used for oxide films the substrate is withdrawn vertically at a controlled speed from a starting solution containing a suitable metal nitrate or chloride and alcohol, when a liquid layer adheres to the substrate surface. It is then baked in a furnace under atmospheric conditions, when the liquid film reacts on the substrate inside the furnace and is converted to a solid film. Undoped and F-doped transparent semiconducting films with tin dioxide as the active material have been prepared by the hydrolysis of stannous chloride which takes place when a substrate is

withdrawn from a methanol solution of $SnCl_2$. $2H_2O$ and baked at a high temperature as described. F-doping is achieved by adding NH_4F to the starting solution. The maximum film thickness obtainable per dipping (dip-withdrawal-bakecycle) is about 0.58 μm, but can be increased by multiple dipping. The films appear to be a mixed phase consisting of crystalline tin dioxide over an amorphous background, probably of Sn(OH)Cl. The film produced by a single dipping consists of a small number of isolated SnO_2 crystallites. But as the film thickness is increased these crystallites increase in number and finally merge into a continuous layer. Typical values of resistivity of F-doped films produced by this method is 2.4 X 10^{-2} Ω cm, with an average transmission of 85% at a thickness of 2.96 μm. This work has been published in the ***"Surface and coating technology"*** Vol. 102 (1998) Page 73-80.

For the preparation of copper oxide (CuO) films, a methanolic solution of cupric chloride ($CuCl_2.2H_2O$) was used. These films were prepared at three different baking temperatures. ASTM data confirms that the films are of CuO phase. The optical band gap of the films calculated from optical absorption measurements is 1.85 eV which is quite comparable with the reported in the literature.

The third chapter describes the deposition and study of various properties of sulphide films. For the preparation of sulphide films, the starting solution contains a suitable compound of sulphur like thiourea or amonium thiocyanate in adddition to a metallic chloride or nitrate. The films prepared were of $Zn_xCd_{1-x}S$, SnS & SnS_2, MoS_2 and Cu_2S.

For preparation of $Zn_xCd_{1-x}S$ ($0 \leq x \leq 1$) alloy thin films by this technique, an alcoholic solution of the corresponding metal nitrates and thiourea was taken as a starting solution from which the substrate was withdrawn and baked at 400° C - 600° C. X-ray diffractometric study suggests that for zinc atomic fraction $x \leq 0.6$ films prepared at a baking temperature of 500° C are homogeneous with a hexagonal (wurtzite) structure. Increase in the proportion of zinc in the starting solution is found to produce a

decrease in the lattice parameter. SEM studies reveal an increase in grain size with Zn atomic fraction x upto a value of 0.6. For $x > 0.6$, the films appear to have an amorphous character, as no distinguishable peaks can be seen in the X-ray diffractograms. The SEM micrographs also do not show any clearly defined grains over this range. Values of bandgap obtained from optical absorption measurements as well as from spectral response of photoconductivity, are in good agreement with each other and vary monotonically from 2.30 eV (CdS) to 2.69 eV ($Zn_{0.6}Cd_{0.4}S$) over the range $0 \leq x \leq 0.6$. For $x > 0.6$, the films appear to develop an amorphous nature and the optical band gaps obtained from optical absorption measurement are much less than those obtained from photoconductive measurements. This work has been published in the ***"Thin Solid Films"*** Vol. 322/1-2 (1998) Page 117-122.

For the preparation of SnS and SnS_2 films the starting solution was prepared by dissolving $SnCl_2$ and thiourea in methanol. The structure and photoconductive properties of these films and their conversion to tin dioxide by annealing in atmospheric condition have been studied. XRD and SEM data suggest that good quality SnS and SnS_2 films are obtained at a baking temperature of 300° C and 360° C respectively. Values of bandgap for SnS and SnS_2 obtained from spectral response of photoconductivity are 1.4 eV and 2.4 eV respectively. The bandgap values for SnS_2 also agree with that obtained from optical absorption measurements. Optical absorption data for SnS_2 and Sb-doped SnS_2 films shows an increase in bandgap with increasing dopant concentration. However, increasing dopant concentration is accompanied by a loss in crystallinity as observed from XRD data. Annealing in atmospheric condition both of SnS and SnS_2 films at 400° C converts them to transparent conducting SnO_2.

In the last two sections of this chapter, preparation of MoS_2 and Cu_2S thin film and their optical & structural properties have been discussed briefly.

In chapter four we discuss a new technique developed by us, which is very simple and cost effective. This is the Open Air Chemical Vapour

Deposition (OACVD) technique. This technique was used for the preparation of transparent conducting undoped and doped (Mo, Sb & F) tin dioxide films. In OACVD technique, the substrate was placed vertically in the central region of a long tube heated from outside of the tube in atmospheric condition by winding a heater coil on its outer surface. When the substrate attained the desired temperature then the starting material (for SnO_2 film; $SnCl_2.2H_2O$ with few drops of water) kept in another container placed at the bottom of the tube was heated separately. White fumes, which contained $SnCl_4$ vapour, were given off by the paste and deposited SnO_2 films where they came into contact with the hot substrate. The electrical, optical, XRD & SEM properties were studied. Films were deposited on glass and mica substrates. The grain size of the film deposited on mica substrate was larger compared to those prepared on glass substrate. Optimum concentration for each dopant, at which the sheet resistance is a minimum, was determined. 4.5 at% F-doped SnO_2 films show the lowest resistivity ~ 4 X 10^{-4} Ω cm and average optical transmission of 80% at a thickness of 3500 A°. This work has been published in the ***"Thin Solid Films"*** Vol. 307 (1997) Page 221-227.

The fifth chapter summarizes the work presented in the thesis and future work that may be carried out in the field is suggested.

CHAPTER - 1

*THIN FILM DEPOSITION TECHNIQUES -A REVIEW

1.1. INTRODUCTION

Thin film technology has become extremely important today for fundamental studies in many fields of physics, electronics, and chemistry and is also employed in numerous practical applications. The tremendous progress in the field of thin film physics has been stimulated and widened to a large degree by the recent development of most efficient high and ultra-high vacuum systems up to many feet in diameter in which thin films can be deposited with great ease by the high vacuum evaporation technique. In addition, new instrumentation for measuring pressure, gas composition, and deposition rates during the evaporation, and novel evaporation sources, which are often automatically controlled, now permit the preparation of thin films under precisely controlled and completely reproducible conditions.

Some workers use such films to obtain information about the properties of solids in general, since certain measurements can be made more conveniently using thin films. Others are more interested in fundamental properties of solids in thin film forms, since these may differ considerably from those of the bulk material. Examples of such research include studies of the optical, electrical, magnetic and superconducting properties, investigations of structural order, dislocation, migration phenomena and phase transitions, and of various surface reactions and surface phenomena. The results obtained by such fundamental studies are also of great interest to those concerned with the practical and commercial applications of thin films. Examples of such applications which are most important for the fields of optics and electronics are: highly reflecting mirror coatings, protective layers, antireflection films, beam-splitters, reflection and transmission type interference filters with narrow and wide band widths, polarizer; radiation

detectors, coatings for image-forming devices, light intensifiers, and solar energy converters, surface films for controlling the temperature of satellites, for passive and active electronic device film components, thin film circuits, and superconducting thin film devices [1].

Thin films form when it is built up as a thin layer of solid substance on a solid support called the substrate by controlled condensation of the individual atomic, molecular or ionic species, either directly by a physical process, or via a chemical and/ or electrochemical reaction.

We present in this chapter a brief review of different deposition techniques. Though thin film deposition techniques are discussed in detail in various standard books [2], it is discussed here in brief to place the deposition methods described in the present work (dip deposition technique and open air chemical vapour deposition technique) in their proper perspective.

A thin fiilm deposition process involves three basic steps: (i) creation of atomic/molecular/ionic species, (ii) transport of these species through a medium (vapour, stream or spray/ or liquid) and (iii) condensation of the species on a substrate. Depending on whether the vapour species has been created by a physical process (such as thermal evaporation and sputtering) or by chemical or electrochemical means, the thin film deposition processes can broadly be divided into two classes.

(i) Physical Methods of deposition or Physical Vapour Deposition (PVD) and

(ii) Chemical Methods of deposition.

By combining these two methods, hybrid techniques such as reactive evaporation/sputtering and plasma deposition have been developed.

Although genuine differences exist between the two classes, the line of demarcation is not really sharp and in many cases the techniques involve features of both classes; nevertheless, the two are discussed separately.

1.2. PHYSICAL VAPOUR DEPOSITION (PVD)

As already stated, PVD techniques are those where vapour of the materials to be deposited has been created by a physical process, mainly based on evaporation and sputtering.

1.2.1. Evaporation technique: The evaporation of a material requires heating to a sufficiently high temperature to produce the desired vapour pressure. The vapour atoms traverse the medium and are made to condense on a substrate surface to form a thin film. The rate of condensation/deposition of the vapour atoms depends on the vapour-source-substrate geometry and the condensation co-efficient on the surface under given physical conditions.

Among the evaporation techniques thermal evaporation is comparatively simple and very convenient. In this method, solid material vaporizes when heated to a sufficiently high temperature and then the condensation of the vapour onto a cooler substrate, yields thin solid films. This is achieved by carrying out the deposition in a vacuum of such magnitude that the mean free path of the ambient gas molecules is greater than the dimensions of the deposition chamber and the source - substrate distance. Because of collisions with ambient gas atoms, a fraction of the vapour atoms proportional to $e^{-d/l}$ will be scattered. Here 'd' is the distance during their transfer through gas and 'l' is the mean free path and its value at 25° C is about 450 cm at 10^{-5} Torr. Other evaporation techniques such as vacuum evaporation, arc evaporation, co-evaporation, flash evaporation, laser evaporation, electron-beam evaporation, activated reactive evaporation (ARE) are also commonly used for the deposition of thin films. A variety of sources is used to evaporate different materials, depending on wheather they are available in wire, foil or powder form.

Figure 1.1 shows a few evaporation techniques which are commonly used for the deposition of thin films. Flash Evaporation [Fig.1.1.(a)], a rapid evaporation of a multicomponent alloy or compound, which tends to distill fractionally, may be obtained [3,4] by continuously dropping fine particles of the materials onto a hot surface so that numerous discrete evaporations occur. It has been used for preparing films of ceramics [5], Bi_2Te_3 [6], III-V compounds [7] etc.

In Arc Evaporation [Fig.1.1.(b)], by striking an arc between two electrodes of a conducting material, sufficiently high temperatures can be generated to evaporate refractory materials such as Nb and Ta. It is widely used for evaporation of carbon for electron-microscope specimens.

The Exploding-Wire techniques [Fig. 1.1.(c)], consists of exploding a wire by a sudden resistive heating of the wire with a transient high current density (approx. 10^6 A/cm^2). It is achieved by discharging a bank of condensers (~10 to 100 μF), charged to a voltage ~ 1 to 10 KV, through a metallic wire.

In case of Laser Evaporation, the enormous intensity of a laser may be used to heat and vaporize materials by keeping the laser source outside the vacuum system and focusing the beam onto the surface of the materials to be evaporated [Fig. 1.1(d)].

The evaporated films are generally not uniform because the amount of the material reaching the substrate depends on the angle (θ) between source and the substrate area [8]. The rate of deposition follows a $Cos\theta/r^2$ variation for a point source and $Cos^2\theta/r^2$ variation for evaporation from a small area, r being the distance between the source and the substrate. By proper selection of source, source-substrate geometry and substrate rotation, it is possible to get highly uniform films over large areas.

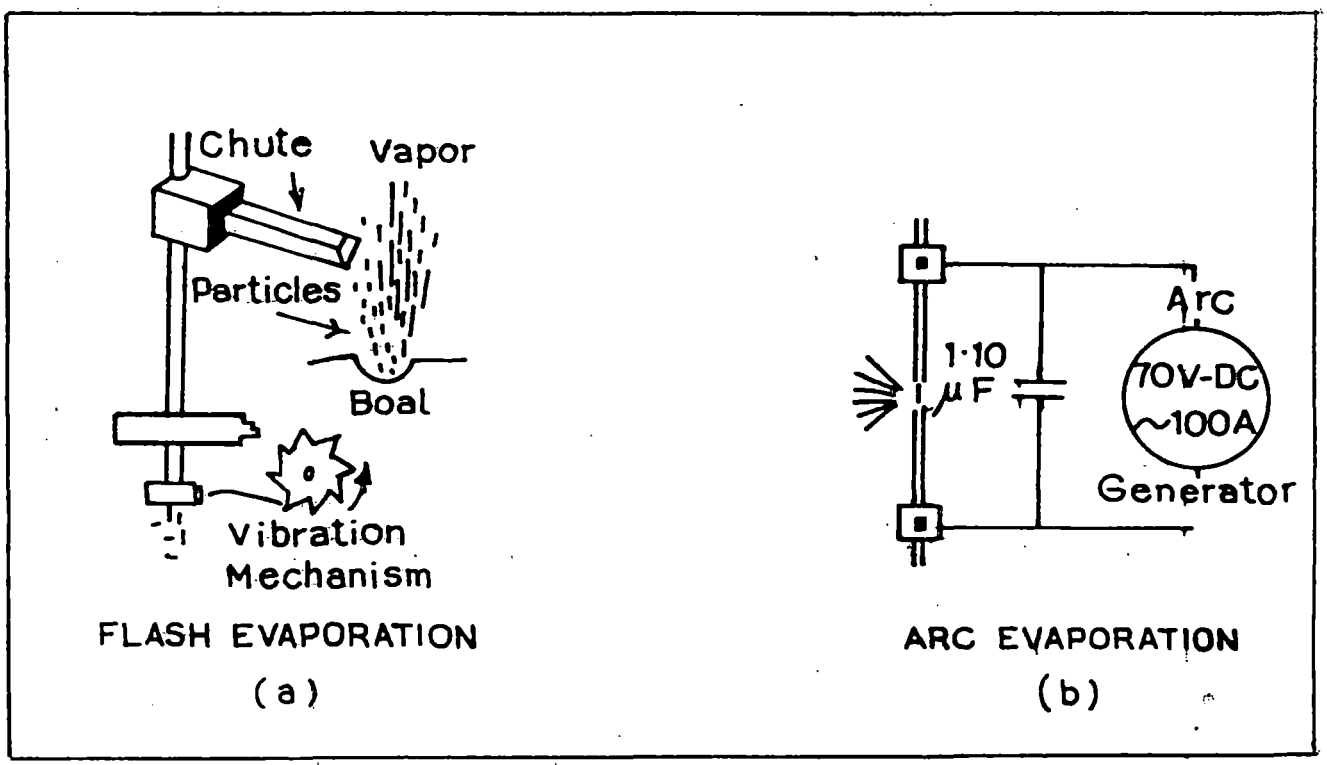

Figure 1.1. Schematic diagram of different evaporation technique (a) Flash evaporation, (b) Arc evaporation.

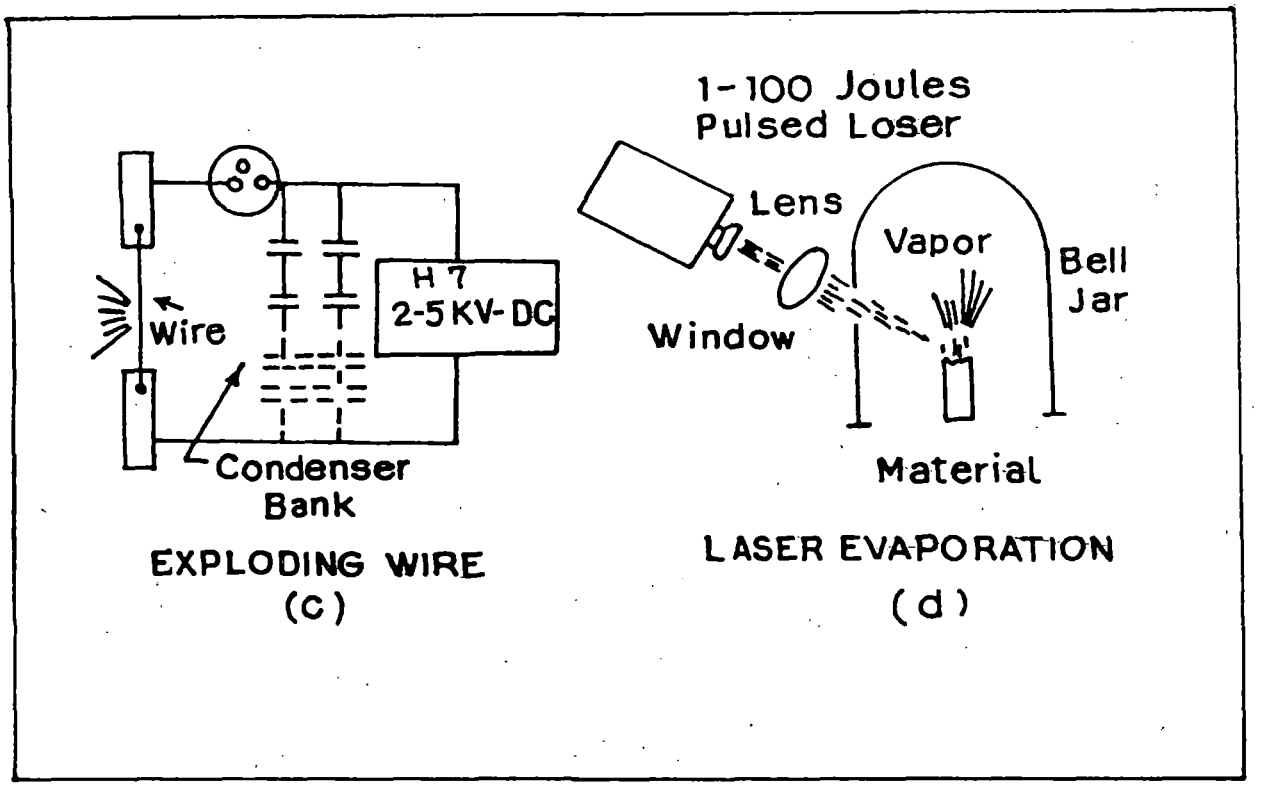

Figure 1.1. Schematic diagram of different evaporation technique (c) Exploding-wire evaporation, (d) Laser evaporation.

1.2.2. Sputtering techniques: Vapour species may be created by kinetic ejection from the surface of a material (called the target) by bombardment with energetic and non-reactive ions. The ejection process, known as sputtering, takes place as a result of momentum transfer between the impinging ions and the atoms of the target surface. The sputtered atoms are condensed on a substrate to form a film. Various sputtering techniques are used for deposition of thin films.

Several systems have been employed for deposition of films by sputtering. These sputtering variants are shown schematically in figure 1.2. The simplest and most widely used one utilizes the glow discharge between two electrodes and is commonly referred to as a diode arrangement [Fig. 1.2.(a)]. The substrate in such a diode system is normally placed on the anode and kept at anode potential. It will acquire a negative potential of several volts relative to the anode and attracts gas ions, leading to contamination of the film. On the other hand, if the substrate is held at a large negative potential, the film will subjected to steady ion bombartment throughout its growth. This technique [Fig. 1.2.(b)] employed by Maissel and Schaible [9], is called "bias sputtering". The idea of sputter deposition with simultaneous sputter cleaning by bombardment was originally conceived by Frerichs [10], and his arrangement is shown in figure 1.2.(c). Here an asymmetric alternating rather than d.c. is applied between cathode and substrate so that more material is deposited on one half-cycle than is removed by reverse sputtering in the other half-cycle. Bombardment removes absorbed gases and responsible for good bonding of the film.

The effect of sputter-cleaning of an evaporated film is utilized in a system [Fig. 1.2.(d)] called "ion plating" [11]. The films are obtained by evaporation from a filament and the deposit is simultaneously bombarded with accelerated gas ions.

The efficient gettering action of films for reactive gases during deposition was put to advantage by Theuerer and Hauser [12] in the technique [Fig. 1.2.(e)], called "getter sputtering". In this case , two cathodes of the material to be sputtered are

symmetrically located with respect to a Ni anode cylindrical can. The first cathode is used to maximize the gettering action of active gases where they enter near the bottom of the cylindrical can. After sputtering for a few minutes, the sputtered materials from the second cathode is allowed to deposit on the substrate.

Auxiliary electrons may be supplied thermionically from a filament. Both the total ionization and the ionization efficiency are increased by accelerating the electrons by means of a third electrode and injecting them into the plasma. This sputtering [Fig.1.2 (f)] process, is called "triode sputtering".

Ionization of the gas can be produced by suitable electromagnetic radiations such as rf, uv, x-rays, and γ-rays. High ionization yield may be obtained conveniently by the use of rf of several megacycles (RF sputtering). The rf may be applied directly to the anode through a capacitor [Fig.1.2.(g.1.) for metal sputtering], or via a high-frequency coil inside [Fig.1.2.(g.2.)] or outside the discharge vessel. Gawehn [13] used the electrodeless technique with rf of 1.8 to 12 Mc/sec to sputter at low pressure. Note that rf may be used additionally in any one of the Fig 1.2.(a) to 1.2.(f) sputtering arrangements to obtained increased sputtering rates at lower pressures.

Davidse and Maissel [14] described the application of the rf technique to sputtering of insulator films. A transmitter or a standerd rf heating power suply (1 to 20 Mc/sec, 2 kW at 2 kV) may be used to couple directly to the insulator target mounted on a metal plate. Two cathodes in a push-pull arrangement may be used [Fig. 1.2.(g.3)]. The direct coupling of rf is somewhat sensitive to the design of the feed through for the insulator cathode and to the rf power input. The reflective losses from the power supply into the sputtering apparatus necessitate water cooling of the leads. For supporting and stabilizing the high-frequency discharge, a magnetic field is frequently applied. It also makes operation possible at low pressures of a few milli-torr. Very pure films can be obtained by this technique because chances of contamination are less at the low pressure involved. Quartz and various glasses may be readily deposited to form films at rates of up

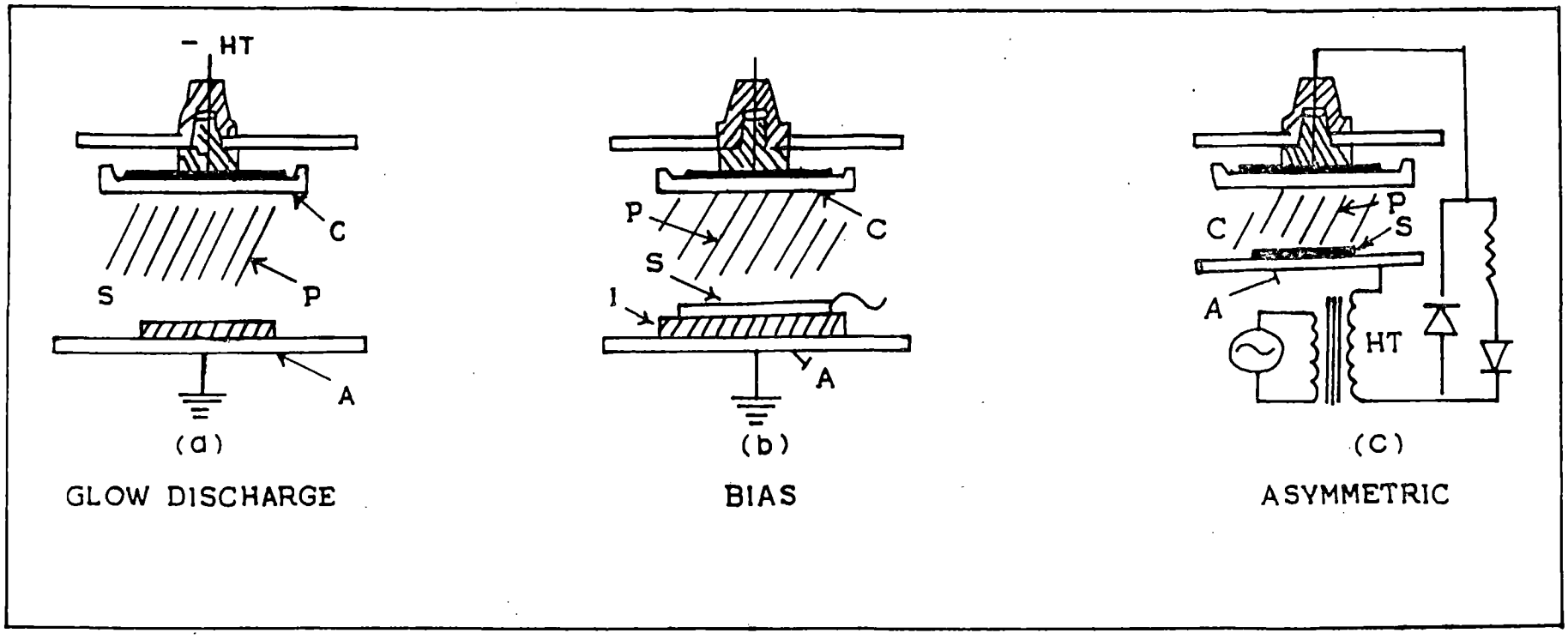

Figure 1.2. Schematic arrangement for several sputtering variants:

(a) Diode sputtering; (b) dc bias; (c) ac asymmetric (or bias);

The notations are P, plasma or discharge; C, cathode; A, anode; S, substrate; LT, lowtension; HT high tension.

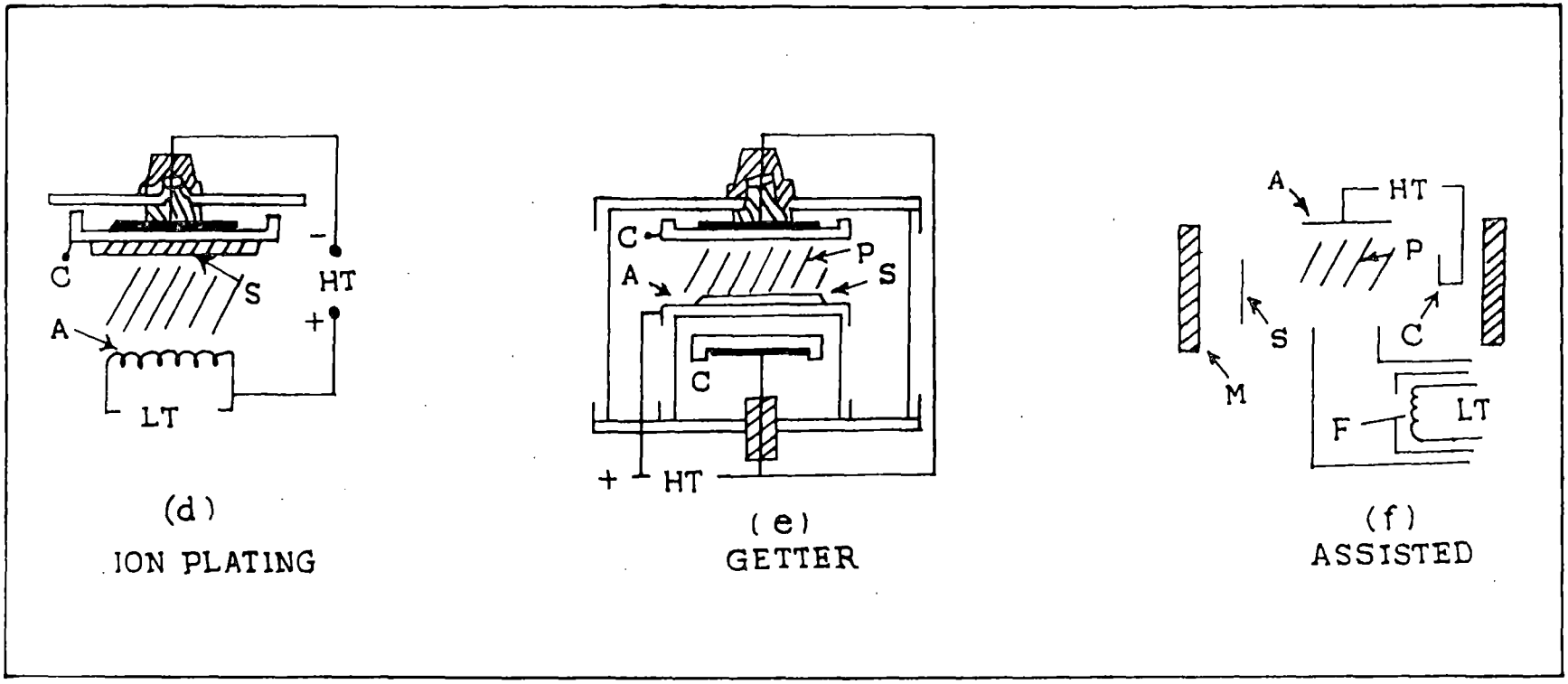

Figure 1.2. Schematic arrangement for several sputtering variants:
(d) ion plating; (e) getter sputtering; (f) thermionically and/or magnetically assisted glow discharge;

The notations are P, plasma or discharge; C, cathode; A, anode; S, substrate; LT, lowtension; HT high tension; M, magnet; F, filament (electron source);

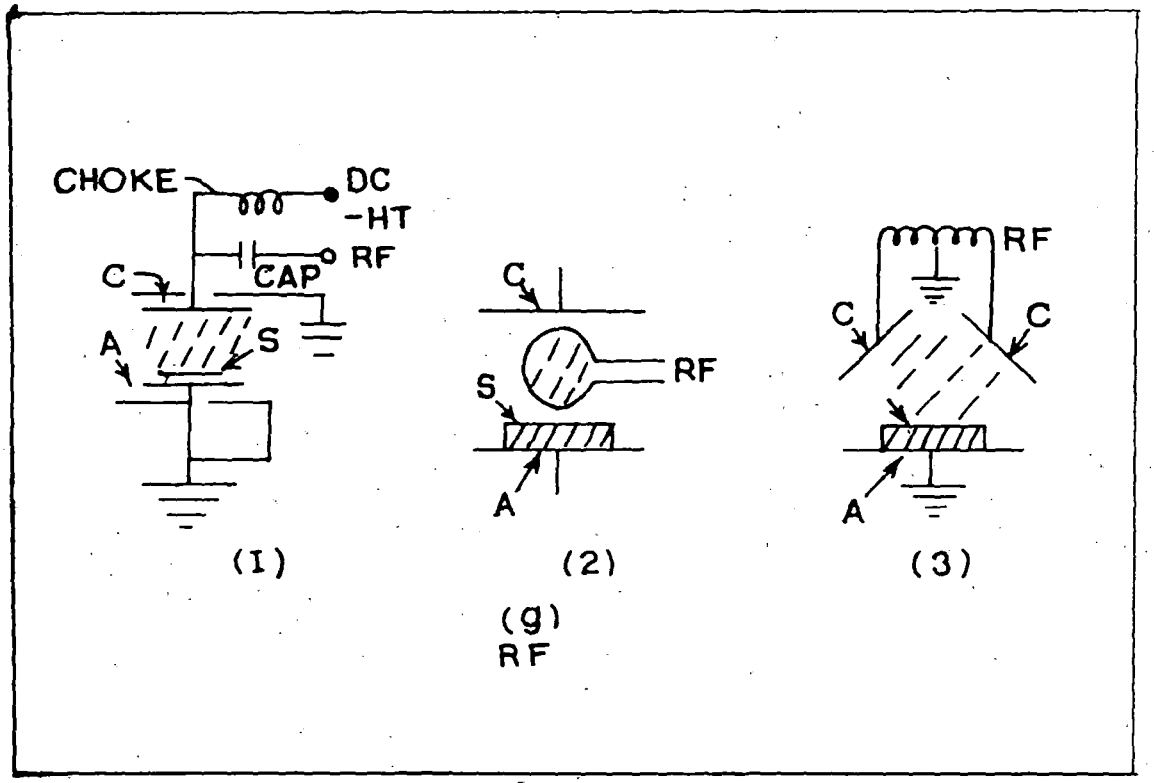

Figure 1.2. Schematic arrangement for several sputtering variants:

(g) rf sputtering with **(1) capacitor coupling for sputtering of metals and the inductor coupling for isolating dc from rf power supply, (2) indirect or induced rf coupling and (3) push-pull double cathode;**

to 30 Å/sec under typical operating conditions of a 13.56 Mc/sec, rf power of 800 W at 3,000 V peak to peak and an axial magnetic field of 0.011 T.

These processes are best suited for depositing films of many type of multicomponent materials.

1.3. EPITAXIAL DEPOSITION

Both for the case of single component and multicomponent compounds, it is possible to monitor and control the kinetics of condensation and thermodynamic reactions of the various ad-atoms so that the deposition takes place literally monolayer-by-monolayer on a single-crystal substrate and the atomic arrangement in the film follows that in the single-crystal. It has been used primarily for basic single-crystal growth studies and for specialized micro-electronic applications. Hot Wall Epitaxy (HWE), Molecular Beam Epitaxy (MBE) and Grapho-epitaxy are commonly known. MBE is a sophisticated and expensive method. For this method ultra-high-vacuum (UHV) is required to provide a clean ambient. With the help of MBE technique it is possible to deposit epitaxial layers of compound semiconductors, such as $Zn_xCd_{1-x}S$ [15], GaAs and CdTe having precisely controlled properties. A schematic diagram of an MBE system is shown in figure 3.

In the above, very brief accounts of the important Physical Vapour Deposition (PVD) techniques have been given. The deposition processes which are related to our techniques belong to the chemical methods of deposition. So in the next section the chemical methods of deposition are discussed in more detail. More elaborate accounts are available in the standard text books [2 & 16-20].

Chemical methods may be classified in two categories:

(i) Chemical vapour deposition and

(ii) Solution deposition technique.

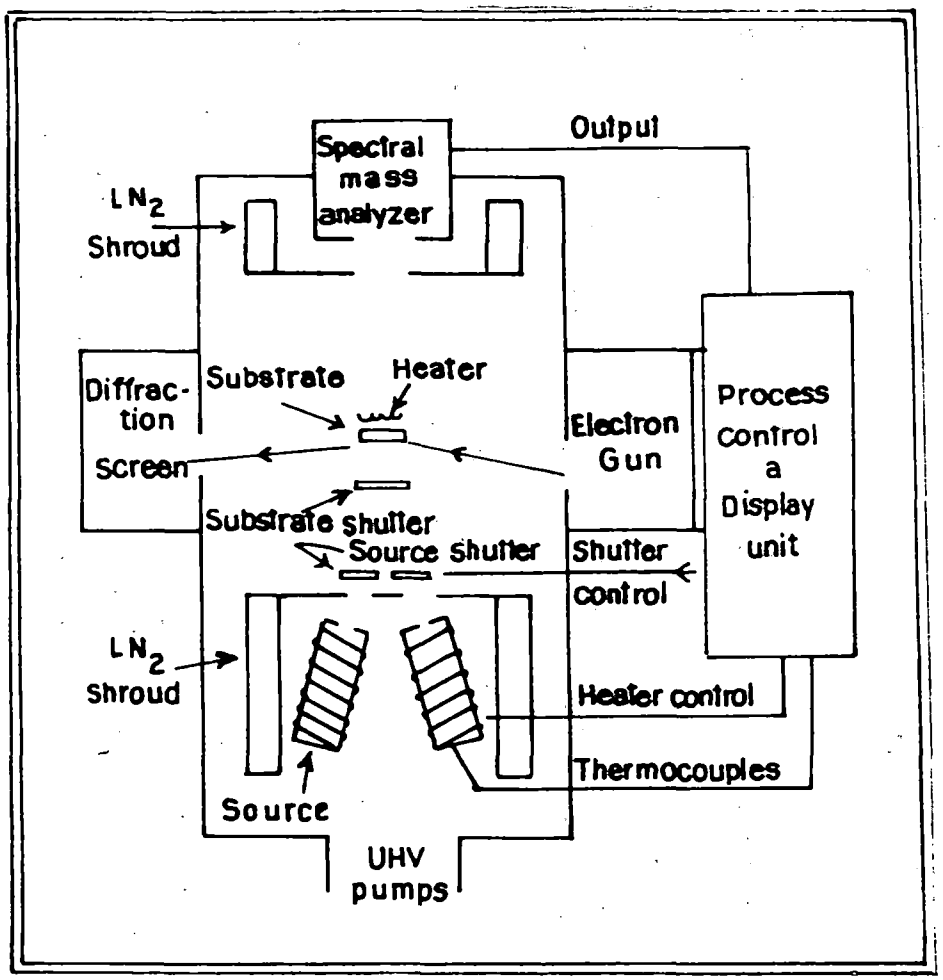

Figure 1.3. Schematic diagram for an MBE system.

1.4. CHEMICAL VAPOUR DEPOSITION

When a volatile compound of the substance to be deposited is vaporised, and the vapour is thermally decomposed or reacted with other gases, vapours, or liquids at the substrate to yield non-volatile reaction products which deposit atomistically (atom by atom) on the substrate, the process is called Chemical Vapour Deposition [21, 22]. Since a large variety of chemical reactions are available, CVD is a versatile and flexible technique in producing deposits of pure metals, semiconductors and insulators.

The chemical reactions utilized in CVD processes can be classified as: (i) decomposition reactions, (ii) reduction reactions, (iii) chemical transport reactions, etc.

1.4.1. Thermal decomposition:- Some compounds (such as organometallics, halides or metal hydrides) decompose at a high temperature on the substrate to yield metallic or semiconductor films. A general decomposition reaction can be written as

$$AB(gas) \rightarrow A(solid) + B(gas) - - - (1.1.)$$

A typical example of the decomposition process activated by heat (pyrolytic decomposition) is

$$SiH_4(gas) \xrightarrow{800-1300^0 C} Si(solid) + 2H_2(gas) - - - (1.2.)$$

Most organo-metallic compounds decompose at relatively low temperatures (< 600°C) and metal halides, particularly the iodides, are decomposed at higher temperatures. It is more convenient to use organo-metallic compounds as the processing can be carried out at lower temperatures. For example, thin films of Al_2O_3 can be prepared by thermal decomposition of aluminium tri-ethoxide at 550° C and aluminium tri-isopropoxide at 420° C.

1.4.2. Reduction:- A reduction reaction may be considered as a decomposition reaction aided by the presence of another vapour species, called the reductant. A reduction reaction occurs at temperatures much lower than the unaided decomposition reaction.

A typical example of CVD by reduction is the preparation of Si from the corresponding halide vapours using H_2 or Zn as the reducing agent, according to the reaction

$$SiCl_4 + 2H_2 \rightarrow Si + 4HCl \text{---} (1.3.)$$

The use of H_2, which is not a very strong reductant, offers the advantage that it can be premixed with the halide vapours without causing a premature reaction in the gaseous phase which gives rise to powdery deposits.

1.4.3. Chemical Transport: - The term chemical transport refers to the process of transferring of a nonvolatile deposit material to the substrate with the help of a highly volatile chemical vapour which converts it to a volatile compound by a chemical reaction. The volatile compound, formed as a consequence of this reaction, then decomposes on the substrate to yield a film of the source material. A typical example is the transport of Si in I_2 vapours.

$$Si(solid) + 2I_2(gas) \xrightarrow{1100^0C} SiI_4(gas) \text{----} (1.4.)$$
$$Si(solid) + SiI_4(gas) \xrightarrow{1100^0C} 2SiI_2(gas) \text{---} (1.5.)$$
$$2SiI_2(gas) \xrightarrow{900^0C} Si(solid) + SiI_4(gas) \text{----} (1.6.)$$

Among the important materials which can be deposited by CVD techniques are semiconductors such as II - VI and III - V compounds, Si, and conducting doped oxides of Sn, In, and V, insulators such as SiO_2, Si_3N_4, BN, Al_2O_3, Ta_2O_5, TiO_2 , Nb_2O_5 , and AlN, and a number of metals [23 - 27].

The commonly used CVD systems cover a wide range from extremely simple laboratory setups to highly sophisticated, completely automated, electronically controlled and computerized industrial reactors. The systems can be either closed, permitting complete recovery of the reagent species and recycling, or open, requiring an external supply of source material and extraction of the reaction components. A typical CVD system used for the deposition of Si p-n junction structures is shown in Fig.1.4.

1.4.4. Major advantages of the CVD technique

(i) In general, low-vacuum facilities are required and, thus a relatively simple setup and fast recycling are possible;(ii) high (~ 1 μm / min.) deposition rates are possible; (iii) it is possible to deposit compounds with easily controlled stoichiometry; (iv) it is relatively easy to dope the deposit with controlled amounts of impurities; (v) it is possible to deposit multicomponent alloys; (vi) refractory materials can be deposited at relatively lower temperatures as compared to vacuum evaporation; (vii) epitaxial layers of high perfection and low impurity content can be easily grown; (viii) objects of complex shapes and geometries can be coated; and (ix) in situ chemical vapour etching of the substrates prior to deposition is possible.

1.4.5. Drawbacks of the CVD technique

(i) The generally complex thermodynamics and reaction kinetics are poorly understood; (ii) comparatively higher substrate temperatures are required than those in the corresponding Physical Vapour Deposition (PVD) techniques ; (iii) the reactive gases used for deposition and the volatile reaction products formed are, in most cases, highly toxic, explosive, or corrosive; (iv) the corrosive vapours may attack the substrate, the deposited film, and the materials of the deposition setup; (v) the volatile

products generated during the deposition process may lead to incorporation of impurities in the film; (vi) the high substrate temperatures may lead to diffusion, alloying or chemical reaction on the substrate surface, thus restricting the choice of the substrate; (vii) high substrate temperatures may also give rise to segregation effects when metastable multicomponent materials are being deposited; (viii) masking of the substrate is generally difficult.

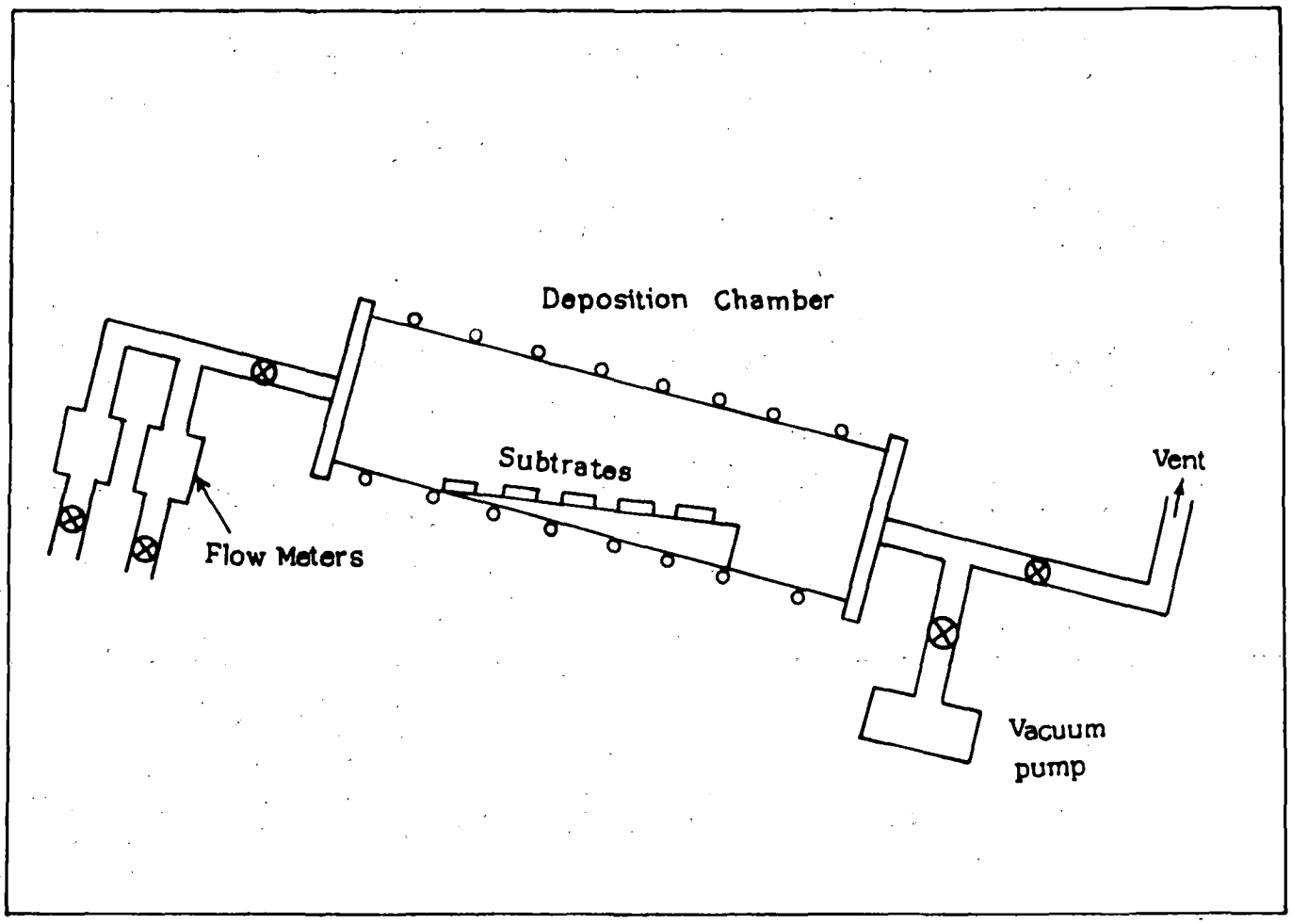

Figure 1.4. A typical chemical vapour deposition system.

1.5. Solution Deposition Techniques

In these techniques, the material to be deposited are dispersed in a liquid medium (generally aqueous) and are always present in ionic form. Solution deposition techniques, therefore, inherently involve chemical and / or electrochemical reactions for the formation of the deposit material. The solution deposition techniques may be classified into two categories: (i) electrochemical deposition (ECD) and (ii) chemical solution deposition (ESD).

1.5.1. Electrochemical Deposition (ECD)

Electrochemical deposition techniques require an external source of current for deposition. Obviously, they also require electrically conducting substrates. Various ECD techniques are used for deposition of films, and electrodeposition is one of them.

1.5.1.1. Electrodeposition:- The occurrence of chemical changes due to the passage of electric current through an electrolyte (salt solution or molten salt) is termed electrolysis, and the deposition of any substance on an electrode as a consequence of electrolysis is called electrodeposition. The main constituent of the electrolyte which serves to provide ions either in their simple form or in complex form. Additional chemicals such as wetting agents, brightening agents, alkalis, and acids may be added with the electrolyte as required. Almost all metals (except for highly electronegative ones) can be electrodeposited from aqueous solutions. Alloys can be deposited by coelectrolysis, for which the electrode potentials should be brought very close to each other. Electrodeposition of compound semiconductors like CdSe, CdTe, Ag_2Se and GaAs is possible by co-depositing the two components in elemental form by cathodic reduction of their corresponding ions and their subsequent reaction to form

the corresponding compound. For example, deposition of CdTe film involves electrolytic codeposition of Cd and Te from Cd^{+2} and TeO_3^{-2} ions. Similarly, CdSe and GaAs are electroeposited from Cd^{+3} and SeO_3^{-2} ions and Ga^{+3} and AsO_2^{-2} ions, respectively. The reaction involved at the cathode, for example, in the case of CdSe, are

$$Cd^{+2} + 2e \rightarrow Cd \quad ----(1.7.)$$

$$SeO_3^{-3} + 3H_2O + 4e \rightarrow Se + 6OH^- \quad --(1.8.)$$

$$Cd + Se \rightarrow CdSe \quad ----(1.9.)$$

A schematic block diagram of the experimental setup for electrodeposition technique is shown in figure 1.5. Using this technique semiconducting metal chalcogenides such as CdS, HgS, PbS, Ti_2S, Bi_2S, Cu_2S, NiS CoS and SnS/SnS_2 thin film can be deposited on various substrates.

1.5.1.2. Anodization:- When a current is passed through an electrolyte; an anode (metal substrate) is converted to one of its compounds. This conversion process is called anodization. The chemical composition of the film depends on the type of electrolyte. Acidic or basic electrolytes lead to oxide films, whereas thiourea and ammonia in the anodizing solution produce sulphide and nitride films respectively.

1.5.1.3. Cathodic conversion:- This is an electroconversion process for the deposition of Cu_2S films on CdS. In this method, $CuSO_4$ taken as an electrolyte, CdS thin film is used as a cathode and a copper plate as an anode. On passing a current Cu_2S films can be deposited on CdS film according to the following reaction.

$$CdS + 2Cu^{+2} + 2e \rightarrow Cu_2S + Cd^{+2} \quad ---(1.10.)$$

In this reaction Cd^{+2}, goes into the solution.

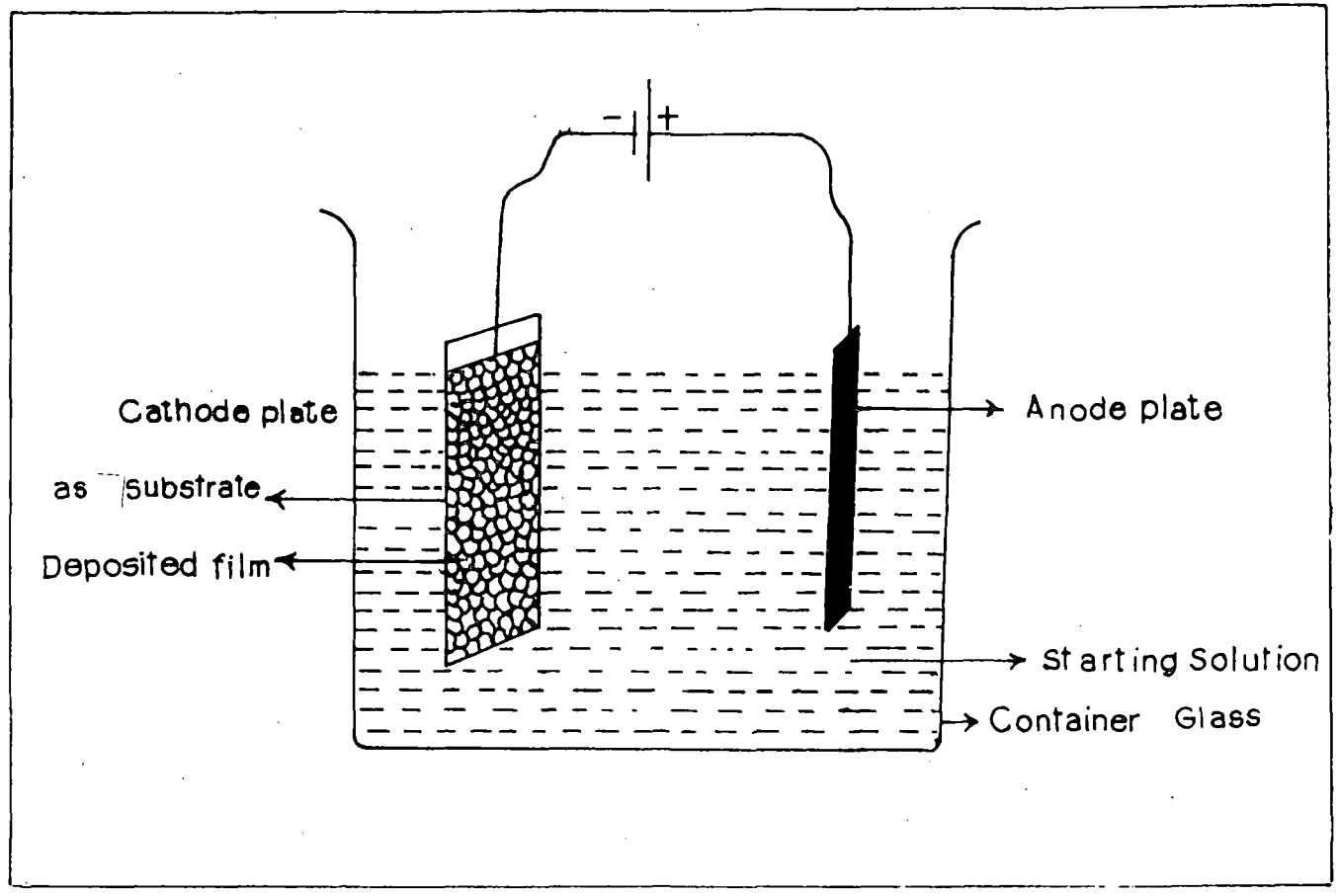

Figure 1.5. Schematic diagram of electrodeposition technique.

1.5.2. Chemical Solution Deposition (CSD)

Chemical solution deposition techniques are generally immersion technique in the sense that they involve simply dipping of the substrate into the reaction mixture for some time depending of the thickness required. Spray Pyrolysis, Solution Growth and Sol-gel techniques are the most popular among Chemical Solution Deposition techniques. The main advantages of these techniques are:-

(i) uniform deposition takes place, (ii) Both conducting and insulating substrates can be coated and (iii) No power supply is required. The various CSD techniques are:

1.5.2.1. Spray Pyrolysis:- A large number of metallic salt solutions when sprayed onto a hot substrate decompose to yield oxide films. Similarly films of sulfides or selenides can be prepared by pyrolytic decomposition of a solid complex compound formed on the surface of a substrate by spraying a mixed solution of the corresponding metalic salt and a sulphur / selenium-bearing compound. For example, $CdCl_2$ and $(NH_2)_2CS$ (thiourea) solutions when mixed at room temperature do not react to form CdS, but when sprayed onto a substrate held at ~ 400^0 C, a solid complex of composition $CdCl_2.(NH_2)_2CS$ is formed, which decomposes on the substrate to yield CdS films.

A schematic block diagram of a typical spray-pyrolysis setup for deposition of metallic oxide, metallic sulfide and metallic selenide thin films is shown in figure 1.6. The atomization of the chemical solution into a spray of fine droplet is effected by the spray nozzle with the help of a filtered carrier gas which may or may not be involved in the pyrolytic reaction. For example, oxygen (O_2) is used as a carrier gas for the deposition of SnO_x film whereas the carrier gas plays no role in the deposition of CdS films. The carrier gas and the solution are fed into the spray nozzle at pre-

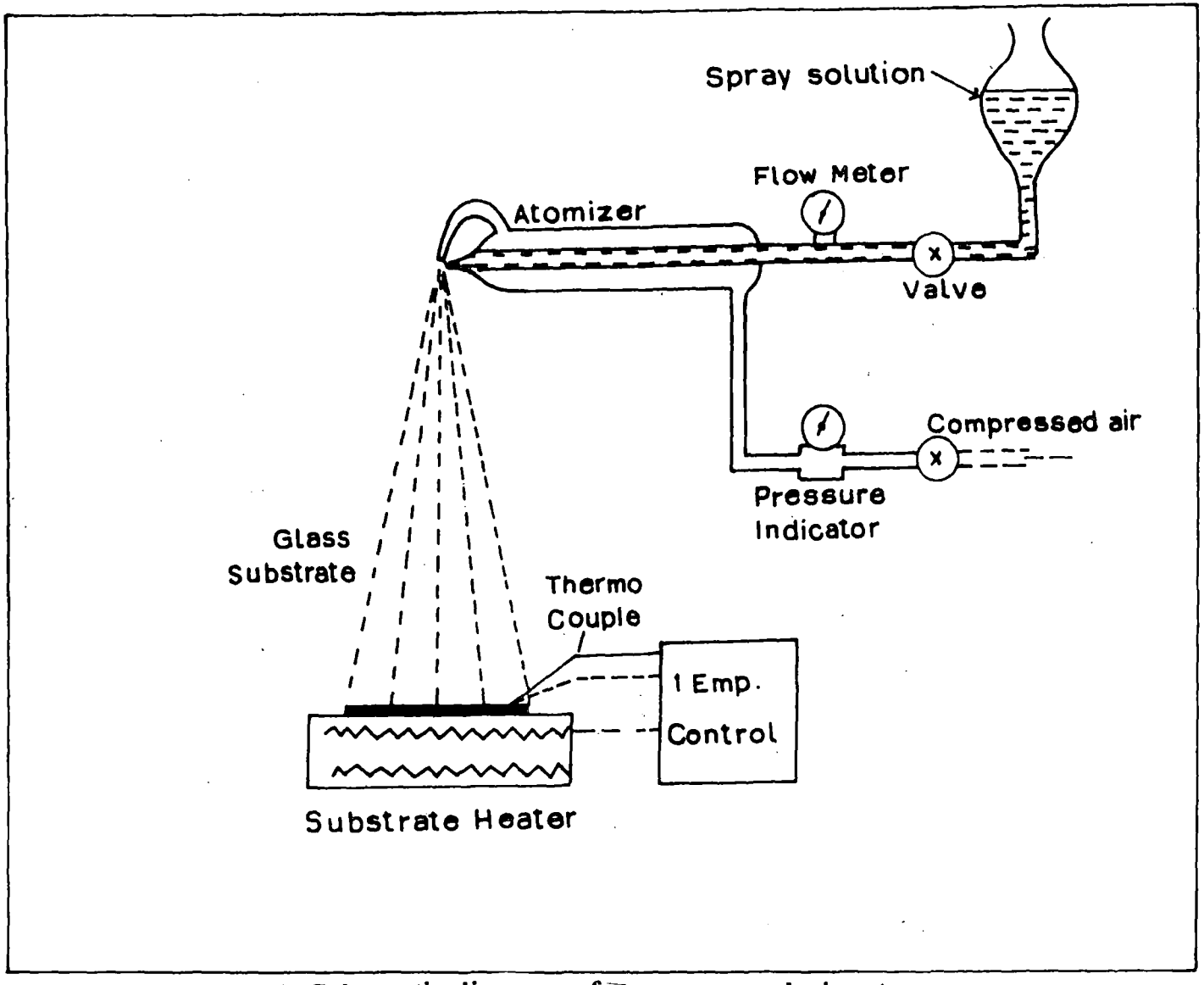

Figure 1.6. Schematic diagram of spray pyrolysis setup.

determined and constant pressure and flow rates. The substrate temperature is maintained with the help of a feedback circuit.

By this method doped and mixed films can be prepared very easily, simply by adding to the spray solution a soluble salt of the desired dopant or impurity. Two very important examples of the materials deposited by this technique [23 - 38] for device fabrication are (i) CdS for solar cells and (ii) In F-or Sb-doped SnO_2 for conducting glass.

1.5.2.2. Chemical Solution Growth:- The chemical solution growth technique, well known for chalcogenide films, has been extended to the deposition of oxide films (MnO_2, Fe_2O_3, ZnO and SnO_2). Metal ions in aqueous solution, under certain conditions, form solid phases of hydroxides $M(OH)_n$ or hydrous oxides ($M_2O.X\ H_2O$) which on heating yield the corresponding metal oxides. With the help of controlled homogeneous precipitation from solution, S and Se compound films like CdS, PbS, ZnS, Bi_2S_3, CdSe, PbSe, ZnSe etc. have been successfully deposited by this technique [39, 40]. The major parameters which control the deposition process are the composition of the deposition bath, its pH and its temperature. The experimental setup to obtain film deposition is shown schematically in fig 1.7. The substrates are immersed vertically in the reaction bath, which is stirred continuously with a magnetic stirrer. The temperature of the bath is monitored by a cotract thermometer that forms a part of a feedback circuit controlling the heater to maintain a constant temperature. When ionic product (IP) of the metal and chalcogenide ions exceeds the solubility product (SP) of the corresponding chalcogenide, a metal chalcogenide film is formed on the substrate by an ion-by-ion condensation process.

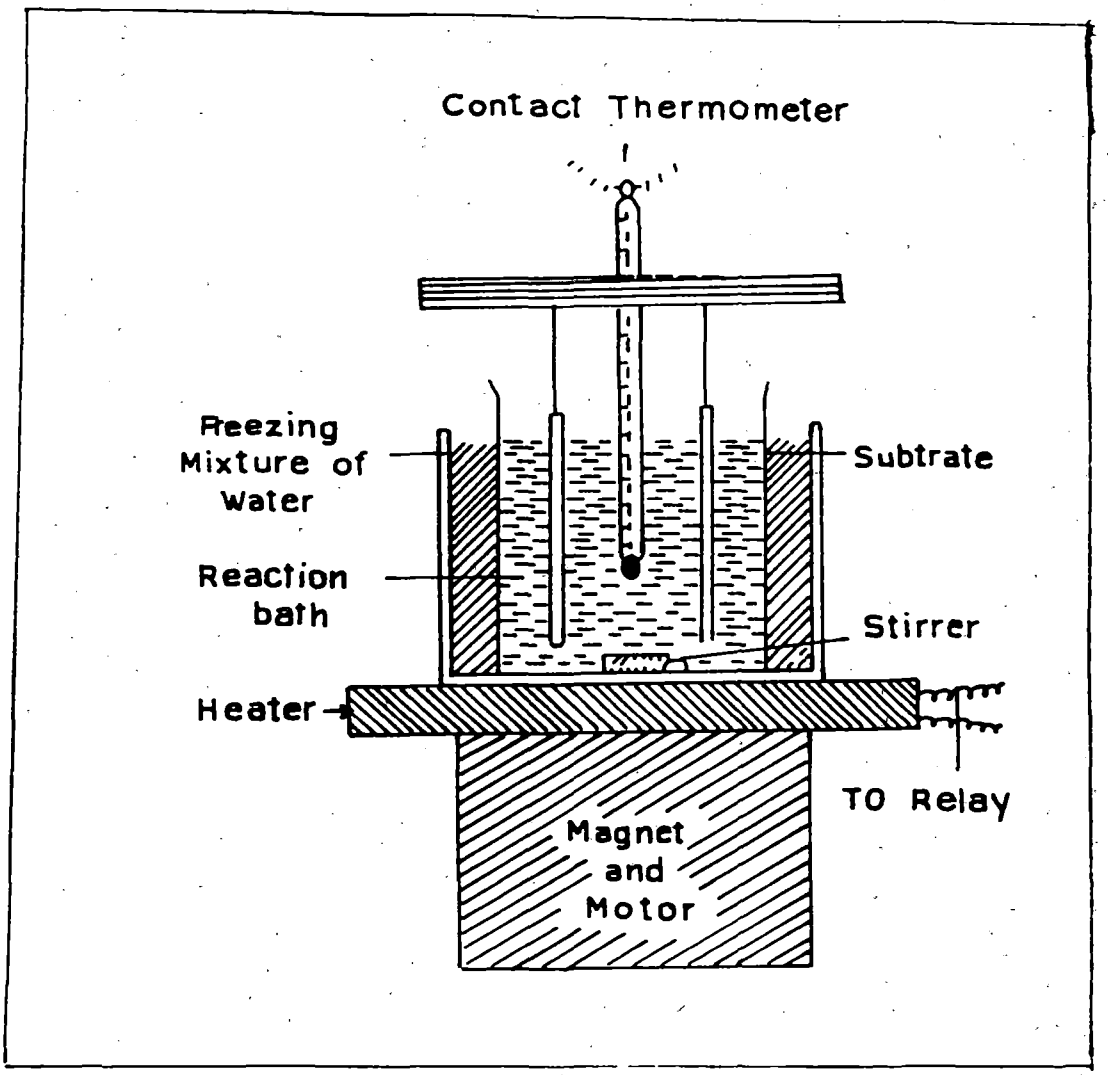

Figure 1.7. Experimental arrangement for solution growth setup.

1.5.2.3. Sol-Gel Method:- In this method for the preparation of thin films, a homogeneous solution is first prepared using metal alkoxides. The solution changes to a sol and then to a gel at room temperature. This gel forms thin gel-sheets which are converted to a glassy layer on heating to a high temperature. For instance, thin SiO_2 layers can be obtained from silicon tetra-ethoxysilane $Si(OC_2H_5)_4$ at a temperature of 500° C - 900° C. The films presents the possibility of obtaining thin glass sheets of thickness ranging from several tens to several hundreds of micrometers. With the help of this method one can also prepare bulk glasses and glass fibres. Fibres like silica-alumina or pure silica can be prepared by heating after drawing from alkoxide solution at near room temperature.

1.5.2.4. Dip Technique:- The dip technique [41-43] consists essentially of inserting the substrate into a solution containing hydrolysable metal compounds and pulling it out at a constant speed in atmospheric condition, when a liquid layer adheres to the substrate surface. It is then baked at high temperature, when a chemical reaction takes place producing the desired thin films. Any hydrolysable compound including halides or nitrates, preferably metallo-organics are suitable for this process. A typical reaction in the case of metal alkoxides is

$$Al(OR)_3 + 3H_2O \rightarrow Al(OH)_3 + 3ROH \quad --(1.11.)$$
$$2Al(OR)_3 \rightarrow Al_2O_3 + 3H_2O \quad --------(1.12.)$$

The important control parameters are the viscosity of the solution, the pulling speed and the firing temperature. The rate of heating also needs to be controlled to avoid cracking of the films.

This technique has not been very popular, because so far it was limited to oxide films only. But as described in detail in chapter 2, it can be used to deposit sulphide thin films also.

1.5.3. Major advantages of Solution Deposition Techniques

(i) Experimental setups are much less sophisticated compared to those in vapour deposition techniques; (ii) no expensive equipment such as vacuum systems is not required for the deposition; and (iii) deposition is carried out at much lower temperatures (< 100^{o} C).

1.5.4. Drawbacks of Solution Deposition Techniques

Solution deposition techniques suffer from the drawback that preparation of ultraclean substrates using in situ techniques, such as plasma etching and ion bombardment as in the case of vapour deposition techniques, is not possible. Also the choice of the substrate is limited to only water-insoluble materials.

1.6. MISCELLANEOUS METHODS

1.6.1. Electrophoretic deposition

In this process, electrically charged particles suspended in a liquid are deposited on an electrode by applying an elecrtic field. Using this method, mainly metal alloys, compounds, polymers and mixture of various components can be deposited.

1.6.2. Screen printing

Schematic representation of the screen printing process is shown in figure 1.8. It involves positioning the substrate on a carriage, which is then brought beneath the screen so that the substrate is in accurate registration with the pattern on the screen. The pattern on the screen is photolithographically defined so that open mesh areas in the screen correspond to the configuration to be printed. The substrate, when in the printing position, is placed a short distance beneath the screen. A small amount of the paste is dispensed onto the upper surface of the screen. A flexible wiper, called the squeegee, then moves across the screen surface, deflecting the screen vertically and bringing it into contact with the substrate and forcing the paste through the open mesh areas. On removal of the squeegee, the screen regains its original posoition by its natural tension, leaving behind the printed paste pattern on the substrate. The substrate carriage is then removed from beneath the screen and the substrate replaced and the process continues.

1.6.3. Spin coating

Spin coating differs from dip - coating in that the deposition film thins by centrifugal draining and evaporation. Bornside et al. [44] divide spin - coating into four stages: deposition, spin - up, spin - off and evaporation. An excess of liquid is dispensed on the surface during the deposition stage. In the spin - up stage, the liquid fiows radially outward, driven by centrifugal force. In the spin - off stage ,

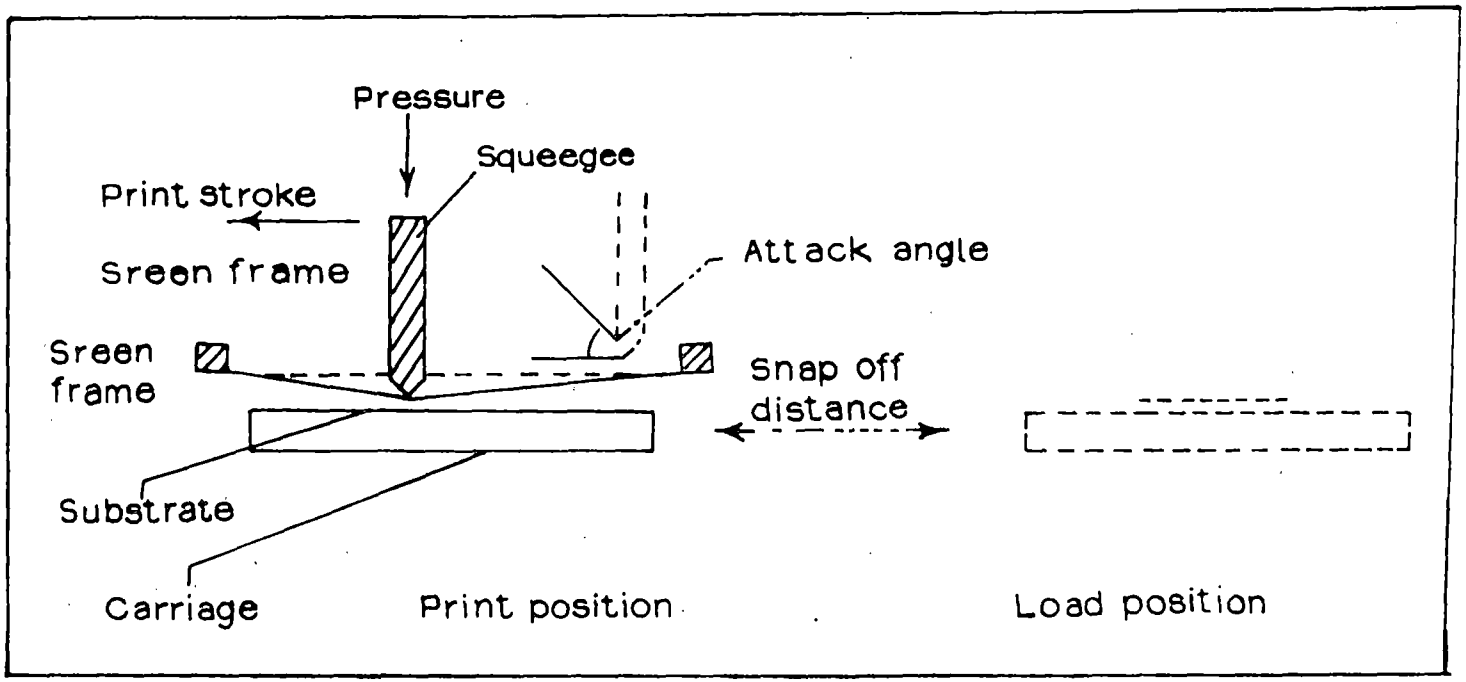

Figure 1.8. Schematic diagram of the screen printing process.

excess liquid flows to the perimeter and leaves as droplets. As the film thins, the rate of removal of excess liquid by spin - off slows down, because the thiner the film, the greater resistance to flow, and because the concentrarion of the non - volatile components increases, raising the viscosity. In the final stage, evaporation takes over as the primary mechanism of thinning. According to Scriven [45] the main advantage of spin - coating is that a film of liquid tends to become uniform in thickness during spin - off and, once uniform, tends to remain so, provided that the viscosity is not shear - dependent and does not vary over the substrate.

1.6.4. Solution Casting

In this method the solution is poured a horizontally placed substrate and leaving it for the solvent to evaporate. And then very thick (~ 100μm) films can be formed on the substrate. The dried film can be stripped off the substrate very easily.

1.7. CONCLUSIONS

A large variety of methods for depositing thin solid films at rates ranging from a fraction of an angstrom to 10^6 A°/sec have been successfully utilized by various workers. Several of these methods, notably thermal evaporation and sputtering, permit automatic monitoring and controlling of the rate of deposition and hence film thickness. The fact that the properties of the films depend on various deposition parameters should be considered in the choice of a particular deposition technique. The parameters are the rate of deposition, temperature or kinetic energy of the vapour atoms, angle of incidence of vapour, electrostatic changes carried by vapours, the substrate temperature and vapour-source materials, concentration of the solution, composition of the ambient atmosphere, and thermal accommodation and condensation coefficients of the vapour atoms and the ambient gas atoms. These parameters may vary from technique to technique.

References:

01. Georg Hass 1963 *Physics of thin films vol. 1.* **Academic Press. New York.**

02. K. L. Chopra 1969 *Thin Film Phenomena* **Mc Graw-Hill, New York.**

03. L. Harris and B. M. Siegel 1948 *J. Appl. Phys.* **19** 1623.

04. W. R. Beam and T. Takahashi 1964 *Rev. Sci. Instr.* **35** 1623.

05. W. Himes, B. F. Stout and R. E. Thun 1962 *9th Natl. vacuum symp.* **The Macmillan Company, New York** p.144

06. E. K. Muller, B. J. Nicholson and G. L'E. Turner 1963 *J. Electrochem. Soc.* **110** 969.

07. J. L. Richards in *"The use of Thin Film for Physical Investigations"* **(J. C. Anderso, ed) Academic Press** p.71.

08. L. Holland 1956 *"Vacuum Deposition of Thin Films"* Chapman and Hall London.

9. L. I. Maissel and P. M. Schaible 1965 *J. Appl. Phys.* **36** 273.

10. R. Frerichs 1962 *J. Appl. Phys.* **33** 1898.

11. G. M. Mattox 1964 *Electrochem. Tech* **2** 295.

12. H. C. Theuer and J. J. Hauser 1964 *J. Appl. Phys.* **35** 554.

13. H. Gawehn, Z Angew 1962 *Angew. Phys.* **14** 126

14. P. D. Davides and L. I. Maissel 1966 *J. Appl. Phys.* **37** 574; P. D. Davides 1967 *Vacuum* **17** 139

15. T. Karasawa, K. Ohkawa. T. Mitsuya, 1991 *J. Appl. Phys.* **69** 3226.

16. L. Holland 1956 *Vacuum Deposition of Thin Films* **Wiley, New York.**

17. L. I. Maissel and Glang, eds.1970 *Handbook of Thin Film Technology* **Tata McGraw 1l, New York.**

18. R. W. Berry, D. M. Hall and M. T. Harris, eds. 1968 *Thin Film Technology* **Van Nostrand, Princeton.**

19. J. L. Vossen and W. Kern eds.1978 *Thin film Processes* **Academic Press, New York.**

20. J. C. Anderson ed. 1966 *The Use of Thin Films in Physical Investigations* **Academic Press, New York.**

21. H. Schafer, 1964 *"Chemical Transport Reactions"* **Academic Press Inc., New York.**

22. C. F. Powell, J. M. Blocher, Jr. (eds.) 1966 *"Vapour Deposition"*, **John Wiley & Sons, Inc., York.**

23. J. Proscia, R. G. Gordon 1992 *Thin Solid Films* **214** 175.

24. Yan Dawel, Ma Xiaocui, Wang Zongchang, Wu Jam 1993 *Thin Solid Films* **224** 257.

25. A. Fujisawa, T. Nishino, Y. Hamakawa 1988 *Jpn. J: Appl. Phys.* **27(4)** 552.

26. M. R. Kadam, N. Vittal, R. N. Karekar, R. C. Aiyar 1990 *Thin Solid Films* **187** 199.

27. B. J. Baliga, S. K. Gandhi 1976 *Electrochem. Soc.* **123** 941.

28. E. Santhi, V. Dutta, A. Banerjee, and K. L. Chopra 1980 *J. Appl. Phys.* **52 (12)** 4443.

29. E. Santhi, V. Dutta, A. Banerjee, and K. L. Chopra 1980 *J. Appl. Phys.* **51 (12)** 6243.

30. E. Santhi, A. Banerjee, and K. L. Chopra 1982 *Thin Solid Films* **88** 93.

31. G. Gordillo, L. C. Moreno, W, de. la cruz, P.Teheran 1994 *Thin Solid Films* **252** 61.

32. A. L. Unaogu and C. E. Okeke 1990 *Solar Energy Mater.* **20** 29.

33. H. Kim, H. A. Laitinen, 1975 *J.Am. Ceram. Soc.* **58** 23.

34. E. Santhi, V. Dutta, A. Banerjee, and K. L. Chopra 1982 *Appl. Phys.* **53** 1615.

35. G. Maurodien, M. Gajardziska, Novkovski 1984 *Thin Solid Films* **113** 93.

36. J. Bruneaux, H. Cachet, M. Froment, A. Messad 1991 *Thin Solid Films* **198** 129.

37. T. A. Chynoweth, R. H. Bube 1980 J. *Appl. Phys.* **51** 1844.

38. A. Mzerd, D. Sayah, I. J. Saunders and B. K. Jones 1990 Phys. Stat. Sol. A **119** 487.

39. G. K. Padam , G. L. Malhotra and S. U. M. Rao 1988 *J. Appl. Phys.* **63** 770.

40. Y. F. Nicola and J. C. Menard 1988 *J. Cryst. Growth* **92** 128.

41. W. Geffcken and E. Berger, Jenaer Glaswerk Schott and Gen., Jena, G. D. R. 1939 *G. D. R. Patent* 736, 411.

42. H. Schroeder 1969 *Phys. of Thin Films* **5** 87.

43. H. Dislich and E. Hussmann 1981 *Thin Solid Films* **77** 129.

44. D. E. Bornside, C. W. Macosko and L. E. Scriven 1989 *J. Appl. Phys.* **66** 5185.

45. L. E. Scriven, 1988 in: *Better Ceramics Through Chemistry III ed.* C. J. Brinker, D. E. Clark and D. R.Ulrich. *Mater. Res. Soc. Symp. Proc.,* **121 (materials Research Society, Pittsburgh)** 717.

CHAPTER-2

*OXIDE FILMS PREPARED BY THE DIP TECHNIQUE

2.1. INTRODUCTION

The dip technique provides a very simple and cost-effective method for the deposition of thin films. It does not require any complex sophisticated specialized setup. In this chapter we describe the dip technique in detail and its use for the deposition of oxide films and their characterisation.

2.2. DIP TECHNIQUE

The earliest investigations concerning oxide coatings deposited from solution were those of Geffcken and Berger [1] and of Geffcken [2] about 60 years ago. Further work on this technique was carried out by Schroeder [3-6] and later by Dislich [7-8]. It was Geffcken [1-2] who laid the cornerstone by showing how to convert relatively simple hydrolysable metal compounds into well-defined layers of metal oxide. Schroeder [3-6] made a thorough analysis of the film forming process and discussed its application to the deposition of a large number oxide films.

In 1980, H. Dislich and Eckart Hussmann [8] showed that it is possible to synthesize by dip coating thin films of glasses, crystals and glass ceramics which are not easy to fabricate in bulk form. Dislich et al. [8] has deposited amorphous and crystalline oxide films from organometallic solution using dip-coating technique. They used large panes (nearly 3m X 4m) for deposition of oxide films, which are carefully cleaned, inserted into an organometallic solution, and then withdrawal and baked in an atmosphere. In this process, atmospheric hydrolysis and condensation process take place until transparent metal oxide layers are obtained. The liquid film partly flows down the plate and partly adheres to it and solidifies after evaporation of the solvent. Finally the

film is hardened in a high temperature (300° C - 400° C) cycle until a transparent metal oxide film has been formed. In this process, film- forming oxides are mainly those of the elements of groups 3-8 of the periodic table (provided that these lead to stable oxide) and especially oxides of the following elements: Al, Si, Zr, Sn, Pb, Ta, Cr, Fe, Ni, Co, and some other earth elements. The technique has also been used to deposit mixed oxides such as SiO_2-TiO_2 [9] whose refractive index could be varied over the range from 1.45 (SiO_2) to 2.20 (TiO_2) depending on the composition. These oxides may be amorphous or crystalline depending on the treatment at higher temperatures, or the influence of the surface of the substrate. It should be possible to deposit transparent conducting oxides such as cadmium-tin-oxide (CTO) and zinc stannate by this technique. Dislich et al. also found that dip-coating method using metal alkoxides is very useful for modifying the properties of large surfaces and provide substrates with new active properties. The first saleable products for optical applications were made in 1953. Since 1969 large panes of window glass have been coated by this method for sun-shielding windows. These are sold under the trade name Calorex [10]. Schott have been producing vehicle rear-view mirrors by the dip-coating procedure since 1959 and anti-reflection layers on glass panes since 1964 [11].

As briefly mentioned in chapter 1, in this technique, the substrate is withdrawn vertically from a solution containing suitable metal compounds (e.g. nitrate or chloride or alkoxides) in an organic solvent, at a controlled speed, when a liquid layer adheres to the substrate. It is then subjected to a high temperature treatment, when a chemical reaction takes place, leading to the formation of the corresponding metal oxide film onto the substrate surface.

The solution (starting solution) which is to be used for deposition by dip technique should have the following characteristics.

(i) Adequate solubility of the starting material and at the same time very little tendency of the dissolved substances towards crystallization during evaporation of the solvent.

(ii) Sufficiently small contact angles between the solution and the substrate to be coated in order to obtain good wetting of the latter. Wettability of a substrate can be improved in some cases by the addition of wetting agents to the solution.

(iii) Adequate durability of the solution and constancy of processing conditions.

During the formation of liquid film on the substrate in this technique, the lifting movement of the carrier holding the substrate should be kept completely smooth and shockless. If the irregularities in the liquid level and uncontrolled air currents are avoided then the liquid film develops in a horizontal dipping line alone the substrate. The uniformity in the film can be checked by observing the interference fringes, which are formed due to the evaporation of the solvent from the substrate surface.

In an excellent review of this topic, Scriven [12] states that when the substrate is withdrawn from the solution or solution is dragged out from the substrate then the thickness of the deposited films is dependent upon many factors. These factors are viscous drag on the liquid by the moving substrate, force of gravity, resultant force of surface tension in the concavely shaped meniscus, inertial force of the boundary layer liquid arriving at the deposition region, surface tension gradient and the disjoining or conjoining pressure.

According to Scriven when the liquid viscosity, η and substrate speed (v) are high enough to lower the curvature of the gravitational meniscus, the deposited film thickness of the liquid layer, h, is that which balances the viscous drag (η v/h) and gravity force (ρgh) [12]:

$$h = c_1(\eta v/\rho g)^{1/2} \quad \text{----(2.1)}$$

where the constant c_1 is about 0.8 for Newtonian liquids. When the substrate speed and viscosity are low (often the case for sol-gel dip coating film deposition), this balance is modulated by the ratio of viscous drag to liquid-vapour surface tension, η, according to the relationship derived by Landau and Levich [13]:

$$h = 0.94(\eta v)^{2/3} / \eta_{1v}^{1/6} (\rho g)^{1/2} \quad \text{----(2.2)}$$

However, the quality of the films and thickness depend on the concentration of the starting solution and the speed of withdrawal. Factors like viscosity, surface tension and vapour pressure, which are characteristics of each solution, can be summarized in a constant value. This constant also depends on ambient temperature and humidity.

The thickness of the film also depends upon the angle of inclination (θ) of the substrate relative to the horizontal line. The usual value of θ is 90°, i.e. vertical withdrawal.

2.3. DIP DEPOSITION SETUP

The setup used by us for the deposition of thin films by the dip technique is shown in figure 2.1.

Here, the precleaned substrate in its holder, moves freely at the end of a thread. The thread passes through a pulley which is driven by a geared motor arrangement. The substrate is immersed into the solution in such a way that the holder remains just outside the liquid level. For smoothly drawing the substrate out of the liquid, air currents are avoided. The liquid is usually kept inside a long cylinder. Often it is found that abrupt exposure to air after withdrawal of the substrate leads to patchy films with cracks. To avoid this shock, the substrate with its liquid film is kept for a few minutes in an atmosphere of the solution vapour within the long cylinder before its transfer to the furnace for baking.

2.3.1.SUBSTRATE CLEANING

The cleanliness of the substrate surface exerts a decisive influence on film growth and adhesion. The choice of cleaning technique depends on the nature of the substrate, the type of contaminants present in it and the degree of cleanliness required. Residues from manufacturing and packaging, lint, fingerprints, oil and airbone particulate matter are examples of frequently encountered contaminants. Ordinary soda-glass, mica, conducting glass (SnO_2-coated) and aluminium substrate have been used for deposition of films. When the glass substrate is polished during manufacture, the surface develops an electrostatic charge, which firmly holds minute particles on the cleaned surface. In addition, a small amount of grease may also be present. To remove these contaminants, acid cleaners such as chromic acid is used to convert them to more soluble compounds. The effectiveness of solvents is probably more dependent on the ability to wet the substrate than their solvent action. The solvent to be used must be of a high purity.

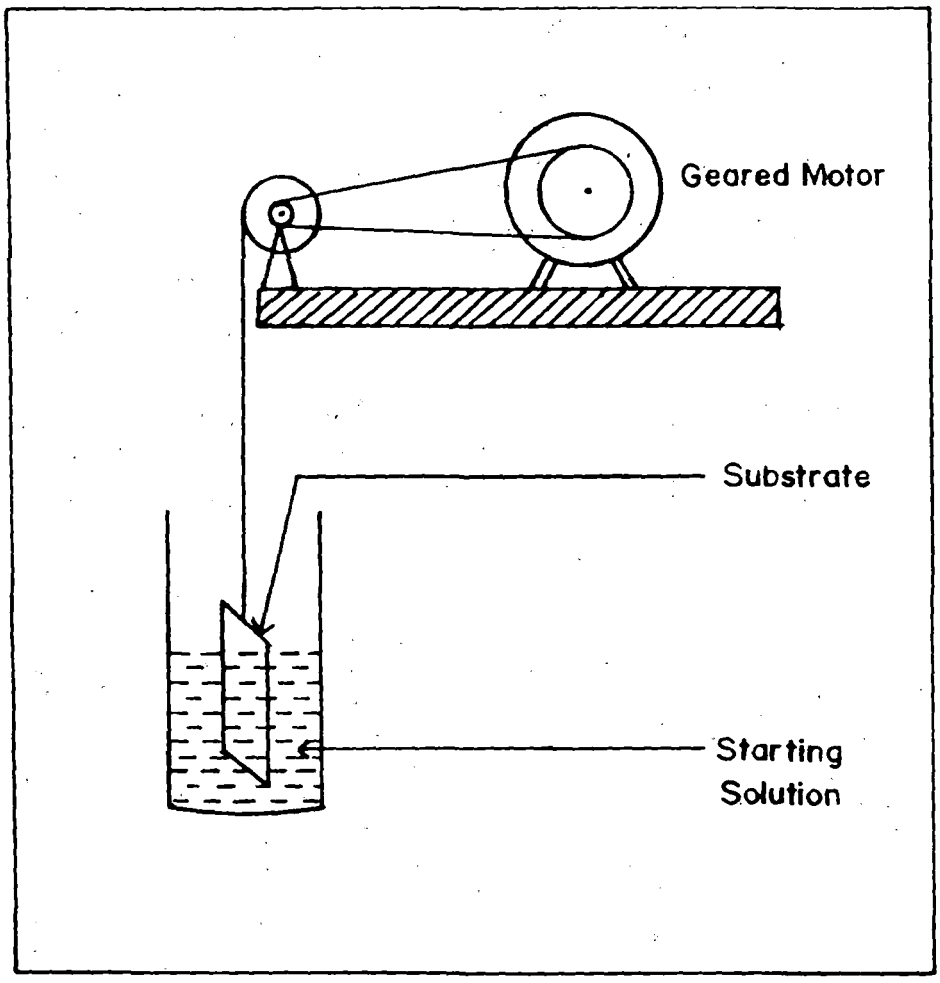

Figure 2.1. Experimental setup of dip technique for deposition of thin films.

Common solvents used in cleaning are methanol, acetone, trichloro-ethylene and distilled water. In this method substrates were initially cleaned in detergent solutions, dipped into chromic acid, then again in detergent solution and finally washed in running water.

The preferred method for degreasing a substrate is to expose it to solvent (methanol) vapours by keeping it above the boiling liquid in a vapour degreasing chamber. The solvent vapours condense on the substrate and fall back into the liquid. In this way, the substrate is cleaned by the action of the pure solvent.

By cleaning test, it can be confirmed whether the substrates have been properly cleaned or not. A common such test is to slowly withdraw the clean substrate from a container filled with pure water, when a continuous film of water will be observed to remain on the substrate surface if the cleaning has been properly done. This method is known as water-break test.

Substrates cleaned by the above method shows a remarkably high coefficient of friction for the liquid layer which adheres strongly to the surface. For all types of substrates used, dipping in chromic acid, washing in soap solution and then distilled water followed by vapour degreasing was found to produce surfaces which were sufficiently clean for the deposition of films by the dip technique.

Thus with the help of the above setup, one can obtain a uniform liquid film on the substrate. It is then subjected to a high temperature treatment to convert it into a solid one.

2.3.2. DEPOSITION PROCESS

Film formation by the dip technique requires heating as an essential step. This is advantageous because heating forms chemical bonds between the film and the substrate leading to strong adhesion. Relatively low ($\sim 300^{0}$ C) baking temperatures are sufficient in most of the cases, hence highly heat - resistant substrates are not essential. As previously mentioned, the precleaned substrate is withdrawn vertically from a starting

solution and baked at a high temperature in a furnace for a few minutes in atmospheric condition, when the adhered liquid chemicals in the form of a uniform liquid layer reacted on the substrate surface and formed the desired solid film. The liquid layer adhering to the substrate is mostly uniform, except for a region of ~1-2 mm wide near the bottom and the side of the substrate. This non-uniform portion of the substrate usually known as the trouble zone is dependent on the lifting speed as well as concentration of the starting solution. If the lifting speed is very small (~ 1 mm) or the solution is very dilute, then the length of the trouble zone is quite negligible (< 1 mm).

However, the film thickness was found to be uniform over a central region of few cm length. Studies were carried out on this uniform central part of the films.

2.3.3. THICKNESS OF THE FILM

Film thickness depends primarily on the lifting speed of the substrate and the concentration of the metal compounds present in the starting solution. Although as previously mentioned, a number of factors, such as viscosity and surface tension of the starting solution, atmospheric humidity and the angle of inclination (θ) determine the thickness of the liquid layer sticking to the substrate as it is pulled out, and thus the thickness of the final film. But for practical purposes characteristics of the solution and ambient condition is essentially constant and films are deposited by vertical withdrawal ($\theta=90^{o}$). So, thickness of the films is varied by key parameters such as lifting speed of the substrate, concentration of the solution and multiple dipping (dip-withdrawal-bake cycle) for thicker films.

A characteristic of the dip technique is the thickness of the film. With the help of this technique the thicknesses ranging from 50 A^{o} - 5000 A^{o} can be obtained in one dip-bake cycle. The small thickness is an advantage for films for electronic applications; while it is usually a disadvantage for protecting layers. Thicker films can also be obtained by this technique by repeating the whole process of dipping-withdrawal-

baking a number of times. Since multiple deposition is somewhat laborious, this technique is not very suitable for films of several micrometers thickness and thicker films.

In the following articles, deposition of tindioxide-based (SnO_2) transparent semi-conducting oxide and copper oxide (CuO) thin films by the dip technique have been described.

*2.4. TIN DIOXIDE-BASED (SnO_2) TRANSPARENT SEMICONDUCTING THIN FILMS

Transparent and conducting tin dioxide films have assumed importance in research as well as in technology owing to their applications in the field of electronics, ferroelectric memories, selective coatings etc. The presence of various impurities and the deposition parameters drastically alter the properties of the tin dioxide films, thereby influencing the efficiency of various devices such as photoconductive and solar cells, thin film transistors and electroluminescent cells etc. Several deposition techniques for preparation of tin dioxide films have been widely used [14-34].

For transparent conducting oxide applications, in electronics for instance, a very high quality of the films is required, and this method is able to lead to very high-quality SnO_2 layers, as far as the structure and morphology are concerned. However, there are not many reports in the literature on SnO_2 films prepared by this technique, which tend to have resistivity at least an order of magnitude higher than those prepared by other techniques such as CVD [35]. This high value of resistivity, while not suitable for photovoltaic cells, would however not be a problem for low current applications, such as liquid crystal displays.

---

* **Published in the "Surface and coating technology" Vol. 102 (1998) Page 73-80.**

To prepare the transparent semi-conducting tin dioxide based films in this technique, the starting solution was prepared by dissolving a requisite amount of stannous chloride ($SnCl_2$ $2H_2O$) into methanol such as 0.33 kg. $SnCl_2$ $2H_2O$ in one litre methanol. A clean substrate was then dipped into the starting solution and withdrawn vertically at a controlled speed (1.33 mm/sec), under atmospheric conditions using the setup described previously (section 2.2). After withdrawal, the substrate with its liquid film adhering to it is baked at 400° C - 500° C for five minutes. In this method, as also in the related sol-gel method [29,30] a metal oxide (SnO_2) film is produced by hydrolysis of the corresponding metal alkoxide, nitrate or chloride on a substrate and subsequently heat treated at a high temperature.

For F-doped film preparation, requisite amount of ammonium fluoride is added to the starting solution. In this method undoped and doped films were prepared for different baking temperatures. Variation of their thickness with lifting speed and concentration was studied. Thicker films could be obtained by repeating the whole cycle (dip-withdrawal-bake) a number of times. Films were deposited on soda-glass microscope slides and mica sheet. The characterization was mostly done on those deposited on glass substrate.

2.4.1. EXPERIMENTAL RESULTS

In this section, electrical and optical properties as well as surface morphology and crystal structure of undoped and F-doped tin dioxide-based transparent semiconducting thin films deposited by the dip technique have been discussed.

The films were deposited at different baking temperatures and at various lifting speeds. It was found that at 1.33 mm/sec lifting speed and the baking temperature of 400° C - 500° C was necessary to obtain films of useful quality in terms of low sheet resistance and high optical transmission. Within this temperature range there is no noticeable variation in the film properties. Results reported in this section refer to films prepared at a baking temperature of 400° C. The films were highly homogeneous and mechanically and chemically stable.

2.4.1.1. THICKNESS

The thickness of resulting films depends only on the lifting speed and concentration of the solution if the starting solution is kept at a constant temperature and humidity condition and the substrate is withdrawan at a fixed angle (90° in this case). Film thickness can be also increased by repeating the whole cycle (dip-withdrawal-bake) a number of times. Figure 2.2 - 2.4 shows the variation of film thickness with speed of withdrawal, concentration and number of dippings, respectively. It is observed that the thickness of the deposition layer increases linearly upto 7-8 dippings, beyond which the rate of increase is slower. Thickness of deposited films was measured by stylus method. In this method a step is made in a deposited film by removing part of the film from the substrate, and then the "shoe" or "skid" of the stylus instrument is placed on the substrate. The stylus instrument, travels across the sample surface with the movement of "shoe" or "skid". The vertical displacement is converted to electrical signals by means of a transducer. The signal is then amplified and recorded on a strip chart. Then the film thickness was measured from the corresponding vertical distance between the lower and upper portions of the trace.

2.4.1.2. X-RAY DIFFRACTOMETRIC STUDY

X-ray diffractometric studies were carried out by PHILIPS diffractometer (model PW 1390) with CuK_{α} radiations (Ni-filter) at 1.54 A°. Figure 2.5 shows the X-ray diffractograms of undoped films on glass substrate for five different numbers of dippings. It is evident from the diffractograms that crystallinity of the films improve with number of dippings upto a value of 20, beyond which a slight reduction in peak height is observed. Single dip films are almost totally amorphous, whose resistivity is rather high, of the order of 2.7 Ωcm. The sheet resistance drops sharply as the thickness increases to about 1 μm.

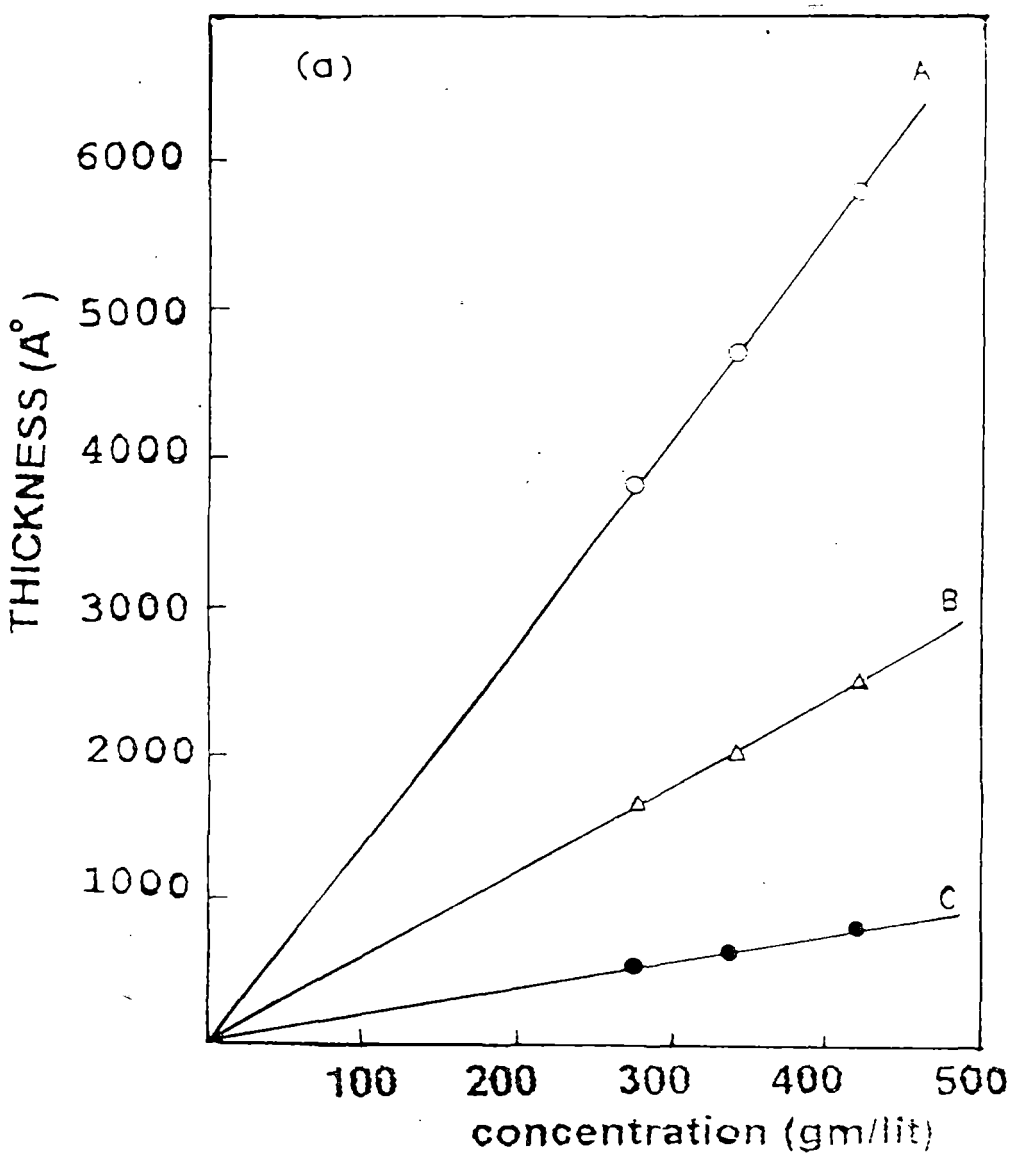

Figure 2.2. Variation of thickness of films deposited on glass substrates with concentration of the starting solution [speed of withdrawal: A = 3 mm/sec, B = 1.3 mm/sec, C = 0.56 mm/sec].

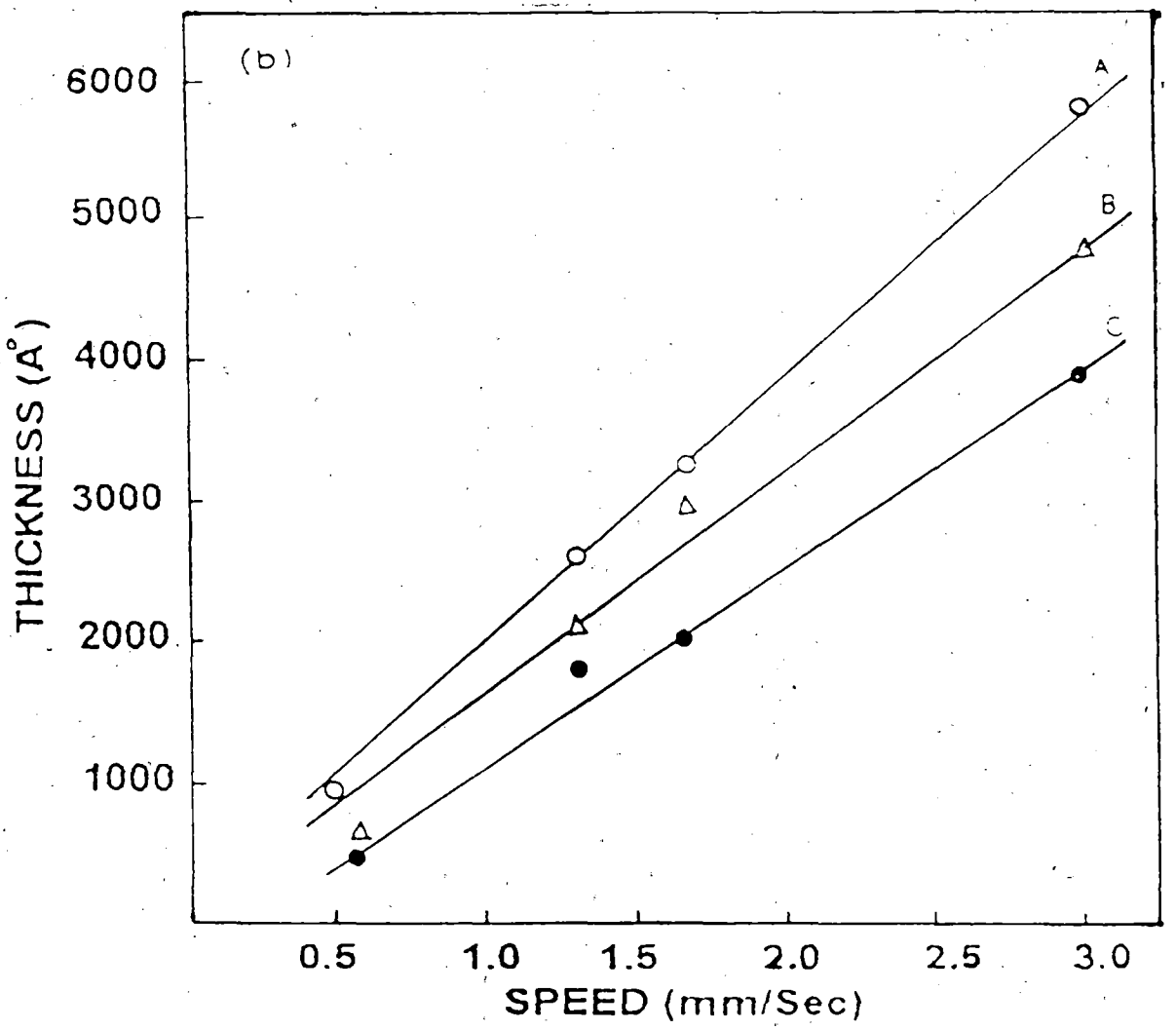

Figure 2.3. Variation of thickness of films deposited on glass substrates with speed of withdrawal [concentration of the liquid starting solution: A = 410 gms/litre, B = 330 gms/litre, C = 250 gms/litre].

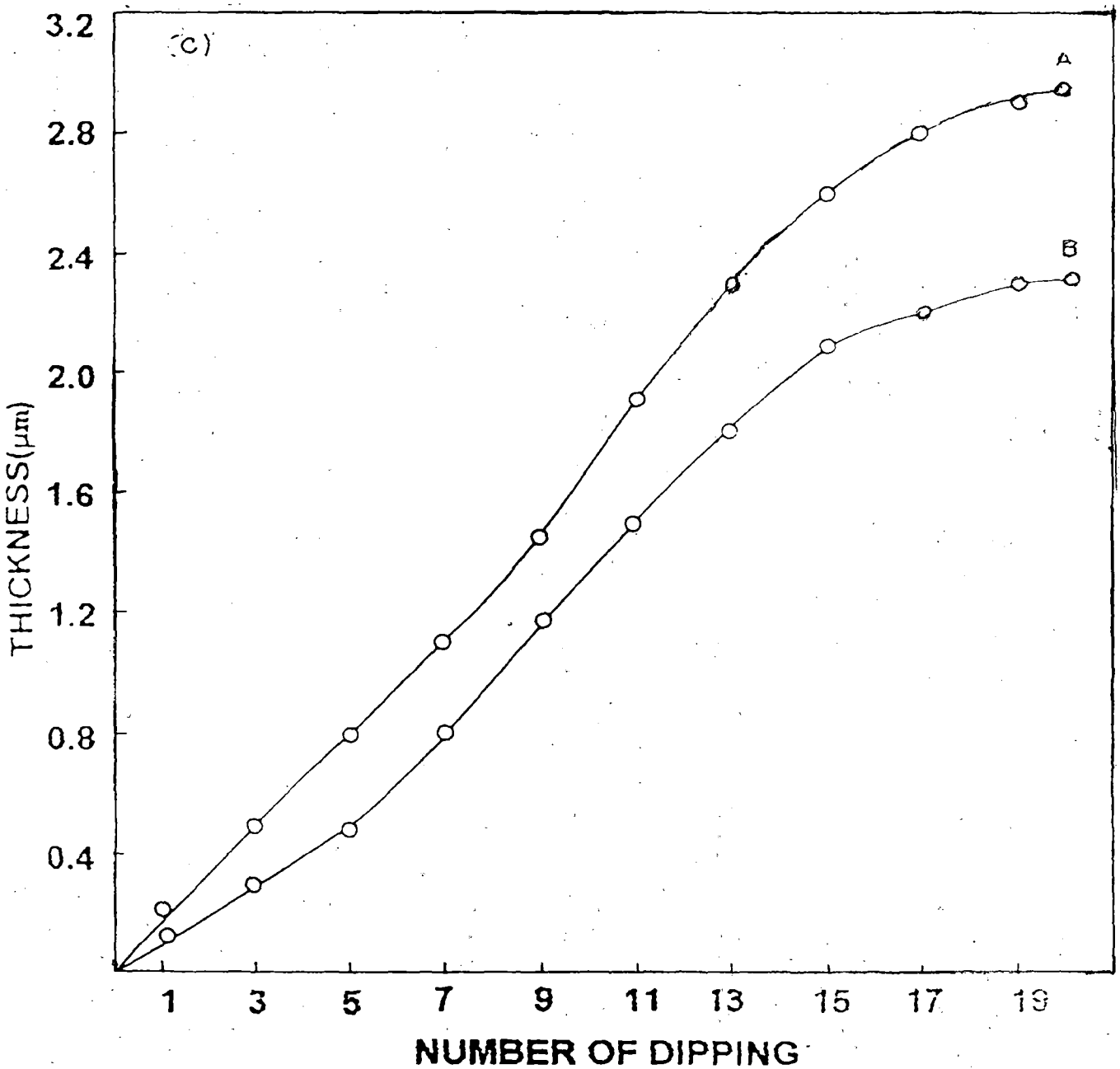

Figure 2.4. Variation of thickness of films deposited on glass substrates with number of dippings at a speed of withdrawal 1.3 mm/sec [concentration of the starting solution: A = 330 gm/litre, B = 250 gm/litre].

This type of behavior has also been observed previously by Procia et. al. [35]. It is possible that at low thickness only isolated small crystallites are formed, which become larger and more densely packed at larger thicknesses [36]. Figure 2.6 shows the X-ray diffractogram of a typical 10-dip film on mica substrate. The peaks are observed to be much sharper compared to those for films deposited on soda-glass substrates. Prominent peaks and their corresponding d- values for typical films deposited on soda-glass (20 dip) and on mica (10 dip) substrate are listed and compared with d-values from ASTM data file in table - 2.1 & table - 2.2 respectively.

Table - 2.1. ***Prominent peak position (2θ values) of x-ray diffraction peaks, corresponding d-values and their identification for SnO_2 - based transparent semi-conducting films deposited on glass substrate.***

(2θ)	Observed d- values (A°)	Comparable d-values (A°) from ASTM data file no 21-1250	h k l
26.6	3.348	3.351	110
33.75	2.653	2.644	101
37.8	2.378	2.369	200
38.9	2.313	2.309	111
51.63	1.769	1.765	211
55.0	1.668	1.675	220
58.12	1.586	1.593	002

Table - 2.2. ***Prominent peaks position (2θ values) of x - ray diffraction peaks, corresponding d-values and their identification for SnO_2 based transparent semi-conducting films deposited on mica substrate.***

(2θ values)	Observed d - values (A°)	Comparable d - values (A°) from ASTM data file no. 21-1250	h kl
26.75	3.330	3.351	110
34.3	2.612	2.644	101
38.1	2.360	2.369	200
45.6	1.988	2.120	210
52.0	1.757	1.765	211
55.4	1.657	1.675	220
58.1	1.586	1.593	002

The position of the peaks are in conformity with the standard tetragonal crystal structure of SnO_2. Comparison with (I/Io) data from ASTM data file indicates that there is no significant preferential growth in any direction.

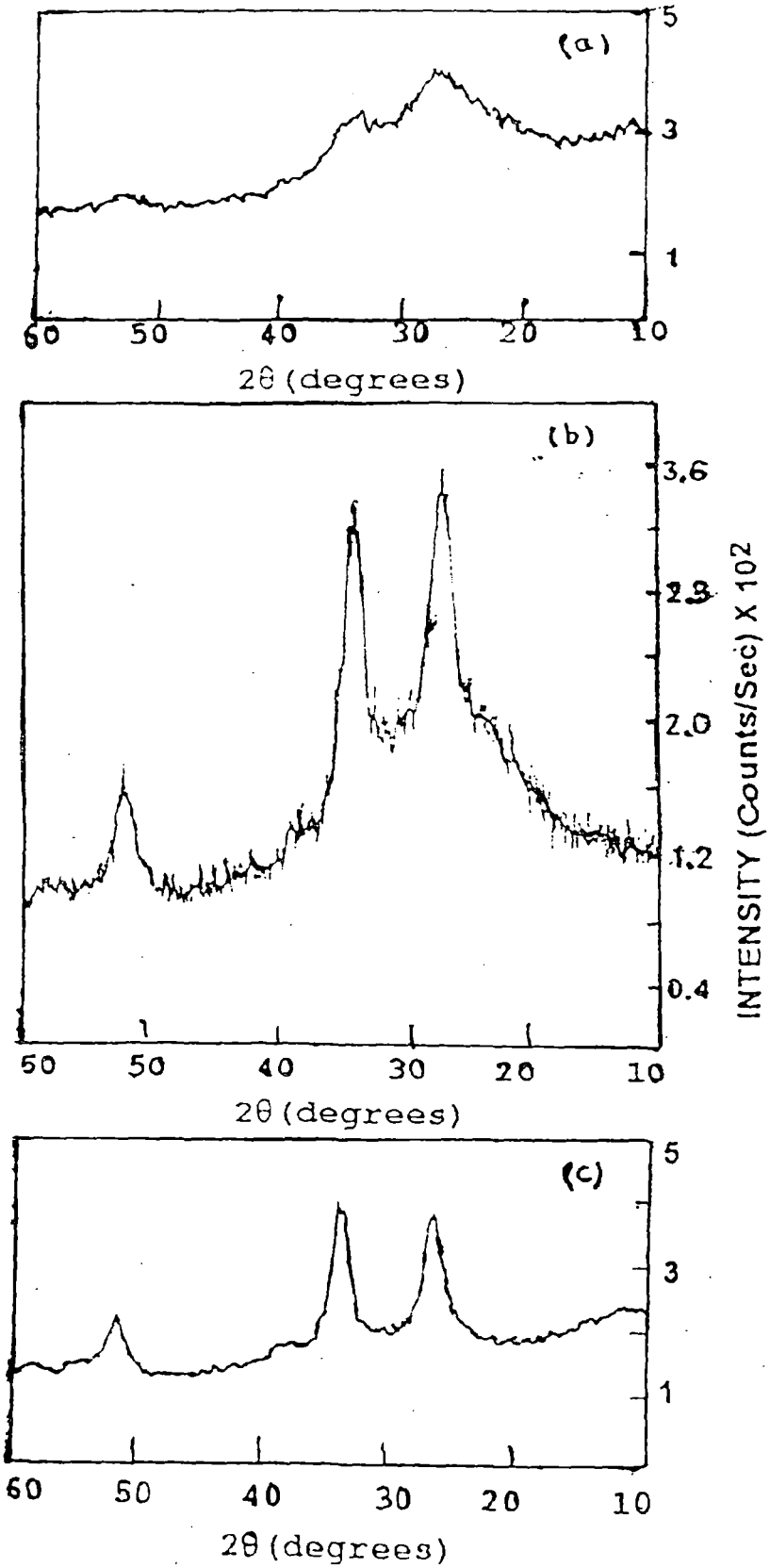

Figure 2.5. X-ray diffractograms of dip coated undoped film on glass substrate (a) 1st dip (b) 5 dip (c) 10 dip

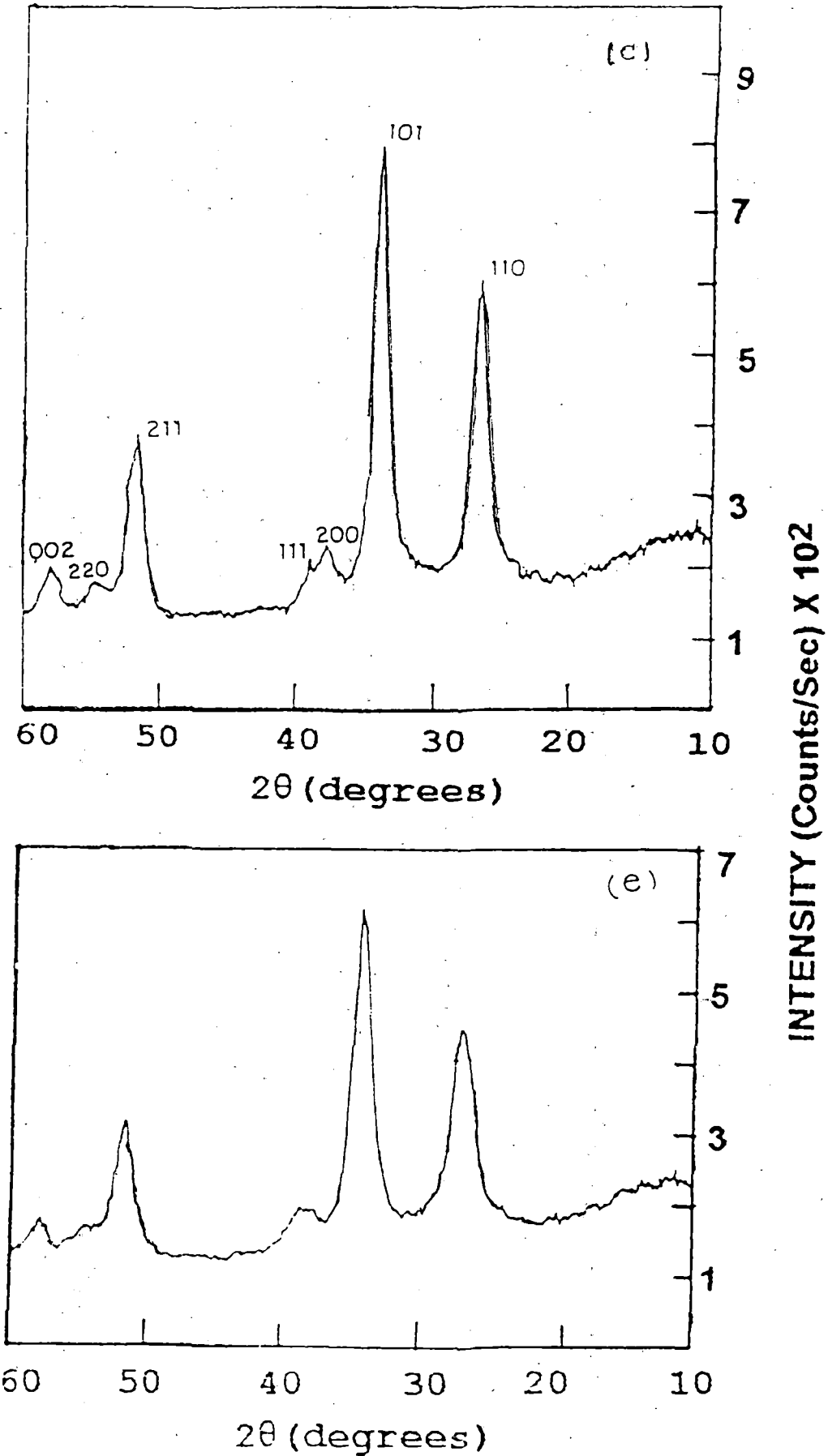

Figure 2.5. X-ray diffractograms of dip coated undoped film on glass substrate (d) 20 dip (e) 25 dip

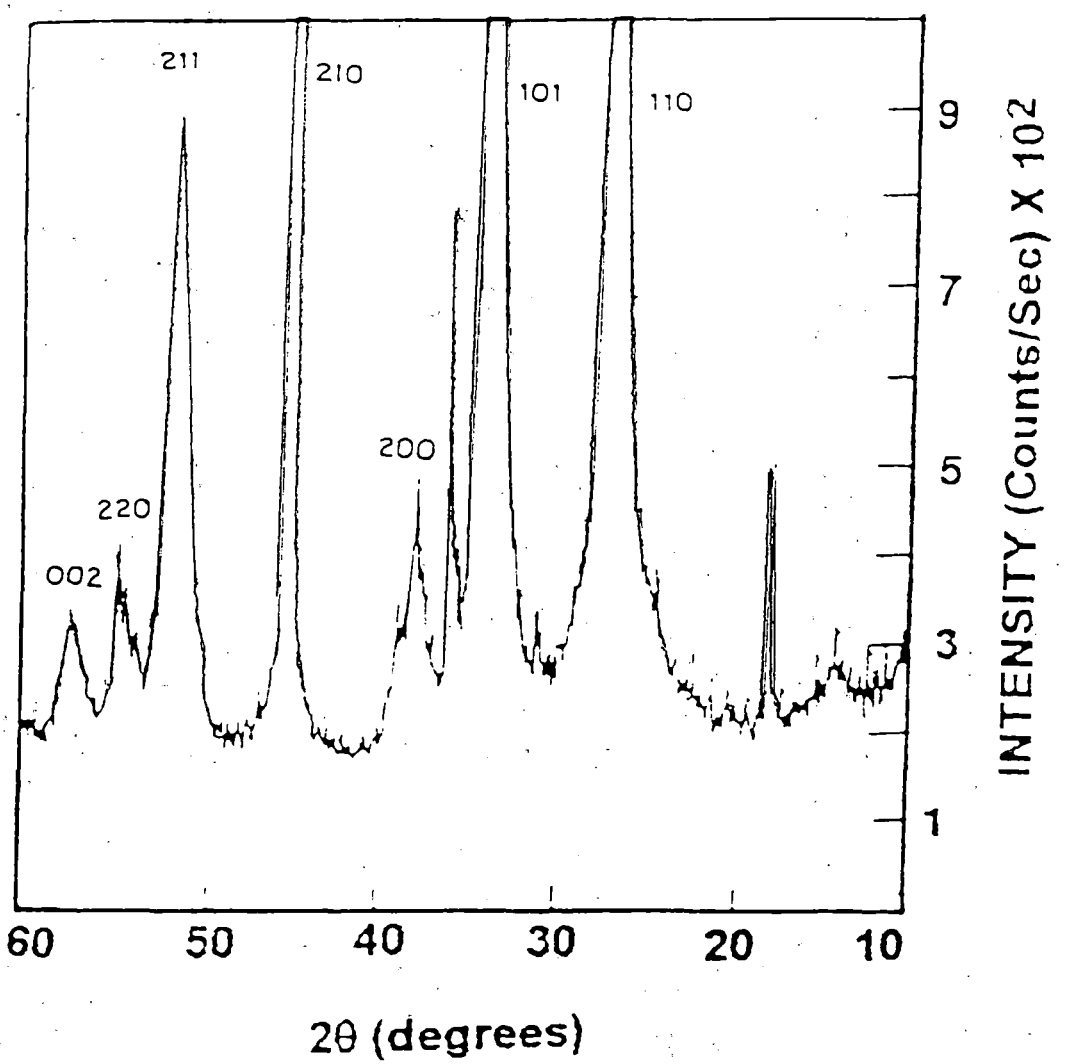

Figure 2.6. X-ray diffractograms of a typical film on mica substrate (10 dip). peaks which are unmarked do not correspond to SnO_2 and probably arises from the substrate itself.

2.4.1.3. ELECTRICAL PROPERTIES

Films of various sheet resistance from 80 - 10^6 Ω/□ could be obtained by varying the concentration of the starting solution, speed of withdrawal and number of dippings. Figure 2.7 shows the variation of sheet resistance of undoped and F-doped films (4.5 at%) with thickness. The sheet resistance was measured by standard four probe arrangement. It is observed from the curves that sheet resistance decreases with the increase in thickness. The lowest value of sheet resistance of undoped and 4.5 at% F-doped films are 300 Ω/□ and 80 Ω/□ respectively for a thickness of 2.96 μm which corresponds to resistivity values of 8.9 x 10^{-2} Ω cm and 2.4 x 10^{-2} Ω cm respectively. It was found that film prepared by single dipping in a high concentration solution has a much higher value of sheet resistance compared to one having the same thickness but prepared by multiple dippings using a lower concentration dip solution. For example, at a thickness of 0.58 μm the sheet resistance of a single dip film was 4 x 10^4 Ω/□, while that prepared by 5 dippings was 8 x 10^3 Ω/□. The possible reason may be that for single dipping, a number of loosely packed crystallites are formed, while for multi-dipping these crystallites formed at every deposition step tend to merge together and produce a continuous conduction path. Support for this argument is obtained from figure 2.7, where the sheet resistance of undoped films is seen to drop sharply at a thickness of about 1 μm. For F-doped films the drop occurs at a thickness of about 0.5 μm.

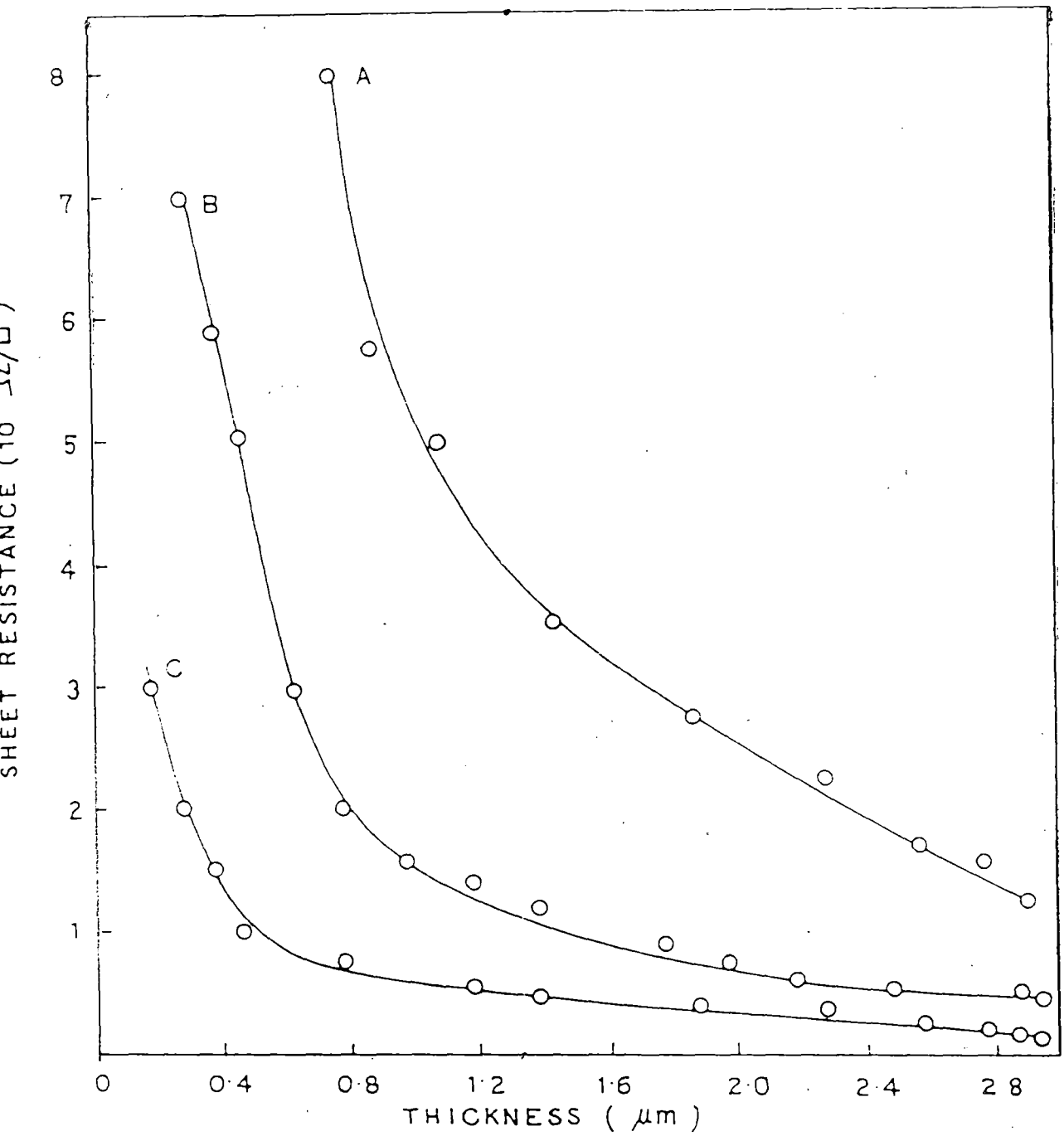

Figure 2.7. Variation of sheet resistance of film deposited on glass substrates with thickness. Undoped: A = 250 gms/litre, B=330 gms/litre and 4.5 at% F-doped: C= 250 gms/litre.

2.4.1.4. SURFACE MORPHOLOGY STUDY BY SEM

Figure 2.8 shows the scanning electron micrograph of undoped and 4.5 at% F-doped film which was studied by HITACHI S-530 scanning electron microscope. It is clear from the micrographs that for the undoped film, grain size increases upto 20 dippings. The initial layer (1st dip) films over an amorphous glass substrate is nearly amorphous, which is evidenced from the XRD pattern also.

Figure 2.9 shows the surface morphology of the films on mica. The grain size is observed to be significantly larger in case of mica substrate than that on glass substrate (Fig. - 2.8.C). The much sharper XRD peaks observed in this case are also consistent with the larger grain size. It is possible that formation of bigger crystallites is facilitated by the single - crystal substrate, which is in contact with the growing film.

2.4.1.5. OPTICAL PROPERTIES

Dip deposited films are highly transparent. Figure 2.10 shows the optical transmission versus wavelength curves for undoped and 4.5 at% F - doped films with different sheet resistance values. These optical transmission data were obtained by SHIMADZU UV-240 double beam spectrophotometer (air reference). It is seen that the optical transmission is reduced as a result of doping. A similar phenomenon has also been observed by chopra et. al. [37] and De et. al. [36] and attributed by them to a high surface roughness of SnO_2 films having low sheet resistance compared to undoped ones. Average optical transmission of 85 % - 90 % for undoped and 75 % - 80 % for doped films are obtained for a thickness of 2.96 μm over a range 400 nm to 800 nm.

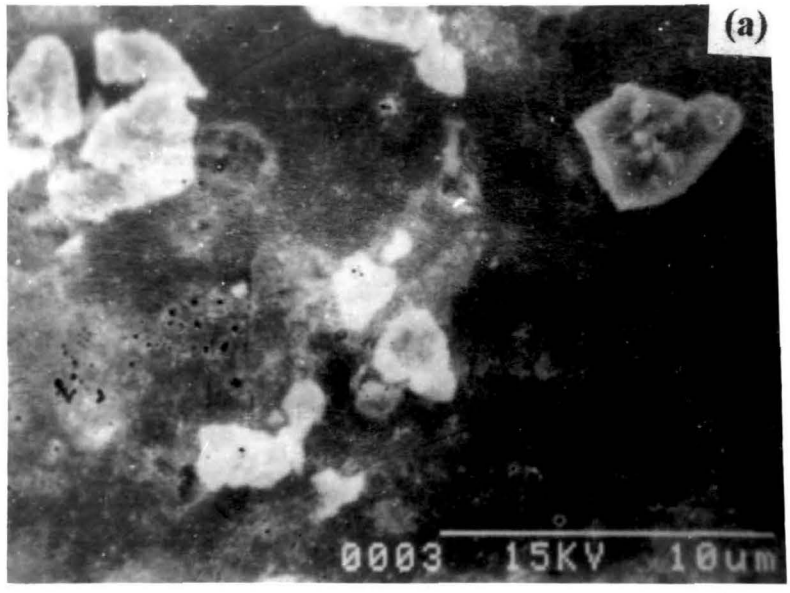

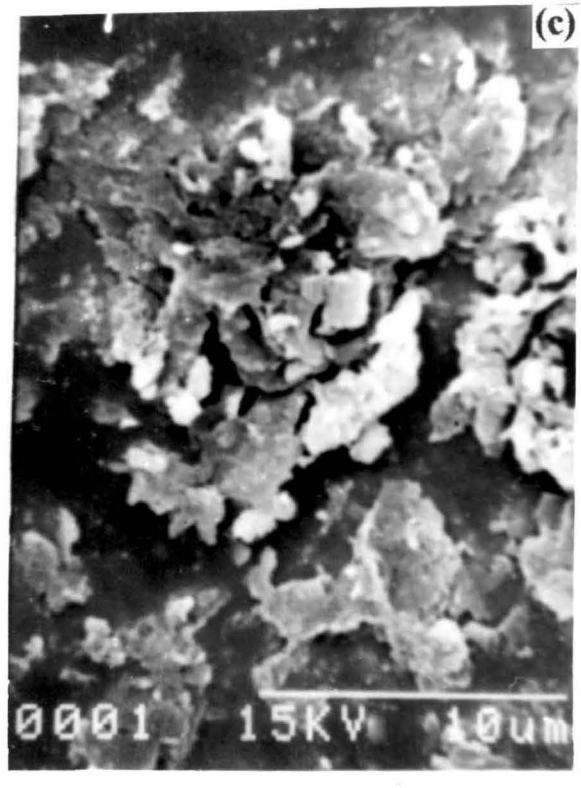

Figure 2.8. Electron micrographs of undoped films on glass substrate undoped: (a) 1st dip, (b) 5 dip, (c) 10 dip.

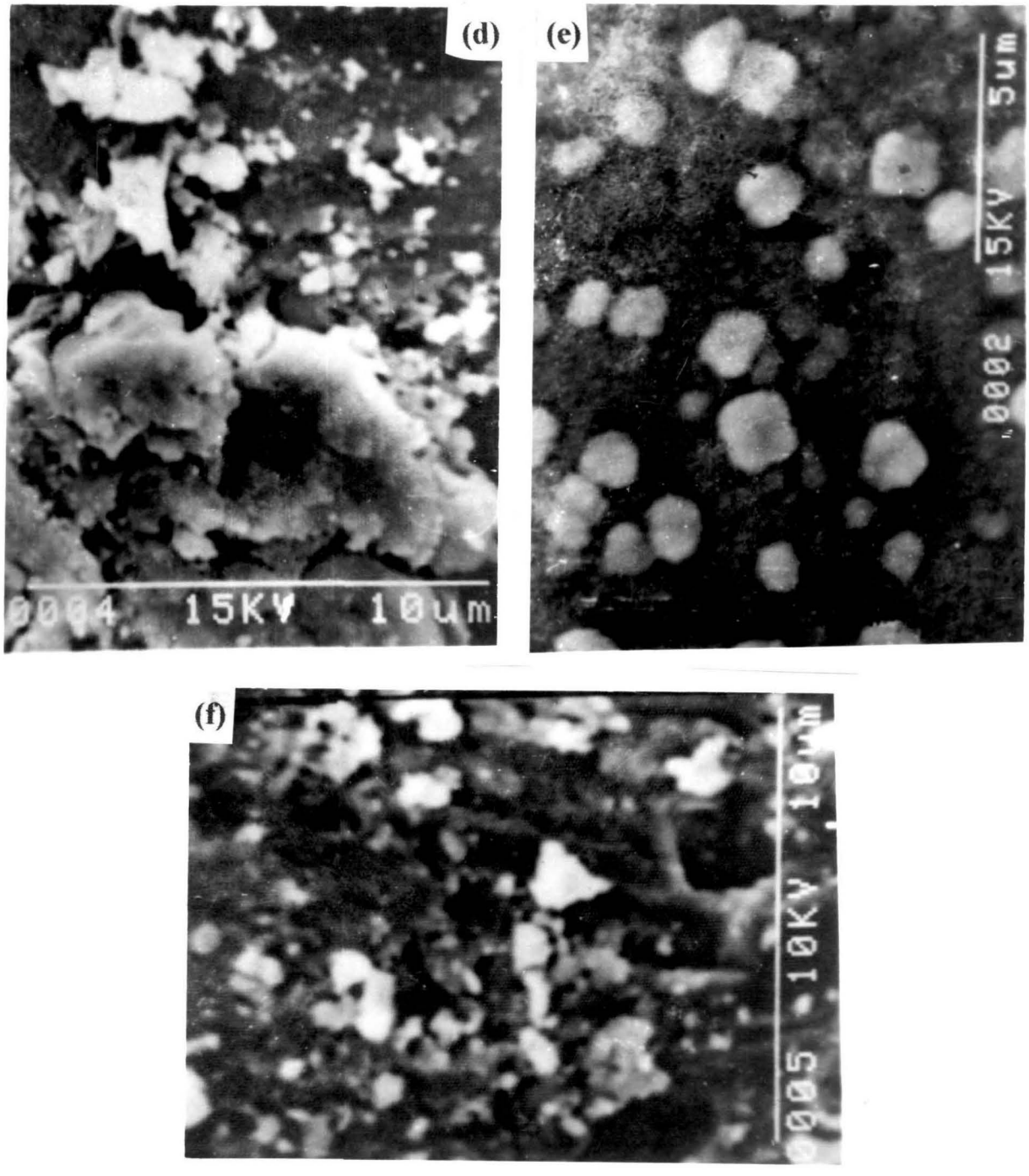

Figure 2.8. Electron micrographs of undoped films on glass substrate undoped: (d) 15 dip, (e) 20 dip, (f) 25 dip.

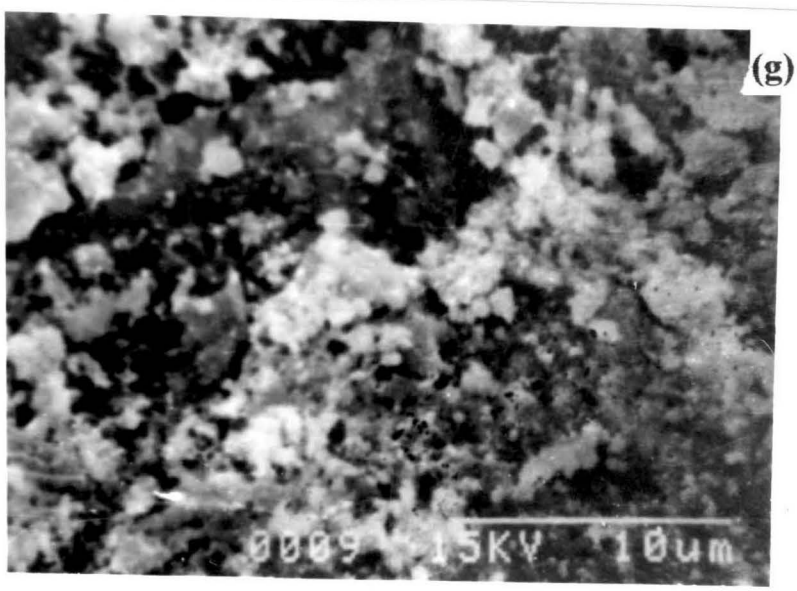

Figure 2.8. Electron micrographs of doped films on glass substrate 4.5 at% F-doped: (g) 20 dip.

Figure 2.8. Electron micrographs of undoped films on mica substrate (10 dip).

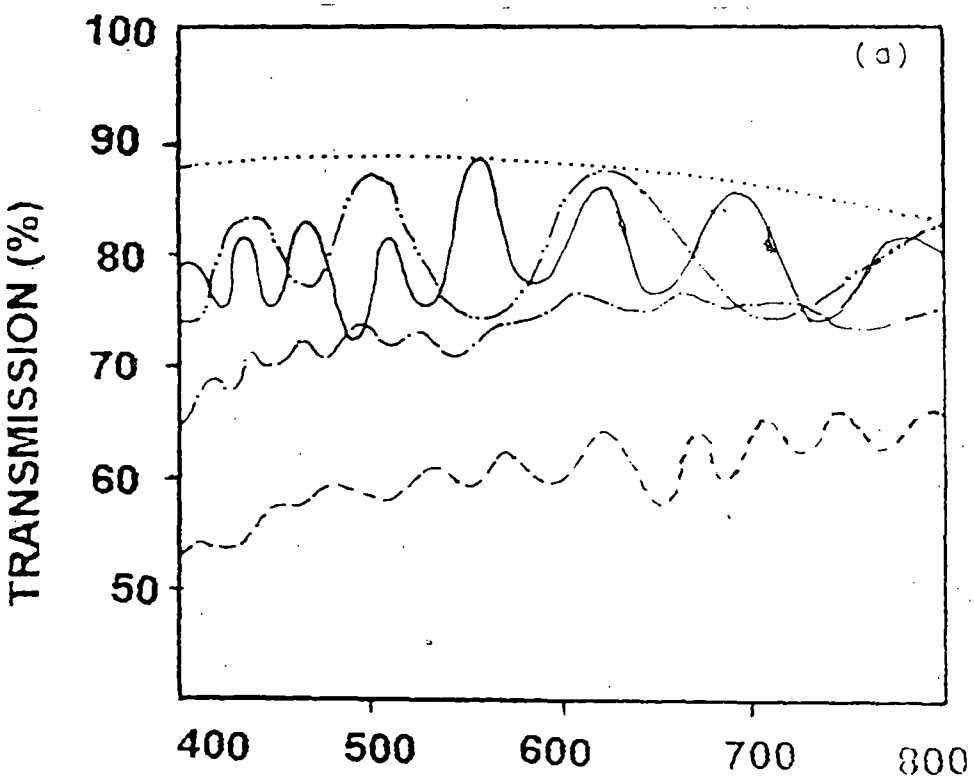

Figure 2.10. Optical transmission versus wavelength for typical films of various sheet resistances (a) Undoped: (.....), bare ubstrate; (_____) 4000 Ω/□; (-..-..-..-) 1250 Ω/□; (-.-.-.-) 600Ω/□; (——) 250 Ω/□.

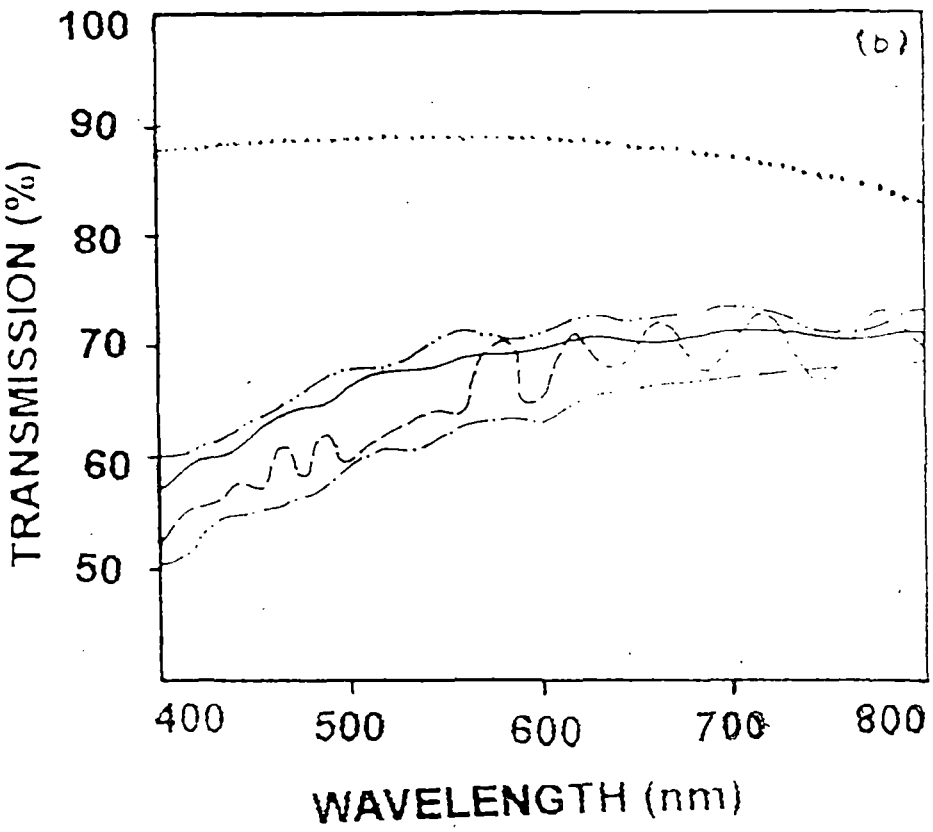

Figure 2.10. Optical transmission versus wavelength for typical films of various sheet resistances (b) 4.5 at% F-doped films:(.....) bare substrate; (_____) 800 Ω/; (-------) 500 Ω/; (-..-..-..-) 200 Ω/; (-.-.-.-) 90 Ω/.

2.4.1.6. DISCUSSION

It is known [38,39] that $SnCl_2$ undergoes hydrolysis in presence of atmospheric oxygen according to the equation

$$6SnCl_2 + H_2O \rightarrow 2SnCl_4 + 4Sn(OH)Cl - - - (2.3)$$

This reaction is relatively slow at room temperature, but is accelerated on heating, $SnCl_4$ in turn, readily hydrolyses to SnO_2 at a high temperature as given below

$$SnCl_4 + 2H_2O \rightarrow SnO_2 + 4HCl - - - (2.4)$$

This forms the basis of preparation of conduction tin dioxide films by the paste-heat or OACVD method [39 & 40, details are given in chapter 4]. In these methods, $SnCl_4$ produced from reaction 2.4 taking place in a separate area is allowed to hydrolyse on the substrate and yield SnO_2 films, which is discuss earlier. In contrast, in the present method the Sn(OH)Cl also remains on the substrate and forms the amorphous matrix, while most of the $SnCl_4$ produced escapes. A small fraction of this $SnCl_4$ however, is hydrolysed on the substrate and produce small SnO_2 crystallites. Repeated dipping increases the number of these crystallites which form a continuous film after about 15-20 dippings. This can be seen from the XRD spectra, the variation of sheet resistance with thickness and the SEM photographs. We see that the sharp drop in sheet resistance, appearance of sharp XRD peaks and merging of SnO_2 grains., all take place at a thickness of about 1 μm. However, even at this stage there is a large amorphous background present., as shown in by the high value of resistivity. viz, 2.4 x 10^{-2} Ω cm compared to 2.4 x 10^{-4} Ω cm for CVD SnO_2 films.It may be interesting to note that in the work of Gordillo et al. [41] also on spray-deposited SnO_2 films, a strong amorphous

background is seen to be present in the XRD pattern when $SnCl_2$ was used as a starting material.

Thus although an amorphous background, most probably Sn(OH)Cl, is present in the films, it is highly transparent and leads to no significant drop in optical transmission. This amorphous background is also responsible for making the resistivity about two orders of magnitude higher than that obtained for CVD films. However, their high optical transmittance makes these films suitable for those display applications where the currents requirement is low, e.g. liquid crystal or electrochromic displays. In addition, the simplicity of the deposition method could make it attractive for enhancing the IR reflectivity at a low cost, e.g. in solar cookers.

The effectiveness of a transparent conducting film depends on its optical transmission as well as its sheet resistance. As already discussed, the high sheet resistance of the dip-deposited films is to a great extent compensated by their large optical transmittance. Haacke [42] has introduced a figure of merit for transparent conducting films defined by the relation $\Phi_{TC} = T^{10}/Rs$, where T is the optical transmittance and Rs is the sheet resistance. This parameter can be used to evaluate the performance of a candidate material from its fundamental parameters. A typical Φ_{TC} value for our 4.5 at% F-doped, dip-deposited film is $2.5 \times 10^{-3}\ \Omega^{-1}$, which compares quite favorably with the value of $2.6 \times 10^{-3}\ \Omega^{-1}$ for CVD SnO_2 films [14, 43].

2.5. COPPER OXIDE (CuO) THIN FILMS BY THE DIP TECHNIQUE

Copper oxide, which is a promising semiconductor material for fabrication of photovoltaic devices like solar cells [44], has been the subject of a number of studies in the past. The investigations carried out concern mainly its growth and optical properties [45-51]. Recently, with the discovery of high temperature superconductivity study of decomposition of CuO/CuO_x employing both metallic and oxide sources has assumed special importance in the preparation of the thin film high temperature superconductors (HTSCS). Thin films of copper oxide have been prepared using various thin film deposition techniques such as chemical vapour deposition, electro-deposition, thermal oxidation and sputtering process [52-54]. Electron - beam evaporation technique also has been reported in the literature for the growth of Cu_2O thin films [45-50].

However, in comparison with other thin films of oxide semiconductors such as In_2O_3, ZnO and SnO_2, few data are available in the literature on the characterization of copper oxide films.

In the following section, preparation of CuO thin films and their structural and optical properties have been discussed.

2.5.1. PREPARATION OF CuO THIN FILM

Methanolic solution of cupric chloride ($CuCl_2.2H_2O$) is taken as a starting solution for the deposition of CuO thin films by the dip technique. The solution was prepared using 0.25 kg cupric chloride in one litre methanol. Cupric chloride ($CuCl_2.2H_2O$) hydrolysed and reacted on the heated substrate inside the furnace at high temperature in open air and formed thin solid films according the following reaction.

$$CuCl_2 + 2H_2O = CuO + 2\,HCl + H_2O \text{ ---------(2.5)}$$

The copper oxide thin films were deposited by the dip technique on glass substrate in atmospheric condition at three baking temperature of 360° C, 400° C and 500° C. The film deposition procedure is same as in the case of SnO_2 film (described in 2.2 section). Films were uniform and black in colour. Films which were characterized had a thickness of the order of one micrometer.

2.5.2. RESULTS AND DISCUSSION

The X-ray diffraction spectra of the CuO films prepared at three baking temperatures are shown in figure 2.11. The relevant diffraction planes are indicated in the spectra. Analysis of diffraction spectra indicates that the peak positions correspond to CuO phase. The films prepared at 360° C show ($\bar{1}11$) and (200) planes whereas films prepared at 400° C and 500° C film show (002) and (111) planes of CuO. Results of peak position observed for the films prepared at three different temperatures and their, comparison with the ASTM data values (file No. 5-661) are given below in the table 2.3.

Table 2.3. ***Comparison of observed value and ASTM data value of CuO thin films deposited by dip technique.***

OBSERVED VALUE			ASTM DATA VALUE			h k l
2θ	d (A°)	(I/Io)	2θ	d (A°)	(I/Io)	
T_B = 360° C						
35.7	2.51	78	35.6	2.52	100	$\bar{1}11$
38.9	2.31	100	38.9	2.31	30	200
T_B = 400° C and T_B = 500° C						
35.3	2.56	78	35.4	2.53	49	002
38.3	2.35	100	38.7	2.32	96	111

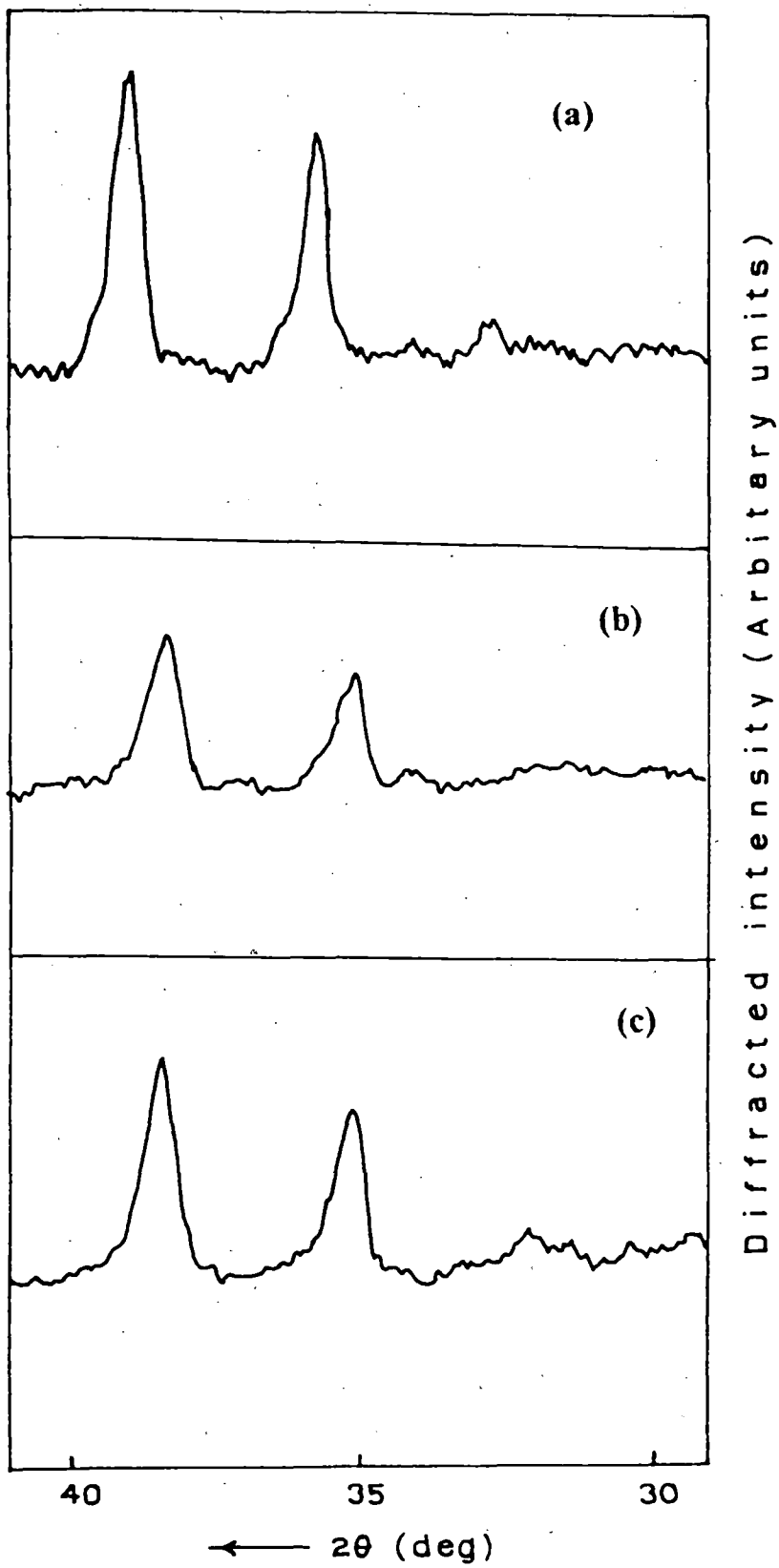

Figure 2.11. X-ray diffractogram of CuO thin films deposited on glass substrate at three different baking temperature [(a), 360° C; (b), 400° C; 500° C].

The optical absorption of the copper oxide thin films was measured using SHIMADZU UV - 240 double beam spectrophotometer in the range 350 - 800 nm. A typical recording for the optical absorption of copper oxide film is shown in figure 2.12. To analyse these results, $(\alpha h\nu)^2$ is plotted against $h\nu$ [Fig. 2.13] and from the intercept of the straight line on the $h\nu$ axis the band gap is estimated. The band gap value thus obtained is about 1.85 eV,which is in good agreement with the value 1.80 eV obtained by Miller et.al. [51].

2.6. CONCLUSION

It has been demonstrated that the dip-coating technique can be used to deposit CuO and SnO_2-based transparent conducting oxide films in a simple manner using metallic chlorides ($SnCl_2.2H_2O$ for SnO_2 and $CuCl_2.2H_2O$ for CuO) as a starting material.

Tin dioxide based transparent conducting films contain crystalline SnO_2 in addition to an amorphous background, probably of Sn(OH)Cl. The resistivity of these films is somewhat higher compared to SnO_2 films prepared by CVD or spray pyrolysis. This is probably due to the presence of the amorphous constituent. However, the films are highly transparent and have a figure of merit value comparable to that for conventionally-prepared SnO_2 films. The films would be potentially useful for low-current application such as display devices.

Copper oxide films are prepared using methanolic solution of cupric chloride ($CuCl_2.2H_2O$) at three baking temperatures. ASTM data confirms that the films are of CuO phase. The optical band gap of the films calculated from optical absorption measurements is 1.85 eV which is quite comparable with the reported value.

Dip technique is a very simple and low-cost method, which requires no Sophisticated specialized setup. Coating of the substrate of a large surface area can be

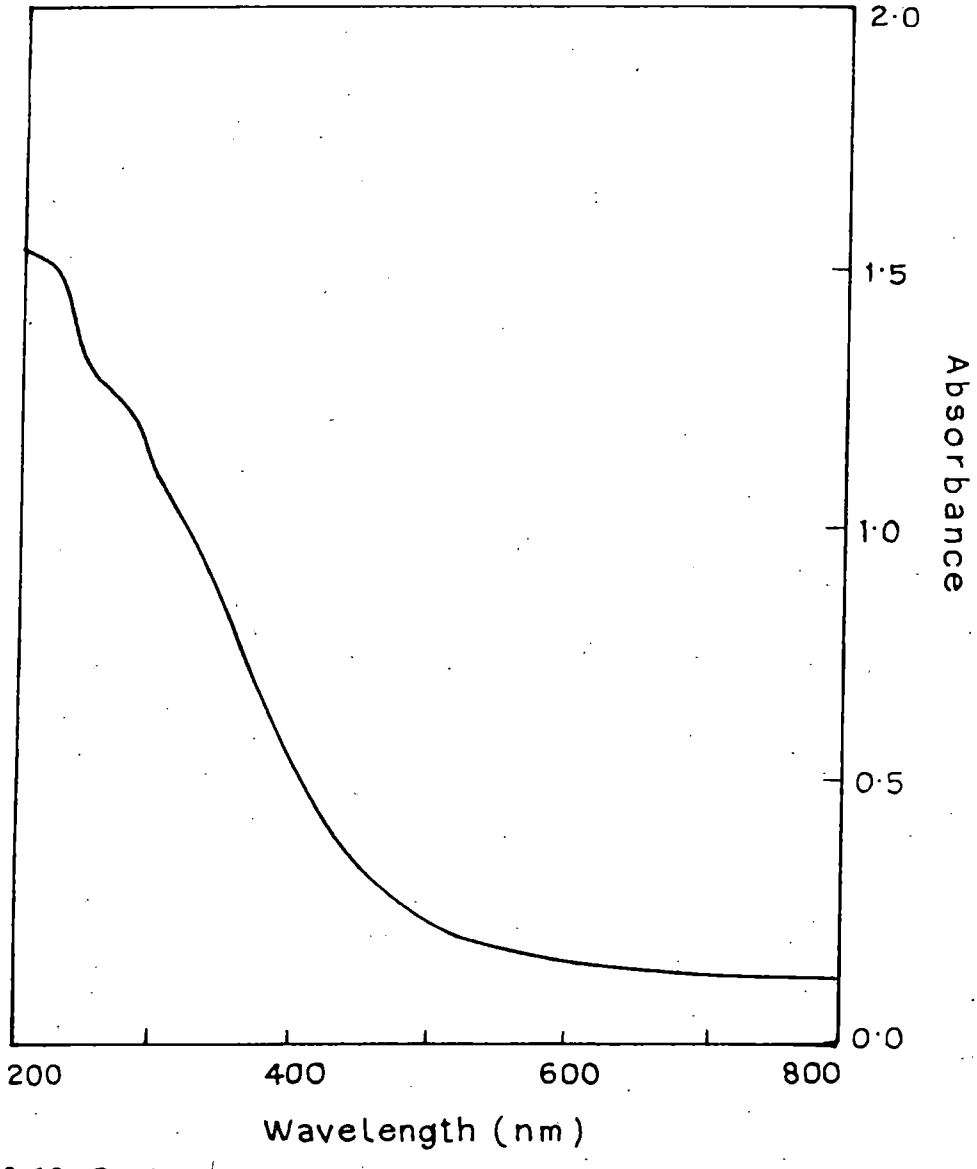

Figure 2.12. Optical absorption spectra of CuO thin films deposited on glass substrate at 400° C.

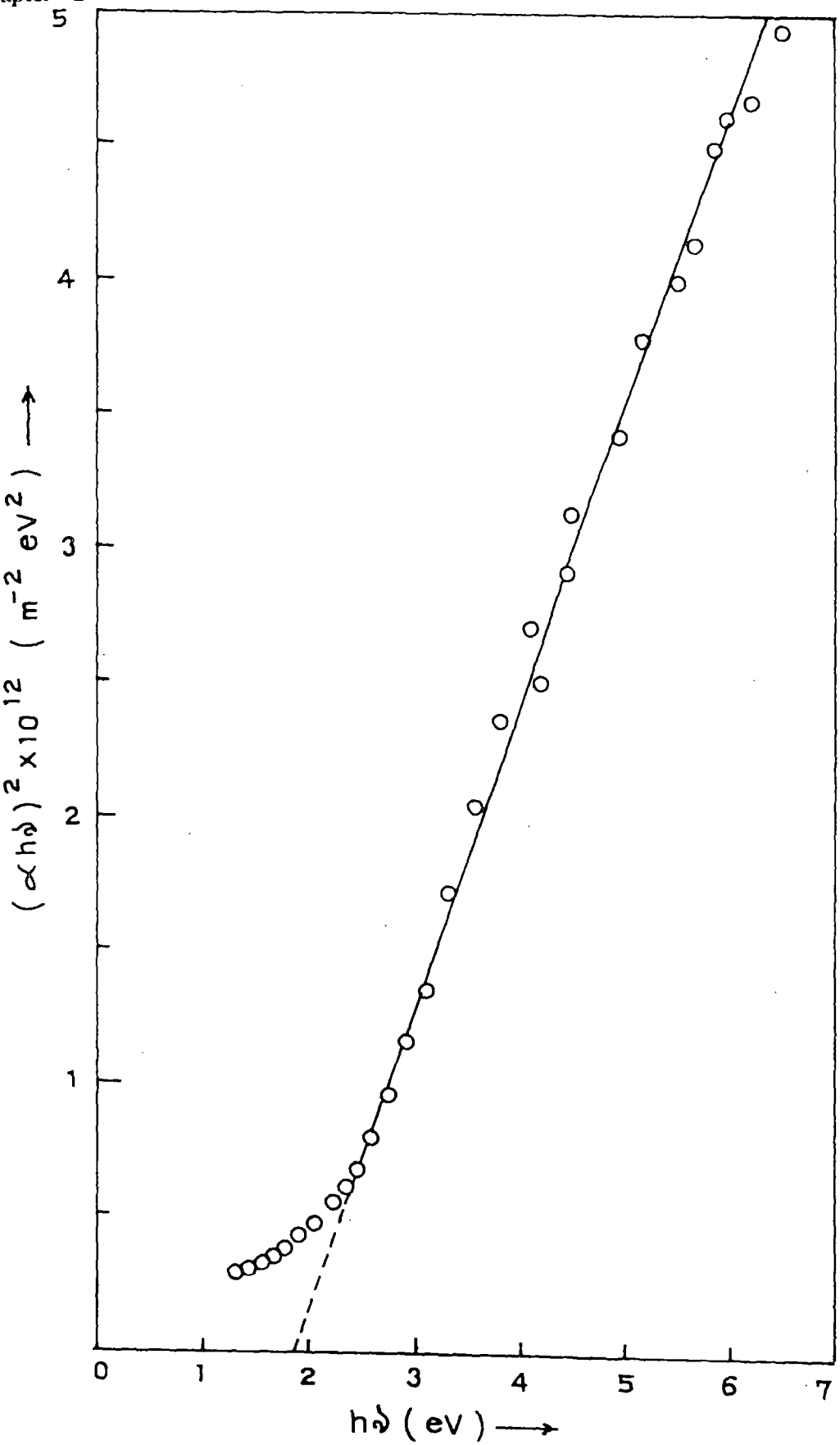

Figure 2.13. Plots of $(\alpha h\nu)^2$ against hν curves for CuO films deposited on glass substrate at 400° C.

easily obtained by this technique compared to that in sputtering, vacuum vapour deposition and spray pyrolysis. Another advantage of the dip technique is that it is very easy to coat both sides of the substrate instead of only one and to deposit otherwise inaccessible surfaces. This method is well suited for applying coating on the inner and outer surfaces of tubes of various diameters and shapes. The main advantage of the dip coating method lies in fact that it is possible to deposit a variety of layers having good homogeneity and mechanical and chemical stability with a very simple setup. Multilayer thin films of different metal oxide layers one after another can be deposited easily by this technique. It should be stressed that both the oxide films produced by the dip technique have been found to be stable after several months observation in laboratory conditions.

REFERENCES:

01. W. Geffcken and E. Berger 1939 *Dtsch. Reichspatent* **736**, 411 **(jenaer glaswerk Schott and Gen., Jena,G.D. R.).**
02. W. Geffcken 1951 *Glastech. Ber.*, **26 (6)** 143-151.
03. H. Schroeder 1962 *Opt. Acta*, **9 (3)** 249.
04. H. Schroeder 1965 *Ins. Glaskonger. Brussel, section* **7.1-7.5**
05. H. Schroeder 1969 *Phys. of thin films* **87-140.**
06. H. Schroeder 1975 *10th Int. Congr. on Glass, Kyoto, Japan* **8.118 - 8.130**.
07. H. Dislich 1971 *Angew. Chem., Int. Ed. Engl.*, **10(6) 363 - 370.**
08. H. Dislich and E. Hussmann 1981 *Thin Solids Films* **77** 129 -131.
09. Sumio Sakka 1985 *Journal of Non-crystalline Solids* **73** 651
10. Prospect Calorex (Trade mark), Jenaer Glaswerk Schoot and Gen., Mainz, 1978.
11. Prospect Glasohne Reflexe, Deutsche spezial glas, Grunenplan, F.R.G.
12. L. E. Scriven 1988 *in: Better ceramics Through Chemistry III ed. C. J. Brinker. D. E. mark and D. R. Ulrich. Matter Res. Soc. Symp.Proc.,* **121** *(Materials Research Society, Pittsburgh)* p.717.
13. L. D. Landau and B. G. Levich 1942 *Acta Physiochim, URSS* **17** 42.
14. J. Kane, H.P. Schweizer and W. Kern 1976 *J. Electrochem. Soc.* **123** 270
15. B. J. Baliga and S. K. Gandhi 1976 *J. electroche. Soc.* **123** 941
16. M. R. Kadam, N. Vittal, R. N. Karckar and R. C. Aiyer 1990 *Thin Solid Films* **187** 199
17. T. P. Chow, M. Ghezzo and B. J. Baliga 1982 *J. Eletrochem. Soc.* **129** 1040
18. J. P. Upadhyay, S. R. Vishwakarma and H. C. Prasad 1989 *Thin Solid Films* **169** 195

19. A. Rohatgi, T. R. Viverito and L. H. Slack 1974 *J. Am. Ceram. Soc.* **57** 57

20. H. Kim and H. A. Laitinen 1975 J. Am. Ceram. Soc. **58** 23

21. E. Shanthi, A. Banerjee, V. Dutta and K. L. Chopra 1980 *J. Appl. Phys.* **51** 6243

22. E. Shanthi, A. Banerjee, V. Dutta and K. L. Chopra 1980 *J. Appl. Phys.* **53** 1615

23. U. R. Chaudhuri, K. Ramkumar and M. Satyan 1990 *J. Phys. D: Appl. Phys.* **23** 994

24. H. Watanabe,1970 *Jpn. J. Appl. Phys.* **9** 1551

25. T. Matsuoka, J. Kuwatov, M. Nishikawa, Y. Fujita, T. tohda and A. Abe 1988 *Jpn. J. Appl. Phys.* **27** 1088

26. H. W. Lehmann and R. Widmer 1975 *Thin Solid Films* **27** 359

27. J. L. Vossen and E. S. Polimiak 1972 *Thin Solid FIlms* **13** 281

28. A. Czapla, E. Kusior and M. Bucko 1989 *Thin Solid Films* **182** 15

29. J. P. Chatelon, C. Terrier, E. Bernstein, R. Berjoan and J. A. Roger 1994 *Thin Solid Films* **247** 162

30. C. Terrier, J. P. Chatelon, R. Berjoan and J. A. Roger 1995 *Thin Solid Films* **263** 37

31. C. J. Brinker, A. J. Hurd, P. R. Schunk, G. C. Frye and C. S. Ashley 1992 *J. Non-Crystalline Solids* **147 & 148** 424

32. Y. Takahashi and Y. Wada 1990 *J. Electrochem. Soc.* **137** 267

33. D. E. Carlson 1975 *J. Electrochem. Soc.* **122** 1334

34. M. K. Karanjai and D. DasGupta 1987 *Thin Solid Films* **155** 309

35. James Proscia and Roy G. Gordon 1992 *Thin Solid Films* **214** 175

36. A. De and S. Ray 1991 *J. Phys. D: Appl. Phys.* **24** 719

37. K.L. Chopra, S. Major and D. K. Pandya 1983 *Thin Solid Films* **102** 1-46

38. Partington J. R. 1950 *A text-book of Inorganic Chemistry 6th edn. (London-Macmillan)* P. 829

39. M. K. Karanjai and D. DasGupta 1988 *J. Phys. D: Appl. phys.* **21** 356

40. Sekhar C. Ray, M. K. Karanjai and D. DasGupta 1997 *Thin Solid Films* **307** 322.

41. G. Gordillo, L. C. Moreno, W. de la Cruz, P. Teheran 1994 T*hin Solid Films* **252** 61

42. G. Haacke 1976 *J. Appl. Phys.* **47** 4086

43. J. Kane, H. P Schweizer and W. Kern 1975 *J. Electrochemcal Soc.* **122** 1144

44. R. Lange, Photoelements and their applications, Reinhold, New York 1939.

45. J. H. Ho and R. W. Vook 1977 *Phtlos Mag.*, **36** 105.

46. C. H. Tsiranovits, J. G. Antonopoulos and J. Stoemenos 1980 *Thin Solid Films* **71** 133.

47. G. B. Marchwicka, L. K. Stepniewska and M. Slaby 1982 *Thin Solid Films* **88** 33.

48. A. E. Rakhshani 1986 *Solid State Electron.* **29** 7.

49. M. E. Abu-zeid, A. E. Rakhshani, A. A. Al-jassor and Y. A. Youssef 1986 *Phys Status Solidi A* **93** 613.

50. K. Santra, C. K. Sarkar, M. K. Mukherjee and B. Ghosh 1992 *Thin Solid Films* **213** 226.

51. D. J. Miller, J. D. Hettinger, R.P. Chiarello and H. K. Kim 1992 *J. Mater. Res.* 7 2828.

52. M. Fujinaka and A. A. Berezin 1983 *J. Appl. Phys.* **54** 3582.

53. H. Wieder and A. W. Czanderna 1962 *J. Phys. Chem.* **66** 816.

54. Cathcart, Petersen and Sparks 1969 *J. Electrochem. Soc.* **116** 664.

CHAPTER - 3

*Sulphide thin films prepared by the dip technique

3. INTRODUCTION

Sulphide thin films are extensively used for the fabrication of a number of solid state devices such as solar cells, photoconductive cells, electroluminescent cells, Schottky diode, thin film transistors etc. A large variety of deposition techniques (discussed in chapter 1) have been used for the preparation of these films. Efforts are under way to develop simple and low-cost methods for the deposition of sulphide films for use in various device applications, especially in solar cells.

Results obtained under various deposition conditions are by no means unique. Different workers have reported different results even under similar deposition conditions.

The dip technique is a simple method for the deposition of device-quality sulphide films. This technique is traditionally used for deposition of oxide films as described in chapter 2, where a solution of corresponding metal chloride in an organic solvent is used as the starting solution. In case of sulphide film preparation, it has been observed that simple addition of a suitable sulphur containing compound to the starting solution prepared originally for the oxide film deposition results in a good quality sulphide film.

In this chapter, we describe the deposition of a number of binary and ternary sulphide films by the dip technique and their characterisation.

*3.1. $Zn_xCd_{1-x}S$ THIN FILMS

3.1.1. INTRODUCTION

Ternary sulphide compounds are some of the most promising man-made materials since they yield new possibilities for tailoring physical properties. Among them the wide band-gap II-VI compound semiconductors have found application in optoelectronic devices. There have been attempts to introduce $Zn_xCd_{1-x}S$ alloy layers instead of CdS for obtaining specific band structure and optical properties [1] for use in solar cells.

These films have been widely used as a wide bandgap window material in heterojunction photovoltaic solar cells [2-7], and in photoconductive devices [8]. In solar cell systems, where CdS thin films have been proved to be useful, partial substitution of Zn for Cd increases the optical window of the heterojunction and also the diffusion potential [9]. Moreover, in heterojunction solar cells using $CuGaSe_2$, use of $Zn_xCd_{1-x}S$ instead of CdS can lead to an increase in photocurrent by providing a match in the electron affinities of the two materials. This hexagonal $Zn_xCd_{1-x}S$ ternary compound is also potentially useful as a window material for fabrication of p-n junctions without lattice mismatch in the devices based on quaternary materials like $CuIn_xGa_{1-x}Se_2$ [10] or $CuIn(S_zSe_{1-z})_2$ [11].

Zn $_xCd_{1-x}S$ thin films have been prepared by a variety of techniques, which include vacuum evaporation [12-13], spray pyrolysis [14-16], rf sputtering [17], solution growth [18-19] and sublimation growth [20]. Metal-organic vapour-phase epitaxy (MOVPE) [21] and molecular-beam epitaxy (MBE) [22] have been recently applied to prepare these films for the fabrication of efficient light-emitting devices.

---

* **Published in the "journal of Thin Solid Films" Vol. 322/1-2 (1998) P. 117-122.**

Ion-beam deposition method makes it possible to fabricate high-quality ZnCdS films at a low substrate temperature without interdiffusion in multilayers and heterojunction devices [23, 25].

As discussed previously (chapter 2), the dip technique and the related sol-gel method have been traditionally used for the deposition of oxide thin films [26-27]. Usually these involve the hydrolysis of the corresponding metal alkoxide, nitrate or chloride on a heated substrate. Previous workers [28] reported a modification of the dip technique for deposition of sulphide films. In this method the substrate is withdrawn from an alcoholic solution of the metal nitrate and thiourea, and with the liquid layer adhering to it, transferred to a furnace maintained at a high temperature. A chemical reaction then takes place on the substrate to yield the solid sulphide films.

As described in ref. [28], attempts to produce $Cd_{0.8}Zn_{0.2}S$ films using a starting solution containing both cadmium and zinc nitrates resulted in the formation of a mixed phase material containing partially crystalline CdS and amorphous ZnS when prepared at a baking temperature of 400° C and baking time (B_T) five minutes. We have found that by increasing the baking temperature to 500° C (B_T = 5 minutes) homogeneous crystalline $Zn_xCd_{1-x}S$ films within the range $0 \leq x \leq 0.6$ could be produced. These films show a continuous variation of lattice parameter and bandgap as a function of atomic fraction x within the range $0 \leq x \leq 0.6$. For $x > 0.6$, the films tend to develop an amorphous character, but the optical properties are not affected and the bandgap varies monotonically from 2.3eV (CdS) to 2.69 eV ($Zn_{0.6}Cd_{0.4}S$) over the range $0 \leq x \leq 0.6$. In this chapter, the preparation of these films and their characterization by x-ray diffractometry, scanning electron microscopy, optical and photoconductivity measurments have been described.

3.1.2. EXPERIMENTAL DETAILS

3.1.2.1. SOLUTION PREPARATION

Three separate saturated solutions of cadmium nitrate [$Cd(NO_3)_2$, $4H_2O2$], zincnitrate [$Zn(NO_3)_2$, $6H_2O$] and thiourea with methanol as solvent were initially prepared. The concentrations are 0.8 kg/litre, 1.0 kg/litre and 0.1 kg/litre respectively. They were then mixed in requisite amounts to prepare the starting solution for deposition of sulphide films. It was observed that the mixing was best achieved without any precipitation taking place if the thiourea solution was initially divided into two parts which were mixed with the two nitrate solutions separately, and finally one of the mixtures slowly added to the other.

3.1.2.2. FILM FORMING PROCESS

Microscope glass-slides were usually used as a substrate. These were cleaned by washing in detergent solution and chromic acid and finally degreased in acetone and methanol vapour. The film forming process is exactly the same as described in chapter 2 for oxide films, which involves dipping of the substrate in the starting solution, its withdrawal at a controlled speed and transfer to a furnace for baking for almost 5 minutes. The chemical reactions for CdS and ZnS films are as follows.

$$Zn(NO_3)_2 + (NH_2)_2CS = ZnS + CO_2 + 2H_2O + 2N_2O \text{ ---------- (3.1)}$$

$$Cd(NO_3)_2 + (NH_2)_2CS = CdS + CO_2 + 2H_2O + 2N_2O \text{ ---------- (3.2)}$$

The minimum baking temperature required for the deposition of a solid films was found to be 300° C. It was observed that single phase crystalline films of a very high quality were obtained when prepared at a baking temperature of 500° C for five

minutes baking time. Thickness of the films could be increased by repeating the whole cycle (dip-withdrawal-bake) a number of times. All the films reported here were baked for a fixed baking time of five minutes within the furnace under atmospheric conditions.

3.1.3. RESULTS AND DISCUSSION

$Zn_xCd_{1-x}S$ films were deposited at 500° C for various concentrations of Zn from x = 0 to x = 1. The value of x was changed by changing the relative concentrations of Zn - nitrate and Cd - nitrate in the starting solution. The $Zn_xCd_{1-x}S$ thin films were smooth, highly uniform, reflecting and strongly adherent to the substrate. Colour of the films was observed to change from yellow-orange to pale yellow with increase in zinc atomic fraction x. Zinc sulphide films (x=1) were white in colour while cadmium sulphide films (x=0) were orange-yellow in colour. Characterization of the films was carried out by optical absorption, X-ray diffractometry, scanning microscopy and spectral response of photo conductivity measurements. Results reported in this chapter were obtained by measurements on films prepared by 10 dippings (dip-withdrawal-bake cycle) from a starting solution containing total 0.93 (Cd + Zn) moles per litre and withdrawn at a speed of 1.33 mm/sec and baked at 500° C for five minutes.

The Zn/Cd ratio in the solid films was determined by Atomic Absorption Spectroscopy. The value of x was found to be essentially the same as the relative proportion of Zn atoms [Zn:(Zn+Cd)] in the starting solution.

3.1.3.1. FILM THICKNESS

Films of different thickness were obtained by changing the lifting speed as well as increasing the number of dippings (dip-withdrawal-bake cycle), keeping the concentration of the solution fixed. Smooth and uniform films could be obtained upto a maximum withdrawal speed of 1.33 mm / sec. For higher speeds, the films tended to be non-uniform. As discussed in chapter 2, at high withdrawal speeds the liquid layer adhering to the substrate, as it is pulled out is quite thick, and turbulence in this layer is also higher. Film thickness was measured by stylus method using α step as described in chapter 2.

Figure 3.1 shows the variation of the thickness of the films for different values of x, when the total number of (Cd + Zn) moles were kept constant in a given volume of the starting solution. It shows that the thickness of the films decreased linearly with the increase in zinc proportion.

3.1.3.2. X-RAY DIFFRACTOMETRIC STUDY

X-ray diffractometry studies were carried out by PHILIPS diffractometer (model PW 1390) with CuK_{α} radiation (Ni-filter) at 1.54 Å. Figure 3.2 shows the XRD patterns of the $Zn_xCd_{1-x}S$ films (x=0.2) deposited at three baking temperatures T_B = 400° C, 500° C and 600° C. It is clear from the diffractograms that the $Zn_xCd_{1-x}S$ films deposited at a baking temperature of 500°C is hexagonal in structure where as that deposited at 400° C is a mixed phase, containing crystalline CdS (cubic) and amorphous ZnS, with a prominent peak at $2\theta = 26.87°$ (d-value 3.32 Å) coresponding to (111) plane of CdS. No prominent peaks were observed in the film deposited at a baking temperature of 600° C.

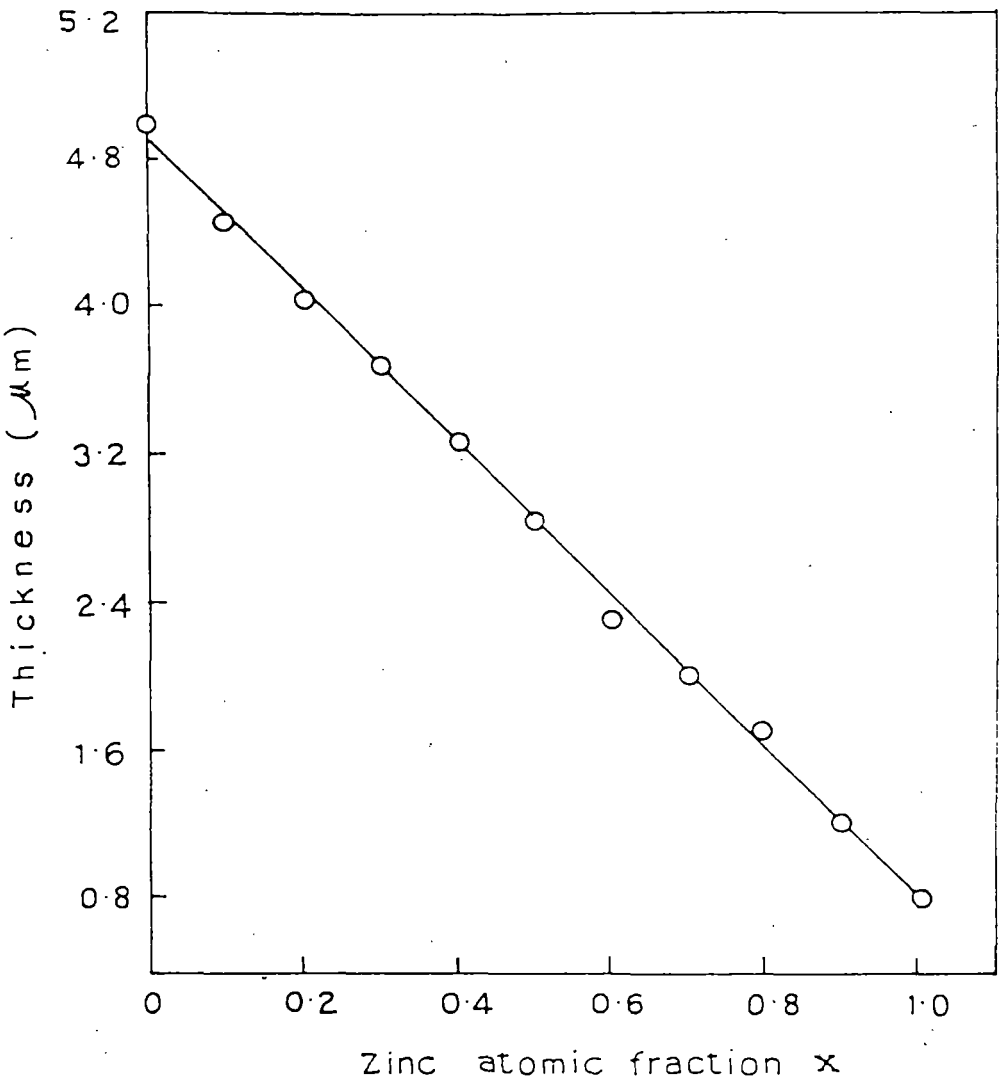

Figure 3.1. Variation of thickness on zinc atomic fraction x of $Zn_xCd_{1-x}S$ thin films ($T_B = 500^o$ C).

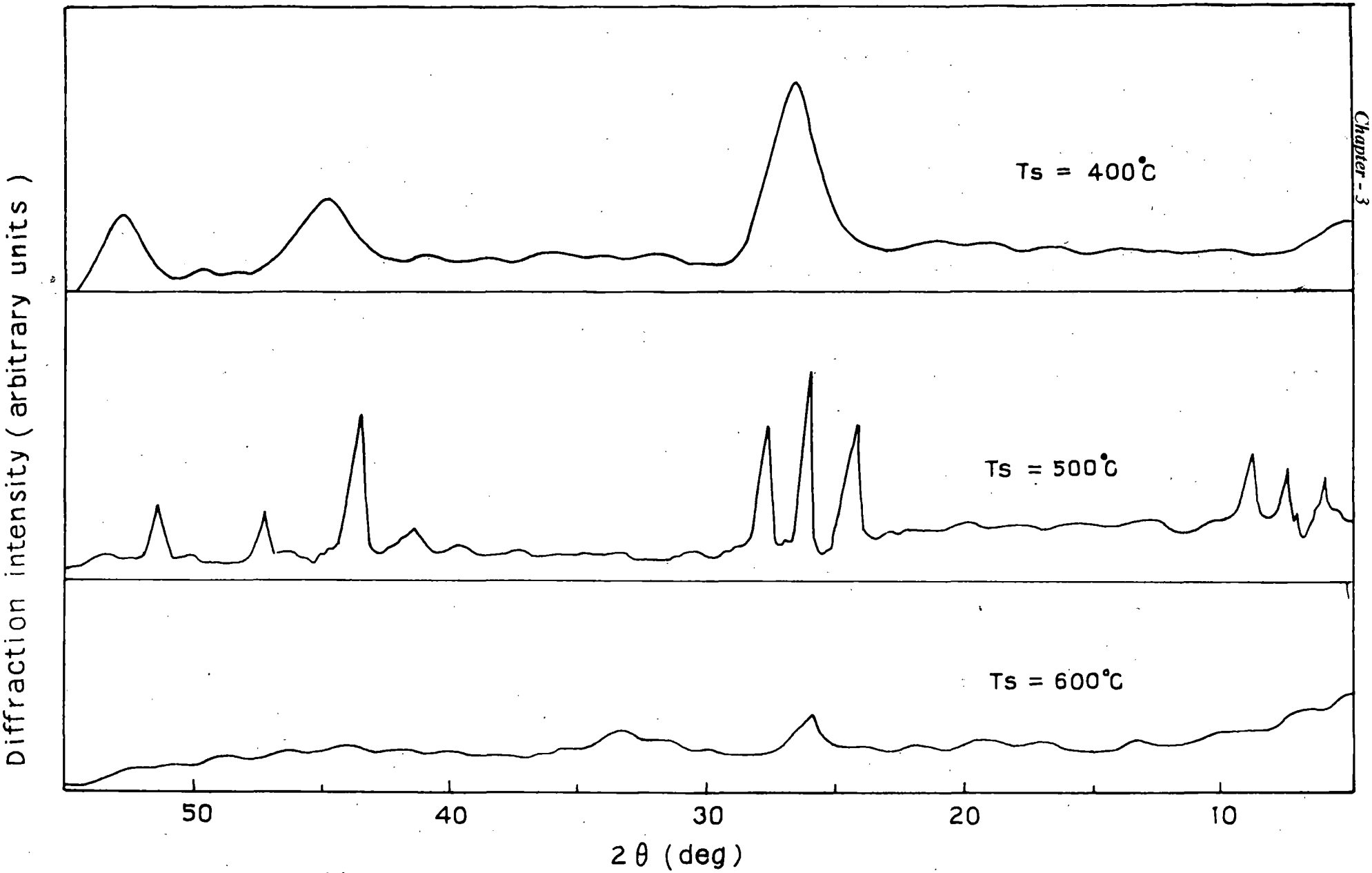

Figure 3.2. X-ray diffractograms of $Zn_xCd_{1-x}S$ (x = 0.2) thin films at various baking temperatures (T_B = 400° C, 500° C, 600° C).

As films with best crystalline properties were obtained for a baking temperature 500° C and a baking time of five minutes, these films were chosen for further detailed study of their properties as a function of atomic fraction x.

In the compositional range $0 \leq x \leq 1$, the crystal structure of the $Zn_xCd_{1-x}S$ films have been determined from x-ray diffraction patterns. The analysis established the presence of hexagonal structure of the polycrystalline $Zn_xCd_{1-x}S$ films in the range $0 \leq x \leq 0.6$. Films with composition corresponding to $x > 0.6$ was found to be nearly amorphous in nature.

A typical XRD pattern for $Zn_xCd_{1-x}S$ (for $x=0.4$) films is shown in figure 3.3. Comparison of the prominent peak position (2θ–value) of the XRD spectra with the JCPDS data file for CdS [29] suggests that the $Zn_xCd_{1-x}S$ film deposited at a baking temperature of 500° C is hexagonal (wurtzite) in structure with the prominent x-ray diffraction peaks corresponding to (100), (002), (101), (110) and (103) planes.

It is observed that the diffraction angle (2θ) shifts to higher angles with increasing zinc atomic fraction x. The peaks, which are quite sharp upto $x = 0.4$, become weaker beyond this and no prominent peaks appear for $x > 0.6$, which means that in this range the films are mostly amorphous.

The diffraction angle shifts towards higher angles with an increase in the composition parameter x, which means that the lattice constant decreases with x. The relationship between the lattice parameter and the zinc atomic fraction x over the range $0 \leq x \leq 0.6$ is shown in figure 3.4. It was observed that the lattice constant decreases with increase in the proportion of Zn. This is consistent with the smaller size of the Zn atoms and also reflected in the decrease in thickness of the films with increasing x as described in section 3.3.1. Similar results were obtained by Yamaquchi et al. [30]. The values of a and c for thin film prepared at $x = 0$ (pure CdS) are 4.13 Å and 6.73 Å respectively. These values are in good agreement with the data for hexagonal CdS films from the JCPDS card [29].

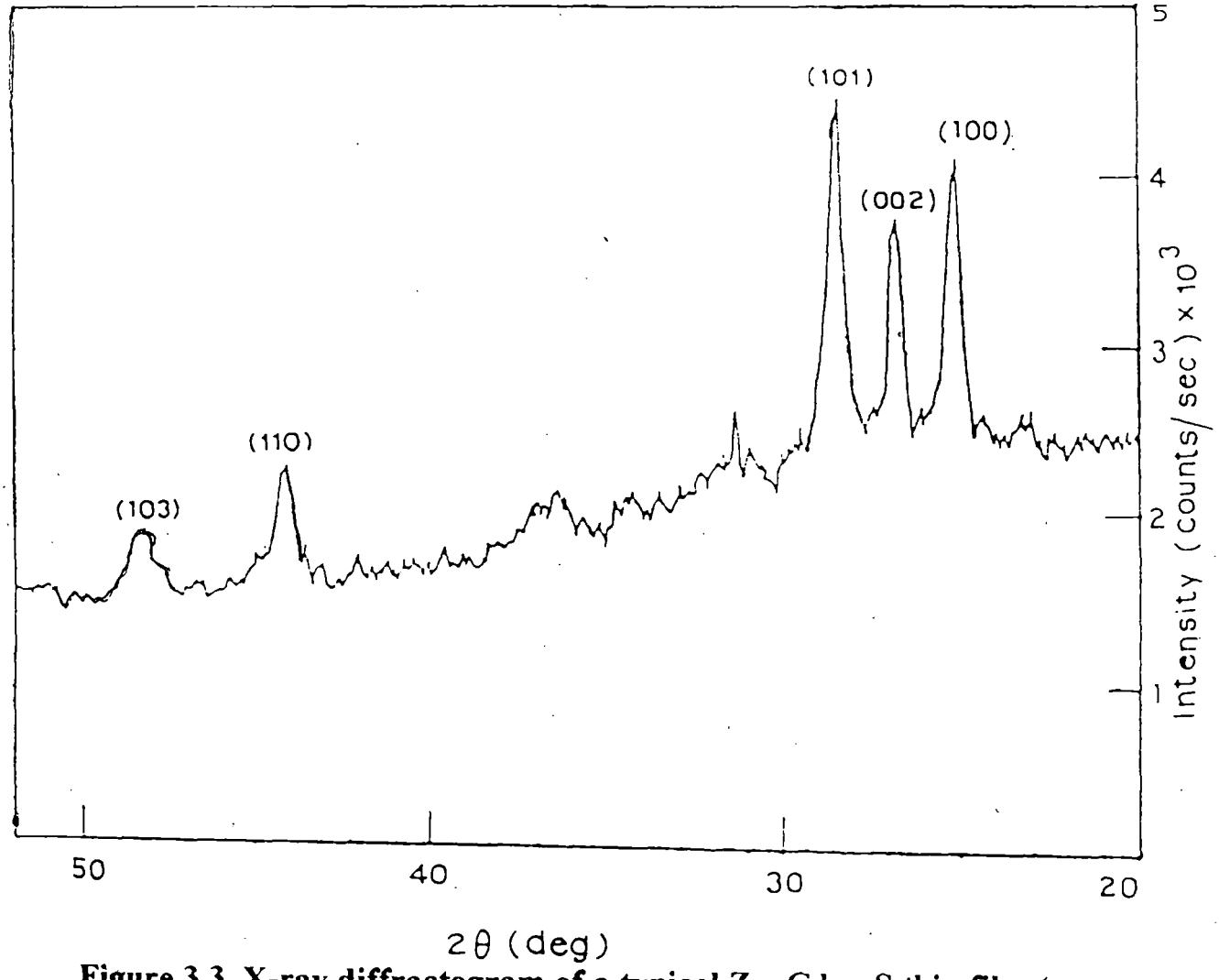

Figure 3.3. X-ray diffractogram of a typical $Zn_xCd_{1-x}S$ thin film (x= 0.4) deposited on glass substrate at 500° C.

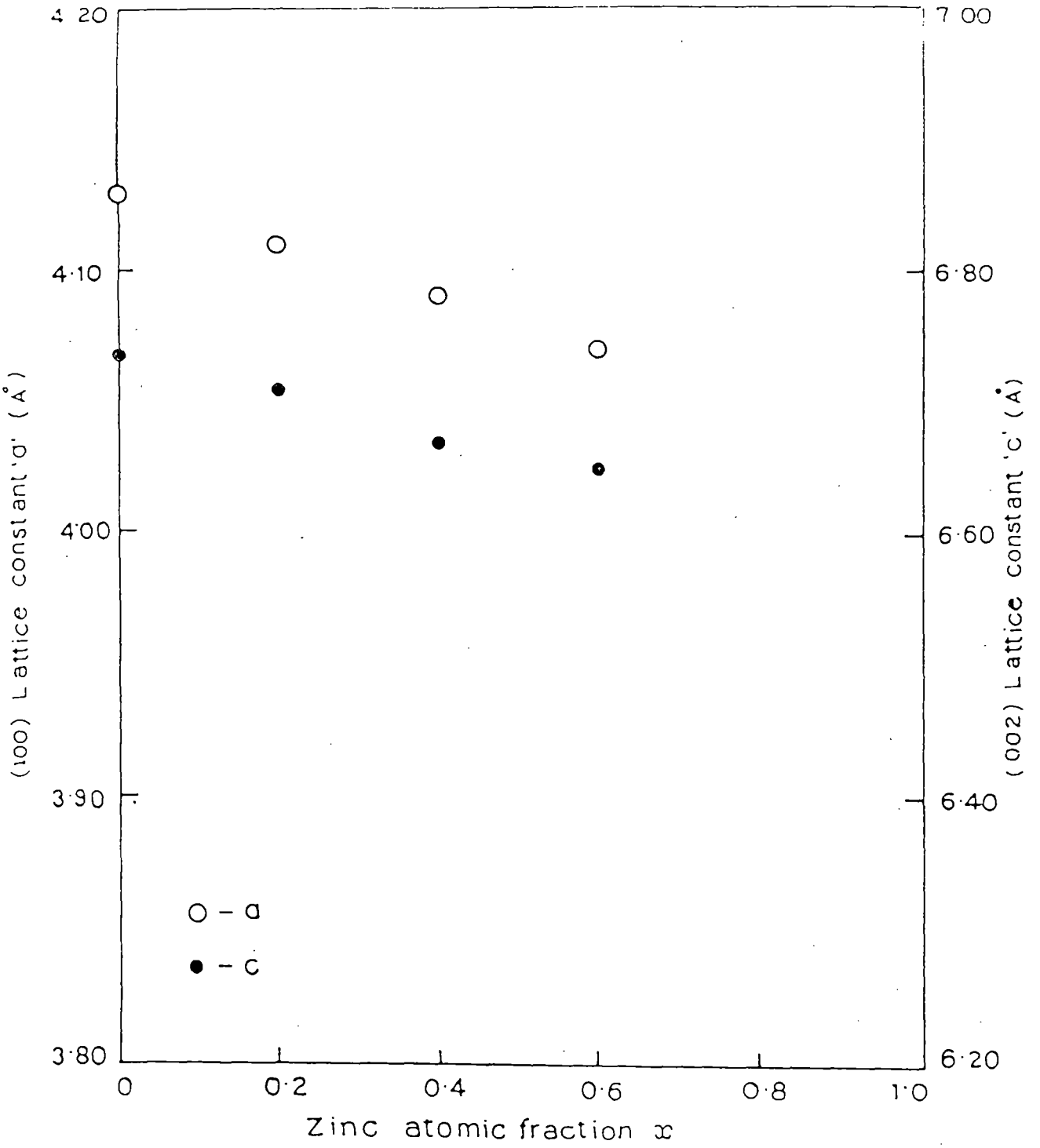

Figure 3.4. Dependence of the lattice constants *c* and *a* on zinc atomic fraction x.

X-ray diffraction of a typical $Zn_xCd_{1-x}S$ film (x= 0.4) deposited at a baking temperature of 500° C upon a dip-deposited polycrystalline CdS film with hexagonal structure is shown in figure 3.5. The underlying CdS thin film of thickness ~ 0.3 μ was deposited initially by the dip technique on crystalline tin-dioxide transparent conducting substrate at a temperature of 500° C. The top layer of $Zn_xCd_{1-x}S$ film (x=0.4) of thickness 0.9 μ was deposited on the CdS. The deposited film is also has a much and more pronounced peak, indicating a higher order of crystallinity and is also hexagonal in structure with preffered orientation along (002) plane.

3.1.3.3. OPTICAL PROPERTIES

3.1.3.3.1. Optical absorption

Optical properties were studied by SHIMADZU UV-240 double-beam spectrophotometer. Optical absorption spectra of $Zn_xCd_{1-x}S$ ($0 \leq x \leq 1$) thin films deposited on glass substrates were obtained in the range 350 nm - 600 nm. (Fig.3.6). The spectra were taken with respect to the bare substrate placed in the reference beam. The absorption edges are quite sharp, indicating that the films are uniform and homogeneous, and these move towards shorter wavelength with increasing Zn atomic fraction x corresponding to increasing bandgap of the material. The optical energy gap (E_g) of the $Zn_xCd_{1-x}S$ thin film was estimated by measuring optical density (O.D) of the films as a function of wavelength in the range 2.2 eV to 3.5 eV, from which absorption co-efficient (α) was obtained. Plots of $(\alpha h\nu)^2$ and $(\alpha h\nu)^{1/2}$ against $h\nu$ were made (Figure 3.7). $(\alpha h\nu)^2$ versus $h\nu$ plots yielded straight line over the range $0 \leq x \leq 0.6$. In contrast, for $x > 0.6$ straight lines were obtained when $(\alpha h\nu)^{1/2}$ was plotted against $h\nu$. This is indicative of the fact that the film are crystalline for $0 \leq x \leq 0.6$ and amorphous beyond this range. The bandgap of hexagonal $Zn_xCd_{1-x}S$ films obtained for the range $0 \leq x \leq 0.6$, using the curve

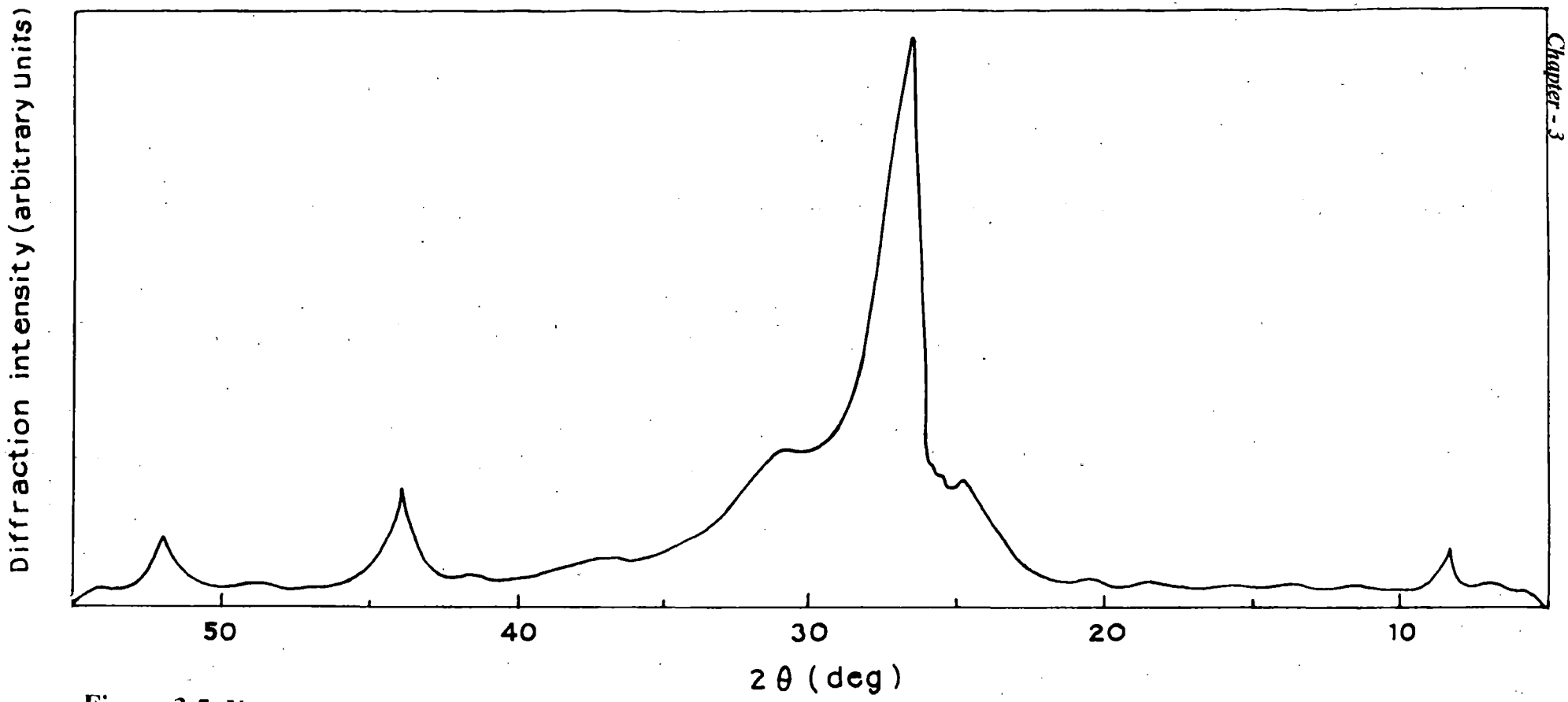

Figure 3.5. X-ray diffractogram of a typical $Zn_xCd_{1-x}S$ thin film (x= 0.4) deposited on a polycrystalline SnO_2-CdS film a 500° C.

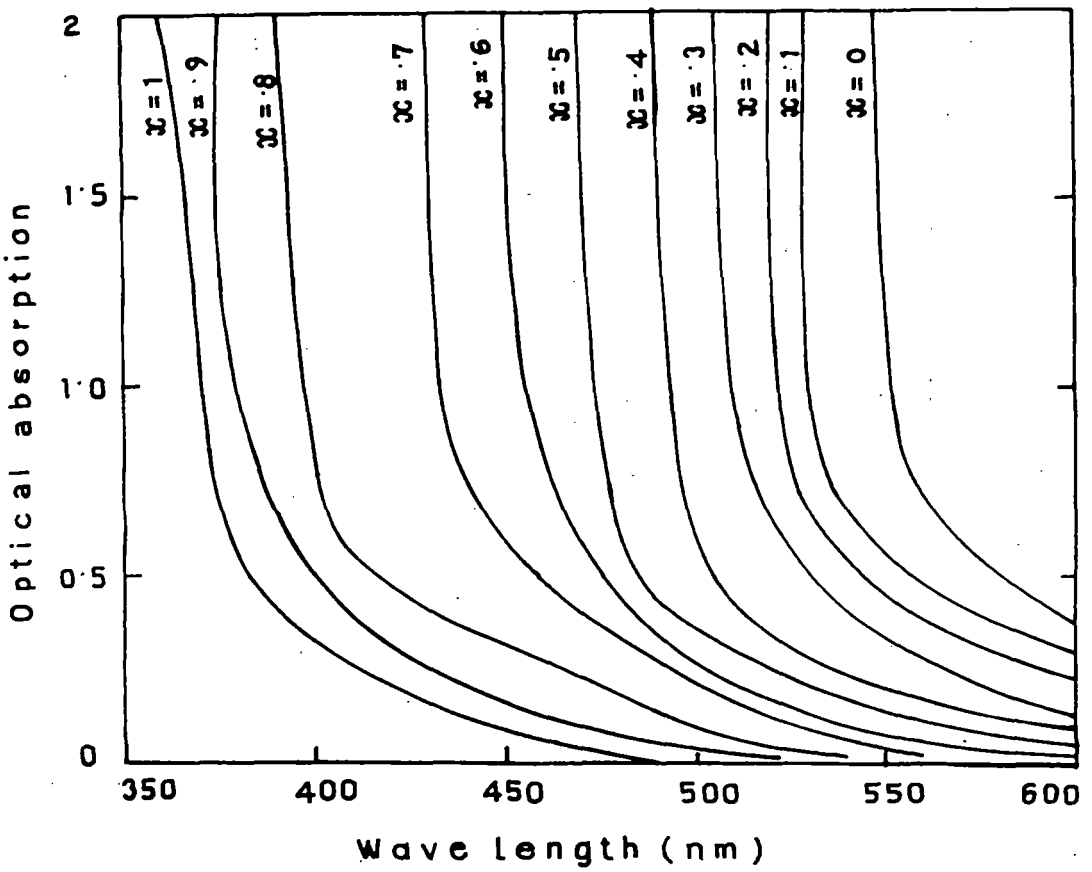

Figure 3.6. Optical absorption spectra of $Zn_xCd_{1-x}S$ ($0 \leq x \leq 1$) thin films.

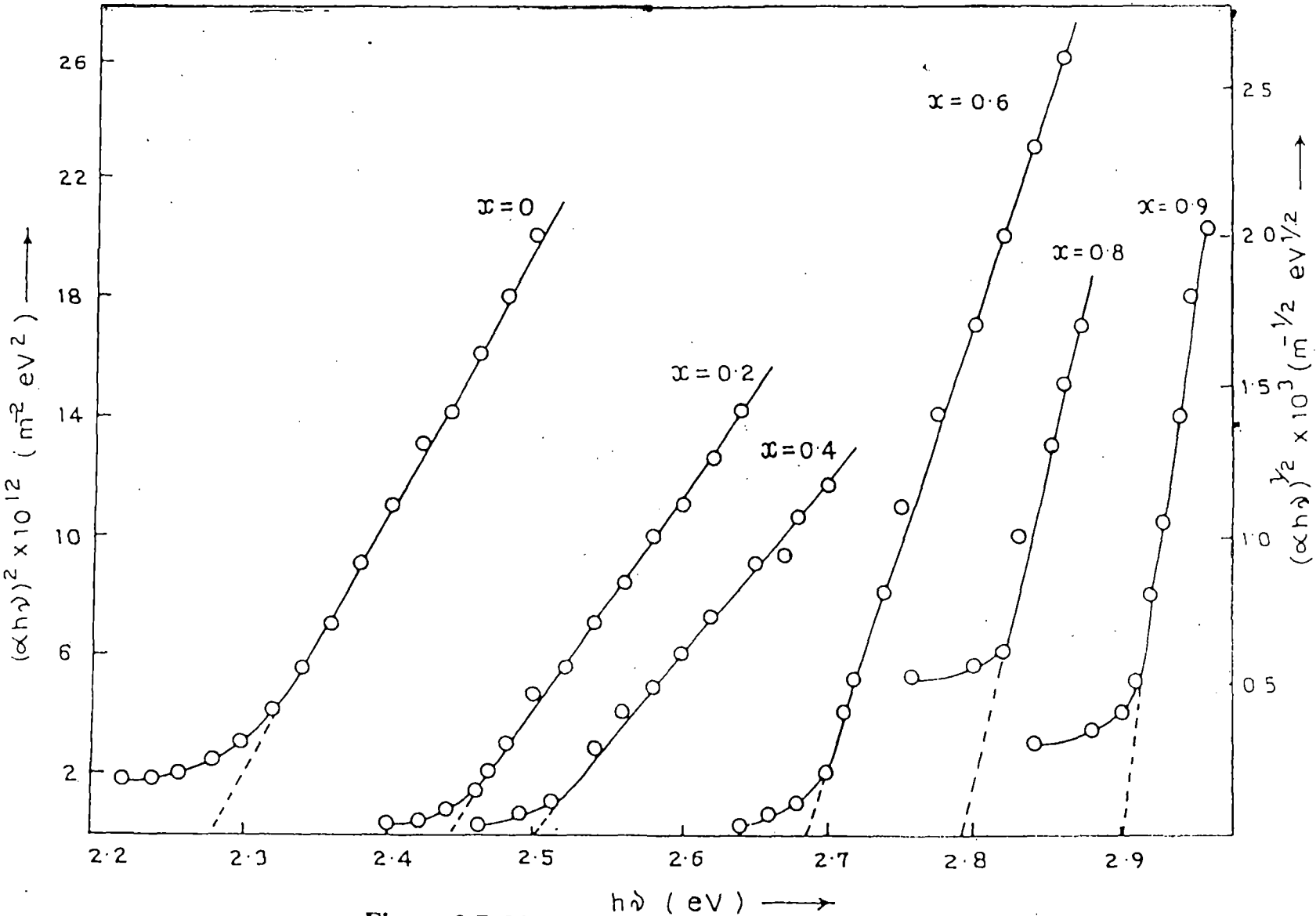

Figure 3.7. Plots of $(\alpha h\nu)^2$ and $(\alpha h\nu)^{1/2}$ against hν curves for $Zn_xCd_{1-x}S$ ($0 \le x \le 1$) thin films.

$(\alpha h\nu)^2$ versus $h\nu$ are in good agreement with other bandgap data obtained from the films deposited by spray pyrolysis [31] or Electron Beam Epitaxy [32].

In the above α was estimated by the following relation.

$$\alpha = \frac{(2.303)X(O.D)}{d} \text{--------(3.3)}$$

where 'd' is the film thickness and O.D. is the optical density, which was converted into transmittance according to the relation given below.

$$O.D. = \log_{10}\left(\frac{I_o}{I}\right) \text{--------(3.4)}$$

and

$$T = \frac{I}{I_o} \text{--------(3.5)}$$

Where I_0 is the intensity of light incident on the film and I is that transmitted beam.

3.1.3.3.2. Spectral response of photoconductivity

To determine the photoconductive (PC) spectral response, a PC cell was fabricated by depositing Ag-electrodes in the usual interdigitated (comb-like) pattern, which was subsequently placed at the detector position of a SPECTROMOM 202 spectrophotometer, and the photocurrent was measured as function of wavelength. The area of the cell was about one square cm. It is known that deposition of Ag after ionic bombardment at high vacuum as was done in this case, produces an ohmic contact with the underlying surface. The pattern of the cell as well as the circuit used for measurement of photocurrent is shown in figure 3.8.

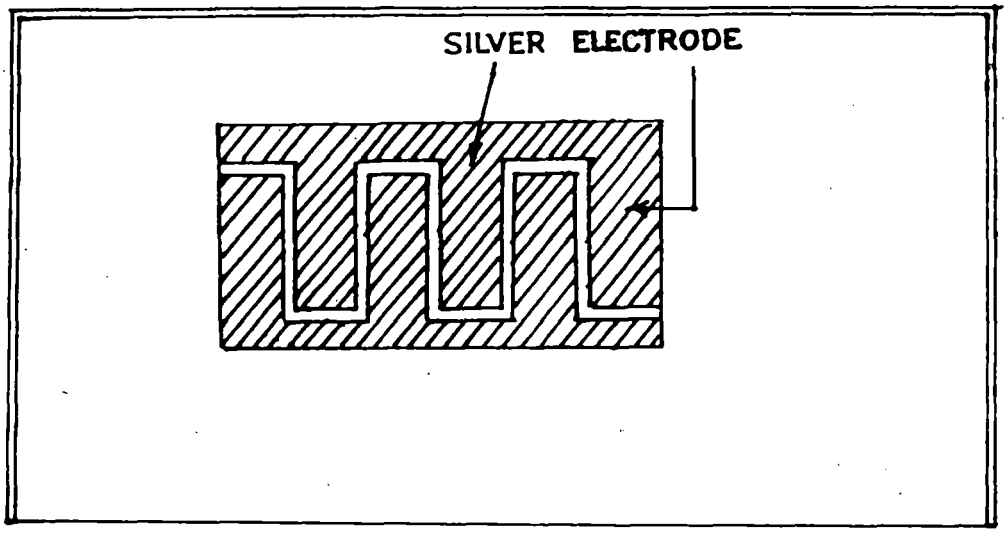

(a)

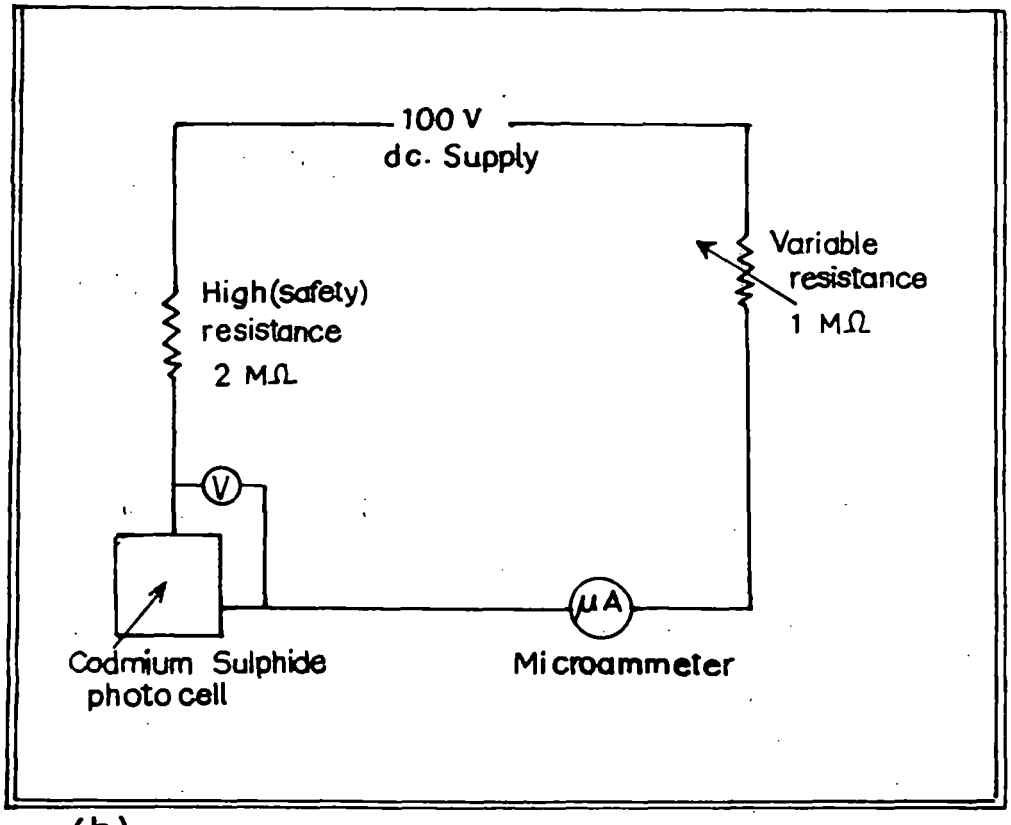

(b)

Figure 3.8. Pattern of the cell and circuit diagram for measurement of photocurrent.

Spectral response of photoconductivity curves are shown in figure 3.9. The photocurrent values are normalized with the peak response for pure CdS taken as 1. No correction was made for the variation of intensity with wavelength of the tungsten filament source used in the spectrophotometer. With increasing x, position of the maximum moves from 540 nm for CdS to 360 nm for ZnS, corresponding to a shift in bandgap from 2.3 eV to 3.4 eV. This continuous change in bandgap with increasing proportion of zinc again confirms the formation of a solid solution.

Figure 3.10 shows the variation with x of (i) bandgap for $0 \leq x \leq 0.6$, (ii) optical gap for $x > 0.6$, and (iii) the photon energy $0 \leq x \leq 1$ at which peak response in photoconductivity is obtained. Curves (i) and (iii) agree quite closely in the range $0 \leq x \leq 0.6$, where crystalline films were obtained. The optical bandgap for $x > 0.6$ are much less than that obtained from photoconductive measurements, which may be due to the amorphous nature of the films in the region.

According to H. Hill [33], the optical bandgap E_x of $Zn_xCd_{1-x}S$ which is a ternary alloy film, can be expressed as

$$E_{(x)} = E_{CdS} + (E_{ZnS} - E_{CdS} - b)x + bx^2 \quad ---(3.6)$$

where b is the bowing parameter and x is the Zn atomic fraction. The value of b for films is about 0.22 eV, estimated from curve fitting with the values of optical bandgap in the range $0 \leq x \leq 0.6$. This value is very close agreement with theory as obtained by Hill [33]. For $x > 0.6$ the value of b changes sharply to 0.07, again indicating a transition from crystalline to amorohous films.

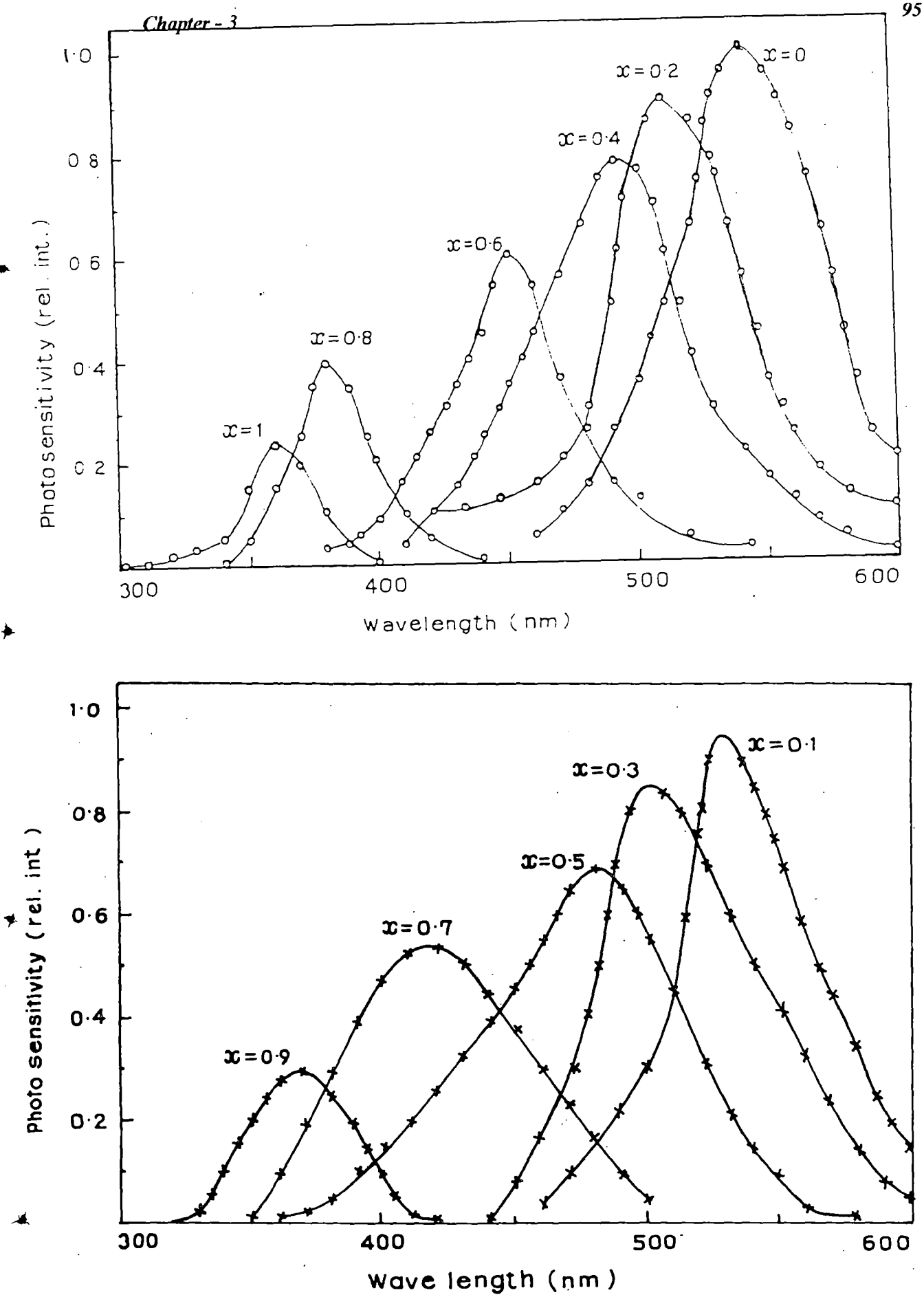

Figure 3.9. Spectral response of photoconductivity curves of $Zn_xCd_{1-x}S$ thin films.

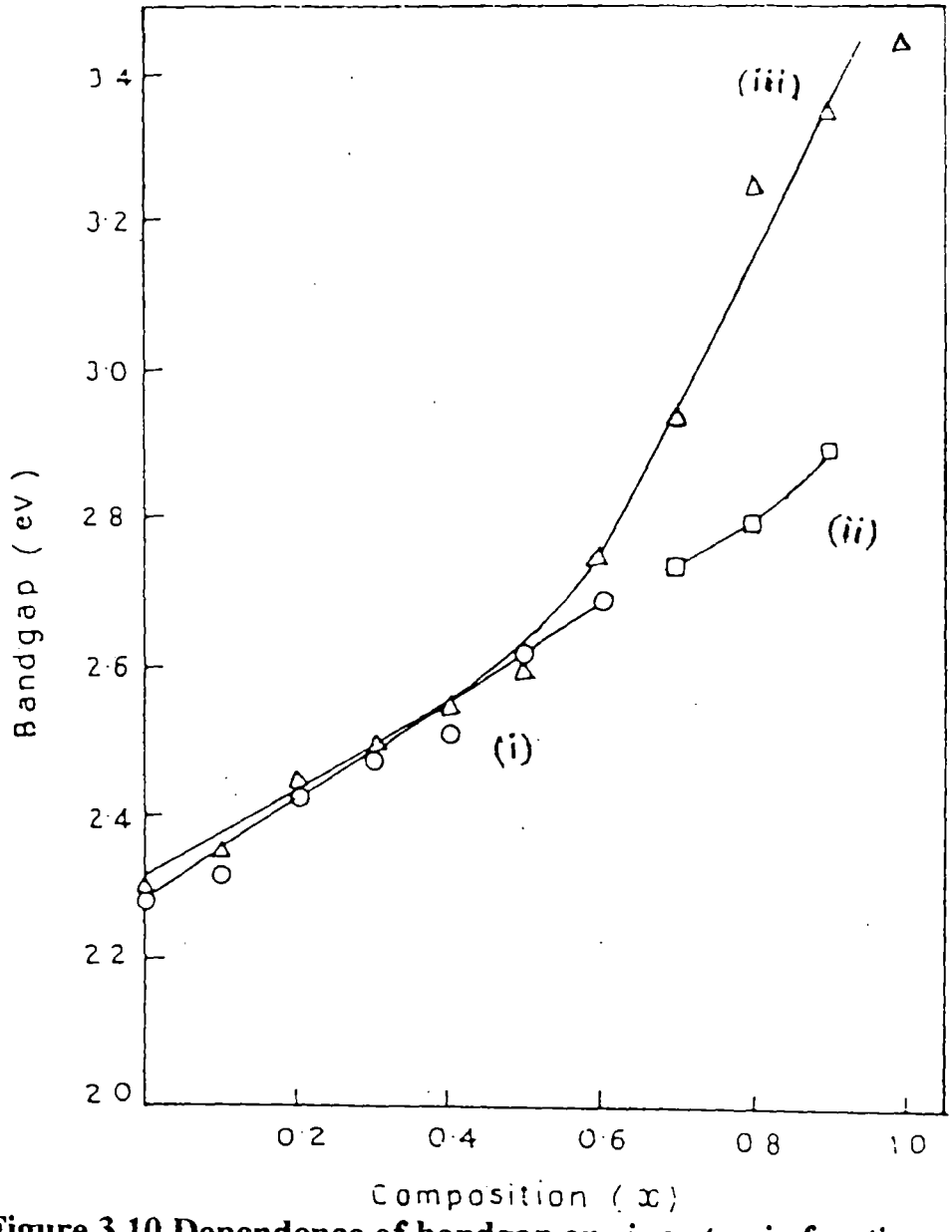

Figure 3.10.Dependence of bandgap on zinc atomic fraction x in $Zn_xCd_{1-x}S$ thin films.

3.1.3.4. SURFACE MORPHOLOGY

Surface morphology studies were carried out by HITACHI S-530 scanning electron microscope. Figure 3.11 shows the SEM micrographs of $Zn_xCd_{1-x}S$ thin films for different values of zinc atomic fraction x. It is evident from the micrographs that the average grain size of the film increases upto x = 0.4, beyond which a tendency of reduction in crystallinity is observed. This is also evidenced in the XRD pattern, where sharp peaks are observed only over the range $0 \leq x \leq 0.4$. The average grain size changes from 0.5 μm (x = 0) to 0.9 μm (x = 0.4), beyond which (x > 0.6) the grains are not properly defined.

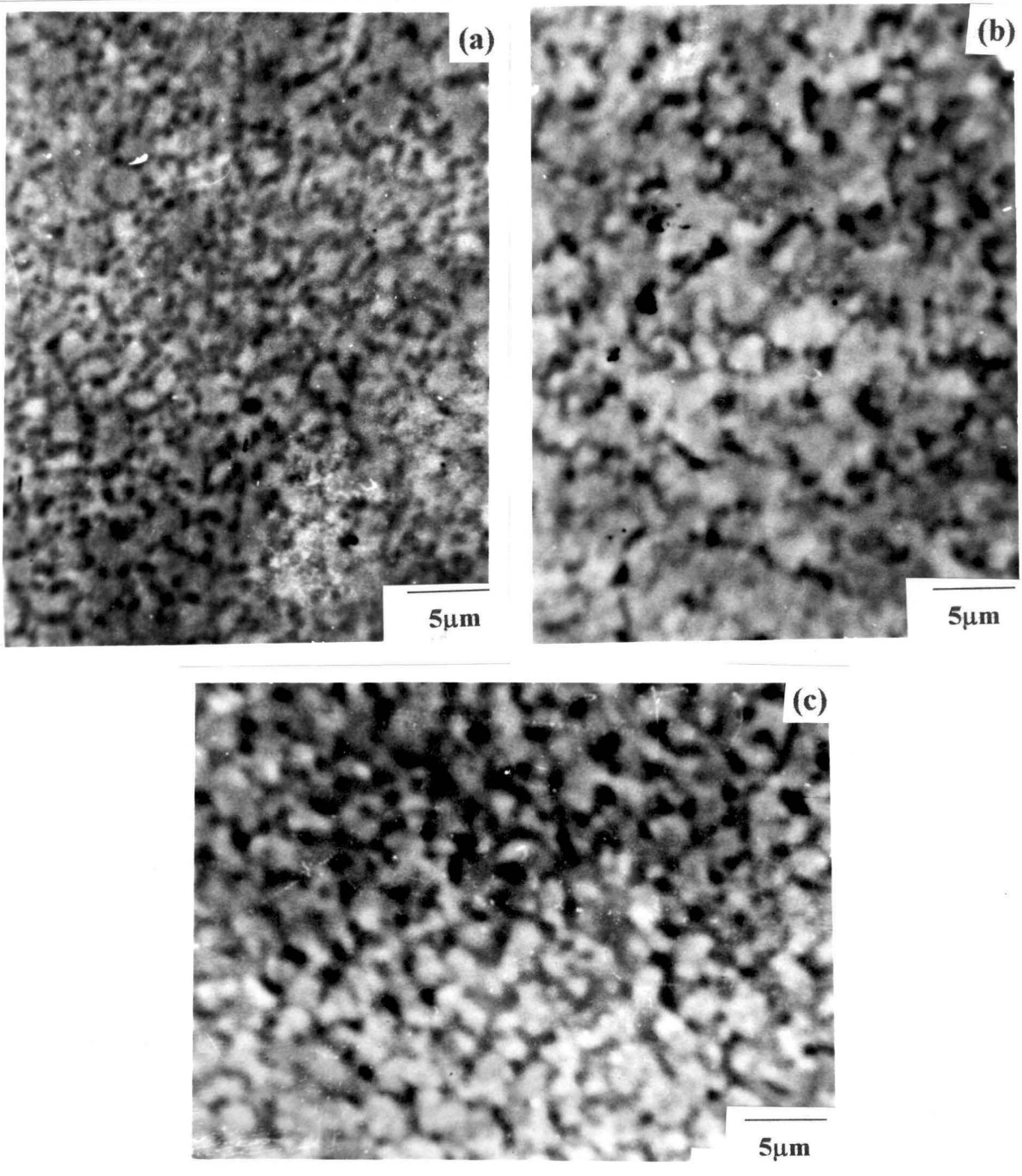

Figure 3.11. Scanning electron micrographs of $Zn_xCd_{1-x}S$ thin films,

(a) X=0, (b) x=0.1, (c) x=0.3.

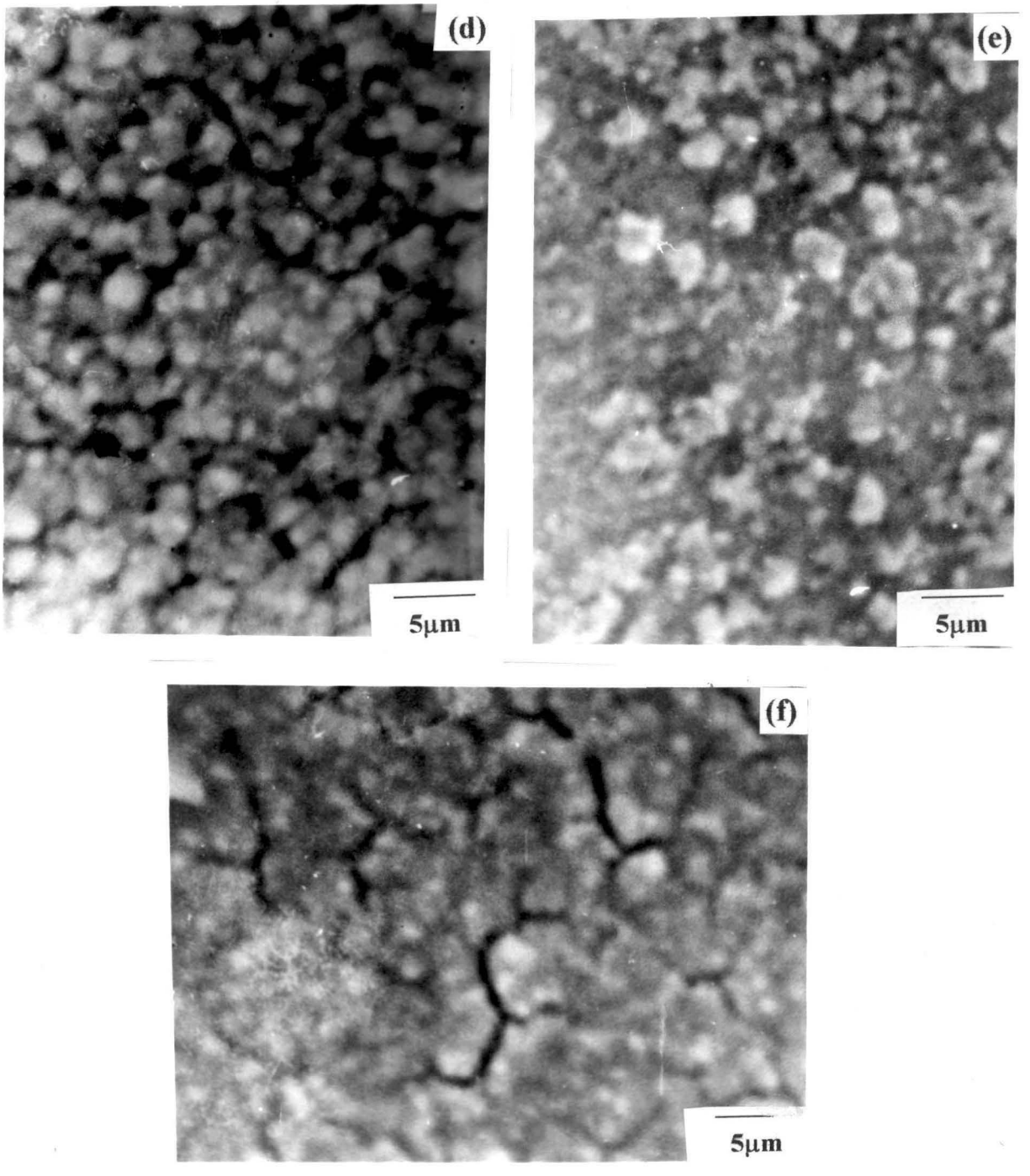

Figure 3.11. Scanning electron micrographs of $Zn_xCd_{1-x}S$ thin films, (d) X=0.4, (e) x=0.5, (f) x=0.6.

*3.2. TIN SULPHIDE (SnS & SnS_2) THIN SOLID FILMS

3.2.1. INTRODUCTION

Efforts have been made currently in finding new materials for energy conversion. Two important factors that should be considered in production of these materials are the band gap energy matching the solar spectrum and the competitiveness of production cost. The first criterion is met by several materials such as Si and GaAs which are being used currently. However, the costs are extremely high for large scale production and can be brought down only by simplifying the manufacturing process.

In the present decade, semiconducting chalcogenide thin films have received much attention because of their world-wide application in the various field of science and technology [34]. In addition, a drastic cut in the cost of production of semiconductor devices is also possible by the use of semiconducting thin films in place of single crystal. Among other materials of recent interest are metal chalcogenides such as CdS and CdSe which fall in the group of II-VI compounds. Among the chalcogenide thin films, tin sulphides show promise because of their possible application in solid state devices, such as photovoltaic [35-38], photoelectrochemical cells (PEC) [39], photoconductive cells [40] and intercalation battery systems [41]. However, compounds of tin sulphide have not been extensively studied.

Tin forms several binary sulphides, such as SnS (orthorhombic) [42-43], SnS_2 (trigonal) [44], Sn_2S_3 (rhombic) [45], and Sn_3S_4 (tetragonal) [46]. All these are semiconducting materials.

---

* **Communicated to the " Thin Solid Films" July 1998.**

Polycrystalline SnS which is usually a p-type semiconductor, with optical and thermal bandgaps of 1.08 eV and 1.20 eV respectively [35-36, 47], may be very interesting for the photovoltaic coversion of solar energy into electrical energy, since its bandgap is comparable to that of silicon [40].

Tin disulphide (SnS_2) is also a very interesting material, both for its layered structure and for the antisotropy of its properties, which makes it a good candidate for utilisation in photochemical solar cells. This compound crystallizes in the CdI_2 type structure with layers of atoms in a close packed arrangement. Within each layer the bonding is mainly covalent, while the layers interact with each other through van der Waals forces. The bandgap of SnS_2 films is about 2.2 eV which is more suitable for photoconductive and photoelectrochemical cells [39-40].

However, comparatively few reports are available for preparation, study and application on these films.

A number of deposition techniques, which include chemical deposition [40,48], evaporation technique [34], chemical vapour transport [49] and electrodeposition [50] have been used for the preparation of these films.

Development of the dip technique for the deposition of SnS and SnS_2 thin films would of practical interest, since dip technique is both simple and economic. An attempt was therefore made to deposit mono and di-sulphides of tin by simple variation of stoichiometry.

These tin sulphide films could be converted easily to tin dioxide by simple annealing in air, thus providing another route for the preparation of transparent conducting tin oxide films.

In this section, we describe in detail the preparation of SnS and SnS_2 films by the dip technique and their characterization by Scanning Electron Microscopy (SEM), X-ray diffractometry (XRD), studies of optical and photoconductive properties, and their conversion to SnO_2 films by air annealing in atmospheric condition.

3.2.2. EXPERIMENTAL DETAILS

Two separate saturated solutions of $SnCl_2.2H_2O$ and thiourea with methanol as solvent were initially prepared. Then they were mixed in requisite amounts together slowly to yield the starting solution for the preparation of SnS and SnS_2 thin films. As a rough guide, 15 gms $SnCl_2.2H_2O$ in 30 cc methanol and 5 gms thiourea in 50 cc methanol was taken for preparation of SnS films whereas for SnS_2 films, 5 gms of more thiourea with 50 cc methanol was added in the above solution .

The films were prepared using the same setup and technique as mentioned in Chapter 2, where speed of withdrawal was 1.33 mm/sec and freshly prepared solutions were used. The films were prepared on soda-glass substrate at different baking temperature in the range 200° C - 360° C for 5 minutes baking time. The formation of SnS and SnS_2 films on the surface of the substrate takes place according to the following reactions.

$$SnCl_2 + (NH_2)_2CS + 2H_2O \rightarrow SnS + 2NH_4Cl + CO_2 \text{ ----(3.7)}$$

To prepare SnS_2 films, a starting solution having $SnCl_2$ and thiourea in 1:2 molar ratio was used and the corresponding equation is given below.

$$SnCl_2 + 2(NH_2)_2CS + 2H_2O \rightarrow SnS_2 + 2NH_4Cl + CO_2 \text{ ----(3.8)}$$

It may be mentioned that the various intermediate chemical reactions and products in the above reactions are quite complex and not known in detail.

SnS and SnS_2 films were deposited at baking temperatures of 200° C, 300° C & 360° C and for a baking time of 5 minutes. Optical absorbtion, photoconductive (PC) spectral response and microstructural studies were carried out using SHIMADZU UV-240 double-beam spectrophotometer, SPECTROMOM 202 spectrophotometer,

PHILIPS diffractometer (model PW 1390) with CuKα radiation (Ni-filter) at 1.54 Å, HITACHI S-530 scanning electron microscope respectively as mentioned earlier (section 4.2). As described earlier, the thickness of the films was measured by stylus method using α step.

SnS and SnS_2 films were baked in a furnace in atmospheric condition at 400° C for different times (10 - 120 minutes) to convert them to transparent conducting tin dioxide film. The SnO_2 films were characterized by XRD, SEM, optical transmission measurements, and variation of their sheet resistance were recorded, using standard four probe method. Optical absorption and doping effects were studied using SnS_2 films only.

3.2.3. RESULTS AND DISCUSSION

Tin mono and di-sulphide films were smooth, shiny and strongly adherent to the substrate. The films were also highly uniform except for the trouble zone at the bottom and sides as described in Chapter 2. The colour of SnS and SnS_2 films was black and golden yellow respectively.

3.2.3.1. THICKNESS

Films of different thickness were obtained by changing multiple dippings. Figure 3.12 shows the thickness variation with number of dippings of SnS_2 films at a baking temperature of 360° C. It is seen that the thickness per dipping is lower for first dip compared with the subsequent dippings. This may be due to the fact that first deposition is on amorphous glass substrate whereas the subsequent depositions are on crystalline SnS_2 layer itself. Similar results were obtained by Karanjai et al. for CdS films [28]. Thickness variation of SnS films with number of dippings follows same nature as

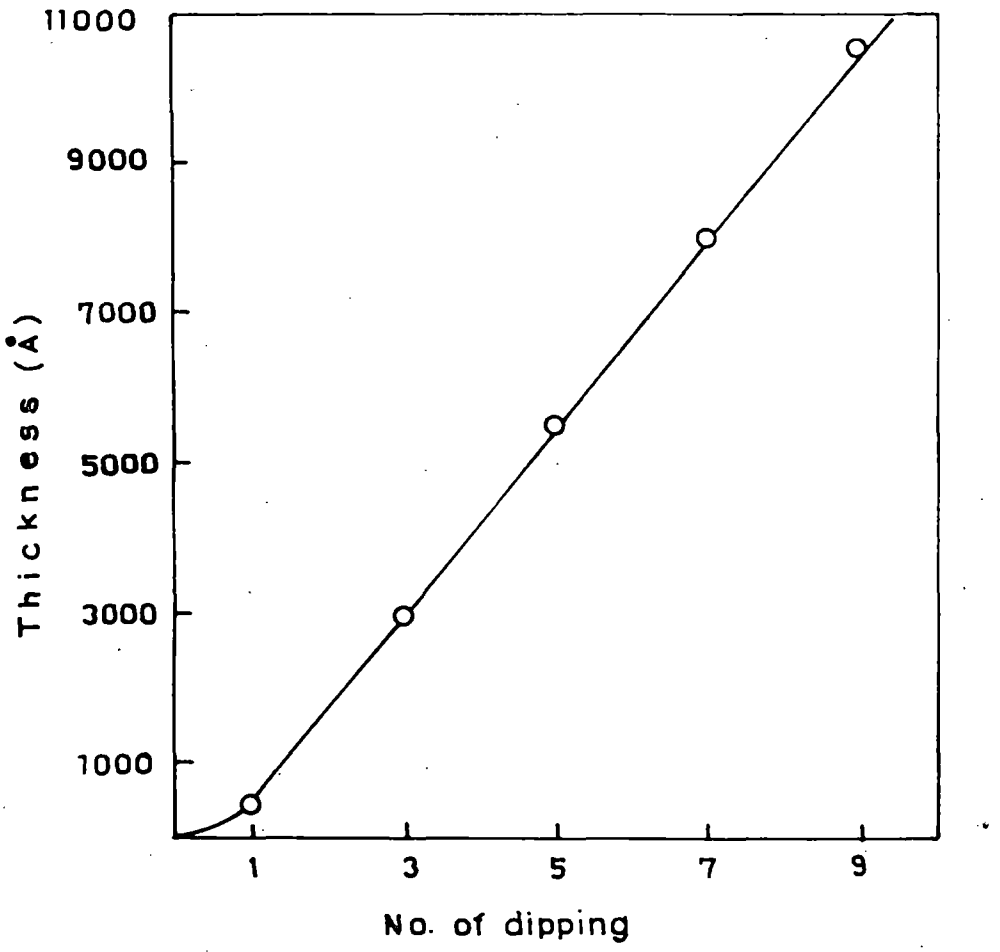

Figure 3.12. Dependence of thickness on number of dippings of SnS_2 thin films (speed = 1.33 mm/sec), $T_B = 360^o$ C).

that of SnS_2 films. But the thickness in case of SnS films is less than that for SnS_2 films for a particular dipping.

Characterization results reported in this chapter are for films prepared by 5 dippings corresponding to a thickness of 0.50 μm for SnS and 0.55 μm for SnS_2 films.

3.2.3.2. X-RAY DIFFRACTOMETRIC STUDY

Figure 4.13 shows the X-ray diffraction patterns for SnS thin films at three different baking temperatures (200° C, 300° C and 360° C) and 5 minutes baking time. Only one peak was observed at 31.95° which was found to be strongest for films prepared at a baking temperature of 300° C. The corresponding 'd' value was found to be 2.8 A°, which is identical to the (040) spacings of SnS.

The X-ray diffraction pattern for a typical SnS_2 thin films prepared at a baking temperature of 360° C, is shown in figure 3.14. It was observed from the XRD pattern that there is only one peak at $2\theta = 15°$. The 'd' value calculated from the 2θ value and was 5.9 A°, corresponding to spacing of (001) plane of SnS_2. Peak position and corresponding 'd' values of both SnS and SnS_2 films were compared with the standard JCPDS data file (No. 14-620 for SnS and No.23-677 for SnS_2), which confirmed the successful deposition of SnS and SnS_2 films. Prominent peaks and their corresponding d-values for SnS and SnS_2 films deposited on soda-glass substrate are listed and compared with d-values from JCPDS data file in table -3.1

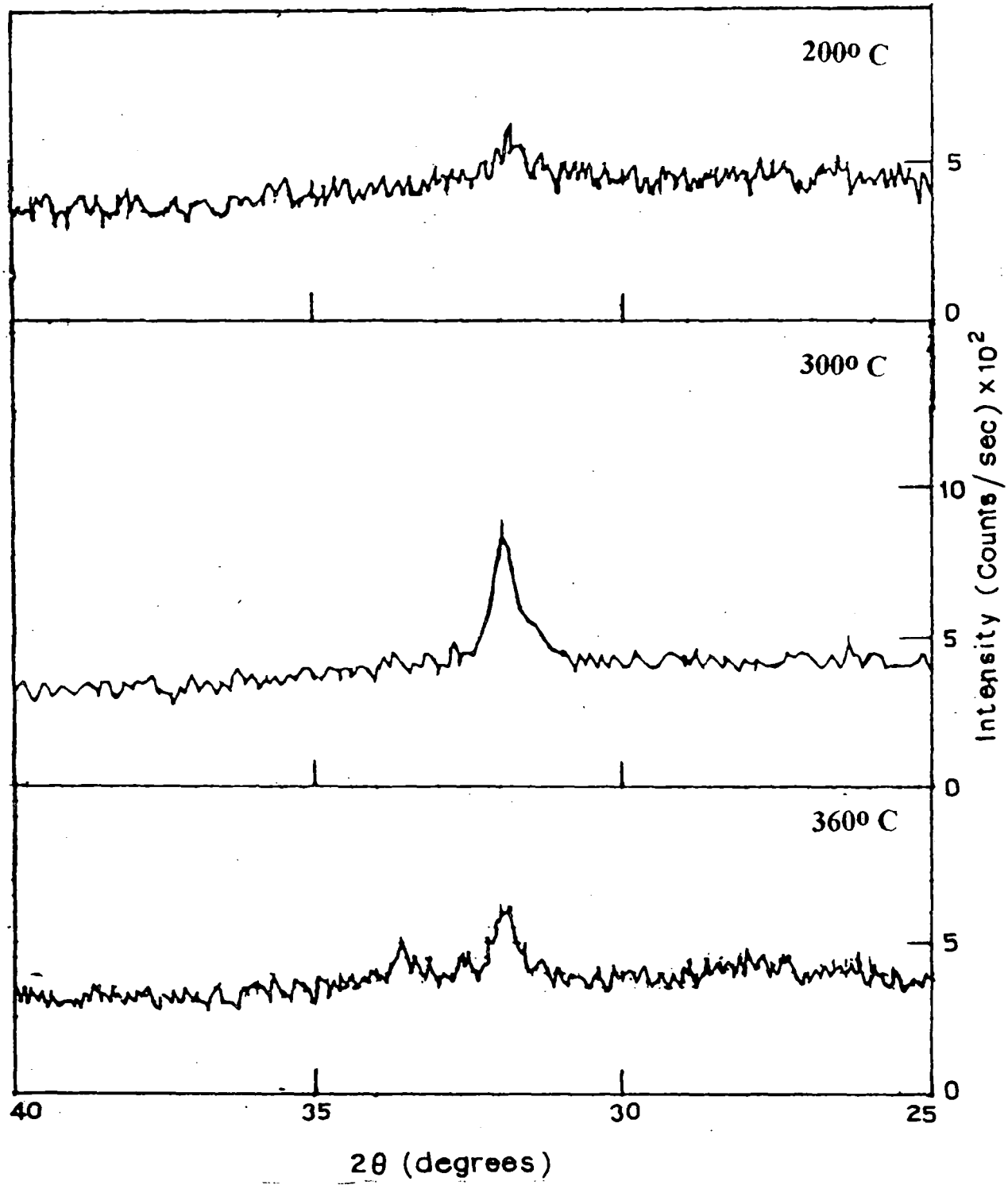

Figure 3.13. X-ray diffractograms of SnS thin films at various baking temperatures (T_B = 200° C, 300° C, 360° C).

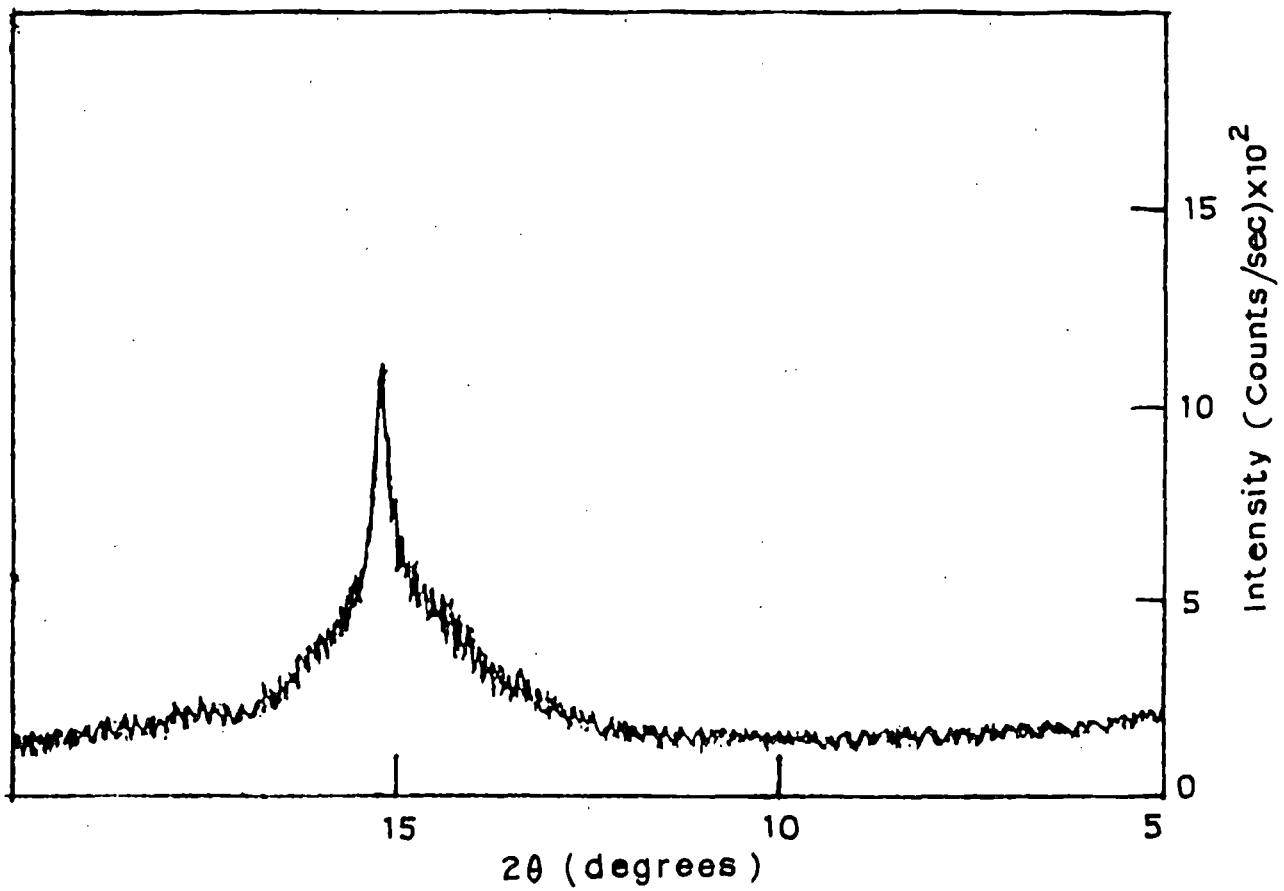

Figure 3.14. X-ray diffractograms of SnS_2 thin films (T_B = 360° C).

Table - 3.1. Prominent peak position (2θ values) of x-ray diffraction peaks,corresponding d-values and their identification for SnS and SnS_2 films deposited on glass substrate.

OBSERVATION			*COMPARISON WITH JCPDS FILE*			*hkl*
Peak position (2θ)	Observed d- values (A°)	Intensity (I/I_0)	Peak position (2θ)	Comparable d- values (A°)	Intensity (I/I_0)	
SnS Film ***(JCPDS data file No. 14-620)***						
31.95	2.80	100	32.00	2.79	100	040
SnS_2 Film (JCPDS data file ***No.23-677).***						
15.02	5.89	100	15.02	5.89	100	001

In each case, appearance of only one sharp peak appears to indicate a preferred orientation, along the (040) planes for SnS and (001) planes for SnS_2 respectively.

SnS_2 films prepared at 200° C and 300° C showed no sharp peaks and only a broad hump indicating that they were possibly amorphous.

Thus, baking for 5 minutes in 300° C and 360° C resulted in oxide-free SnS and SnS_2 films by the dip technique. It may be mentioned that no evidence of any oxide (SnO_2) peak was found over a 2 θ range 10° to 80°.

3.2.3.3. SURFACE MORPHOLOGY

SEM micrographs of SnS thin Films deposited at three different baking temperatures (200° C, 300° C and 360° C) are shown in figure 3.15. It is clear from the micrographs that grain size of the films deposited at 300° C is the largest compared to others. As already mentioned, these films also show the strongest XRD peaks.

Figure 3.16 shows the SEM micrographs of an SnS_2 thin film prepared at a baking temperature of 360° C. Average grain size for both SnS and SnS_2 films as observed from the micrograph is about 1 μm.

3.2.3.4. PHOTOCONDUCTIVE PROPERTIES

The spectral response of photoconductivity curves for SnS and SnS_2 thin films are shown in figure 3.17. In figure 3.17 the photocurrent values are normalised with the peak response for SnS_2 film taken as 1. The maximum photocurrent for SnS film is seen to occur at 840 nm, corresponding to a band gap of 1.4 eV which is comparable to values reported in the literature [39]. In case of SnS_2 films, the maximum photocurrent was observed at 500 nm which corresponds to a band gap of 2.4 eV, and compares quite well with values reported by other workers [39-40].

3.2.3.5. OPTICAL ABSORPTION PROPERTIES

In the following, the optical absorption of undoped and Sb-doped SnS_2 films are discussed. It was not possible to carry out optical absorption measurements on SnS films as the absorption edge lies in the infrared and the soda-glass substrate strongly absorbs in this range.

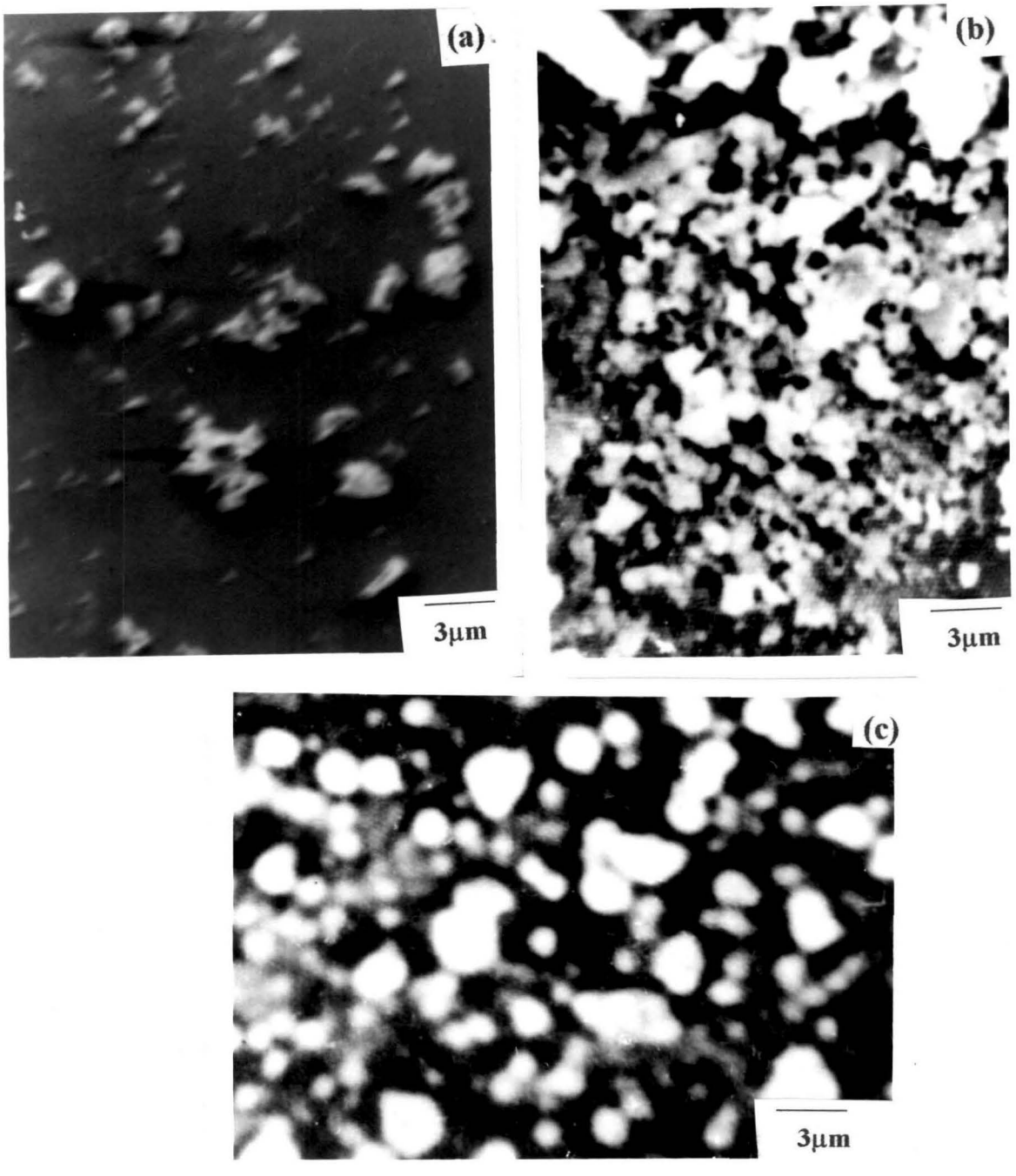

Figure 3.15. Scanning electron micrographs of SnS thin films at three different baking temperatures, (a) 200° C, (b) 300° C, (c) 360° C.

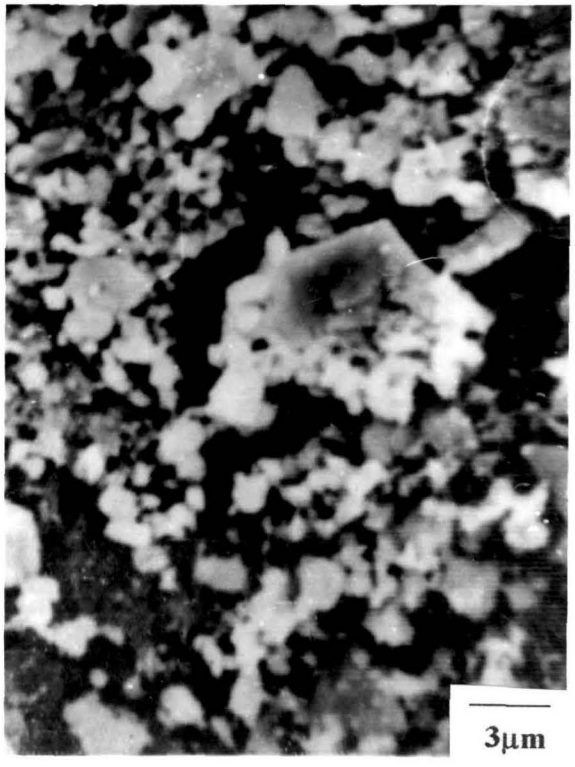

Figure 3.16. Scanning electron micrograph of SnS_2 thin films deposited on glass substrate at 360° C.

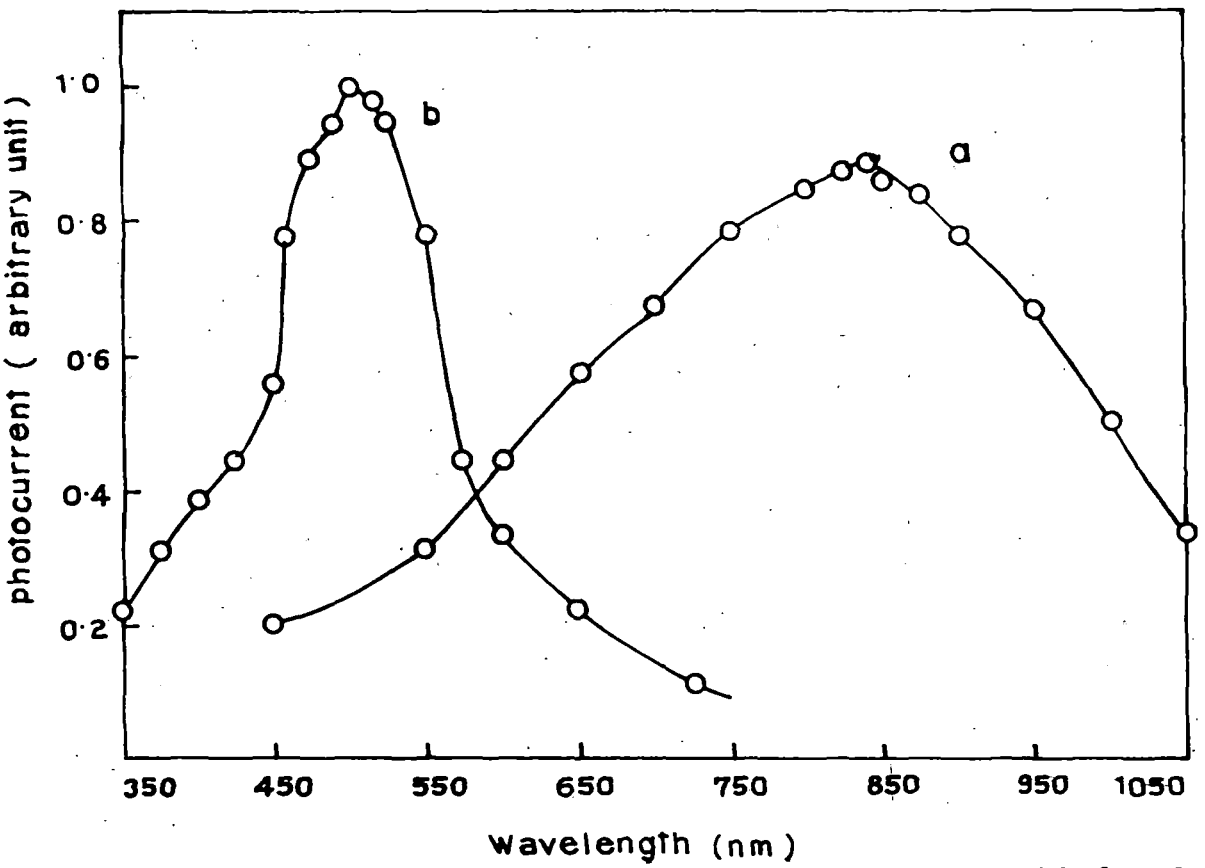

Figure 3.17. Spectral response of photoconductivity curves of SnS and SnS_2 thin films at baking temperature 300° C and 360° C respectively (a) SnS thin film and (b) SnS_2 thin film.

3.2.3.5.1. Undoped SnS_2 films

Optical absorption spectra of SnS_2 films is shown in figure 3.18. In this figure (a) shows the absorption spectra of pure SnS_2 film. The spectra is taken with respect to the bare substrate placed in the reference beam. The rise in absorption is quite steep, indicating that the films are homogeneous and the optical band gap was measured from the extrapolation of the linear portion of the $(\alpha h\nu)^2$ versus $h\nu$ curve shown in figure 3.19. The optical band gap of SnS_2 films is 2.4 eV (from figure 3.19), which is the same as obtained from photoconductive response data.

3.2.3.5.2. Sb-doped SnS_2 films

SnS_2 thin films of thickness about 0.55 μm deposited at a baking temperature of 360° C for 5 minuits baking time were doped with antimony (Sb) for different at%. It was observed from the optical absorption data in figure 3.18, that the absorption edges of these spectra are shifted towards shorter wavelength as a result of increasing Sb concentration corresponding to an increase in band gap from 2.4 eV to 3.0 eV (for 3 at%doping), which was calculated from the curve $(\alpha h\nu)^2$ versus $h\nu$ shown in figure 3.19.

X-ray diffractometric studies were carried out for doped SnS_2 films. It is observed that introduction of antimony (Sb) as a dopant in the SnS_2 film reduces the peak height. In the X-ray diffractogram shown in figure 3.20, thus at 0.12 at% Sb doped SnS_2 film the peak height is reduced and for 0.3 at% Sb doping the peak has disappeared. Thus it can be concluded that Sb-doping has a strong effect on the crystallinity of SnS_2, and a very small concentration (0.3 at%) of Sb being sufficient to make it completely amorphous. A similar result was observed by Banerjee et al. [51], who found that the introduction of Sb as dopant in CdS reduces its crystallinity and, at 3 at% doping, the structure becomes completely amorphous.

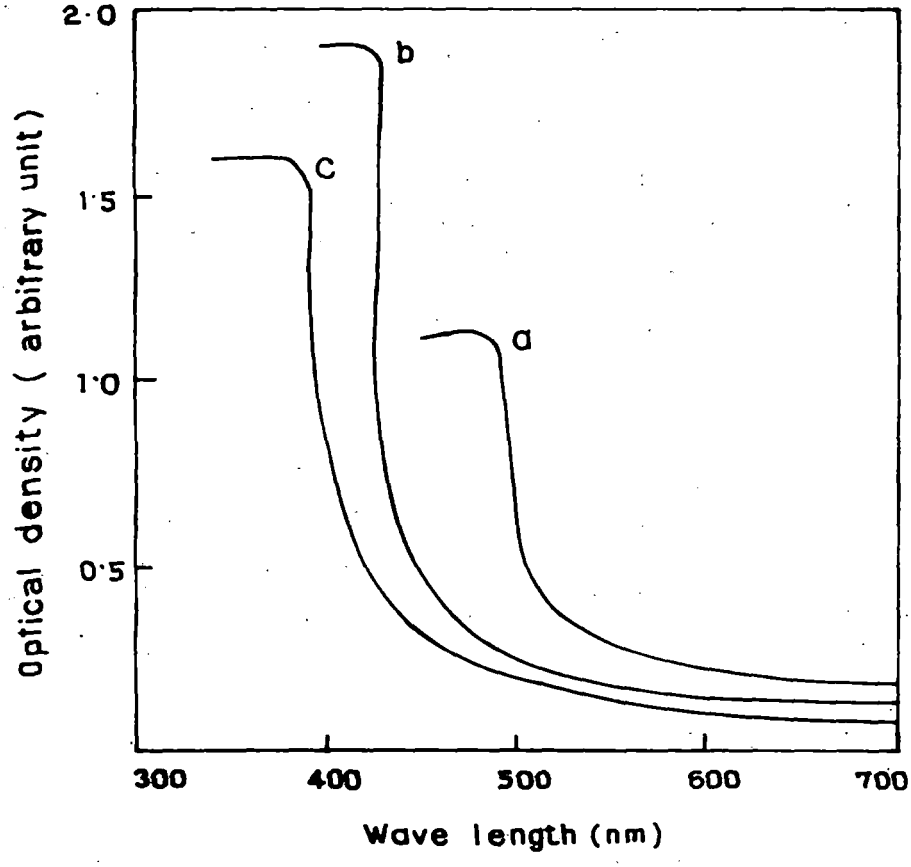

Figure 3.18. Optical absorption spectra of undoped SnS_2 and different at% dopped SnS_2 thin films at baking temperature 360° C ;(a) undopped SnS_2 , (b) 0.12 at% Sb dopped SnS_2 and (c) 0.32 at% sb dopped SnS_2 thin films.

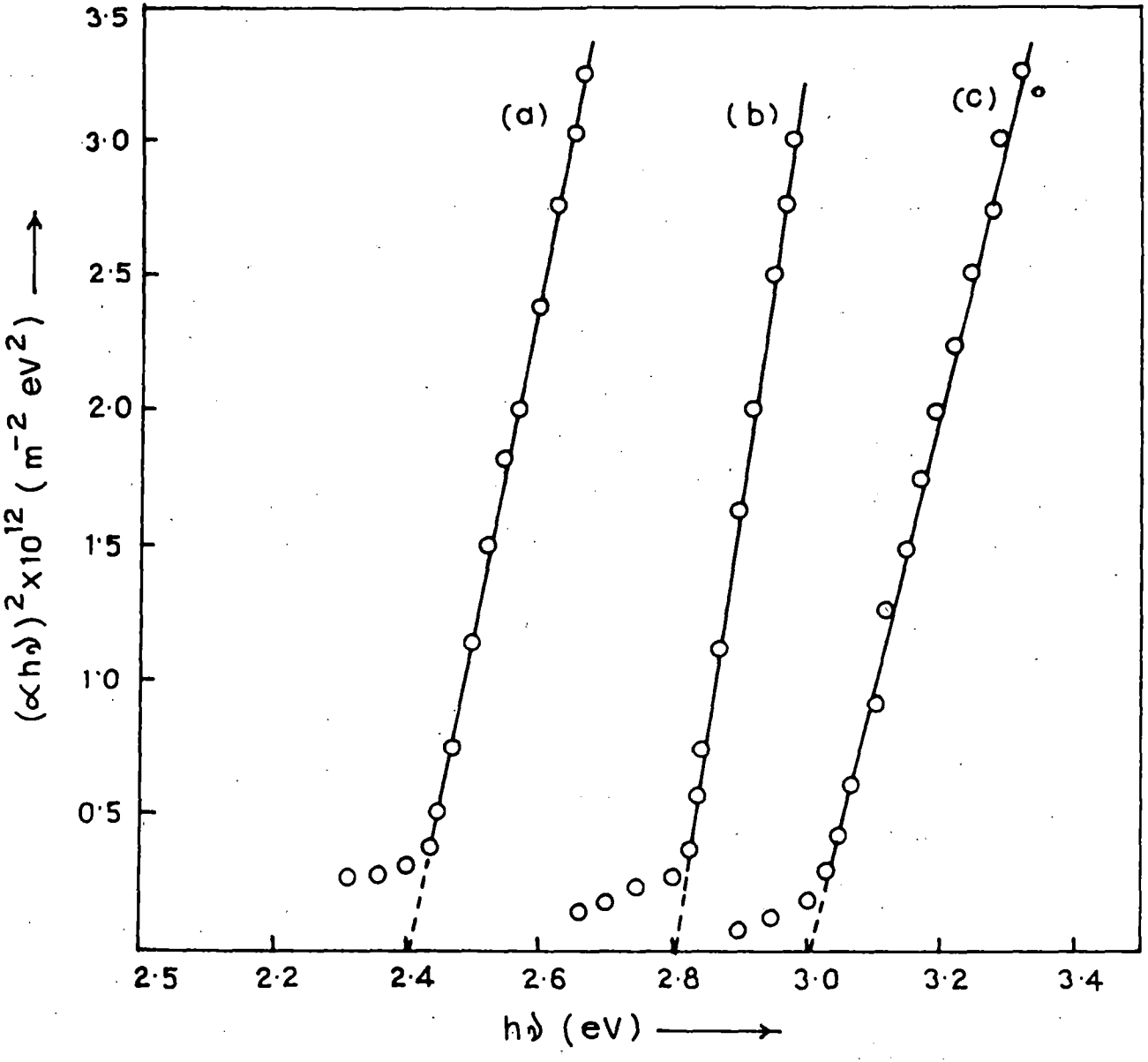

Figure 3.19. Plots of $(\alpha h\nu)^2$ against hν curves of undoped and Sb-doped SnS_2 thin films. (a) Undoped SnS_2 films; (b) SnS_2:Sb 0.12 at%; (c) SnS_2:Sb 0.32 at%.

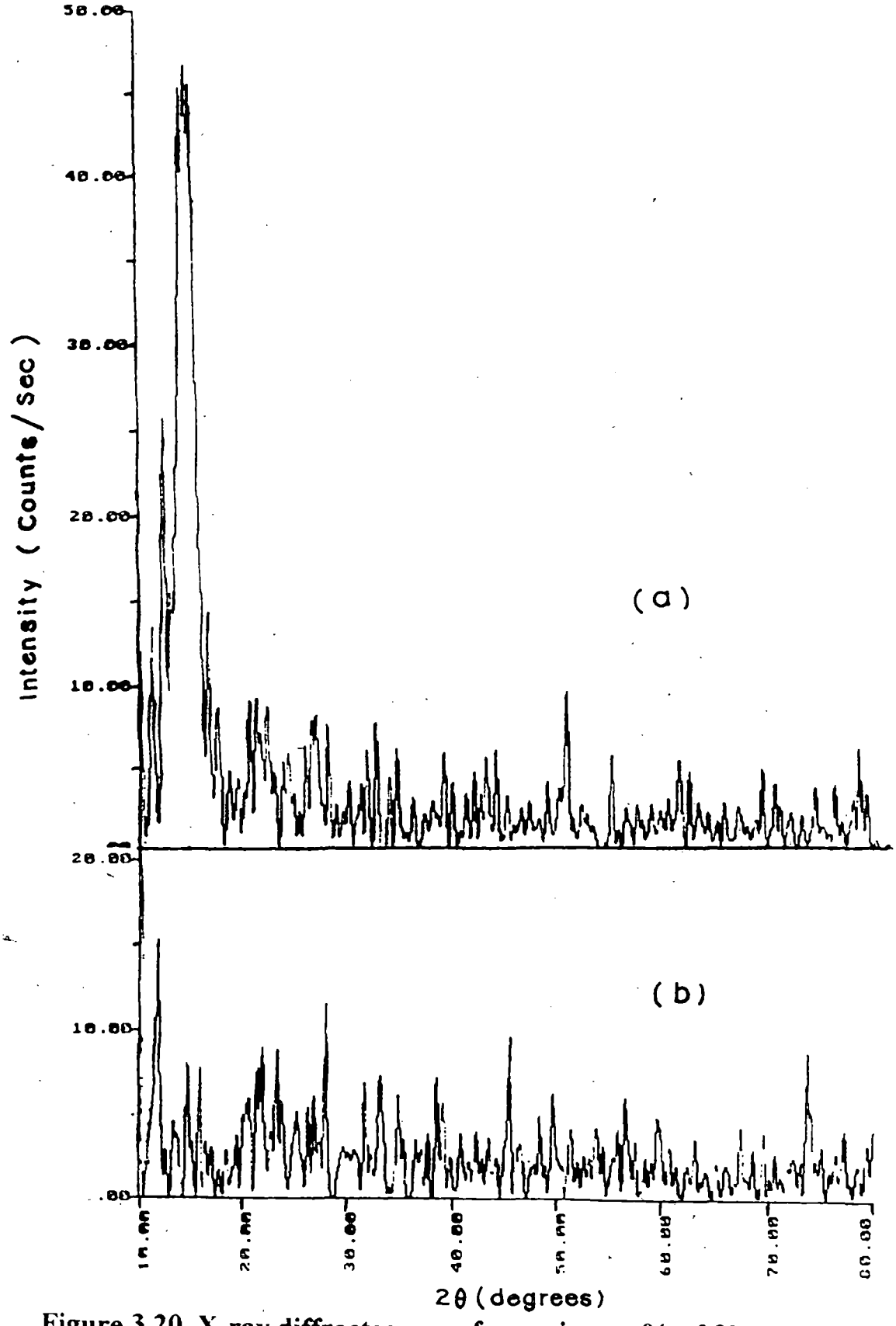

Figure 3.20. X-ray diffractograms for various at% of Sb dopped SnS_2 thin films at baking temperature 360° C (a) 0.12 at% and (b) 0.3 at%.

3.2.3.6. EFFECT OF ANNEALING

Effect of annealing was studied by baking SnS and SnS_2 films, prepared at a baking temperature of 300° C and 360° C for 5 minutes to a higher temperature of 400° C in the furnace at atmospheric condition for various baking times.

We found that when SnS and SnS_2 films are annealed in a furnace at 400° C for more than 10 minutes, these are converted into SnO_2 transparent conducting films in the presence of atmospheric oxygen, according to one of the following reactions.

$$SnS + 2O_2 = SnO_2 + SO_2 \text{ ---------(3.9)}$$

$$SnS_2 + 3O_2 = SnO_2 + 2SO_2 \text{ -------(3.10)}$$

Figure 3.21 shows the effect of annealing in atmospheric condition at 400° C for different baking times on the sheet resistance of SnS and SnS_2 films. It was observed that good quality SnO_2 films in terms of crystallinity as well as optical transmission could be obtained by air annealing of tin disulphide films prepared by dip technique for about 50 minutes. The electrical conductivity SnO_2 films obtained by this method are quite reasonable, the sheet resistance being 2 X 10^3 Ω/□ with an optical transmission of 90%.

It was observed that for prolonged annealing (>120 min.) of SnS and SnS_2 films the sheet resistance become very high and of the order of 10^6 Ω/□ with no change in optical transmission.This is probably due to the filling of the oxygen vacancies resulting in a near-stoichiometric materials. These high-sheet-resistance SnO_2 films may be useful as an insulator layer [52] as well as a protective layer [48] in semiconductor device structures. It was observed that due to increase in annealing time the optical transmission of the films is increase (fig. 3.22). XRD and SEM of a typical SnO_2 films obtained by this method by annealing of SnS_2 is shown in figures 3.23 and 3.24. The XRD pattern of the

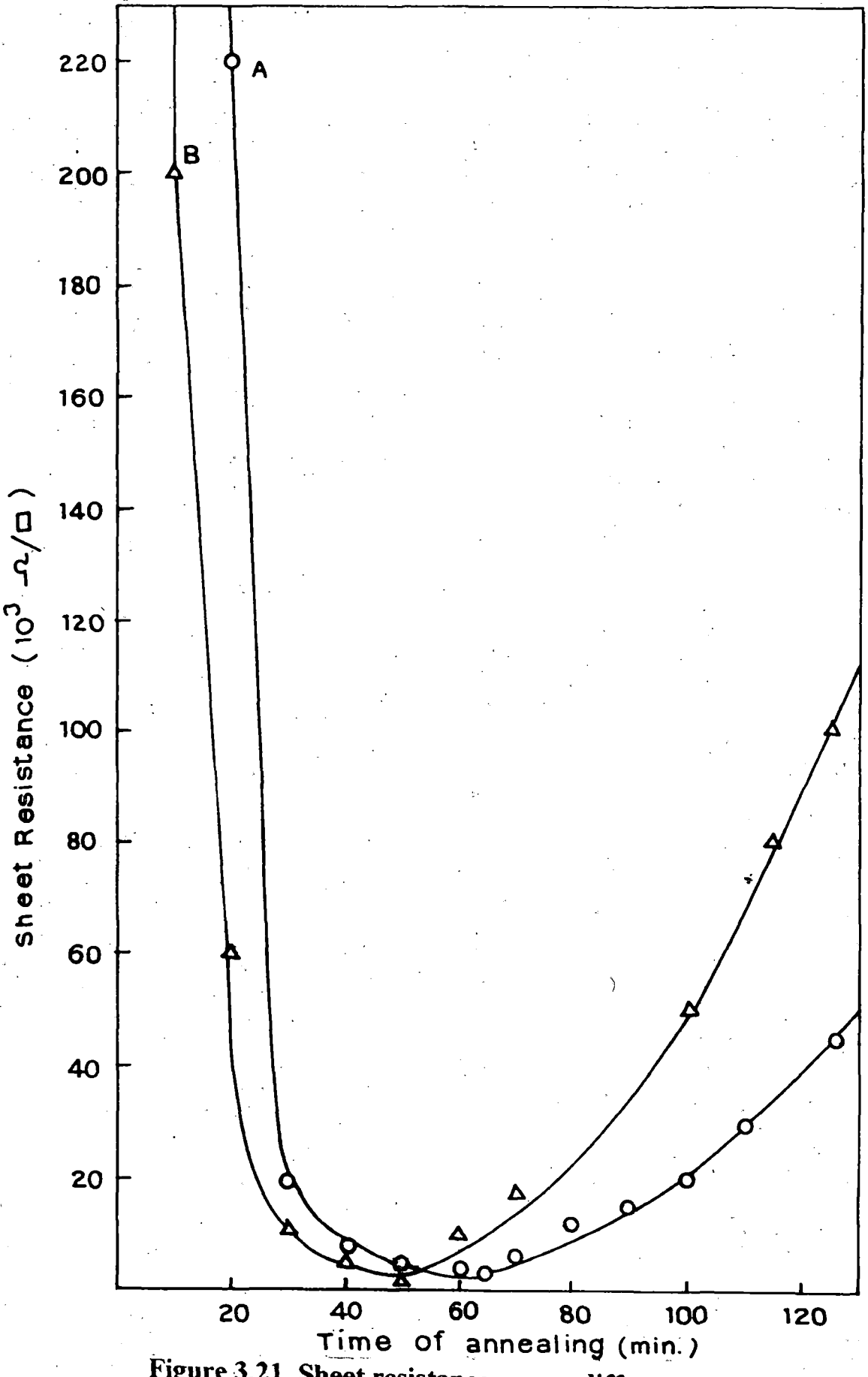

Figure 3.21. Sheet resistance versus different baking time of annealing of A, SnS; B, SnS_2 films at 400° C.

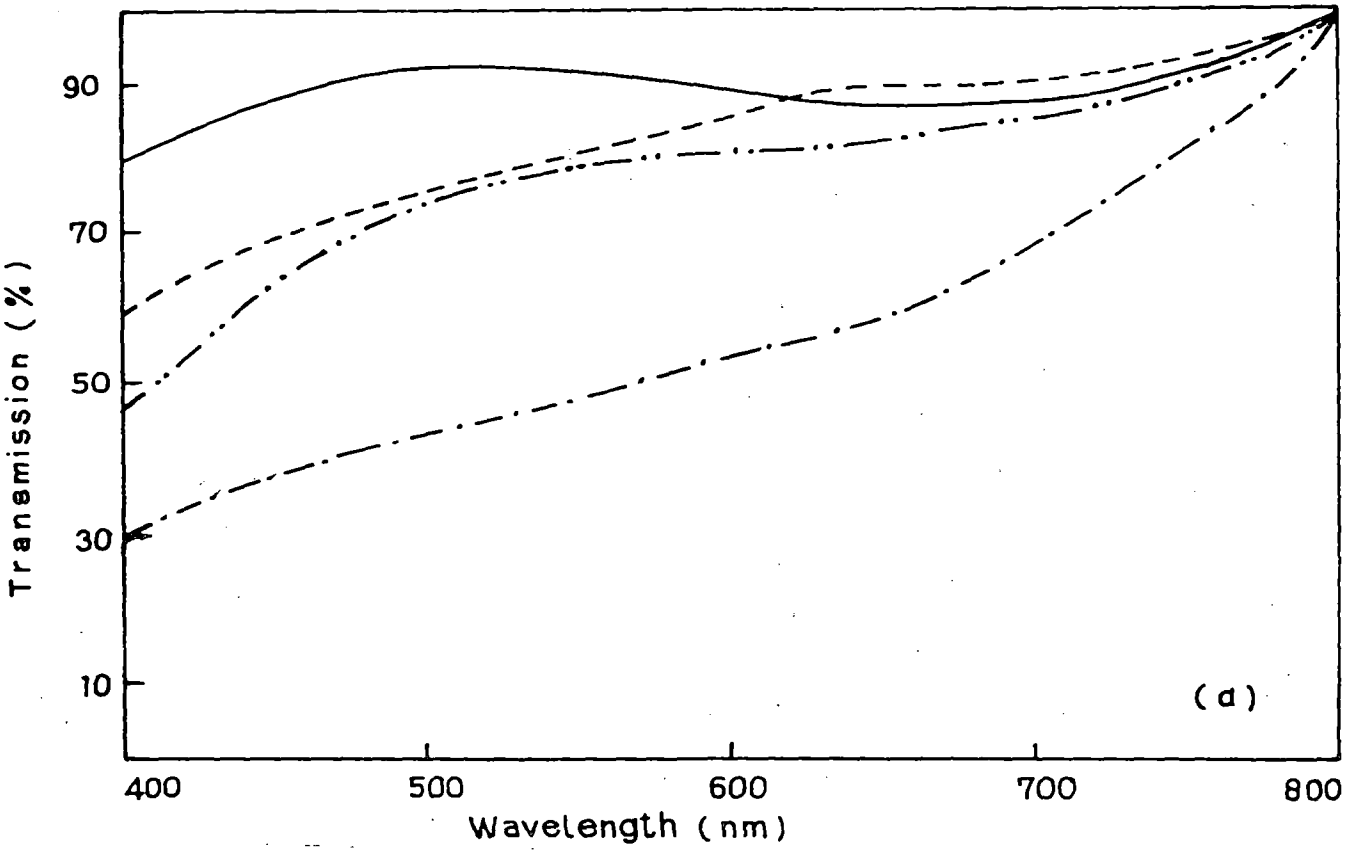

Figure 3.22. Optical transmission versus wavelength for annealed SnS thin films of various annealing /baking time(T_B).
(a) Annealed SnS thin film: (-.-.-.-.), T_B =30min.; (-..-..-..-..), T_B=60 min.; (———), 75 min.; (_____), T_B=90 min.

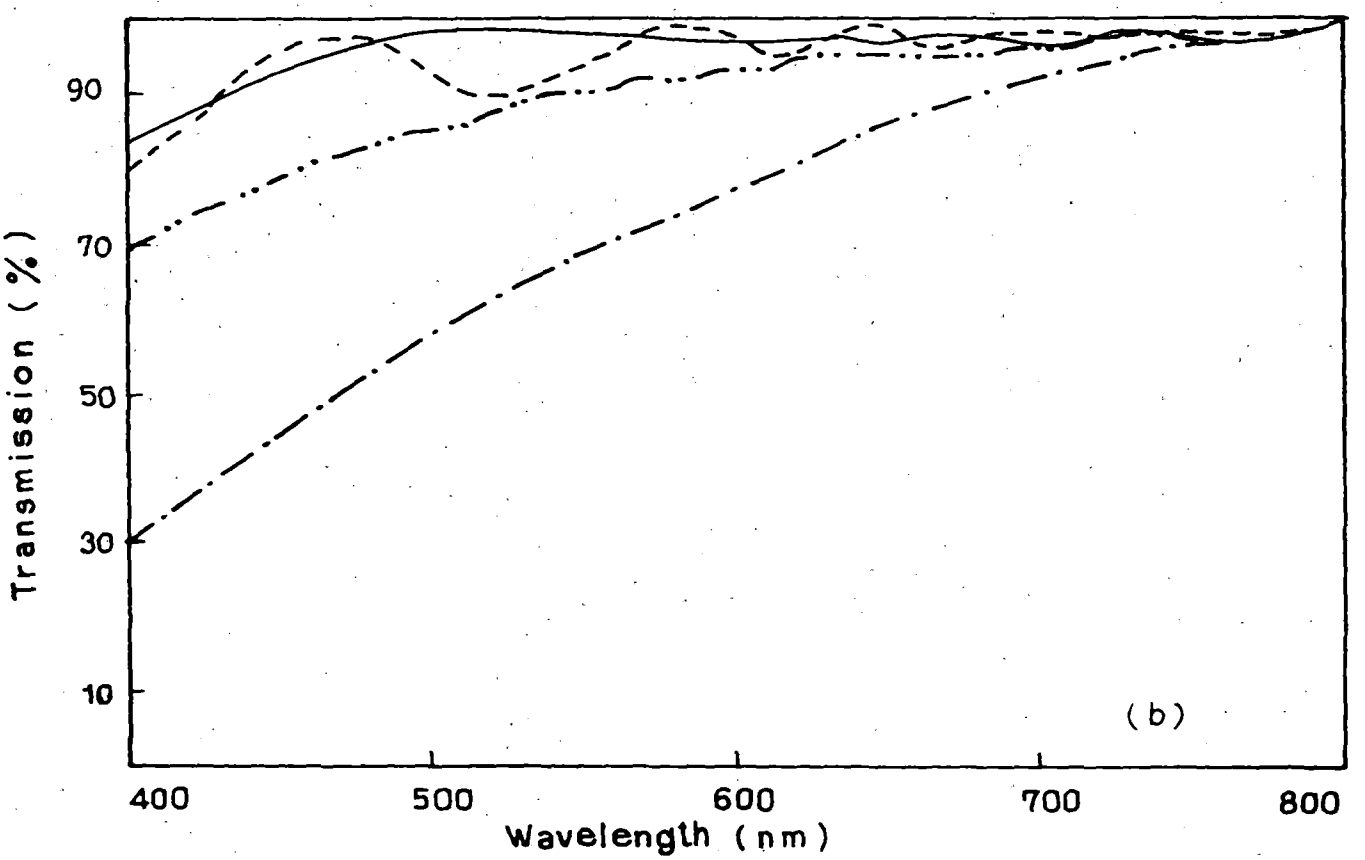

Figure 3.22. Optical transmission versus wavelength for annealed SnS_2 thin films of various annealing /baking time(TB).
(b) Annealed SnS_2 thin film: (-.-.-.-.), T_B =30min.; (-..-..-..- ..), T_B=50 min.; (———),T_B=75 min.; (_____),T_B=90 min.

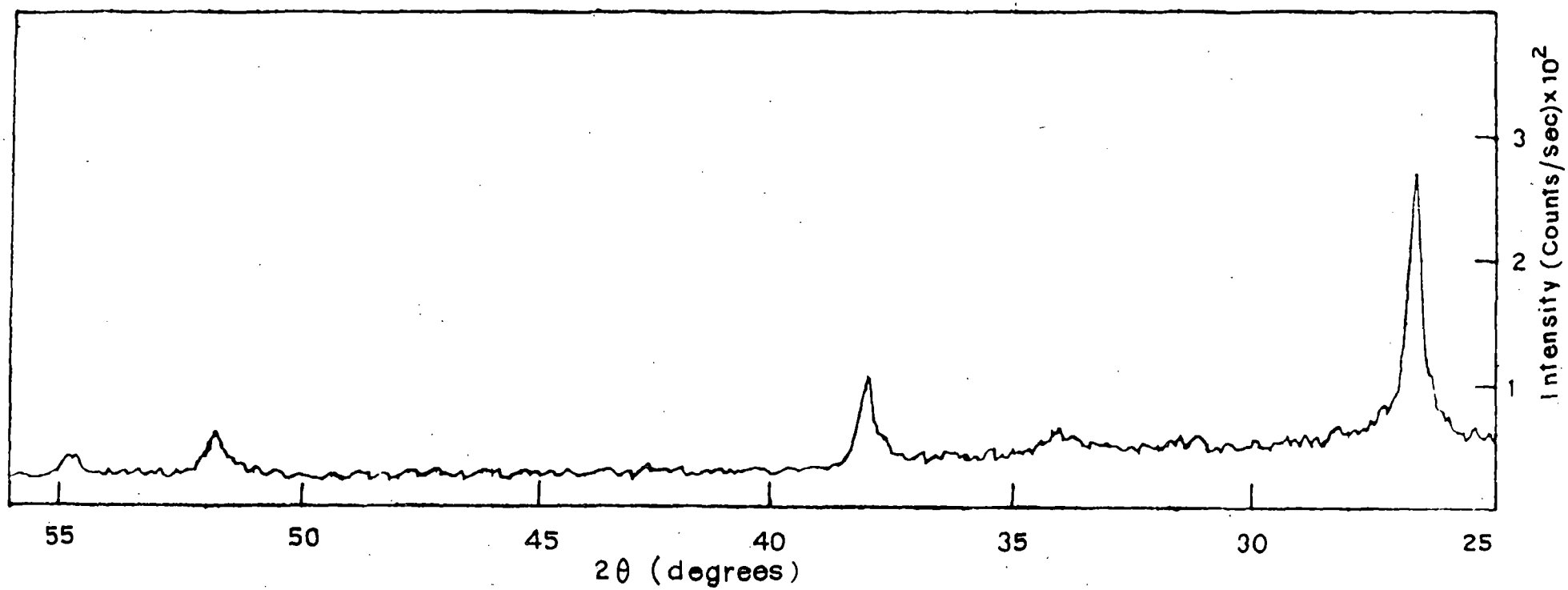

Figure 3.23. X-ray diffractograms for SnO_2 film obtained from SnS_2 film by atmospheric annealing at 400° C.

transformed films matches well with the XRD powder pattern simulated from the data for SnO_2 [53] as well as with JCPDS file 21-1250 data for SnO_2 mineral sample. Prominent peaks, corresponding d-values and their intensity for these SnO_2 films are listed and compared with JCPDS data file in table -3.2

Table - 3.2. Prominent peak position (2θ values) of x-ray diffraction peaks, corresponding d-values and their identification for SnO_2 film obtained from SnS_2 film (annealing time = 50 minutes).

OBSERVATION			*COMPARISON WITH JCPDS DATA FILE NO. 21-1250*		*hkl*
Peak position (2θ)	Observed d- values (A°)	Intensity (I/I_o)	Comparable d- values (A°)	Intensity (I/I_o)	
26.65	3.34	100	3.35	100	110
38.00	2.36	40	2.37	25	200
51.85	1.76	22	1.76	65	211
54.80	1.67	15	1.67	18	220

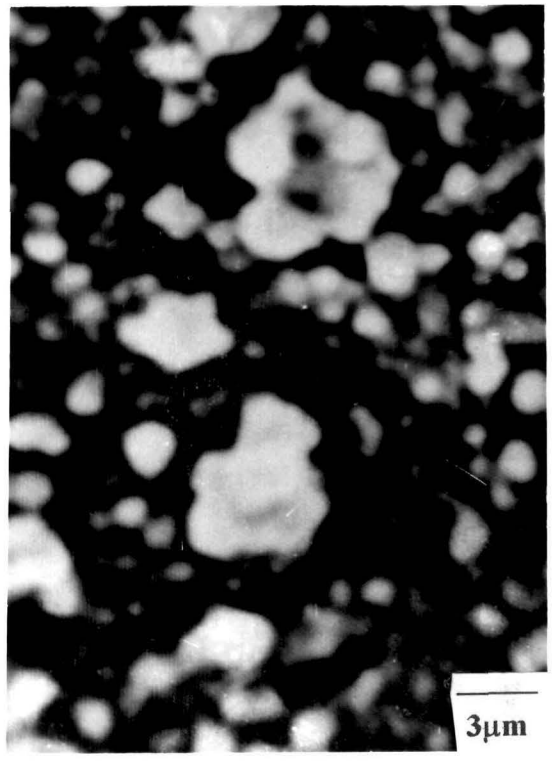

Figure 3.24. Scanning electron micrograph of SnO_2 thin film obtained from SnS_2 film by atmospheric annealing at 400° C.

3.3. A FEW MORE SULPHIDE FILMS

A few more sulphide films were also deposited using dip technique. In the following section deposition and characterisation of Mo-sulphide and Cu-sulphide films have been discussed in brief.

*3.3.1. MOLYBDENUM DISULPHIDE (MoS_2) THIN FILM

3.3.1.1. INTRODUCTION

Molybdenum dichalcogenides appear to be very promising semiconductor materials for various applications such as solar cells [54-55], rechargeable batteries [56] and solid lubricants for metallic and ceramic surface in environments where hydrocarbon or other fluid-based lubricants are unsuitable, such as in high vacuum or high temperature applications [57-58]. It has been also widely used in space-technology where its low co-efficient of friction in vacuum is of particular value [59]. These applications arise from the optical, electrochemical and mechanical properties of these compounds. They exhibit a layer-type structure in which monolayers of Mo are sandwiched between monolayers of sulphur, which are held together by relatively weak van der Waals forces. These materials have band gaps (1.78 eV) well-matched to the solar spectrum [60]. A number of methods exist for the production of MoS_2 thin films, including sputtering [61-63], electrochemical deposition [60,64], and pulsed laser deposition [65-68].

In this section, the preparation of MoS_2 thin films by dip technique and to study their structural and optical properties have been described.

***Presented at the "Fifth West Bengal State Sc. Cong." Proceedings, University of North Bengal, 21-23 March, 1998, Page 140.**

3.3.1.2. EXPERIMENTAL DETAILS

Film deposition procedure exactly follows the same technique as discussed earlier, where lifting speed were 1.33 mm/sec and the starting solution was taken by mixing of methanolic solution of ammonium molybdate (5 gms ammonium molybdate in 50 cc methanol) and ammonium thiocyanate (3.88 gm ammonium thiocyanate in 40 cc methanol). The deposition was performed on soda-glass substrate at different baking temperature from 300° C to 450° C for 5 minutes baking time. The substrate was cleaned as discussed before in detergent solution, water and chromic acid and finally degreased in acetone and methanol vapour.

Characterization of the films were carried out by X-ray diffractometry, Scanning electron microscopy and optical absorption using PHILIPS diffractometer (model PW 1390) with CuK_{α} radiation (Ni-filter) at 1.54 Å, HITACHI S-530 scanning electron microscope and SHIMADZU UV-240 double-beam spectrophotometer respectively.

3.3.1.3. RESULTS AND DISCUSSION

MoS_2 thin films are smooth, uniform and strongly adherent to the substrate. The films are gray in colour. The thickness of the films prepared for characterization is estimated to be one micrometer.

Figure 3.25 shows the XRD spectra of MoS_2 thin films prepared at three different baking temperature 300° C, 360° C and 450° C. From the XRD spectra we observed that the films prepared at 300° C is completely amorphous in nature but films prepared at 360° C and 450° C are crystalline. Comparison of the prominent peak positions (2θ - values) of the XRD spectra with the ASTM data file for MoS_2 (File No. 24-515) suggests that the films deposited at baking temperature 360° C and 450° C are

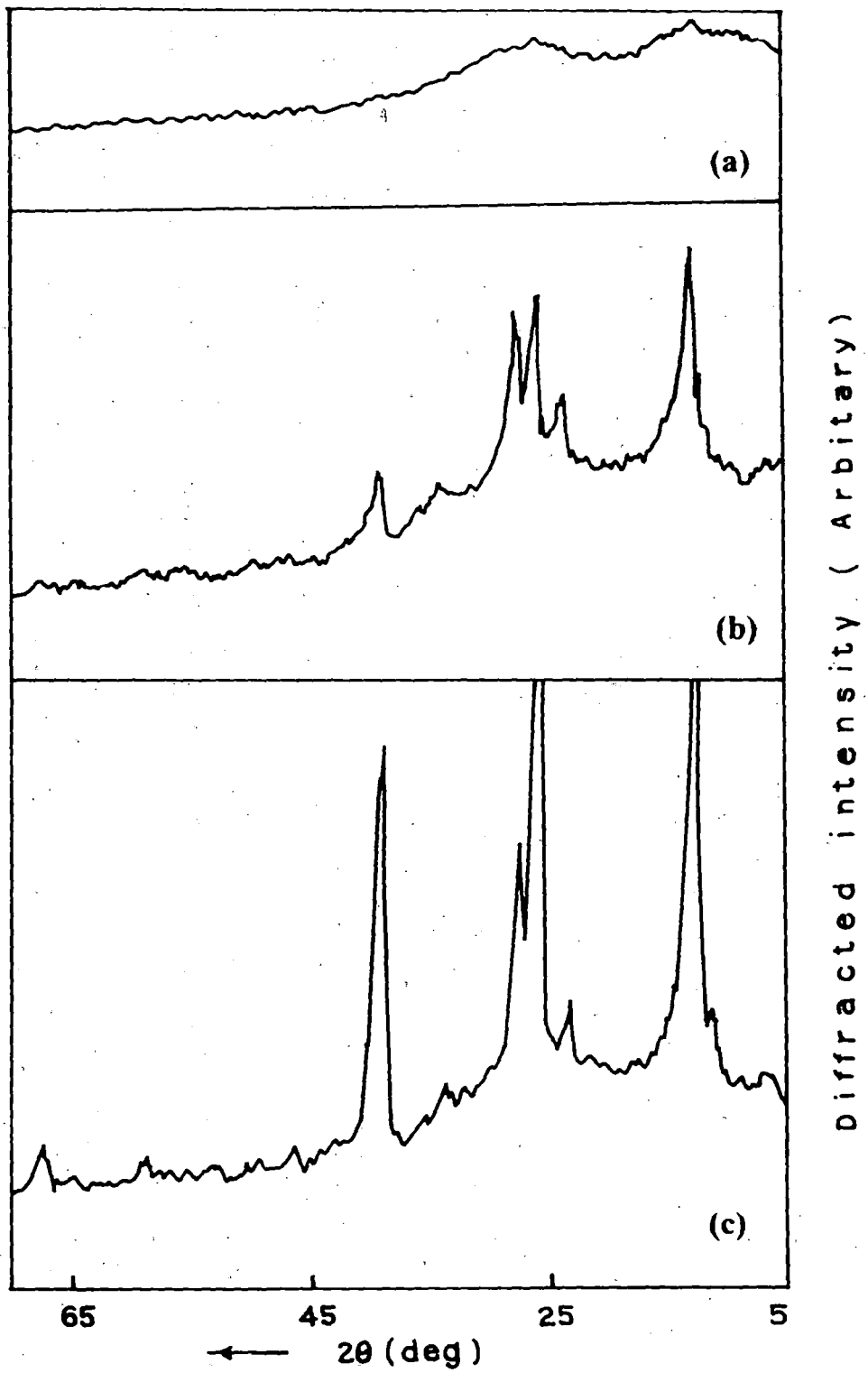

Figure 3.25. X-ray diffractogram of MoS_2 thin films deposited on glass substrate at three different baking temperature [(a), 300° C; (b), 360° C; (c), 450° C].

hexagonal in structure. The planes of MoS_2 are indicated in the XRD spectra. These planes are (002), (012), (104), (107) and (113). The peaks which are unmarked do not correspond to MoS_2 films. These unmarked peaks correspond to MoO_3 which were confirmed from the ASTM data file no. 5-0508. Prominent peaks, corresponding d-values and their intensities for MoS_2 films prepared at 450° C are listed and compared with JCPDS data file (24-515) in table -3.3

Table - 3.3. Prominent peak position (2θ values) of x-ray diffraction peaks, corresponding d-values and their identification for MoS_2 films.

OBSERVATION			*COMPARISON WITH JCPDS DATA FILE NO. 24-515*		*hkl*
Peak position (2θ)	Observed d- values (A°)	Intensity (I/I_0)	Comparable d- values (A°)	Intensity (I/I_0)	
13.25	6.30	100	6.20	100	002
33.75	2.65	33	2.63	21	012
39.00	2.30	88	2.35	27	104
46.40	1.95	28	1.90	14	107
59.00	1.56	25	1.53	8	113

Figure 3.26 shows the scanning electron micrographs of MoS_2 films deposited on glass substrates at three different baking temperatures. These micrographs shows that the grain size of MoS_2 films when deposited at 360° C and 400° C are larger than the that size of films deposited at 300° C.

Figure 3.27 shows the optical absoption of MoS_2 films deposited on glass substrate. From the steepness of the absorption edge we conclude that the films are homogeneous. The optical bandgap is calculated from the plot of $(\alpha h\nu)^2$ versus $h\nu$ (Fig. 3.28) and is found to be 1.80 eV. This is comparable with the value 1.78 eV obtained by Ponomarev et al.[60].

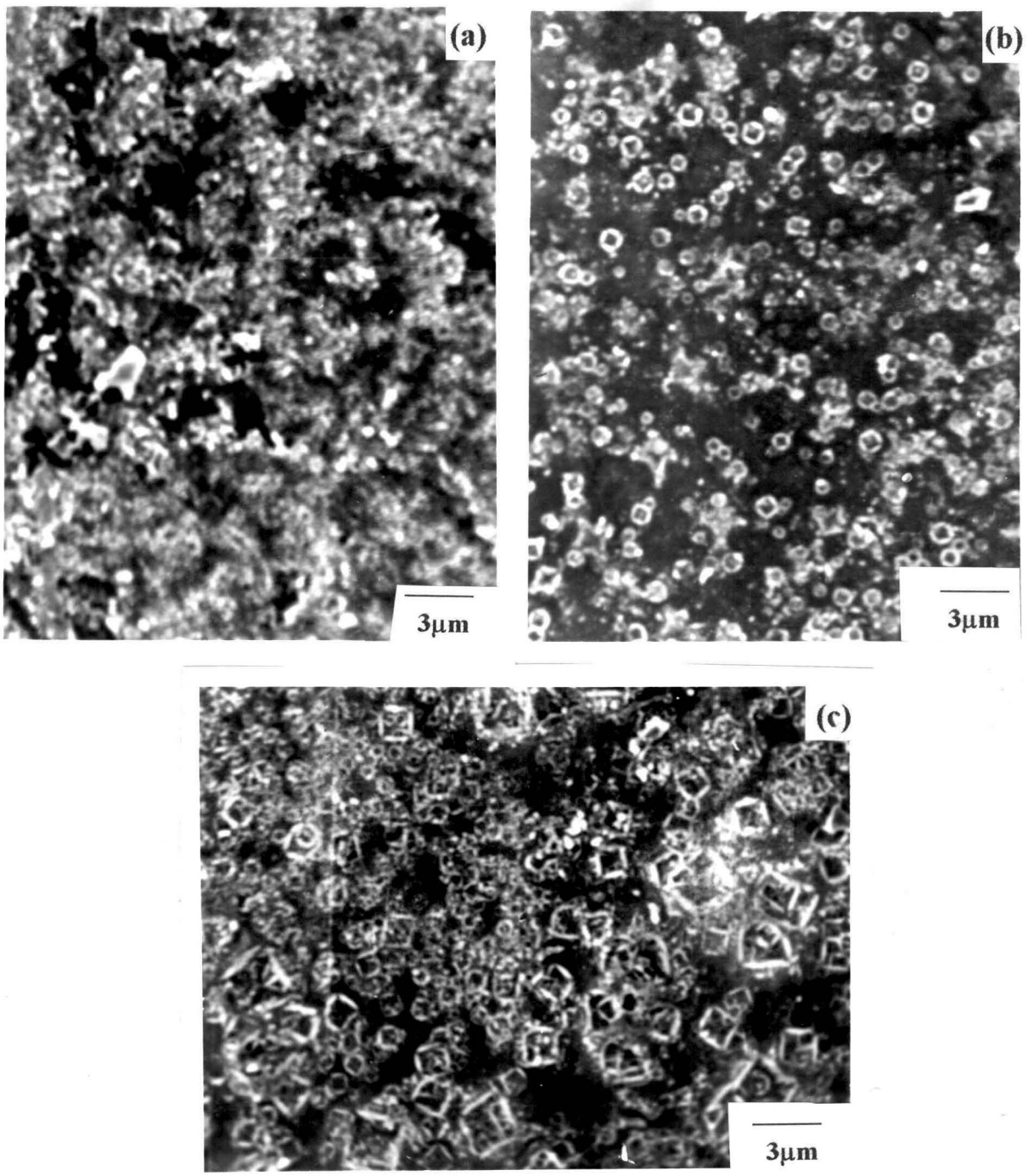

Figure 3.26. Scanning electron micrograph of MoS_2 thin film obtained from deposited on glass substrate at three different baking temperatures [(a), 300° C, (b) 360° C, (c) 450° C.]

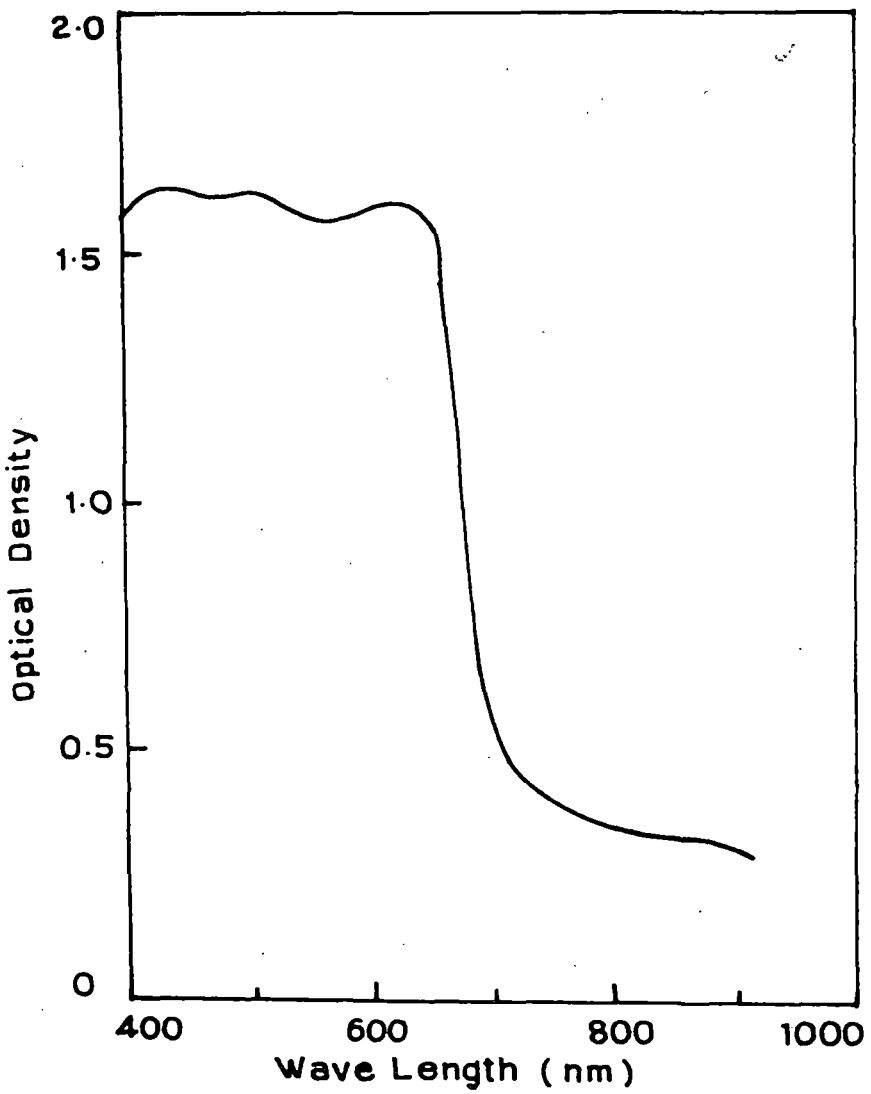

Figure 3.27. Optical absorption spectra of MoS_2 thin films deposited on glass substrate.

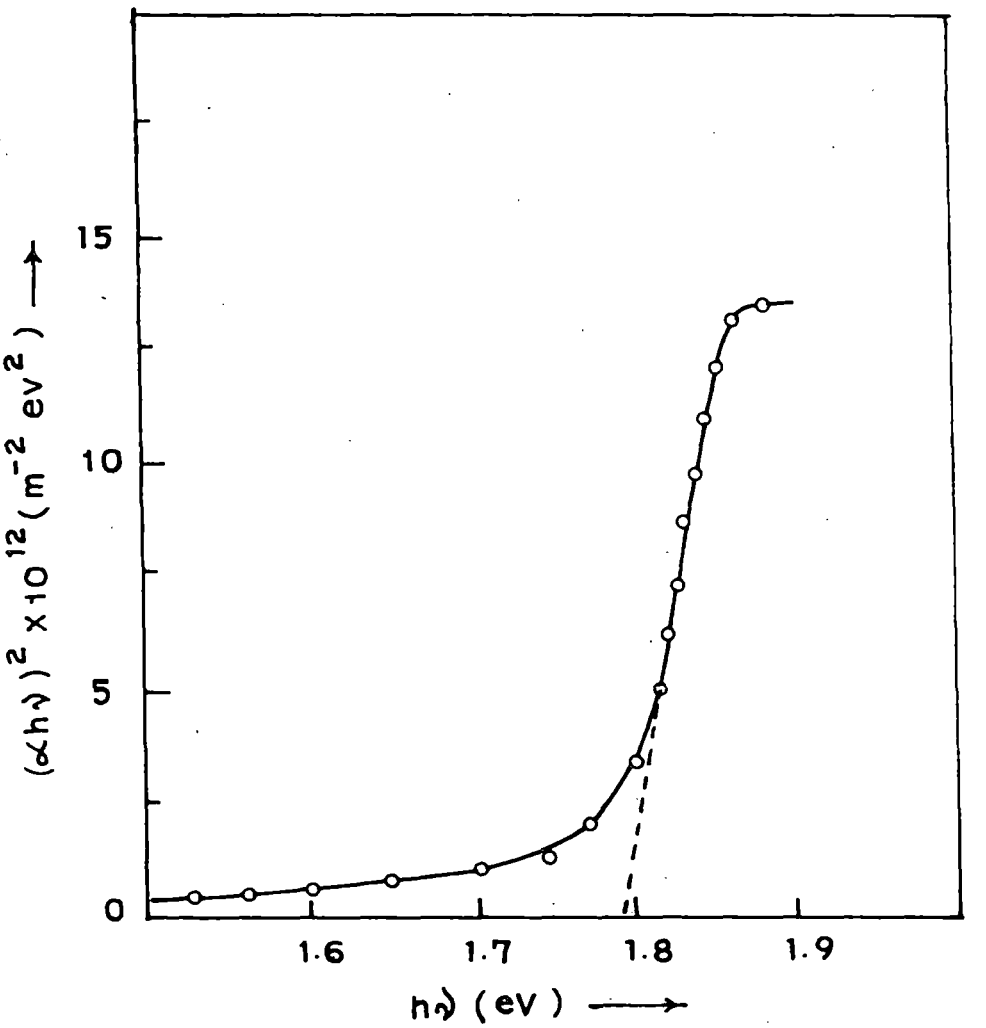

Figure 3.28. Plots of $(\alpha h\nu)^2$ against hν curves of MoS_2 thin films.

3.3.2. COPPER SULPHIDE (Cu_2S) THIN FILM

3.3.2.1. INTRODUCTION

The copper-sulphide Cu_xS ($1 \leq x \leq 2$) system forms a number of phases, which are well known for their application as optoelectronic materials, and continue to be interesting semiconductor materials due to the variation in properties depending on the value of x [69-72]. At least four stable phases are known [73] to exist at room temperature for which their mineralogical names are often used. On the 'copper rich' side of the copper sulphide phase diagram are the orthohorhombic chalcocite (Cu_2S), djurlite ($Cu_{1.95}S$) and anilite ($Cu_{1.75}S$), while in the 'sulphur rich' side is covellite (CuS). Mixed phases are also known in the intermediate composition [74]. The structure of the copper sulphide compounds is quite complicated [75]. Even the structures of Cu_2S and CuS, which appear to be stoichiometric, are not consistent with their formulation as Cu(I) and Cu(II) sulphides. Chalcocite (Cu_2S) can come in its low-temperature from with a rather complex structure or in its high-temperature from of disordered rearrangements of Cu atoms in a close-packed array of S atoms [76]. Likewise, the compound CuS, which occurs as the mineral covellite, has one -third of its metal ions surrounded by three neighbouring S atoms at the corners of a tringle and the remainder have four S neighbours arranged tetrahedrally.

Copper sulphides exhibit a range of electrical properties, from metallic to semi-metallic and semiconductor-like. Due to these characteristics, by suitably adjusting their composition copper sulphides are exploitable in the fabrication of electronic devices [76-77].

Deposition of these films can be made by different techniques, such as vacuum evaporation [78], activated reactive evaporation [79] and chemical bath deposition [80-84].

In this section, the preparation, structural and optical properties of dip deposited Cu_2S thin films have been described shortly.

3.3.2.2. EXPERIMENTAL DETAILS

Film preparation and other parameters was the same as discussed earlier, the only difference being the starting material and the baking temperature. For depositon of Cu_2S films, methanolic solution of copper nitrate (10 gms of copper nitrate in 40 cc methanol) and ammonium thiocyanate (1.6 gms ammonium thiocyanate in 20 cc methanol) were mixed together slowly to yield the starting solution. Films were deposited on soda-glass substrates at three different baking temperature 360° C, 400° C and 500° C for five minutes baking time. Multicoating (5 dip) films having thickness of about 1μm was taken for the characterization of the films. The colour of the films are brown.

For structural properties x-ray diffractometry and surface morphology studies were carried out by PHILIPS diffractometer (model PW 1390) with CuKα radiation (Ni-filter) at 1.54 A° and HITACHI S-530 scanning electron microscope respectively whereas optical absorption data were taken by SHIMADZU UV-240 double-beam spectrophotometer for measurement of optical band gap.

3.3. 2.3. RESULTS AND DISCUSSION

Figure 3.29 shows the XRD patterns of Cu_2S thin films at baking temperature of 400° C, 500° C. Cu_2S peaks are identified from the ASTM data file and shown in table 3.4. A few peaks of CuO also arise in this spectra. Probably some of the copper is oxidised to CuO at this high temperature. The films prepared at the other two baking temperature (360° C & 400° C) are amorphous in nature. A typical scanning electron micrographs of Cu_2S film at 500° C is shown in figure 3.30.

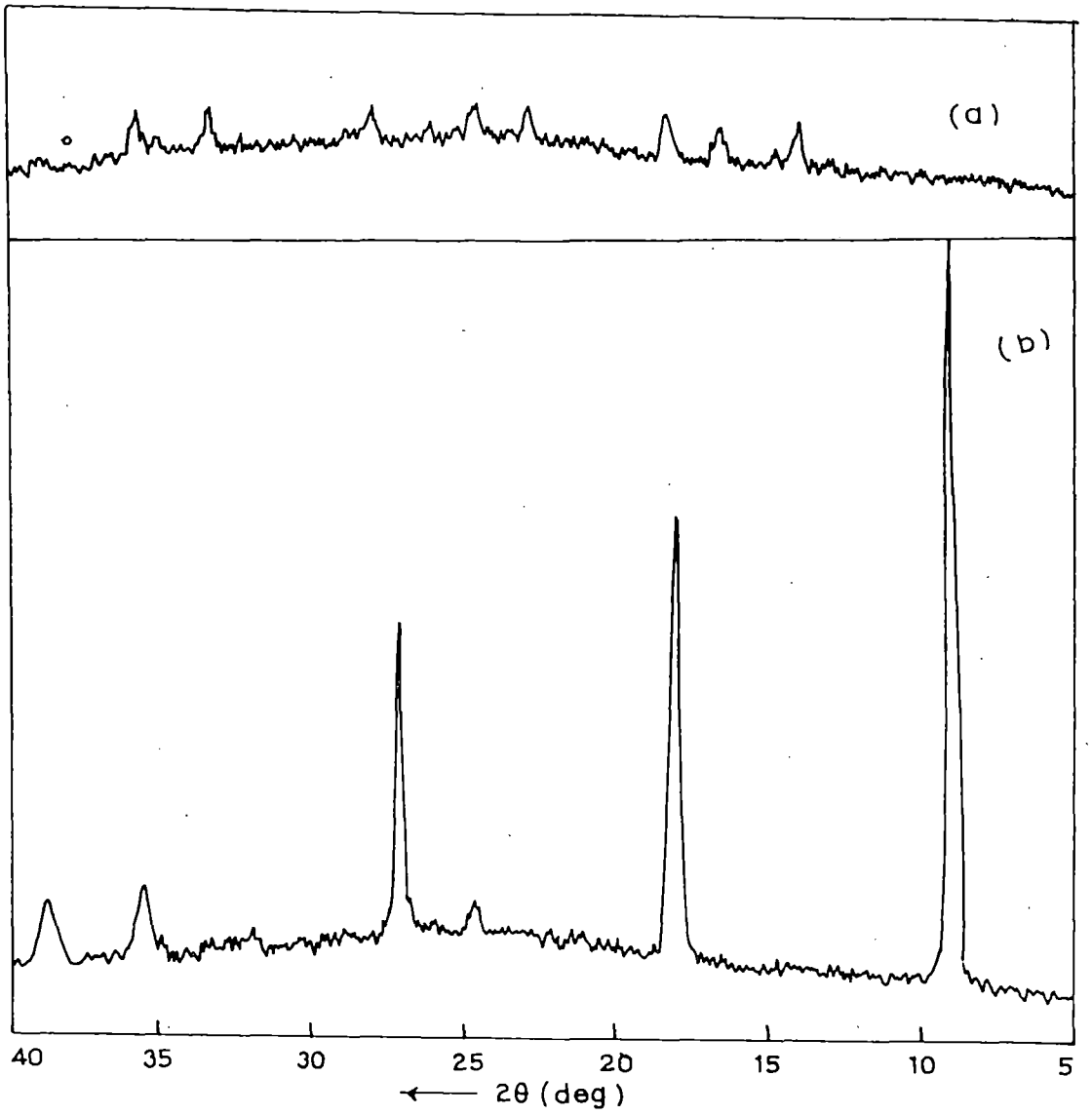

Figure 3.29. X-ray diffractogram of Cu_2S thin films deposited on glass substrate at two different baking temperature [(a), 400° C; (b), 500° C]

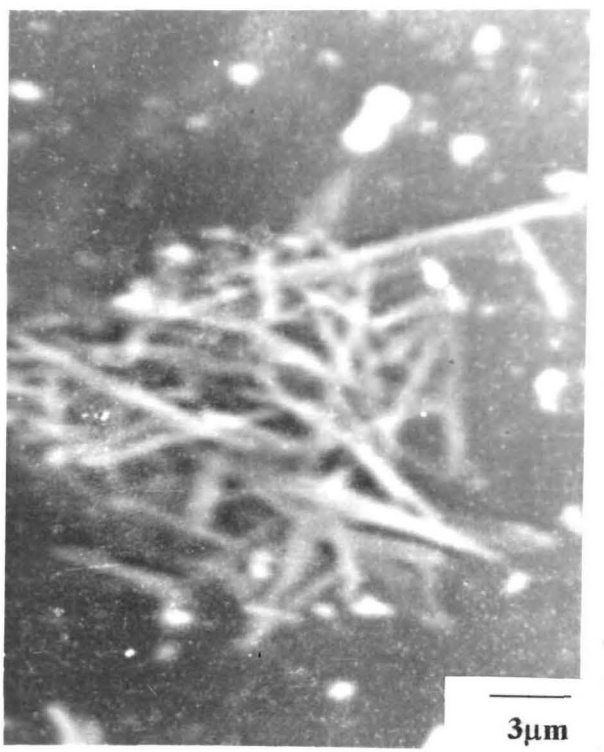

Figure 3.30. A typical scanning electron micrograph of Cu_2S thin film deposited on glass substrate at 500° C

Table - 3.4. Prominent peak position (2θ values) of x-ray diffraction peaks, corresponding d-values and their identification for Cu_2S film.

OBSERVATION			*COMPARISON WITH JCPDS DATA FILE NO. 23-961*		*hkl*
Peak position (2θ)	Observed d- values (A°)	Intensity (I/I_0)	Comparable d- values (A°)	Intensity (I/I_0)	
24.80	3.59	16	3.59	16	162, 203
27.00	3.30	57	3.31	25	322
35.70	2.51	19	2.52	40	$0\underline{1}02^{+}$
38.80	2.32	17	2.32	40	$2\underline{1}02, 471^{+}$

Figure 3.31 shows the optical absoption of Cu_2S films deposited on glass substrtate. The value of the band gap, Eg was determined in the usual way from the intercept of the $(\alpha h\nu)^2$ versus hν plots (fig.3.32) which was a straight line on the hν axis. The optical band gap obtained from this curve is about 1.4 eV. This value is good agreement with the value obtained by other workers [79].

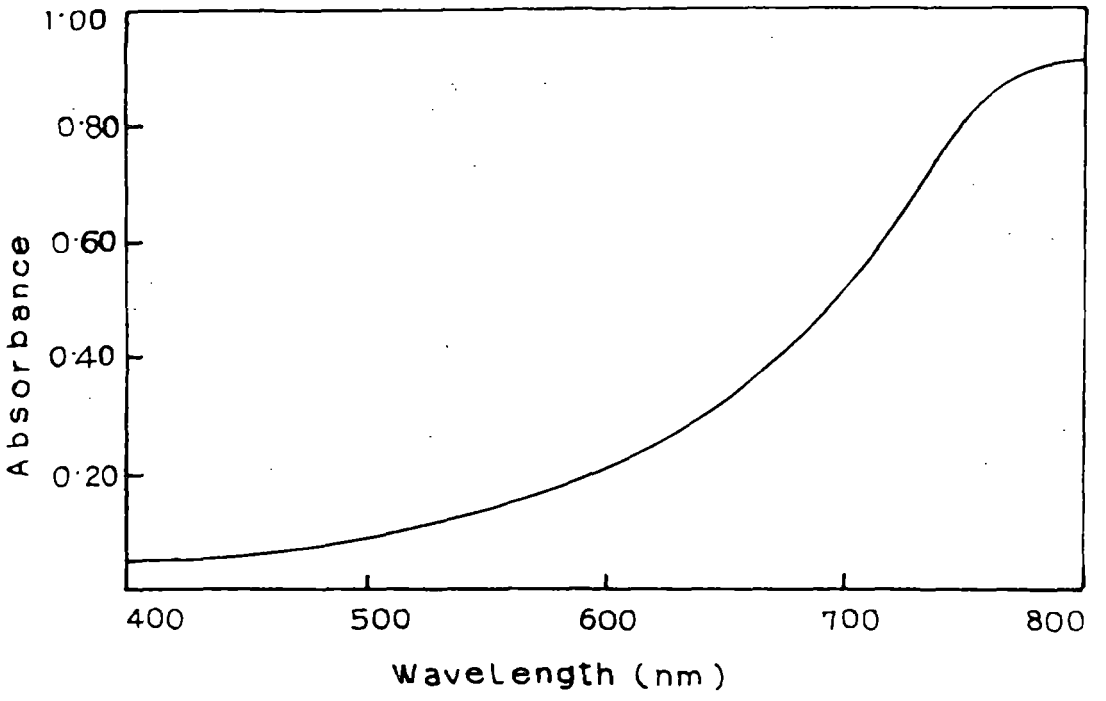

Figure 3.31. Optical absorption spectra of Cu_2S thin films deposited on glass substrate at 400° C.

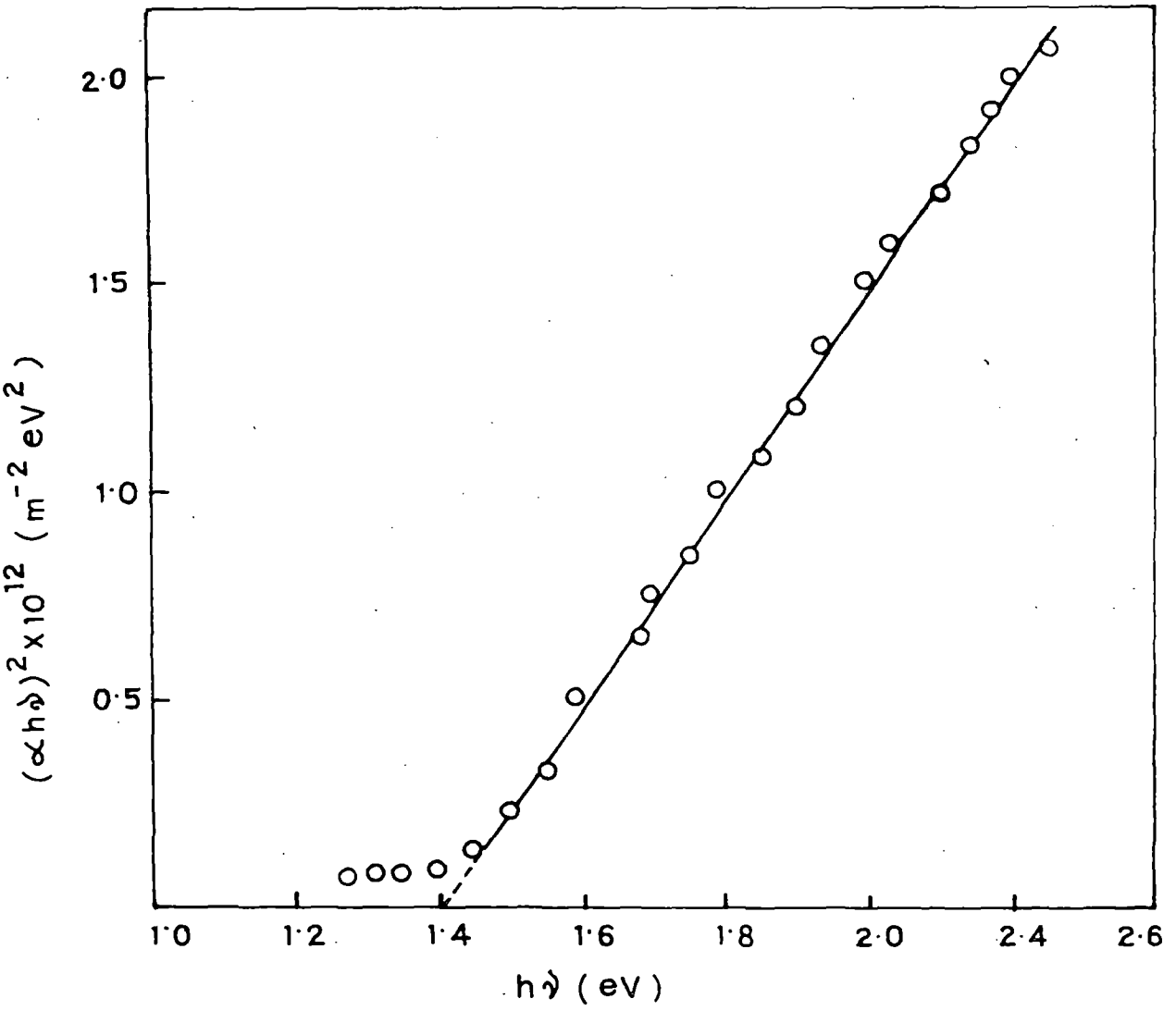

Figure 3.32. Plots of $(\alpha h\nu)^2$ against hν curves of Cu_2S thin film.

3.4. CONCLUSION

Dip technique is a simple and suitable method of obtaining adherent, specular, homogeneous and stoichiometric sulphide thin solid films. In this present chapter, we have prepared successfully a number of sulphide films which may be used in solid state devices. All these films are smooth, uniform and have the usual crystal structure for these materials.

$Zn_xCd_{1-x}S$ ($0 \leq x \leq 0.6$) films were hexagonal in structure, whose lattice parameter ***c*** and ***a*** were found to decrease with increase in x. An increase in x also produces a similar drop in the thickness of the film, the total number of (Cd + Zn) moles in the starting solution remaining constant. This agrees well with the fact that the Zn atoms have a relatively smaller size compared to Cd atoms. The bandgaps obtained from optical absorption and spectral response of photoconductivity measurements are in good agreement with each other and vary from 2.30 eV (CdS) to 2.69 eV ($Zn_{0.6}Cd_{0.4}S$), beyond which the bandgaps obtained from optical absorption measurements (optical bandgap) are much less than that obtained from photoconductive measurements owing to the films becoming amorphous over this range. Surface morphology study by SEM as well as XRD data show that good crystallinity is obtained upto a zinc atomic fraction of 0.4.

SnS ans SnS_2 thin film shows good crystalline structure when prepared at a baking temperature of 300° C for SnS and 360° C for SnS_2 films. Bandgaps obtained from photoconductivity measurements are 1.4 eV and 2.4 eV for SnS and SnS_2 films respectively. Optical absorption measurements on SnS_2 films also yield a value of 2.4 eV. Antimony-doping of SnS_2 films produces an increase in bandgap along with a sharp reduction in crystallinity.

Annealing in air at 400° C both SnS and SnS_2 films convert them to transparent conducting tin dioxide, thus providing an alternative route for its preparation.

MoS_2 thin films show a crystalline structure for a baking temperature of 360° C and 450° C, whereas at 300° C these are amorphous in nature. Optical absorption data shows the films are uniform and homogeneous. The optical bandgap, which was calculated from the absorption data, is 1.80 eV and is comparable with the literature value.

Cu_2S thin films have crystalline structure when the baking temperature was 500° C but has some CuO present because of the oxidation at this high temperature. Optical bandgap, calculated from optical absorption data is 1.4 eV, which is again in agreement with that obtained by other workers.

REFERENCES

1. Y. Endo and T. Taguchi, 1989 *Proc. Mater. Res. Soc.*, Boston,
2. S.Y. Yin, A. L. Fahrenbruch and R.H. Bube 1978 *J.Appl. Phys.* **49** 1294
3. K. T. RamaKrishna Reddy and P. Jayarama Reddy 1992 *J. Phys. D: Appl. Phys.* **25** 1345
4. Kim W. Mitchell, Alan L. Fahrenbruch and Richard H. Bube 1977 *J. of Appl. Phys.* **48** 4365
5. Bulent M. Basol 1984 *J. appl. Phys.* **55** 601
6. Y. K. Jun and H. B. Lm 1988 *J. Electrochem. Society: Electrochemical Science and Technology* **135** 1658
7. Hyeong Soo Kim and Ho Bin Lm 1992 *Thin Solid Films* **214** 207
8. J. Torres and G. Gordillo 1992 *Thin Solid Films* **207** 231
9. Trever A.chynoweth and Richard H. Bube 1980 *J. of Appl. Phys.* **51** 1844
10. T. Yamaquchi, J. Matsufusa and A. Yoshida, 1992 *Jpn. J. Appl. Phys.* **31** L.703
11. T. Walter, M. Ruckh, K. O. Velthaus and H.W. schock, 1992 *Proc. 11th EC Photovoltaic Solar Energy Conf., Montreux,* P.124
12. L. C. Burton and T. L. Hench 1976 *Appl. Phys. Lett.* **29** 612
13. N. Romeo, G. Sberveglieri and L. Tarricone 1978 *Appl. Phys. Lett.* **32** 807
14. O. P. Agnihotri and B. K. Gupta 1979 *Jpn. J. Appl. Phys.* **18** 317
15. R. R. Chamberlin and J. S. Skarman 1966 *J. Electrochem. Soc.* **113** 86.
16. A. Mzerd, D. Sayah, I. J. Saunders and B. K. Jones 1990 *Phys. Stat. Sol. (A)* **119** *487*
17. K. Yamaguchi and S. Sato 1994 *Jpn. J. Appl. Phys.* **23** 126
18. Y.F.Nicolau and J. C. Menard 1988 *J. of crystal growth* ***92*** *128*

19. G. K. Padam, G. L. Malhotra and S. U. M. Rao 1988 *J. Appl. Phys.* **63** 770

20. Y. Sakurai, Y. Kokubun, H. Watanabe and M. Wada 1977 *Jpn. J. Appl. Phys.* **16** 2115

21. S. Yamaga, A. Yoshikawa and H. Kasat 1990 *J. Crystal Growth* **94** 432

22. T. Karasawa, K. Ohkawa and T. Mitsuyu 1991 *J. Appl. Phys.* **64** 3226

23. Takeshi Karasawa, Kazuhiro Ohkawa and Tsuneo Mitsuya 1991 *J. of Appl. Phys* **69** 3226

24.A. Kuroyanagi and T. Suda 1989 *Thin Solid Films* **176** 247

25. A. Kuroyanagi 1990 *J. Appl. Phys.* **68** 5567

26. H. Schroeder. *Oxide layer deposited from organic solutions In G. Hass and R. F. Thun (eds),* 1969 *Physics of Thin Films.* **Vol. 5** Academic Press, New York pp. 87-141

27. C. Terrier, J. P. Chatelon, R. Berjoan and J. A. Roger 1995 *Thin Solid Films* **263** 37

28. M. K. Karanjai and D. DasGupta 1987 *Thin Solid Films* **155** 306

29. JCPDS, Swarthmore, PA Card no. 06 - 0314

30. T. Yamaquchi, Y. Yamamoto, T. Tanaka, Y. Demizu, A. Yoshida 1996 *Thin Solid Films* **281-282** 375

31. R. S. Feigeelson, A. N. Diaye, S. Y. Yin and R. H. Bube 1977 *J. Appl. Phys.* **48** 3162

32. C. M. Mbow, G. W. Cohen-Solal and D. laplaze 1982 Thin Solid Films 87 141

33. R. Hill 1974 *J. Phys C: Solid State Physics* 7 521.

34. K. L. Chopra, R. C. Kainthla, D. K. Pandya and A. P. Thakoorin G. Hass,

M. H. Francombe and J. L. Vossen (eds) 1982 *Physics of thin films* **Vol. 12 Academic Press, New York, P. 167.**

35. W. Albers, C. Hoss, H. I. Vink and I. D. Wassher 1961 *J. Appl. Phys.* **32** 2220.
36. P. M. Nikolic and D. M. Jodoruvic 1986 *J. phys. C. Solid State Physics* **20** 39.
37. M. Sharon, K. Basavaswaran and N. P. Sathe 1985 *J. Sci. Ind. Res.* **44** 593.
38. M. Sharon and K. Basavaswaran 1987 *Solar Cells.* **20** 323.
39. M. Sharon and K. Basavaswaran 1988 *Solar Cells* **25** 91.
40. K. Kawano, R. Nakata and M. Sumita 1989 *J. Phys. D: Appl. Phys.* **22** 136.
41. M. S. Whittingham and A. J. Jacobsen 1982 *Fds. Intercalation Chemistry* **(Academic Press, New York)**
42. W. Hofman 1935 *Z. Kristallogr.* **92** 161.
43. S. Bucchia, J. Jumas and M. Maurir 1981 *Acta Crystallogr. B* **37** 1903.
44. J. Offedol 1928 *J. Phys. Chem.* **134 No. 3/4** 301.
45. D. Mootz and A. Puhl 1967 *Acta Crystallogr.* **23 No.** 3 471.
46. L. D. C. Bok and J. C. A. Boeyens 1957 *J. S. Afric Chem Inst.* **10 No. 2** 49.
47. I. S. Anderson, M. C. Morton 1945 *Proc R. Soc. A* **48** 83.
48. M. Ristov, G. J. Sinadinovski, I. Grozdanov and M. Mttocski 1989 *Thin Solid Films* **173** 53.
49. T. Shibata, Y. Muranushi, T. Miura and T. Kishi 1991 *J. of Material Science* **26** 5107.
50. Zulkarnain Zainal, Mohd Zobir Hussein and Arniza Ghazali 1996 *Solar Energy Materials and Solar Cells* **40** 347.

51. R. Banerjee, Swati Ray and A. K. Barua 1984 *Indian J. Physics* **58** 166.

52. P. K. Nair, M. T. S. Nair, Ralph A. Zingaro and Edward A. Meyers 1994 *Thin Solid Films* **239** 85.

53. W. H. Bauer 1956 *Acta Cryst.* 1 515.

54. H. Tributsch 1980 *Faraday Discuss.* **70** 1.

55. H. Tributsch and J. C. Bennelt 1977 *J. Electroanal.Chem.* **81** 97.

56. T. A. Recoraro and R. R. Chaianelli 1981 *J. Catal.* **67** 430.

57. R. Reichelt and G. Mair 1978 *J. Appl. Phys.* **49** 1245.

58. T. Spalvins 1978 *Thin Solid Films* **53** 286.

59. T. Spalvins 1969 *ASLE Trans.* **12** 36.

60. E. A. Panomarev, M. Neumann-Spallart, G. Hodes, C. Levy-Clement 1996 *Thin Solid Films* **280** 86.

61. J. Moser and F. Levy 1994 *Thin Solid Films* **240** 56.

62. P. Gribi, Z. W. Sun and F. Levy, 1989 *J. Phys. D. Appl. Phys.* **22** 238.

63 H. Dimigen, H. Hubsch, P. Willich and K. Reichelt 1985 . *Thin Solid Films* **129** 79.

64. L.F. Schneemeyer and U. Cohen 1983 *J. Electrochem. Soc.* **130** 1536.

65. N. T. McDevill, J. S. Zabinski and M. S. Donley 1994 *Thin Solid Films* **240** 76.

66. J. S. Zabinski, M. S. Donley, V. J. Dyhouse and M. T. Mcdevitt 1992 *Thin Solid Films* **214** 156.

67. V. Yu. Fominski, A. R. Markeev, V. N. Nevolin, V.B. Prokopenko and A. R. Vrublevski 1994 *Thin Solid Films* **248** 240.

68. E. Bucher, *Photovoltaic properties of solid state junctions of layered Semiconductors, in A. Aruchany (ed), Photoelectro chemistry and Photovoltaics of layered Semiconductors, Kluwer, Dordrecht,* 1992, **pp. 36.**

69. J. J. Loferski,J. Shewehum, S. D. Mittleman , E. A. De Meo, R. Arnott, H. L. Hwang, R. Beauliew and G. Chapman 1979 *Solar Energy Mater.* **1** 152.

70. M. Savelli and J. Bougnot, in B.O. Serophin (ed) 1979 *Solar Energy Conversion: Topic In Applied Physics* **Vol. 31 Springer, Berin** P. 231.

71. K. Okamoto and S. Kawai 1973 *Jpn . J. Appl. Phys.* **12** 1130.

72. S. Couve, L. Gouskov, L. Szepessy, J. Vedel and E. Castel 1973 *Thin Solid Films* **15** 223.

73. I. Grozdanov, C. K. Barlingay, S. K. Dey, M. Ristov and M. Najdoski 1994 *Thin Solid Films* **250** 67.

74. A.F. Well 1962 *Structural Inorganic Chemistry, Clarendon Press, Oxford, 3rd edn.* P. 883.

75. S. Djurle 1958 *Acta Chem. Sand.* **12** 1415.

76. E. Ramli, T. B. Rauchfiuss and C. l. Stern 1990 *J. Am. Chem. Soc.* **112** 4043.

77. H. Fjellvag, F. Gronvold, S. Stolen. A. F. Andersen, R. Mullerkafer and A. Simon 1988 *Z. Kristallogr* **184** 111.

78. B. Rezig, S. Duchemin, F. Guastavino 1979 *Sol. Energy Mater.* **6** 53.

79. H. S. Randhawa, R. F. Bunshah, D. G. Brock, B. M. Basol and O. M. Staffsudd 1982 *Sol. Energy Mater.* **6** 445.

80. R.N. Bhattacharya and P. Pramanic 1981 *Bull Mater Sci.* **3** 403.

81. M. T. S. Nair and P. K. Nair 1989 *Semicon. Sci. Technol.* **4** 191.

82. K. M. Gadave and C. D. Lokhande 1993 *Thin Solid Films* **229** 1.

83. M. Inoue, C. Cruz-Vazquez, M. B. Inoue, K. B. nebesny and Q. Fernando 1993 *Snthetic Metals* **55-57** 3748.

84. Takakazu Yamamoto, Kuniaki Tanaka, Etsuo Kubota and Kohtaro Osakada 1993 *Chem. Mater.* **5** 1352.

CHAPTER - 4

*Transparent conducting Tin dioxide thin films Prepared by open air chemical vapour deposition(OACVD) technique

*4.1 INTRODUCTION

The simultaneous occurrence of high optical transparency (more than 80 %) in the visible region and high electrical conductivity (about 10^3 Ω^{-1} cm^{-1} or more) is not possible in an intrinsic stoichiometric material. Partial transparency and fairly good conductivity may be obtained in thin films of a variety of metals. The only way to obtain good transparent conductors is to create electron degeneracy in a wide band gap (more than 3 eV) oxide by controllably introducing non-stoichimetry and /or appropriate dopants. The most popular transparent coatings are fabricated from metal oxides, in particular the oxides of indium, tin and zinc.

Tin oxide thin films are known to have high mechanical and chemical stability, except for their interaction with oxygen atoms at high temperature. These films have high transmittance in the visible region and a high reflectivity in the infrared region. They also possess a high electrical d.c. conductivity and Hall mobility. Undoped tin oxide films are n-type degenerate semiconductor with a wide band gap (approximately 3.5 - 4 eV) [1-3], and a refractive index of approximately 1.9 [3]. However, the properties of tin dioxide depend crucially on their deviation from stoichiometry, on the nature and amount of impurities, and on the microstructure. All these properties depend on the deposition method and parameters, and on post-deposition processing.

*** Published in the "journal of Thin Solid Films" Vol. 307 (1998) P. 221-227.**

Owing to their high chemical and mechanical stabilities, transparent conductive tin dioxide are largely employed in electrochemistry as transparent electrodes [4, 5] or as substrates for electrodeposition [6] in solid state devices for photovoltaic and optoelectronic applications [7-9] or as spectrally selective coatings [10]. Apart from these applications transparent conducting tin oxide can also be used in thin film resistors, transparent heating element for aircraft and automobile windows, antistatic coatings for instrument windows, heat reflecting mirrors for glass windows and incandescent bulbs, antireflection coatings, liquid crystal display, electrochromic and ferroelectric photoconductor storage, semiconductor / insulator / semiconductor (SIS) heterojunctions, and protective and wear-resistant coatings for glass containers [11]. There is growing interest in newer applications of tin oxide and one of the most important uses is for the detection of toxic and explosive gases in air such as carbon monoxide and methane [12,13].

Tin oxide is a high bandgap semiconductor which is made conductive by n-type dopants which fall into two categories: (i) pentavalent metals such as antimony which substitute for tin atoms, and (ii) halogens such as fluorine or chlorine which replace oxygen. The choice of dopant can be guided by understanding that tin oxide is a fairly ionic compound for which the metal orbitals dominantly form the conduction band, while the oxygen orbitals make up most of the filled valence band. Substituting a metal for tin induces a large local perturbation in the conduction band, frequently scattering the electrons in the conduction band. This reduces the mobility of the electrons, which degrades the conductivity and transparency of the material. A halogen substituting for oxygen, however, mainly disturbs the filled valence band, and only slightly disturbs the electrons in the conduction band. Of the halogens, fluorine causes the least scattering, and fluorine doping leads to tin oxide films with the highest conductivity [11], because these films generally have higher mobilities (about 25 - 50 cm^2

V^{-1} S^{-1}) than undoped SnO_2 films. In either type of substitution, a positively charged scattering center is produced.

Tin dioxide films have been prepared by various techniques such as chemical vapour deposition [14-18], spray pyrolysis [19-23], vacuum evaporation [24], reactive rf sputtering [25-28], sol-gel method [29-32] and glow discharge [33]. In this chapter, Open Air Chemical Vapour Deposition (OACVD) technique has been employed for the preparation of undoped and doped tin dioxide thin films and to study their different properties.

4.2. DEPOSITION OF SnO_2 FILM BY CVD

In the last several years, the deposition techniques for SnO_2 have undergone many changes, mainly as a result of the work of international research groups led by Bube, Bunshah, Manifacier and Chopra [1,8,11]. Many sophisticated deposition techniques have been developed. The foremost characteristics of a Chemical Vapour Deposition (CVD) technique is that it involves a heterogeneous chemical reaction at the surface of a substrate without requiring vacuum as an essential condition for deposition. The chemical reaction in CVD may be activated by the application of light, heat, RF field, x-ray radiation, electrical arc, glow discharge, electron bombardment, or by catalytic activity of the substrate surface.

Metallic oxides are usually deposited by the vaporization of a suitable metal-bearing compound (which is volatile, thermally stable at a temperature sufficiently high to produce an adequate vapour pressure and thermally unstable at higher temperatures of deposition - criteria generally fulfilled by organometallic compounds) and its in situ oxidation with O_2 or H_2O [34]. Argon, O_2 or N_2, are generally used as carrier gases. Some heterogeneous reactions leading to the formation of SnO_2 are given below.

$$SnCl_4(g) + O_2(g) \rightarrow SnO_2(s) + Cl_2 \quad ---(4.1.)$$

$$(CH_3)_4Sn(g) + 8O_2(g) \rightarrow SnO_2(s) + 6H_2O(g) + 4CO_2(g) \quad ---(4.2.)$$

$$SnCl_4(g) + 2H_2O \rightarrow SnO_2(s) + 4HCl(g) \quad ---(4.3.)$$

The mechanism of film formation via the above reactions has been throughly examined by Ghoshtagore [35]. In all cases, the reaction of $SnCl_2$ or $(CH_3)_4Sn$ has been found to take place at the surface with an adsorbed oxygen atom or water molecule. The main control parameters in the process are gas flow and composition, substrate temperature and geometry of the deposition apparatus. The deposition rate depends mainly on the gas flow rate and substrate temperature. Typical rates are about 300-1000 A^o min^{-1}, although much higher rates have been also reported [37,38]. The substrate temperature is generally in the range 350 - 400° C. Higher temperatures favour better crystallinity [34,39] and larger grain size [34,39-40] resulting in higher mobilities [34]. The geometry of the deposition system is of the utmost importance, especially for large-scale applications. A maximum solar transmittance of about 85% - 95% with a minimum resistivity as low as about 7 X 10^{-5} Ω cm is achievable by the CVD method [14-18 & 34-36].

In a previous report, Karanjai et al. [41] had described an extremly simple and low-cost chemical vapour deposition method for tin dioxide films. In that method, the starting material was $SnCl_2.2H_2O$ crystal which were ground with water into a paste and the paste applied in the form of 4-5 mm wide band near, and parallel to the lower edge of a substrate positioned vertically. On heating in air the paste decomposes according to the following equation.

$$6SnCl_2 + H_2O \rightarrow 2SnCl_4 + 4Sn(OH)Cl \quad ---(4.4.)$$

$SnCl_4$, which is generated as one of the reaction products, rises upward due to convection and hydrolyses on the heated substrate to produce a tin dioxide film according to the equation.

$$SnCl_4 + 2H_2O = SnO_2 + 4HCl \quad \ldots\ldots\ldots\ldots (4.5)$$

Doping with antimony can be achieved by mixing requisite amount of $SbCl_3$ with $SnCl_2$ paste. Considering the simplicity of the method, films of reasonable good quality can be obtained.

This so called "paste - heat " method, however suffers from the following disadvantages: (i) the portion of the substrate where the $SnCl_2$ paste was applied must be subsequently cut away before the films can be used, (ii) because of the geometry of the arrangement, the films are non-uniform, being thickest near the paste - coated area and becoming thinner away from it, and (iii) non-planar substrates, as also those with small sizes cannot be used.

4.3. EXPERIMENTAL DETAILS

Open Air Chemical Vapour Deposition (OACVD) method is mainly based on the principle of Chemical Vapour Deposition technique and modification of the above "paste-heat" method [41], which employs the same principle, and maintains essentially the same simplicity, at the same time enabling one to obtain films free from the defects discussed above. Here, the reaction is activated by heat only. It does not require any specialized sophisticated experimental setup, and hence can be carried out in any laboratory. In OACVD method the films were obtained simply by passing $SnCl_4$ vapour using air current due to convection through a long tube on a heated substrate in atmospheric conditions. Using this method, preparation of undoped and doped (Sb, Mo & F) tin dioxide thin films have been prepared and their electrical and optical properties as well as surface morphology and crystal structure are studied.

In this method a 75 cm. long glass tube of internal diameter 5 cm. was placed vertically as shown in Figure 4.1. The tube was heated from outside in atmospheric condition by winding a heater coil on its outer surface over a length of 70

cm. The substrate was placed vertically in the central region of the tube. The starting material was taken in a conical flask placed at the bottom of the tube and heated separately. The temperature of the substrate was measured by a thermocouple placed close to it. The starting material was prepared by mixing crystals of $SnCl_2$, $2H_2O$ with a few drops of water along with any dopant material that might be added and was stirred mechanically to convert it to a paste.

In the film forming process, the substrate was initially heated to attain the desired temperature after which the $SnCl_2$ paste was heated. White fumes were given off by the paste and were seen to deposit SnO_2 films where they came into contact with the hot substrate.

Using this method, it is possible to deposit a number of films in a batch, by attaching them to a holder, which is placed in the central region of the tube. Usually both sides of the substrate are coated by this method, which is advantageous in some special cases [42], but it is also possible to coat one side only by masking the other side, or by fixing two substrates back to back. This method is especially advantageous for inaccessible surfaces and the inside surface of a tube, where one can obtain a coating quite easily, in contrast to rather complex arrangements required in usual CVD methods. The films were usually deposited over microglass slides (7.5 cm. x 2.5 cm.) and showed uniform interference colour over their entire area except at the edges. But uniform films could also be routinely obtained, if necessary, over a larger area of 40 cm. long by 4 cm. wide.

Undoped tin dioxide films of various thicknesses were prepared at substrate temperatures of 350° C, 400° C and 450° C. Soda glass microslides, mica and Al-sheet were used as substrates.

The films were doped with Antimony, Fluorine and Molybdenum by adding Antimony trichloride (15 mg for 1.5 at% Sb-doped), Ammonium fluoride (275

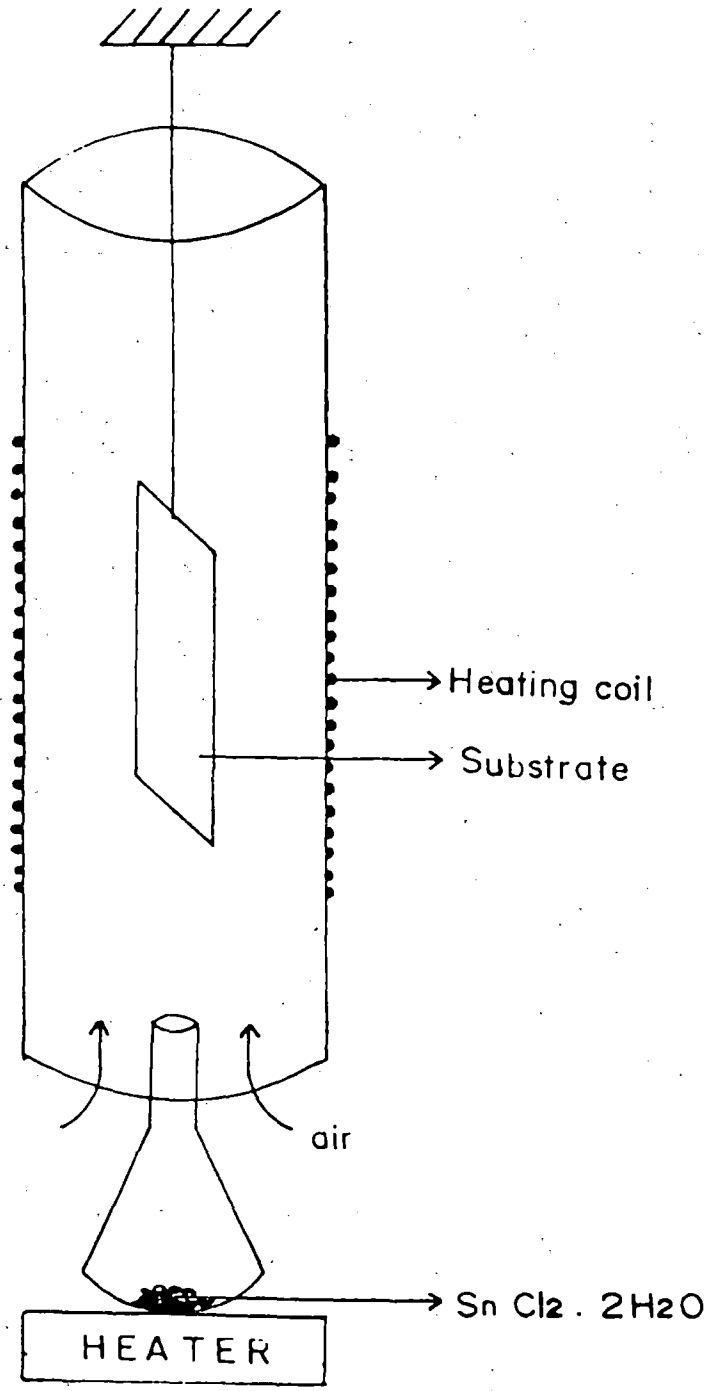

Figure 4.1. Experimental setup of Open Air Chemical Vapour Deposition (OACVD) method for deposition of thin films.

mg for 4.5 at% F-doped) and Ammonium molybdate (70 mg for 6 at% Mo-doped) respectively to the $SnCl_2.2H_2O$ (25 gm) starting material. Electronic grade materials were used for the preparation of these films. Characterization of the films was carried out by optical transmission and electrical conductivity measurments, X-ray diffractometry and scanning electron microscopy.

4.4.EXPERIMENTAL RESULTS

The films were smooth, highly uniform and resistant to peeling - off and acids, and also showed long term stability with respect to their optical, electrical and mechanical properties. They displayed characteristic interference colours. It was found that using this process a substrate temperature of 400° C was necessary to prepare films of the very high quality in terms of conductivity, optical transmission, uniformity and resistance to peeling - off and acids as well as environmental shocks.

4.4.1. X- ray diffractometric study

The undoped and doped tin dioxide films are polycrystalline and have a rutile structure with lattice parameters corresponding to those of bulk tin dioxide. Although the undoped tin dioxide films are randomly oriented, doping leads to orientation effects.

X-ray diffractometric studies were carried out on undoped and doped (Sb, Mo & F) SnO_2 films deposited at a substrate temperature of 400° C using Philips diffractometer (model PW 1390) with CuK_α radiation at 1.54 Å. Diffraction peaks for undoped SnO_2 films having two different thicknesses are shown in figure 4.2(a). Figure 4.2(b) shows the x-ray diffractograms of Sb and F-doped SnO_2 films. The crystal structure is in accordance with the usual tetragonal form of SnO_2 .

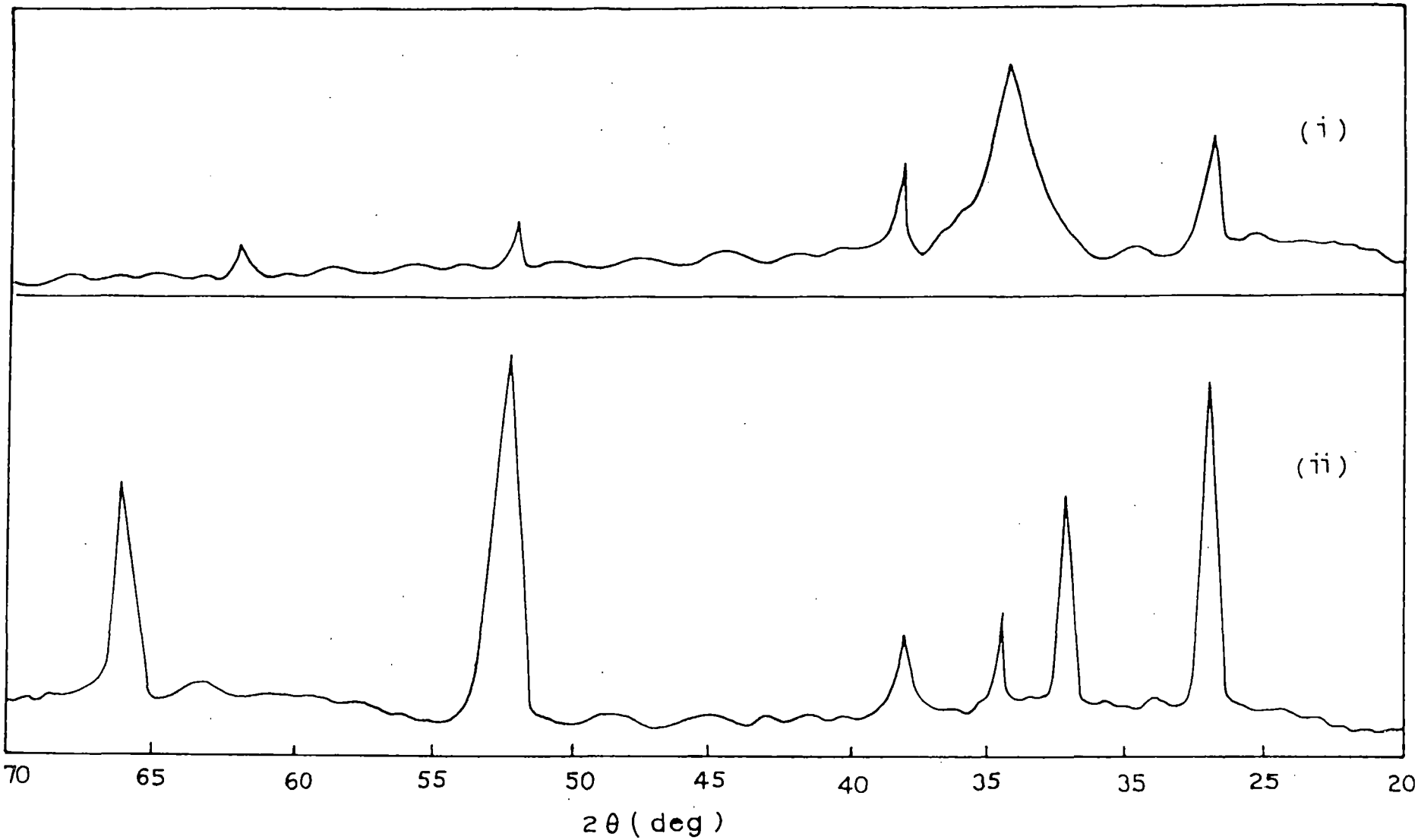

Figure 4.2. (a). X-ray diffractogram of undoped SnO_2 films of two different thickness (T_s = 400° C) (i) 0.6 μm (ii) 2.5 μm.

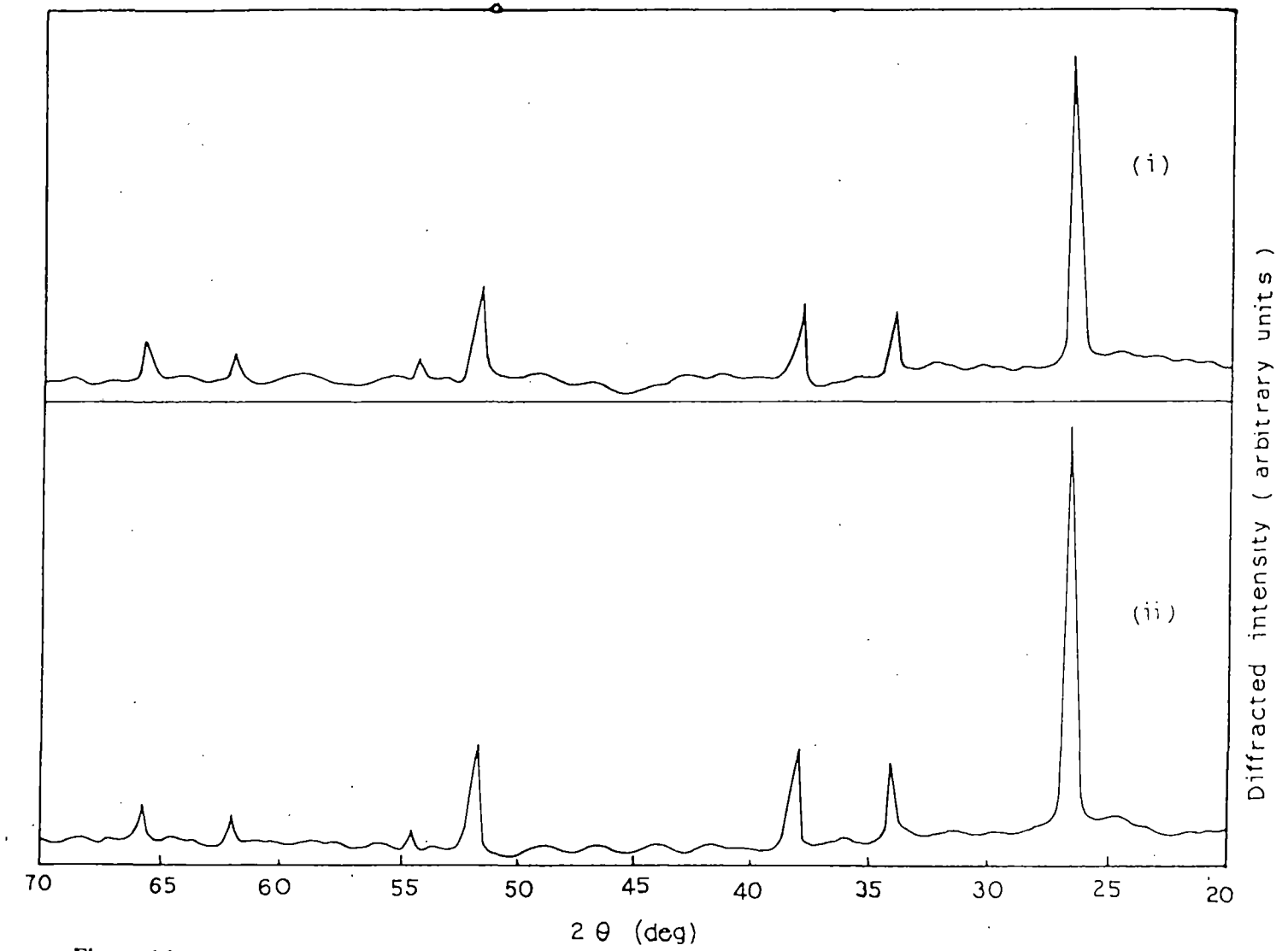

Figure 4.2.(b) X-ray diffractogram of doped SnO_2 films (T_s= 400° C). (i) 1.5 at% Sb-doped, (ii) 4.5 at% F-doped

It is clear from the XRD patterns that there is no amorphous background in the diffractograms of the deposited films. Moreover, none of the undoped films show any preferred orientation, while those doped with Sb and F shows preferred orientation along the (110) planes. Prominent peaks, their d-values and relative intensities (I/I_0) for a typical F-doped films are listed in Table - 4.1.

Table - 4.1. ***Prominent peak position (2θ values) of the X- ray diffraction peaks, corresponding d - values, relative intensities (I/I_0) and their identification for F - doped SnO_2 films.***

Observed Values			**Comparable values from ASTM data file**			
(2θ)	d-values(A^o)	(I/I_0)	(2θ)	d-values(A^o)	(I/I_0)	h k l
26.60	3.347	100	26.57	3.351	100	110
33.90	2.641	21	33.86	2.644	80	101
37.95	2.368	32	37.94	2.369	25	200
51.75	1.764	34	51.73	1.765	65	211
54.85	1.671	12	54.74	1.675	18	220
61.95	1.496	12	61.86	1.498	14	310
65.90	1.415	13	65.94	1.415	16	301

4.4.2. Surface Morphology

Surface morphology studies were carried out by HITACHI S-530 scanning electron microscopy. The scanning electron micrographs of these films indicated that the coarseness of the surface increases with increasing deposition temperature and dopant concentration. Surface topographies of undoped, 6 at% Mo-doped, 1.5 at% Sb-doped, and 4.5 at% F-doped SnO_2 films deposited at a substrate temperature of

400° C are shown in figure 4.3. It is observed that in all cases except that of Mo-doped films large size grains of ~ 1.7 μm are spread through out the film over a background of grain size ~ 0.6 μm. These large grains are observed to disappear when doped with Mo. The average grain size for Sb and F-doped films are found to be larger, while that for Mo-doped films are smaller compared to the undoped ones.

Films were also deposited on different substrates to investigate the substrate effect. Figure 4.4 shows the SEM micrographs of undoped SnO_2 films deposited on mica and aluminium sheet at a substrate temperature of 400° C. It is also evident from figure 4.4 that the grain size of the undoped SnO_2 films deposited on crystalline mica and aluminium substrate is larger than that deposited on glass substrates. Table 4.2 shows the grain size variation of the film deposited.

Table 4.2. *- Grain size variation of doped (on glass) and undoped (on different substrates) SnO_2 films [deposition temperature T_S = 400° C].*

Films	Substrate	Average grain size (μm)
SnO_2-undoped	glass	1.20
SnO_2:Sb	glass	4.00
SnO_2:Mo	glass	0.60
SnO_2:F	glass	4.75
SnO_2-undoped	mica	2.00
SnO_2-undoped	aluminium	1.50

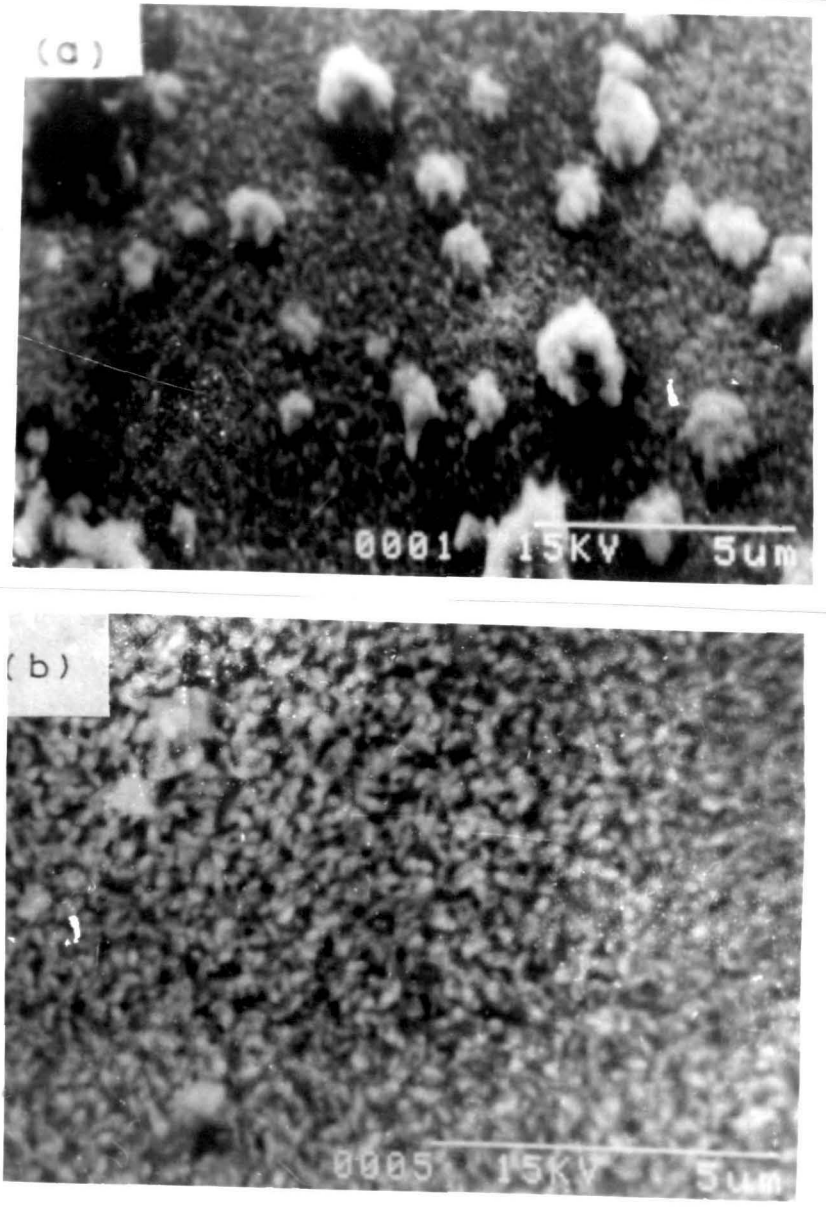

Figure 4.3. Scanning electron microscopes of undoped and doped SnO_2 thin films on glass substrate (T=400^0 C). (a) Undoped SnO_2; (b) SnO_2:Mo (6 at%).

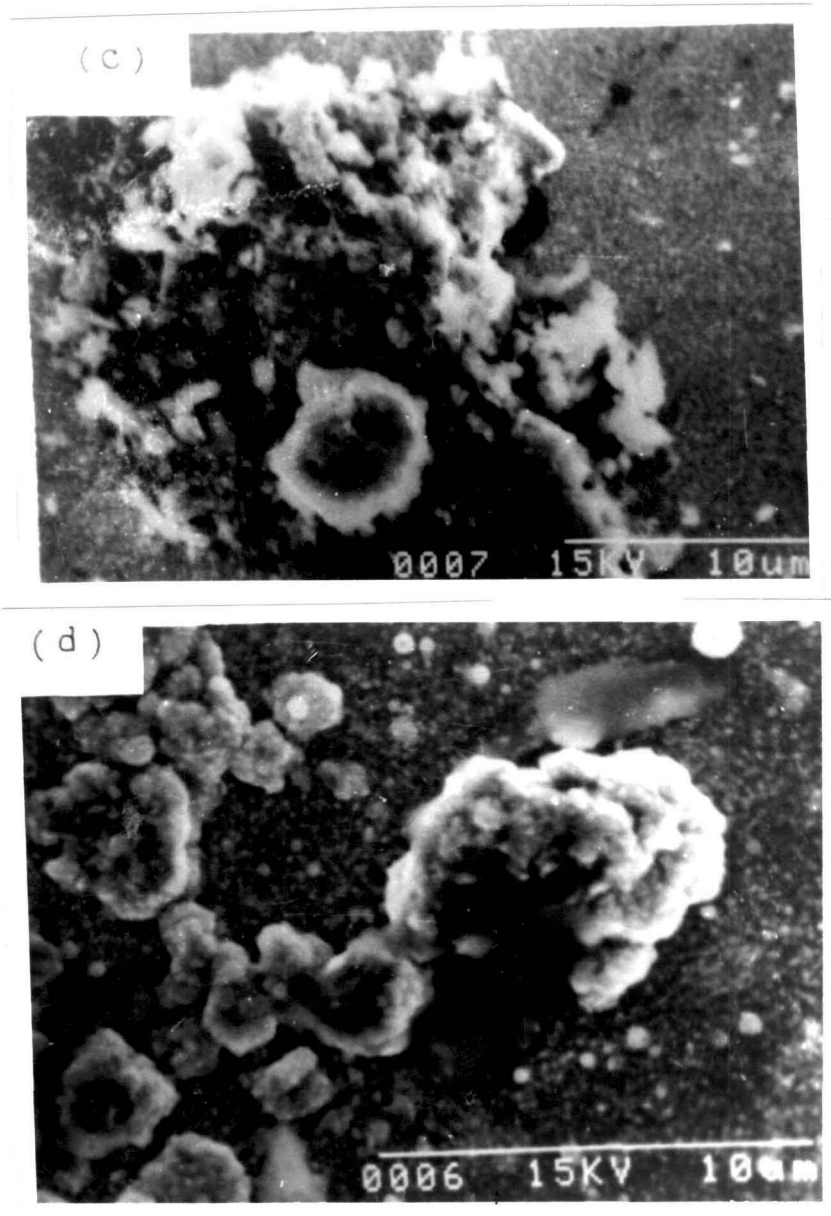

Figure 4.3. Scanning electron microscopes of doped SnO_2 thin films on glass substrate (T=400° C). (c)SnO_2:Sb (1.5 at%) (d) SnO_2:F (4.5 at%).

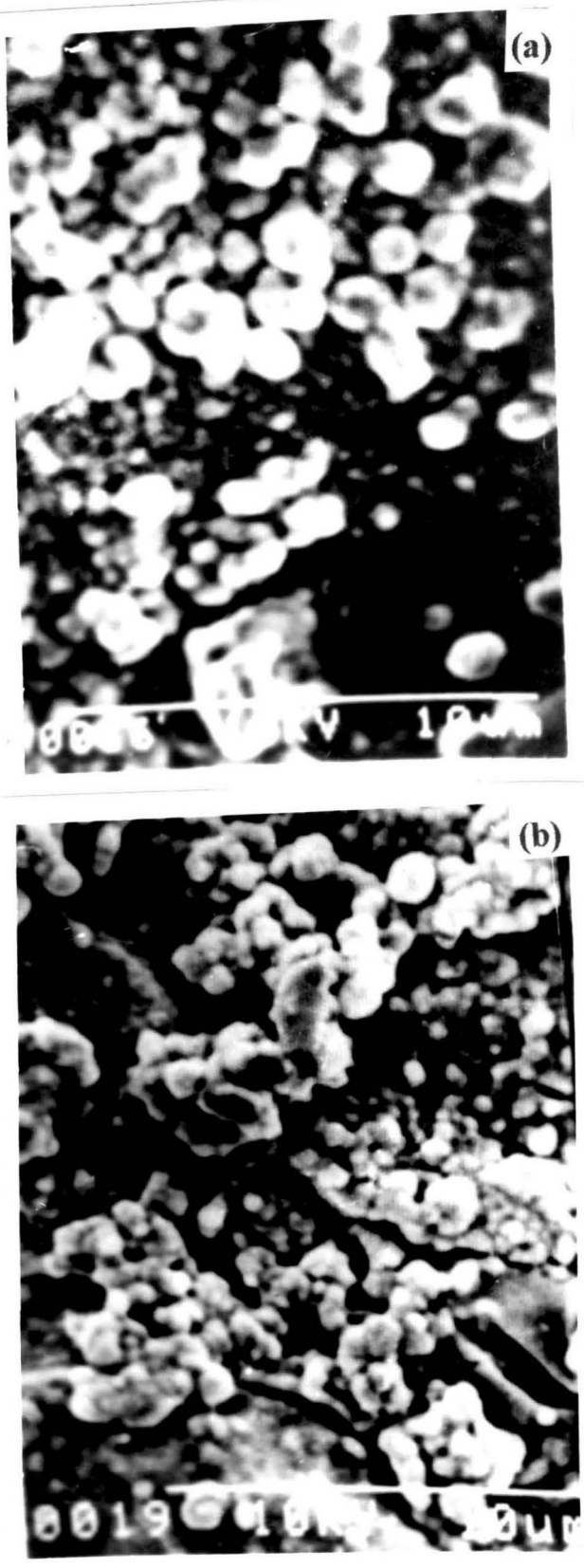

Figure 4.4. Scanning electron microscopes of SnO_2 thin films on different substrates (T=400^0 C) (a) mica (b) On aluminium sheet.

4.4.3. Electrical Properties

Results of detailed measurments of sheet resistance of the films as a function of thickness, temperature and dopant concentration are shown in Figures 4.5, 4.6 and 4.7 respectively. Films of various thickness were obtained by varying the amount of starting material, deposition time and substrate temperature. By observing the change in interference colours as a function of time the order of a particular colour could be known, and from the standard value of mean refractive index of SnO_2 (taken as 2.0 over the range 400 nm - 800 nm) the thickness could be estimated [43]. The sheet resistance of the films were measured by standard four-probe method.

Figure 4.5 shows the variation of sheet resistance with thickness of undoped films deposited at three substrate temperatures. It is evident from the curves that the room temperature resistivity of the undoped films decreases to its minimum value when deposited at a substrate temperature of 400° C but increases again when deposited at a higher substrate temperature of 450° C. This is due to the fact that, on increasing the substrate temperature from 350° C to 400° C, a better degree of crystallinity is achieved, leading to improved electronic, optical and structural properties [44-45]. It is also known that [21] both the carrier concentration and mobility increase with the increase of substrate temperature where mobility variation is larger than that of carrier concentration. Further increase in substrate temperature produces films of increased resistivity. This is due to the fact that in undoped SnO_2, conduction electrons arise from oxygen vacancies, and higher substrate temperature causes increased oxygen evolution from the substrate, leading to more nearly stoichiometric films [14,44]. The resistivity of the undoped films prepared at a substrate temperature of 400° C is estimated to be 4×10^{-3} Ω cm., which agrees well with the values reported earlier in the literature [44].

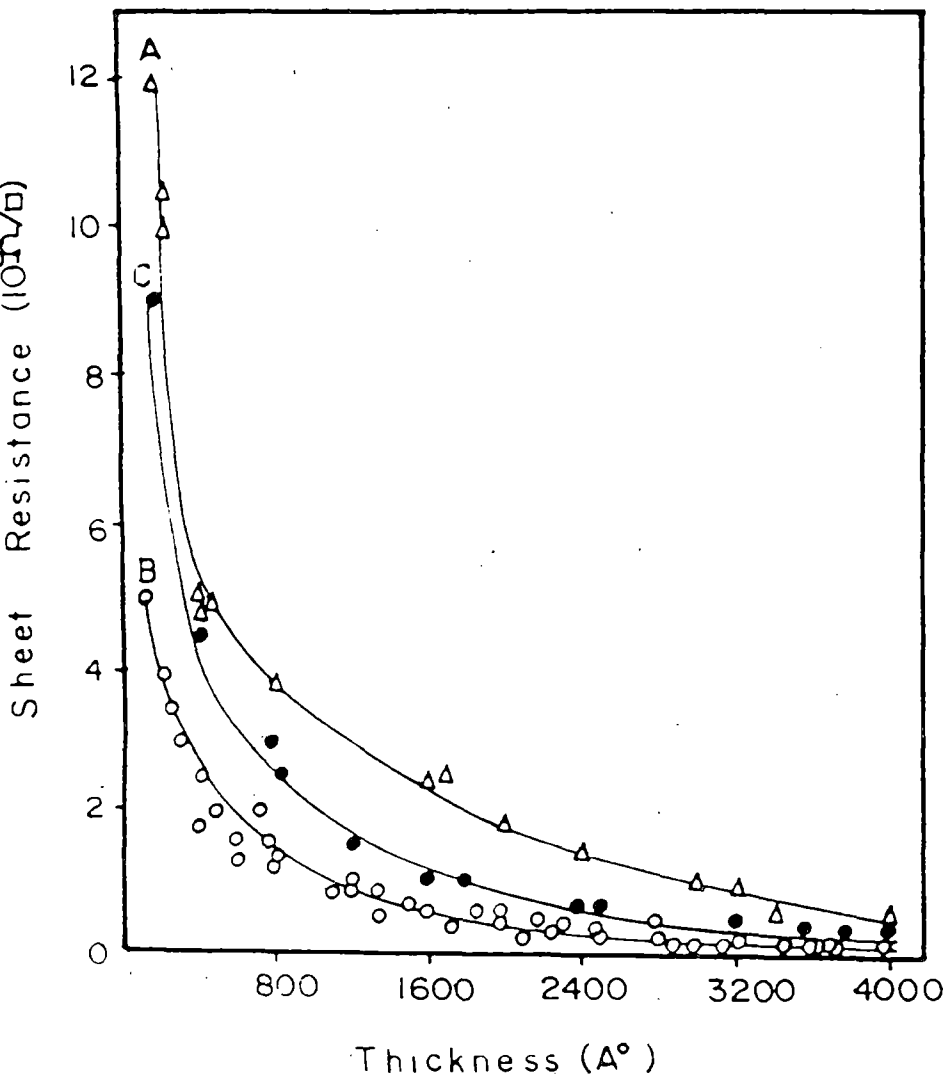

Figure 4.5. Variation of sheet resistance with thickness of undoped SnO_2 thin films deposited at various substrate temperatures. A, 350° C; B, 400° C; C, 450° C.

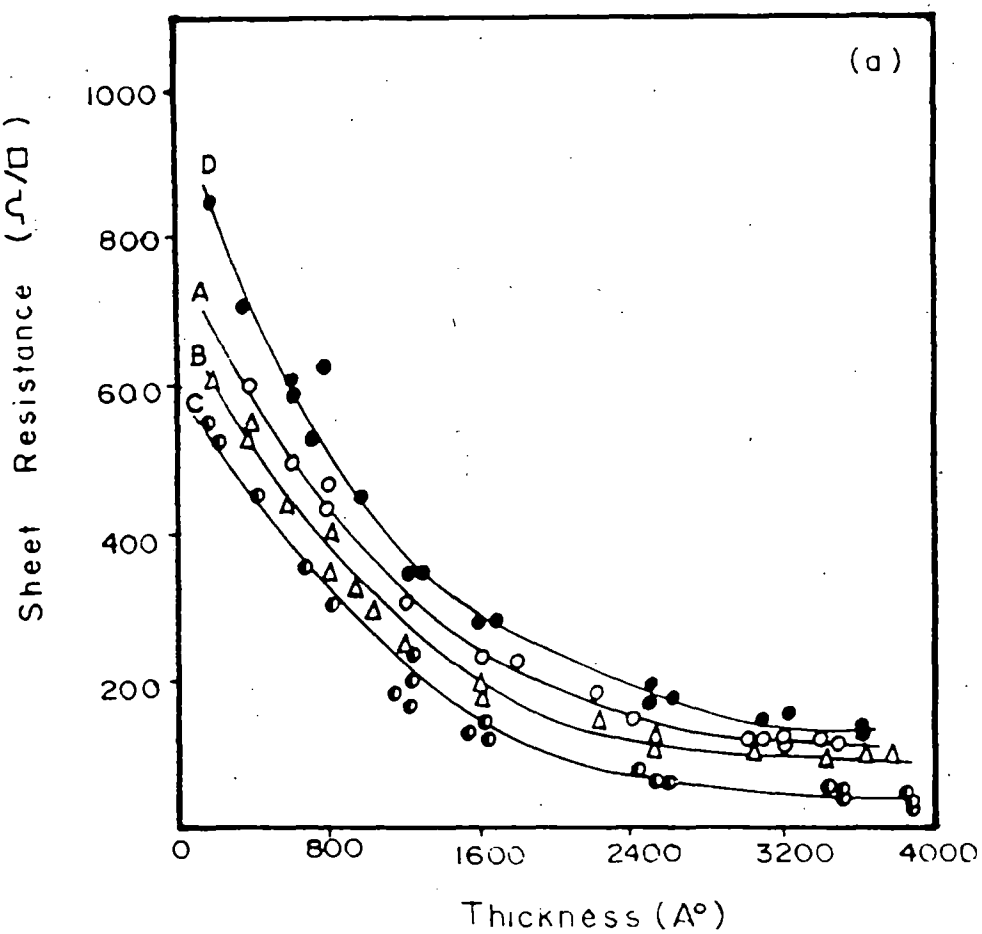

Figure 4.6. Variation of sheet resistance with thickness of doped SnO_2 thin films (T_s = 400° C), (a) Mo-doped SnO_2: A, 4 at%; B, 5 at%; C, 6 at% D, 7 at%.

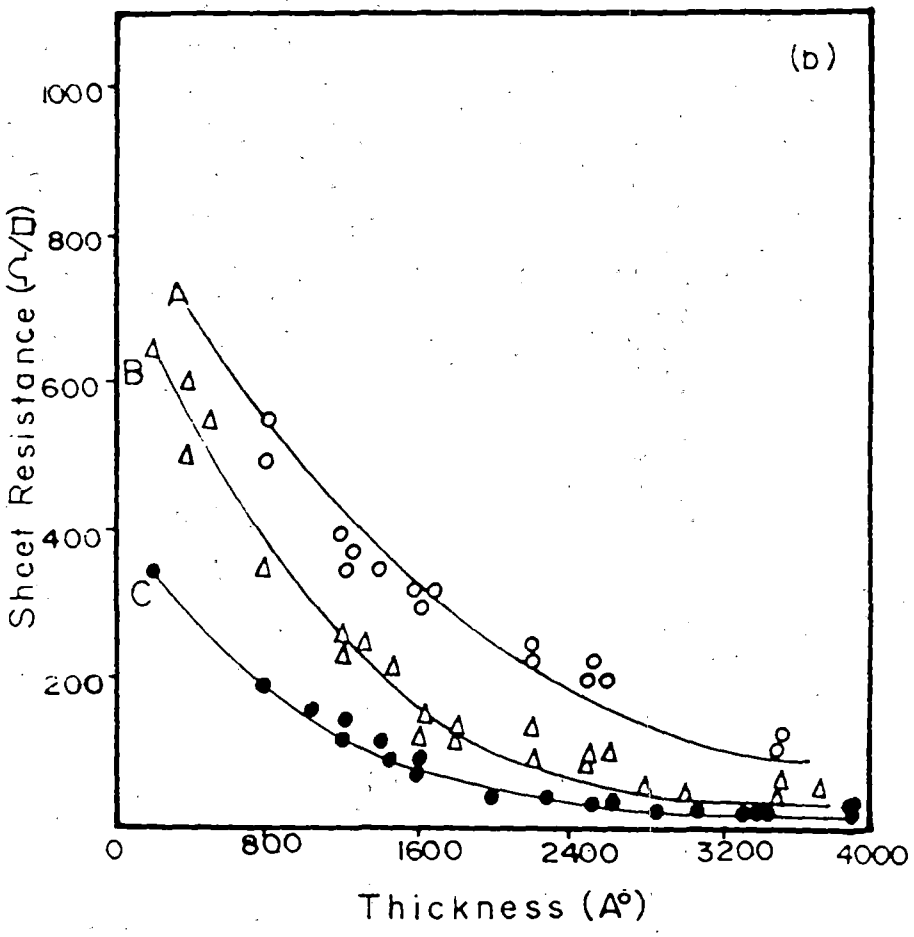

Figure 4.6. Variation of sheet resistance with thickness of doped SnO_2 thin films (T_s = 400° C), (b) Sb-doped SnO_2: A, 0.5 at%; B, 1.0 at%; C, 1.5 at%.

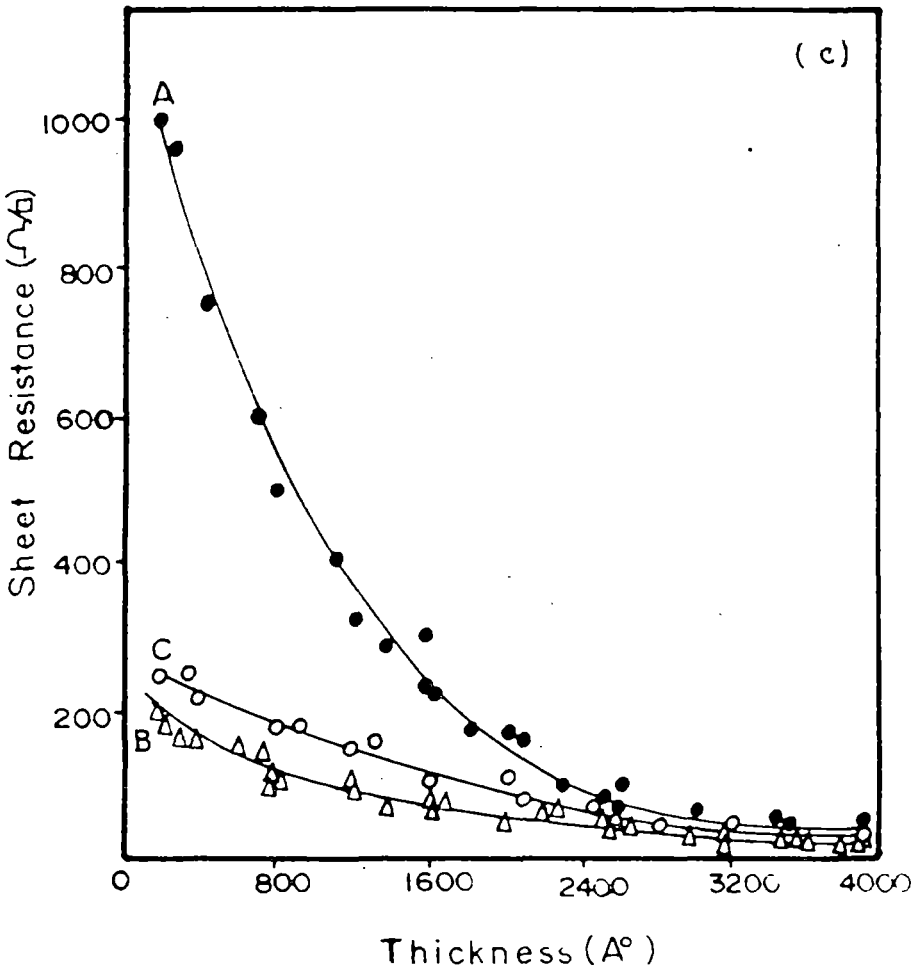

Figure 4.6. Variation of sheet resistance with thickness of doped SnO_2 thin films (T_s = 400° C), (c) F-doped SnO_2: A, 4 at%; B, 4.5 at%; C, 5 at%.

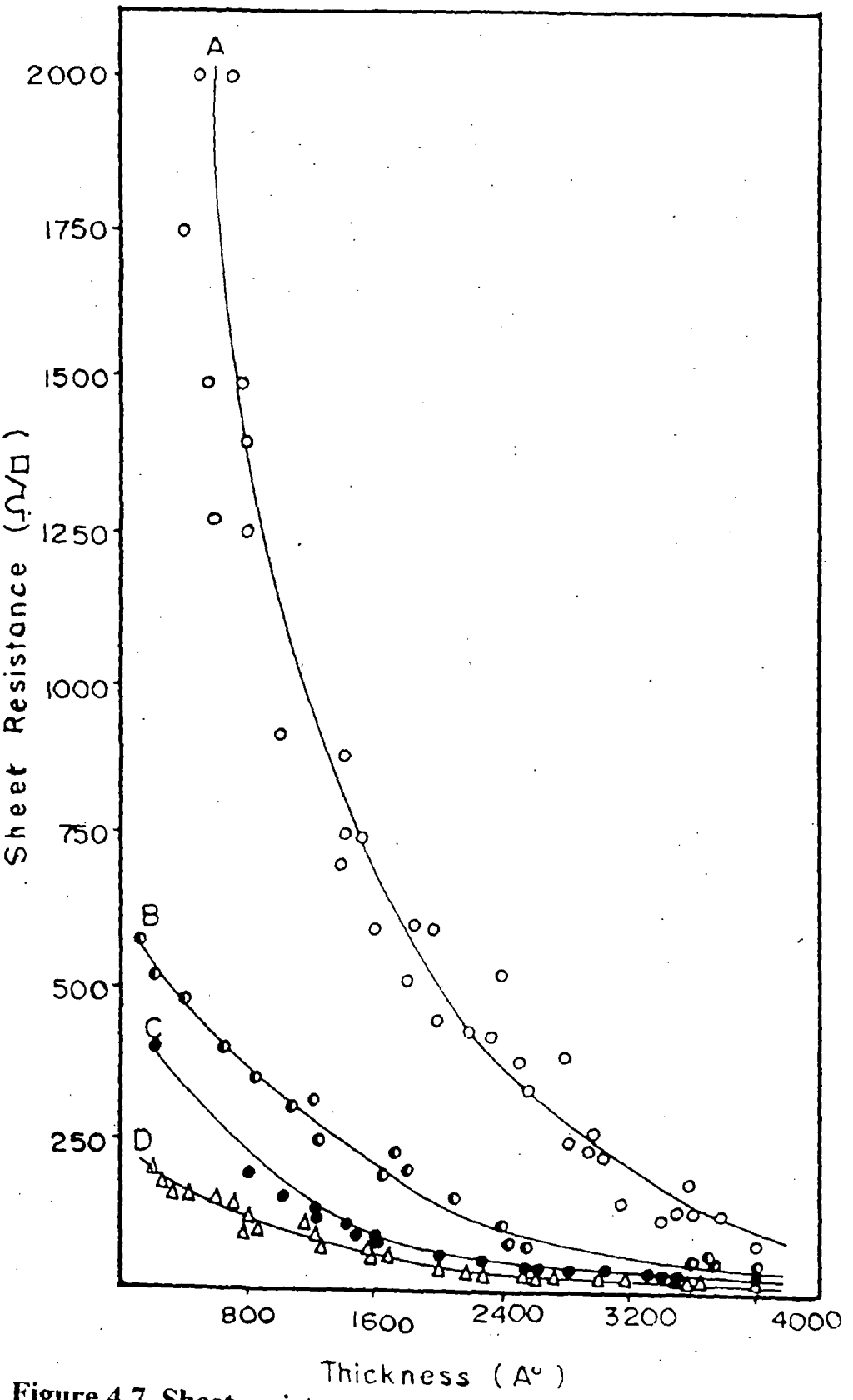

Figure 4.7. Sheet resistance versus thickness relationship for undoped [curvr A] and doped [curve B, SnO_2:Mo (6 at%); curve C, SnO_2:Sb (1.5 at%); curve D, SnO_2:F (4.5 at%)] SnO_2 thin films prepared at a substrate temperature of 400° C.

Effect of dopants [Mo, Sb & F] at various concentration on the resistivity is shown in figure 4.6. It is found that for every dopant, there is an optimum concentration at which the sheet resistance is a minimum. These values are listed in table 4.3.

Table 4.3. ***Minimum resistivity values of undoped and doped SnO_2 films on glass substrate (T_s = 400° C).***

Films	Resistivity (Ω cm.)
SnO2 (undoped)	4×10^{-3}
SnO2:Mo (6at%)	2×10^{-3}
SnO2:Sb (1.5at%)	8×10^{-4}
SnO2:F (4.5 at%)	4×10^{-4}

Thus it is observed that introduction of Mo reduces the resistivity by a maximum factor of two whereas Sb and F reduces it by a factor of five and ten respectively. Similar results are reported by G. Gordillo et al [46]. Relatively higher resistivity and lower optical transmission of the Mo-doped SnO_2 films compared to Sb-doped and F-doped films may due to their small grain size, as observed from the SEM micrograph. It is known that with decrease in grain size the grain boundary potential increase leading to increased grain boundary scattering and a corresponding increase in resistivity [12]. In the case of Sb-doped and F-doped SnO_2 films, the resistivity decreases upto 1.5 at% Sb doping and 4.5 at% F-doping respectively which may be due to (i) increased carrier concentration, (ii) larger grain size and (iii) preferred orientation. Beyond the above concentration the observed increase in resistivity may be due to the increase in contribution from ionised impurity scattering [21].

Variation of sheet resistance with thickness for optimum concentration of the dopants is shown in figure 4.7.

4.4.4. Optical Properties

The high optical transparency of these films in the visible and near IR regions of the solar spectrum in a direct consequence of SnO_2 being a wide bandgap semiconductor ($E_g \geq 3$ eV). The transmission in this region is limited by several factors [11]: (i) reflection losses which include both specular and scattered (diffuse) components (this backward scattering (about 1% - 2%) is primary due to surface roughness and increases with increasing thickness); (ii) absorption (about 1% - 2%) in the films, which is primarily due to free carriers; (iii) Variations in transmittance that may occur due to interference phenomena depending on the thickness of the film with the result that an average visible transmission must be described. The transmitted part of the incident energy also has specular and scattered (diffuse) components. This forward scattering (about 5%) is due to inhomogeneities in the film in the form of unreacted or partly reacted chemical species generated during the complex pyrolytic process, trapped gases, segregated impurity atoms of other oxide phases. Optical transmission as a function of wavelength in the range 400 nm to 800 nm was obtained by SHIMADZU UV - 240 double beam spectrophotometer.

The results for undoped and variously doped films for constant thickness and different sheet resistance values are shown in figure 3.8a, 3.8b, 3.8c and 3.8d. The optical transmission is observed to decrease with decreasing sheet resistance in case of both undoped and doped films. Variation of the average optical transmission as a function of sheet resistance for undoped and doped films are shown in figure 3.9. It is seen for all the films that the optical transmission drops off more rapidly at lower values of the sheet resistance. This is due to an increase in surface roughness of films having low sheet resistance which have a proportionately higher thickness. However, F-doped films are found to have high optical transmission even at a low resistivity of 4 X 10^{-4} Ω cm.

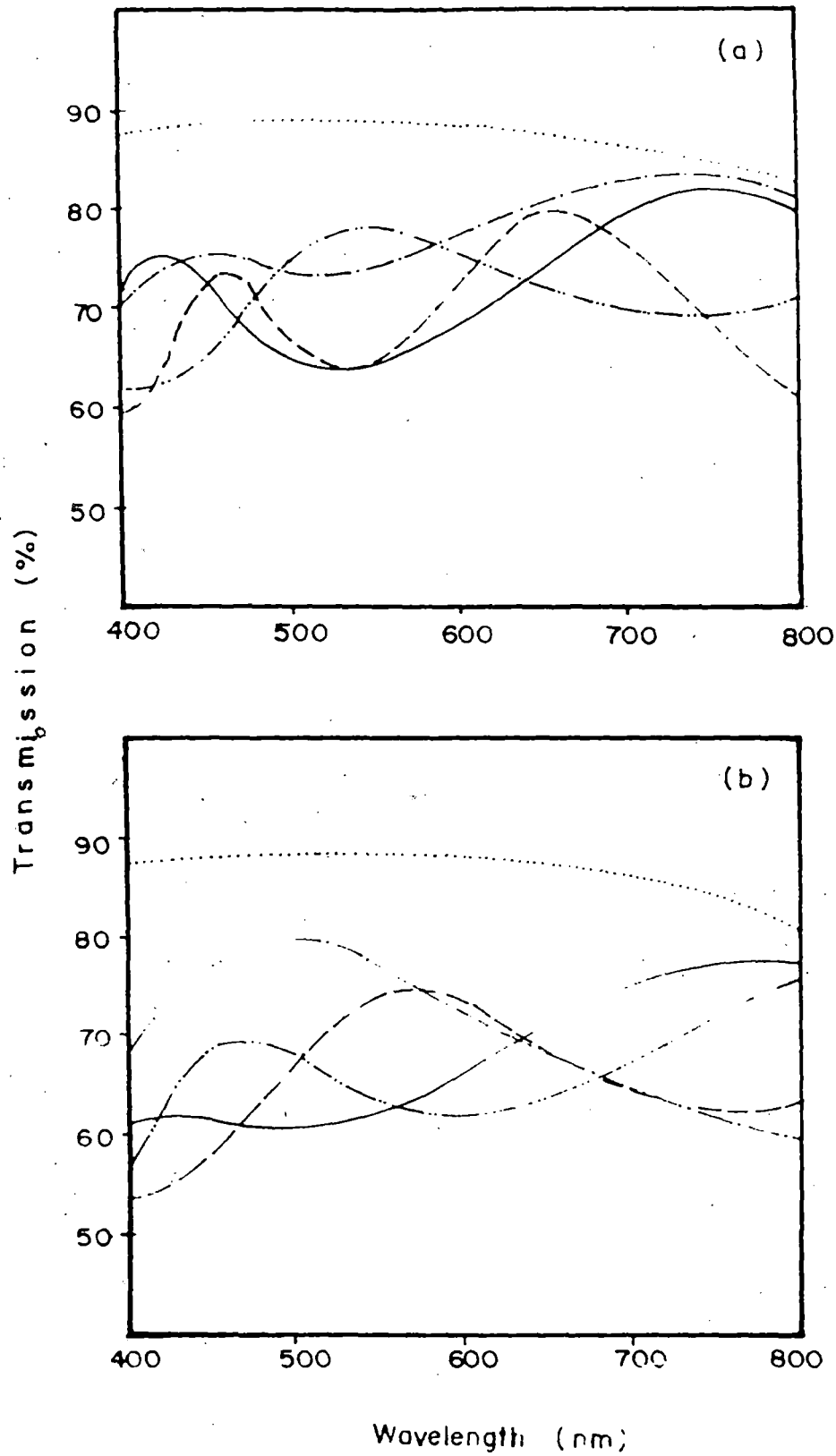

Figure 4.8. Optical transmission versus wavelength for typical SnO_2 thin films of various sheet resistance.(a) Undoped: (.....), bare substrate; (-.-.-.-) 700 Ω/□;(-..-..-..-) 400 Ω/□; (——) 350 Ω/□;(_____),200Ω/□. (b) Mo-doped (6 at%): (.....) bare substrate;(-.-.-.-) 525 Ω/□; (-..-..-..-) 200 Ω/□; (_____) 150 Ω/□; (——) 60 Ω/□.

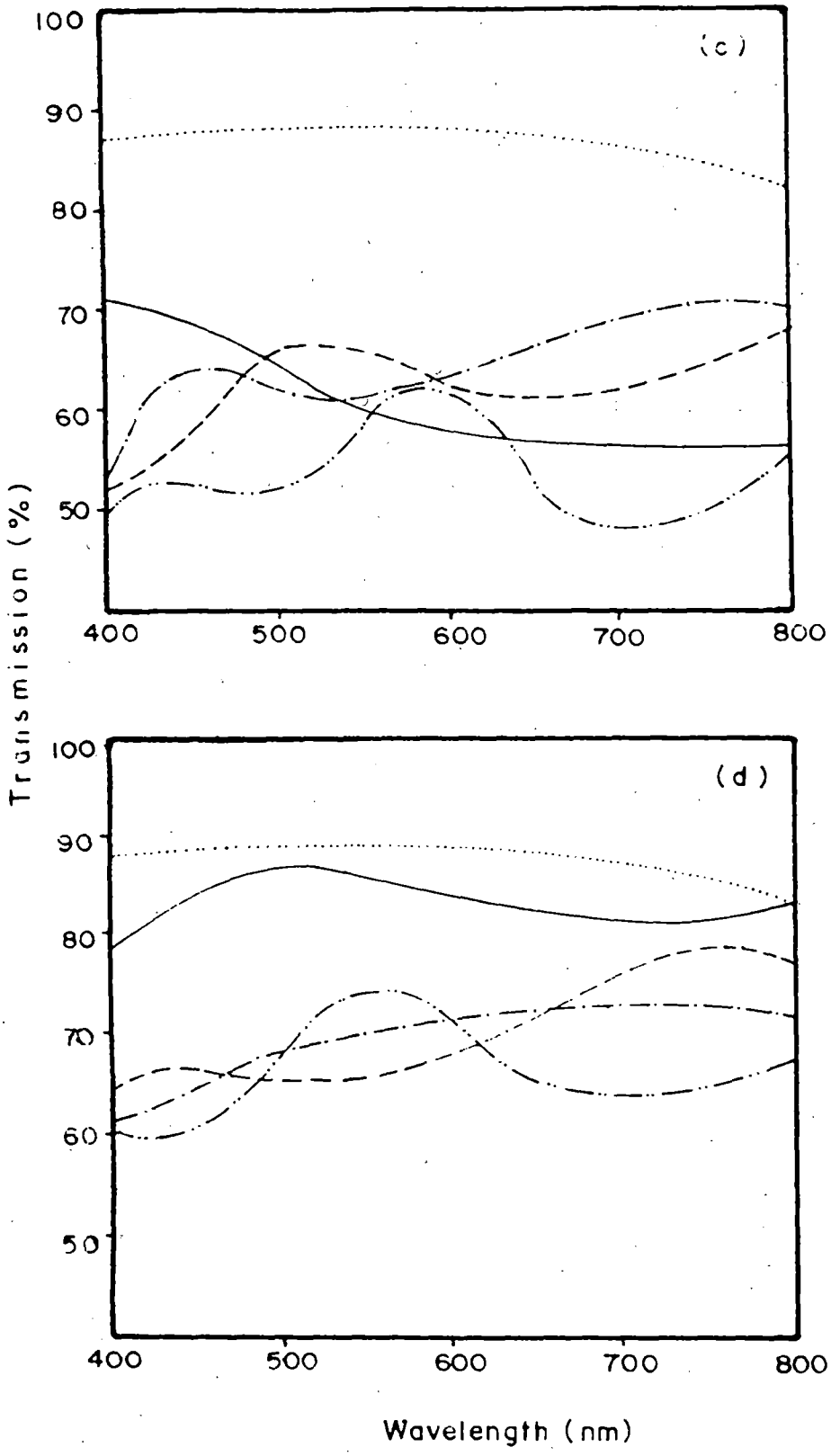

Figure 4.8. Optical transmission versus wavelength for typical SnO_2 thin films of various sheet resistance.(c) Sb-doped (1.5 at%): (.....) bare substrate; (_____)350 Ω/□; (——) 200 Ω/□; (-.-.-.-) 130 Ω/□; (-..-..-..-) 30 Ω/□.(d) F-doped (4.5 at%) : (.....), bare substrate; (_____) 160 Ω/□; (——) 90 Ω/□; (-.-.-.-), 60 Ω/□; (-..-..-..-) 20Ω/□.

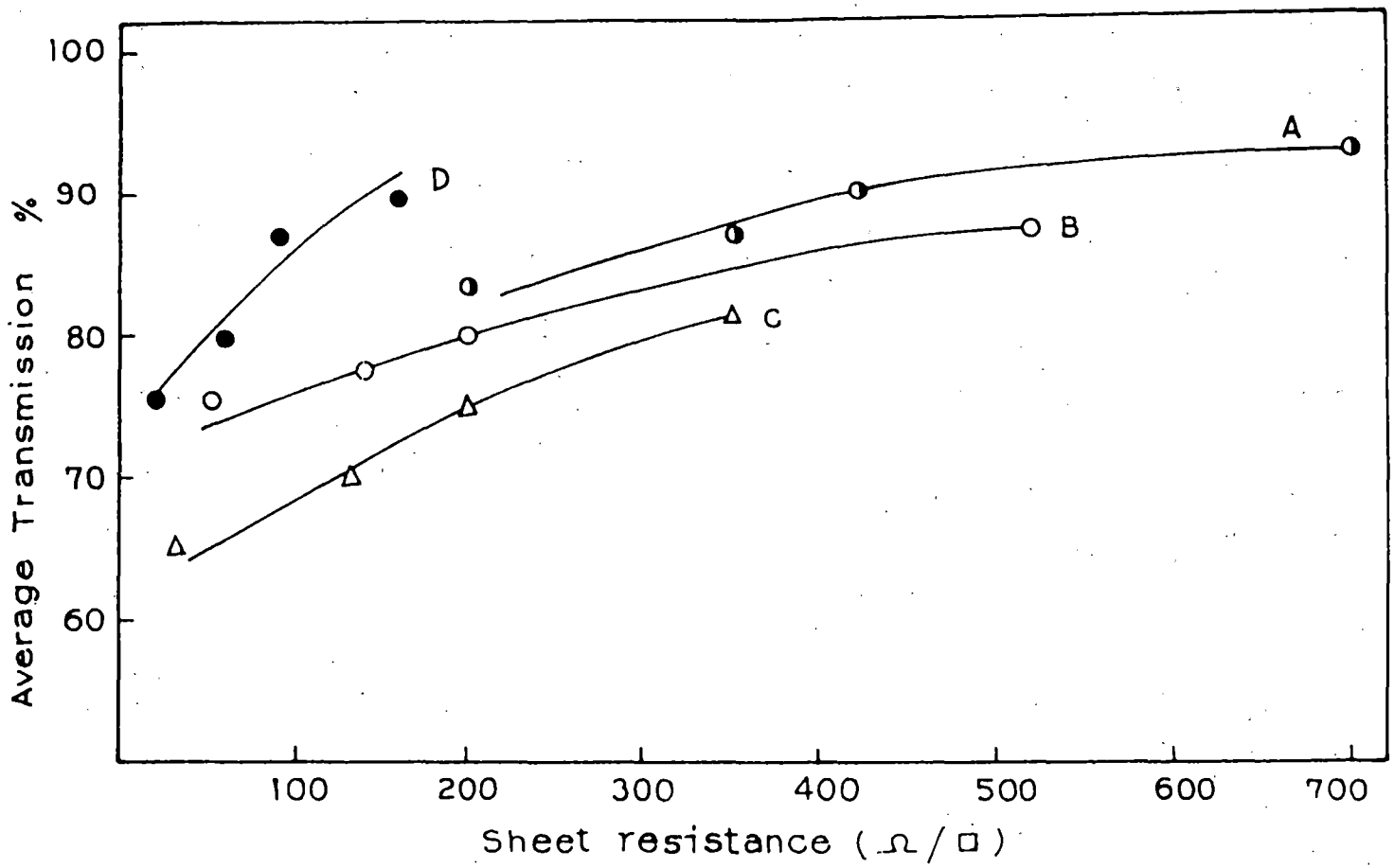

Figure 4.9. Average optical transmission over the range 400 nm - 800 nm versus sheet resistance for undoped [curve A] and doped [curve B, SnO_2:Mo (6 at%); curve C, SnO_2:Sb (1.5 at%); curve D, SnO_2:F (4.5 at%)] SnO_2 thin films prepared at a substrate temperature of 400° C.

4.4.5. Figure of merit

A figure of merit for transparent materials has been defined by the relation $\Phi_{TC} = T^{10}/R_S$ [38], where T is the optical transmission and R_S is the electrical sheet resistance. It is a useful tool for comparing the performance of transparent conductive coating when their electrical sheet resistance and optical transmission are known. Furthermore, the expression derived for Φ_{TC} can be used to predict the transparent electrode properties of a candidate material from its fundamental properties. The figure of merit is calculated for undoped and Mo, Sb and F doped SnO_2 films deposited by this method and compared with other workers. The calculated value and the results of other workers are tabulated in table 4.4.

4.4.6. Comparision of Electrical and Optical properties of tin dioxide films prepared by various workers.

The films are found to compare quite favourably in terms of electrical and optical properties with those prepared by other methods as shown in table 4.4 given below.

Table - 4.4. *Comparison of the electrical and optical properties of tin dioxide films prepared by various workers.*

Material	Deposition technique	ρ (Ω cm.)	R_S (Ω/□)	T (λ_r) % (μm)	ϕ_{TC} ($10^{-3}cm^{-1}$)
SnO_2	Spray pyrolysis [1]	5×10^{-3}	84	85 (0.5-2)	2.4
	CVD [54]	7×10^{-2}	1200	93 (0.3-0.7)	0.41
	Present work	4 x 10-3	100	90 (0.4-0.8)	3.48
SnO_2 :Sb	Spray pyrolysis [11]	4.2×10^{-3}	28	87 (0.3-1)	9.4
	CVD [20]	2×10^{-3}	55	88 (0.4-0.7)	5.06
	Present work	8×10^{-4}	20	75 (0.4-0.8)	2.82
SnO_2:F	Spray pyrolysis [11]	4.6×10^{-4}	10	85 (0.4-10)	19.68
	CVD [55]	5×10^{-4}	20	90 (0.4-0.8)	17.43
	Present work	4×10^{-4}	10	85 (0.4-0.8)	19.68
SnO_2:Mo	Present work	2×10^{-3}	50	70 (0.4-0.8)	2.15

ρ - Resistivity, R_S - Sheet resistance, T (λ_r) - Average optical Transmission (Wavelength), ϕ_{TC} - Figure of merit, **CVD** - chemical vapour deposition.

4.5. CONCLUSION

Undoped and Mo-, Sb- and F-doped tin oxide films of reproducible quality have been deposited by the Open Air Chemical Vapour Deposition (OACVD) technique. The films were smooth, highly uniform and resistant to peeling - off and acids, and also showed a high degree of crystallinity along with long term stability with respect to their optical, electrical and mechanical properties. X-ray diffractometric study suggests that Sb and F-doped SnO_2 films show preferred orientation along the (110) plane. Surface morphology study by scanning electron microscope suggests that for films deposited on glass substrates, the grain size increases in the case of Sb-doped and F-doped SnO_2 films but decreases for Mo-doped SnO_2 films when compared to undoped films. The grain size for undoped films on mica and aluminium sheet substrate is also larger than that for films deposited on glass substrates.

The lowest values of sheet resistance at a particular thickness are obtained for 6 at% Mo-doped, 1.5 at% Sb-doped and 4.5 at% F-doped SnO_2 films on glass substrate. A typical value of resistivity of 4.5 at% F-doped SnO_2 films is 4×10^{-4} Ω cm and that for 1.5 at% Sb-doped SnO_2 is 8×10^{-4} Ω cm.

The films compare quite well in terms of electrical conductivity and optical transmission with those obtained by other methods. The average optical transmission is found to decrease as the sheet resistance decreases for Mo and Sb-doped films. But for F-doped films, negligible increase in transmission loss with decrease in sheet resistance is found to occur.

Transparent conductors will continue to play an increasingly important role in electronic and opto-electronic devices. Further efforts are required to introduce such dopants and develop new processing techniques to satisfy the twin conflicting requirements of high optical transmission along with low resistivity. This is a totally unexplored area.

In conclusion, tin oxide films having a sheet resistance of 10 - 100 Ω Square^{-1} and an average optical transmission of 75% - 90% could routinely be obtained by this method. The merit of this method is its extreme simplicity by which one can deposit useful tin oxide films for device applications either on one side or both sides of a planar substrate or inside of a tube quite easily in any laboratory without using any specialized experimental set up. It is believed that using this method, ZnO, CuO, CdO, $CdSnO_2$ etc. oxide thin films also can be prepared.

REFERENCES

1. J. C. Manifacier, L. Dzepessy, J. F. Bresse and M. Perotin 1979 *Mater. Res. Bull.* **14** 163 (123)

2.W. Spence 1967 J. *Appl. Phys.* **38** 3767

3.Yar-Sun Hsu and Sorab K. Gandhi 1980 *II J. Electrochem. Soc., Solid State Sci. Technol.* **127** 1592

4. J. Bruneaux, H. Cachet, M. Froment, J. Amblard, J. Belloni and M. Mostafavi 1987 **Electrochem. Acta 32** 1533

5. J. Bruneaux, H. Cachet, M. Froment, J. Amblard, J. Belloni and M. Mostafavi 1989 *J. Electroanal chem.* **269** 375

6. P. Cowache, D. Lincot and J. Vedel 1989 *J. Electrochem. Soc.* **136** 1646

7. W. Badway, F. Decker and K. Doblhoffer 1983 *Solar Energy Mater.* **8** 363

8. J. C. Manifacier, J. P. Fillard and J. M. Bind 1981 *Thin Solid Films* **77** 67

9. B. Drevillon, K. Satytendra, P. Rocai Cabarrocas and J M. Siffert 1989 *Appl. Phys. Lett.* **54** 2088

10. P. Grosse, F. J. Schmitte, G. Frank and H. Kostlin 1982 *Thin Solid Films* **90** 309

11. K. L. Chopra, S. Major and D. K. Pandya 1983 *Thin Solid Films* **102** 1-46

12. C. S. Rastomjee, R. S. Dale, R. J. Schaffer, F. H. Jones, R. G. Egdell, G. C. Georgiadis, M. J. Lee, T. J. Tate & L. L. Cao 1996 *Thin Solid Films* **279** 98

13. Ireneusz Kocemba, Tadeusz Paryjczak 1996 *Thin Solid Films 272* 15

14. J. Kane, H.P. Schweizer and W. Kern 1976 *J. Electrochem. Soc.* **123** 270

15. B. J. Baliga and S. K. Gandhi 1976 *J. electroche. Soc.* **123** 941

16. M. R. Kadam, N. Vittal, R. N. Karckar and R. C. Aiyer 1990 *Thin Solid Films* **187** 199

17. T. P. Chow, M. Ghezzo and B. J. Baliga 1982 *J. Eletrochem. Soc.* **129** 1040

18. J. P. Upadhyay, S. R. Vishwakarma and H. C. Prasad 1989 *Thin Solid Films* **169** 195

19. A. Rohatgi, T. R. Viverito and L. H. Slack 1974 *J. Am. Ceram. Soc.* **57** 57

20. H. Kim and H. A. Laitinen 1975 *J. Am. Ceram. Soc.* **58** 23

21. E. Shanthi, A. Banerjee, V. Dutta and K. L. Chopra 1980 *J. Appl. Phys.* **51** 6243

22. E. Shanthi, A. Banerjee, V. Dutta and K. L. Chopra 1980 *J. Appl. Phys.* **53** 1615

23. U. R. Chaudhuri, K. Ramkumar and M. Satyan 1990 *J. Phys. D: Appl. Phys.* **23** 994

24. H. Watanabe,1970 *Jpn. J. Appl. Phys.* **9** 1551

25. T. Matsuoka, J. Kuwatov, M. Nishikawa, Y. Fujita, T. tohda and A. Abe 1988 *Jpn. J. Appl. Phys.* **27** 1088

26. H. W. Lehmann and R. Widmer 1975 *Thin Solid Films* **27** 359

27. J. L. Vossen and E. S. Polimiak 1972 T*hin Solid FIlms* **13** 281

28. A. Czapla, E. Kusior and M. Bucko 1989 *Thin Solid Films* **182** 15

29. J. P. Chatelon, C. Terrier, E. Bernstein, R. Berjoan and J. A. Roger 1994 *Thin Solid Films* **247** 162

30. C. Terrier, J. P. Chatelon, R. Berjoan and J. A. Roger 1995 *Thin Solid Films* **263** 37

31. C. J. Brinker, A. J. Hurd, P. R. Schunk, G. C. Frye and C. S. Ashley 1992 *J. Non-Crystalline Solids* **147 & 148** 424

32. Y. Takahashi and Y. Wada 1990 *J. Electrochem. Soc.* **137** 267

33. D. E. Carlson 1975 *J. Electrochem. Soc.* **122** 1334

34. T. Muranoi and M. Furukoshi 1978 *Thin Solid Films* **48** 309.

35. R. N. Ghoshtagore 1978 *J. Electrochem. Soc.* **125** 110.

36. G. N. Advani, A. G. Jordan, C. H. F. Luges and R. N. Longini 1979 *Thin Solid Films* **62** 361.

37. R. Kalbskopf 1984 *Thin Solid Films* **22** 65.

38. O. Tabata, T. Tanaka, M. Waseca and K. Kumhara 1979 *Surface Sci.* **86** 230.

39. K. B. Sundaram and G.K. Bhagver 1981 *Thin Solid Films* **78** 35.

40. J. A. Aboaf, V. C. Marcotte and N. R. Cronel 1973 *Electrochem Soc.* **120** 701.

41.M. K. Karanjai and D. DasGupta 1988 *J. Phys. D: Appl. Phys.* **21** 356.

42. H. Dislich and E. Hvssmann 1981 *Thin Solid Films* **77** 129.

43. Vossen J. L. 1977 Physics of thin films Vol. 9 ed. G. Hass, M. H. Francombe and R. W. Hoffmann (New York: Academic) P. 1-71.

44. A. L. Unaogu and C. E. Okeke, 1990 *Solar Energy Materials* **20** 29

45. A. De and S. Ray 1991 *J. Phys. D: Appl. Phys.* **24** 719

46. G. Gordillo, L. C. Moreno, W. de la Cruz, P. Teheran 1994 *Thin Solid Films* **252** 61

47. G. Haacke 1976 *J. Appl. Phys.* **47** 4086

48. J. Kane, H. P Schweizer and W. Kern 1975 *J Electrochemcal Soc.* **122** 1144

49. James Proscia and Roy G. Gordon 1992 *Thin Solid Films* **214** 175

CHAPTER - 5

**Concluding remarks*

**Proposed future work*

In this present work, we have reported two techniques for the deposition of thin films. They are the DIP TECHNIQUE and the OPEN AIR CHEMICAL VAPOUR DEPOSITION (OACVD) TECHNIQUE. Using the DIP technique, we have prepared a few oxide (SnO_2 & CuO) and sulphide ($Zn_xCd_{1-x}S$, SnS, SnS_2, MoS_2 & Cu_2S) thin films, while the OACVD technique has been used for the deposition of SnO_2 films only. The films were characterised by various standard methods. The major observations and conclusions drawn from the work reported in this thesis are presented along with suggestions for future work.

I. THE DIP TECHNIQUE

The dip technique has been developed as a simple and inexpensive process for the deposition of oxide and sulphide films. For both types of films, the film-forming process consists of dipping and withdrawal of the substrate from a suitable starting solution and its subsequent baking at a high temperature. The starting solution has methanol as the solvent, in which the corresponding metallic chlorides are disolved for the preparation of oxide films. For sulphide films, it also contains a suitable sulphur containing compound such as thiourea or ammonium thiocyanate in addition to the corresponding metallic chloride or nitrates. These films were smooth, highly uniform and strongly adherent to the substrate.

Undoped and F-doped transparent semiconducting films with tin dioxide (SnO_2) as the active material as also copper oxide (CuO) films have been prepared. The transparent conductor with SnO_2 as the active material film is formed in situ by the hydrolysis of stannous chloride (with NH_4F added for F-doped films) which takes place when the substrate is withdrawn from a methanol solution of $SnCl_2.2H_2O$ and baked at a high temperature as described above. The maximum film thickness obtainable per dipping cycle is about 0.58 μm, but can be increased by multiple dipping. The film consist of a mixed phase consisting of small amount of SnO_2 crystallites over an amorphous background, probably of Sn(OH)Cl. The films have a featureless microstructure and a high resistivity. The high resistivity is thought to be due to the presence of Sn(OH)Cl along with small amounts of crystalline SnO_2. But as the film thickness is increased by repeating the number of dipping, these crystallites increase in number and finally merge into a continuous layer after 15-20 dippings. However, even at this stage there is a large amorphous background present, as shown by the high value of resistivity. viz, 2.4×10^{-2} Ω cm compared to 2.4×10^{-4} Ω cm for CVD SnO_2 films. In spite of the presence of the amorphous background the films are quite transparent and have a high optical transmission. These are suitable for those display application where the current requirment is low, e.g. liquid crystal or electrochromic displays.

The copper oxide films were prepared at different baking temperatures using methanolic solution of $CuCl_2$. The films have the crystalline CuO structure and its optical band gap as determined from the optical absorption data is 1.85 eV.

$Zn_xCd_{1-x}S$ ($0 \leq x \leq 1$) alloy thin films prepared at 500° C using an alcoholic solution of the corresponding metal nitrates and thiourea. $Zn_xCd_{1-x}S$ ($0 \leq x \leq 0.6$) were hexagonal in structure, whose lattice parameter c and a are found to decrease with increase in x. An increase in x also produces a similar drop in the thickness of the film, the total number of (Cd + Zn) moles in the starting solution being kept constant. This agrees well with the fact that the Zn atoms have a relatively smaller size compared to Cd atoms.

The bandgaps obtained from optical absorption and spectral response of photoconductivity measurements are in good agreement with each other and vary from 2.30 eV (CdS) to 2.69 eV ($Zn_{0.6}Cd_{0.4}S$). Beyond this range (x>0.6) the films are amorphous and the bandgaps obtained from optical absorption measurements (optical bandgap) are much less than that obtained from photoconductive measurements due to a change from crystalline to amorphous structure. Surface morphology study by SEM as well as XRD data also confirm that good crystallinity is obtained upto a zinc atomic fraction of 0.6 only.

Tin mono- and disulphide (SnS & SnS_2) were prepared using an alcoholic solution of the corresponding chloride and thiourea. SnS & SnS_2 thin film show good crystalline structure when prepared at a baking temperature of 300° C for SnS and 360° C for SnS_2 films. Bandgaps obtained from photoconductivity measurements are 1.4 eV and 2.4 eV for SnS and SnS_2 films respectively. Optical absorption measurements on SnS_2 films also yield a bandgap value of 2.4 eV. Antimony-doping of SnS_2 films produces an increase in bandgap along with a sharp reduction in crystallinity. Annealing in atmospheric condition at 400° C both SnS and SnS_2 films convert them to transparent conducting tin dioxide, thus providing an alternative route for its preparation.

For MoS_2 and Cu_2S thin films, methanolic solution of ammonium molybdate and copper nitrate respectively along with ammonium thiocyanate as a starting solution were used. MoS_2 and Cu_2S films with good crystallinity were obtained for baking temperature of 360° C, 450° C and 500° C respectively. Optical absorption data shows the films are uniform and homogeneous. The optical bandgaps are 1.80 eV and 1.4 eV for MoS_2 and Cu_2S respectively which were calculated from optical absorption data.

II. OACVD TECHNIQUE

A simple and low-cost technique has been developed in our laboratory for the preparation of transparent conducting tin dioxide films. Using this technique,

transparent conducting undoped and doped (Mo, Sb & F) tin dioxide films have been prepared on glass substrates at 400° C. Here the substrate was placed vertically in the central region of a long tube heated from outside by winding a heater coil on its outer surface. The starting material in the form of $SnCl_2$ paste was heated at the bottom of an open-ended glass tube inside which the substrate was placed. On heating, the $SnCl_2$ decomposed into $SnCl_4$ and H_2O, the former getting hydrolyzed on the heated substrate and depositing SnO_2 film. The films were of a very high quality and showed long term stability with respect to their optical, electrical and mechanical properties. Doping of the films by F, Mo and Sb was achieved by mixing Ammonium fluoride, Ammonium molybdate and Antimoni trichloride respectively. The films were characterised by XRD & SEM as also measurement of electrical and optical properties. The films were deposited on glass and mica substrates. The grain size of the films deposited on mica substrate was larger compared to those prepared on glass substrate. Optimum concentration for each dopant at which the sheet resistance is a minimum, was determined. 4.5 at% F-doped SnO_2 films showed the lowest resistivity ~ 4 X 10^{-4} Ω cm and average optical transmission of 80% at a thickness of 3500 A°.

IV. SUGGESTION FOR FUTURE WORK

(a) To assess the usefulness of the dip technique, it is necessary to prepare films of different materials under various deposition conditions and their subsequent characterisation. For example, Tin sulphide films described here have only SnS & SnS_2 phase, but the same technique may be used to prepare SnS_x ($1 \leq x \leq 2$) films, and even films with composition Sn_2S_3, Sn_3S_4. Other dopants like Cu could also be used for tin sulphide films.

(b) The simple OACVD technique for deposition of SnO_2 film could be used for the deposition and study of films using other dopants, such as Cl, In, Cd, P. In addition,

preparation and characterisation of cadmium-tin-oxide ($CdSnO_2$) or ZnO films in this method could also be used.

It is evident that for the future well-being of nations, a supply of energy, based on a renewable source which is economically and environmentally acceptable need to be developed. Direct conversion of solar energy electric power by thin film PV devices appears to be the ideal solution. In the present work, the films which were prepared are suitable as materials for the above purpose. The above techniques which can be adopted for the preparation of solar photovoltaic energy conversion thin film materials are very simple and low-cost and can be carried out in virtually any laboratory.

We hope that in future these techniques will be found to be useful for long-term success of PV technology as a way of effectively utilizing our solar income due to its simplicity and low-cost.

REPRINTS

ELSEVIER

Thin Solid Films 307 (1997) 221–227

thin solid films

Preparation and study of doped and undoped tin dioxide films by the open air chemical vapour deposition technique

Sekhar C. Ray, Malay K. Karanjai, Dhruba Dasgupta *

Department of Physics, University of North Bengal, Siliguri, Darjeeling 734430, West Bengal, India

Received 11 September 1996; accepted 30 April 1997

Abstract

Highly transparent and conducting undoped and doped (Mo, Sb, F) tin dioxide films have been prepared by the open air chemical vapour deposition technique. The electrical and optical properties have been studied in detail for films deposited on glass substrates. Surface morphology study by scanning electron microscope shows that for films deposited on glass substrates, Sb- and F-doped films have a larger grain size than undoped ones. Mo-doping, in contrast, produces smaller grains. Films deposited on mica and Al sheet substrate have also a larger grain size compared to those on glass substrate. Films of very high quality in terms of crystallinity, electrical conductivity and optical transmission were obtained when deposited at a substrate temperature of 400°C. The optimum concentration for each dopant, at which the sheet resistance is a minimum, has been determined. 4.5 at.% F-doped SnO_2 films show the lowest resistivity, $\sim 4 \times 10^{-4}$ Ω cm, and an average optical transmission of 80% at a thickness of 3500 Å. © 1997 Elsevier Science S.A.

Keywords: Transparent conducting oxide; SnO_2 thin films; CVD

1. Introduction

Tin dioxide has been widely used as a transparent conducting thin film material for application in a number of solid state devices such as solar cells, opto-electronic devices, liquid crystal displays, heat mirrors, photo-thermal converters, thin film resistors and gas sensors [1–4].

The films are also very useful because of the stability of their mechanical, optical and electrical properties. Tin dioxide is a wide band gap electron degenerate semiconductor, whose properties largely depend on the deviation from stoichiometry (oxygen deficiency) as well as on the dopants used. Usually antimony or fluorine is used as a dopant to substitute tin or oxygen atoms, respectively.

Tin dioxide films have been prepared by a large variety of techniques which include spray pyrolysis [5–12], chemical vapour deposition [13–17], sol-gel method [18–20], reactive evaporation [21] and reactive r.f. sputtering [22]. The properties of these films crucially depend on the deposition technique and post deposition treatment.

In a previous report [23] we described an extremely simple and low-cost chemical vapour deposition method for tin dioxide films. In this method, the starting material is $SnCl_2 \cdot 2H_2O$ crystals which are ground with water into a paste and the paste applied in the form of a 4–5 mm wide band near, and parallel to, the lower edge of a substrate positioned vertically. On heating in air the paste decomposes according to the equation

$$6SnCl_2 + H_2O \rightarrow 2SnCl_4 + 4Sn(OH)Cl.$$

$SnCl_4$, which is generated as one of the reaction products, rises upward due to convection and hydrolyses on the heated substrate to produce a tin dioxide film. Doping with antimony can be achieved by mixing the requisite amount of $SbCl_3$ with $SnCl_2$ paste. Considering the simplicity of the method, films of reasonably good quality can be obtained. Details are given in Ref. [23].

This so-called 'paste-heat' method, however, suffers from the following disadvantages: (i) the portion of the substrate where the $SnCl_2$ paste is applied must be subsequently cut away before the films can be used, (ii) because of the geometry of the arrangement, the films are non-uniform, being thickest near the paste-coated area and becoming thinner away from it, and (iii) non-planar substrates, as also those with small sizes cannot be used.

* Corresponding author. Tel.: +91 353 450414; fax: +91 353 450546; e-mail: dhruba@nbu.ernet.in

PII S0040-6090(97)00268-X

In this report, we describe a modification of the above method, which employs the same principle, and maintains essentially the same simplicity, at the same time enabling one to obtain films free from the above defects. The preparation of undoped and doped (Sb, Mo, F) tin dioxide thin films by this method and the study of their electrical and optical properties as well as their surface morphology and crystal structure are described.

2. Experimental details

A 75 cm long glass tube with an internal diameter of 5 cm was placed vertically as shown in Fig. 1. The tube was heated from the outside in atmospheric condition by winding a heater coil on its outer surface over a length of 70 cm. The substrate was placed vertically in the central region of the tube. The starting material was taken in a conical flask placed at the bottom of the tube and heated separately. The temperature of the substrate was measured by a thermocouple placed close to the substrate. The starting material was prepared by mixing crystals of $SnCl_2$, $2H_2O$ with a few drops of water along with any dopant material that might be added and was stirred mechanically to convert it to a paste.

In the film forming process, the substrate was initially heated to attain the desired temperature after which the $SnCl_2$ paste was heated. White fumes were given off by the paste and were seen to deposit SnO_2 films where they came into contact with the hot substrate.

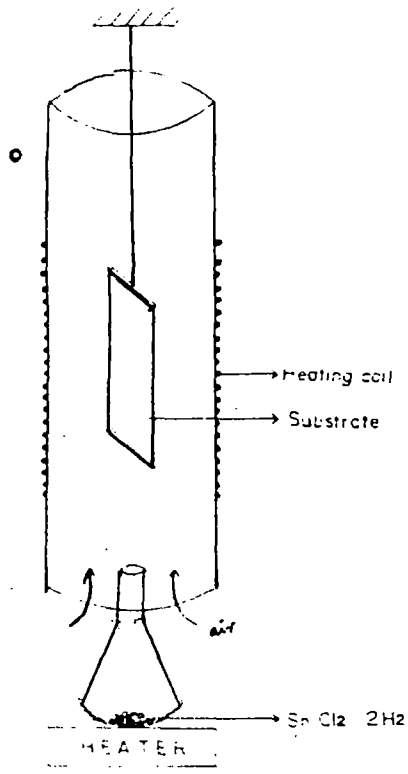

Fig. 1. Experimental arrangement for the deposition of SnO_2 films.

It is possible to deposit a number of films in a batch, by attaching them to a holder, which is placed in the central region of the tube. Usually both sides of the substrate are coated by this method, which is advantageous in some special cases [24], but it is also possible to coat one side only by masking the other side, or by fixing two substrates back to back. This method is especially advantageous for inaccessible surfaces and the inside surface of a tube, where one can obtain a coating quite easily, in contrast to the rather complex arrangements required in the usual CVD methods. The films were usually deposited over soda glass substrates (7.5 cm × 2.5 cm) and showed a uniform interference colour over their entire area except at the edges. But uniform films could also be routinely obtained, if necessary, over a larger area of 40 cm long by 4 cm wide.

Undoped tin dioxide films of various thicknesses were prepared at substrate temperatures of 350°C, 400°C and 450°C. Soda glass microslides, mica and Al sheet were used as substrates.

The films were doped with antimony, fluorine and molybdenum by adding antimony trichloride, ammonium fluoride and ammonium molybdate respectively to the $SnCl_2$ starting material. Characterization of the films was carried out by optical transmission and electrical conductivity measurements, X-ray diffractometry and scanning electron microscopy.

The electrical properties of the films were measured by the standard four-probe method and the optical properties were studied by a Shimadzu UV-240 double-beam spectrophotometer. Surface morphology and X-ray diffractometric studies were carried out by a Hitachi S-530 scanning electron microscope and a Philips diffractometer (model PW 1390) with CuK_α radiation (Ni-filter) at 1.54 Å, respectively.

3. Results and discussions

The films were smooth, highly uniform and resistant to peeling-off and acids, and also showed long-term stability with respect to their optical, electrical and mechanical properties. They displayed characteristic interference colours. Films of various thicknesses were obtained by varying the amount of starting material, deposition time and substrate temperature. By observing the change in interference colours as a function of time the order of a particular colour could be known, and from the standard value of the mean refractive index of SnO_2 (taken as 2.0 over the range of 400–800 nm) the thickness could be estimated [25].

It was found that using this process a substrate temperature of 400°C was necessary to prepare films of very high quality in terms of conductivity, optical transmission, uni-

formity and resistance to peeling-off and acids as well as environmental shocks.

3.1. X-ray diffractometric study

X-ray diffractometric studies were carried out on undoped and doped SnO_2 films deposited at a substrate temperature of 400°C. Diffraction peaks for undoped SnO_2 films having two different thicknesses are shown in Fig. 2(a). Fig. 2(b) shows the X-ray diffractograms of Sb and F doped SnO_2 films. The crystal structure is in accordance with the usual tetragonal form of SnO_2.

It is clear from the XRD patterns that there is no amorphous background in the diffractograms of the deposited films. Moreover, none of the undoped films show any preferred orientation, while those doped with Sb and F show a preferred orientation along the (110) planes. Prominent peaks, their d-values and relative intensities (I/I_0) for a typical F-doped SnO_2 film are listed in Table 1.

3.2. Surface morphology

Surface topographies of undoped, 6 at.% Mo-doped, 1.5 at.% Sb-doped, and 4.5 at.% F-doped SnO_2 films de-

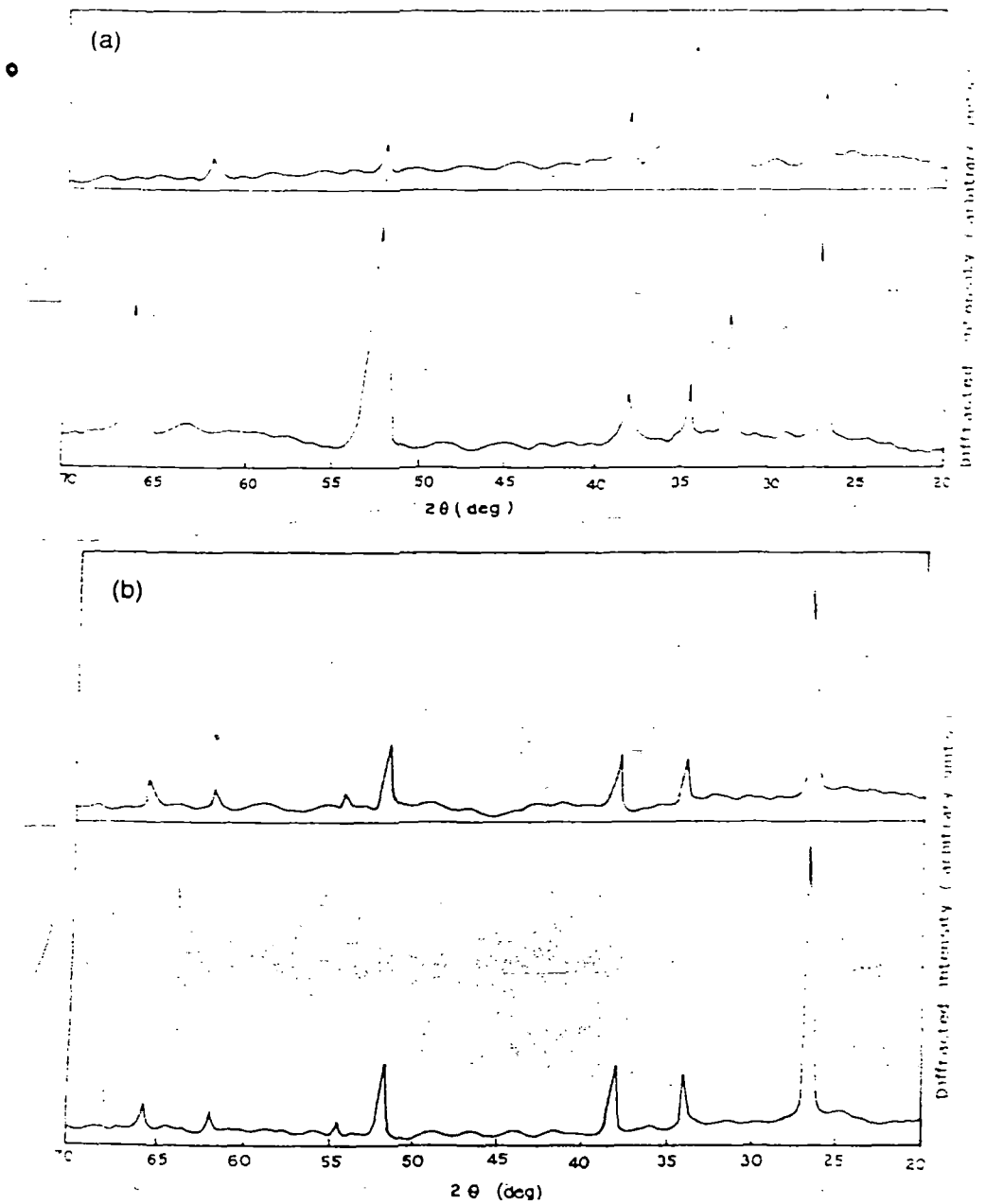

Fig. 2. (a) X-ray diffractogram of undoped SnO_2 films of two different thicknesses (T_s = 400°C). (i) 0.6 μm (ii) 2.5 μm. (b) X-ray diffractogram of doped films (T_s = 400°C). (i) 1.5 at.% Sb-doped. (ii) 4.5 at.% F-doped.

Table 1
Prominent peak positions (2θ values) of the X-ray diffraction peaks, corresponding d-values, relative intensities (I/I_0) and their identification for F-doped SnO_2 films

Observed values			Comparable values from ASTM data file			
2θ	d-value [Å]	(I/I_0)	2θ	d-values [Å]	(I/I_0)	hkl
26.60	3.347	100	26.57	3.351	100	110
33.90	2.641	21	33.86	2.644	80	101
37.95	2.368	32	37.94	2.369	25	200
51.75	1.764	34	51.73	1.765	65	211
54.85	1.671	12	54.74	1.675	18	220
61.95	1.496	12	61.86	1.498	14	310
65.90	1.415	13	65.94	1.415	16	301

posited at a substrate temperature of 400°C are shown in Fig. 3. It is observed that in all cases except that of Mo-doped films large size grains of ~ 1.7 μm are spread throughout the film over a background of grain size ~ 0.6 μm. These large grains are observed to disappear when doped with Mo. The average grain size for Sb- and F-doped films is found to be larger, while that for Mo-doped films is smaller compared to the undoped ones.

Films were also deposited on different substrates to investigate the substrate effect. Fig. 4 shows the SEM micrographs of undoped SnO_2 films deposited on mica and aluminium sheet at a substrate temperature of 400°C. It is also evident from Fig. 4 that the grain size of the undoped SnO_2 films deposited on crystalline mica and aluminium substrate is larger than that deposited on glass substrates. Table 2 shows the grain size variation of the films deposited.

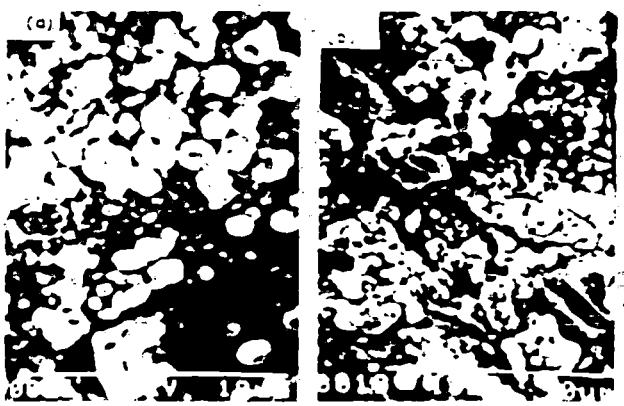

Fig. 4. Scanning electron micrographs of SnO_2 thin films on different substrates (T_s = 400°C). (a) On mica, (b) on aluminium sheet.

3.3. Electrical properties

Results of detailed measurements of the sheet resistance of the films as a function of thickness, temperature and dopant concentration are shown in Figs. 5 and 6.

Fig. 5 shows the variation of sheet resistance with thickness of undoped films deposited at three substrate temperatures. It is evident from the curves that the room temperature resistivity of the undoped films decreases to its minimum value when deposited at a substrate temperature of 400°C but increases again when deposited at a higher substrate temperature of 450°C. This is due to the fact that, on increasing the substrate temperature from 350°C to 400°C, a better degree of crystallinity is achieved, leading to improved electronic, optical and structural properties [8,26]. It is also known that [5] both the carrier

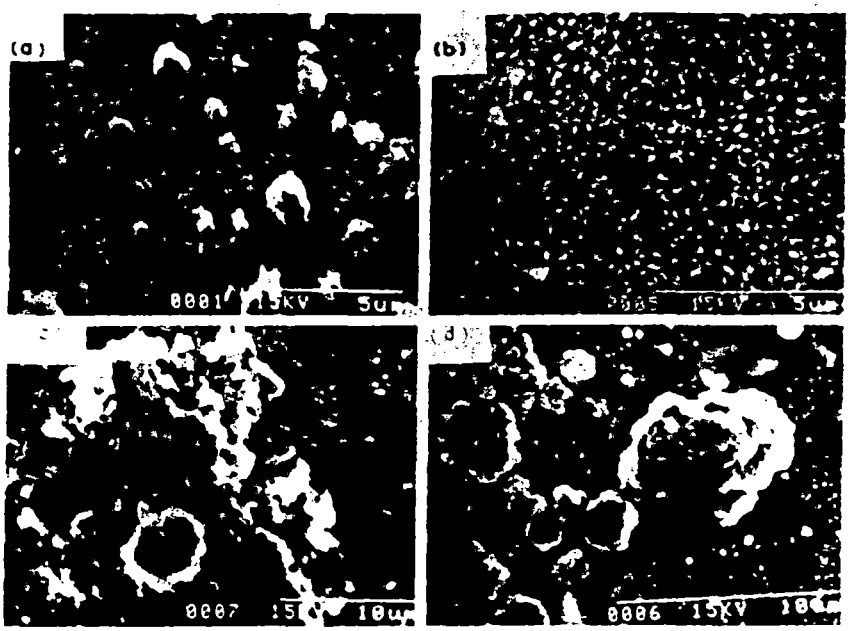

Fig. 3. Scanning electron micrographs of SnO_2 thin films on glass substrates (T_s = 400°C). (a) Undoped SnO_2; (b) SnO_2:Mo (6 at.%); (c) SnO_2:Sb (1.5 at.%); (d) SnO_2:F (4.5at.%).

Table 2
Grain size variation of doped (on glass) and undoped (on different substrates) SnO_2 films (deposition temperature T_s = 400°C)

Films	Substrate	Average grain size [μm]
SnO_2 undoped	glass	1.20
SnO_2:Sb	glass	4.00
SnO_2:Mo	glass	0.60
SnO_2:F	glass	4.75
SnO_2 undoped	mica	2.00
SnO_2 undoped	aluminium	1.50

concentration and mobility increase with the increase of substrate temperature where mobility variation is larger than that of the carrier concentration. A further increase in substrate temperature produces films of increased resistivity. This is due to the fact that in undoped SnO_2, conduction electrons arise from oxygen vacancies, and a higher substrate temperature causes an increased oxygen evolution from the substrate, leading to more nearly stoichiometric films [8,27]. The resistivity of the undoped films prepared at a substrate temperature of 400°C is estimated to be 4×10^{-3} Ω cm, which agrees well with the values reported earlier in the literature [8].

The effect of dopants (Mo, Sb, and F) at various concentrations on the resistivity was studied. It is found that for every dopant, there is an optimum concentration at which the resistivity is a minimum. These values are listed in Table 3.

Thus it is observed that the introduction of Mo reduces the resistivity by a maximum factor of 2 whereas Sb and F reduce it by factors of 5 and 10, respectively. Similar results are reported by Gordillo et al. [7]. The relatively

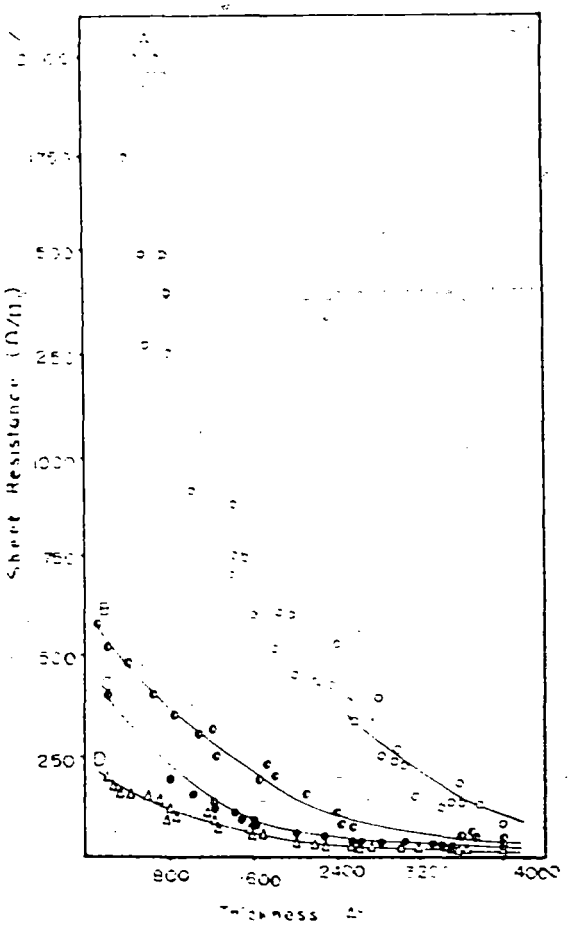

Fig. 6. Sheet resistance–thickness relationship for undoped (curve A) and doped (curve B, SnO_2:Mo (6 at.%); curve C, SnO_2:Sb (1.5 at.%); curve D, SnO_2:F (4.5 at.%)) SnO_2 films prepared at a substrate temperature of 400°C.

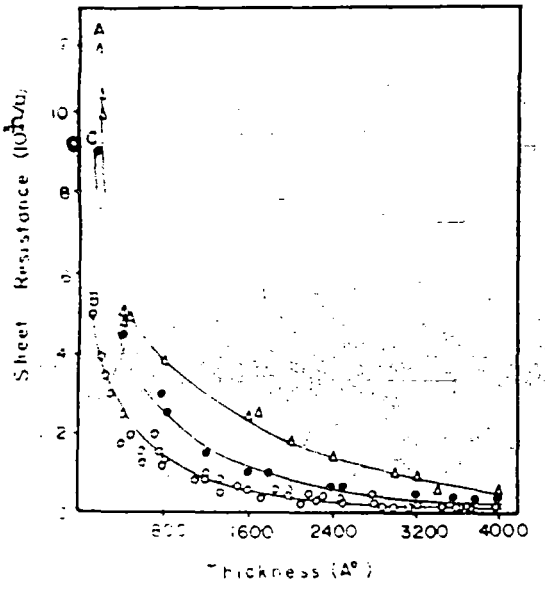

Fig. 5. Variation of sheet resistance with thickness of undoped SnO_2 films deposited at various substrate temperatures. A, 350°C; B, 400°C; C, 450°C.

higher resistivity and lower optical transmission of the Mo-doped SnO_2 films compared to the Sb-doped and F-doped films may be due to their small grain size as observed from the SEM micrograph. It is known that with the decrease in grain size the grain boundary potential increases, leading to an increased grain boundary scattering and a corresponding increase in resistivity [5]. In the case of Sb-doped and F-doped SnO_2 films, the resistivity decreases up to 1.5 at.% Sb-doping and 4.5 at.% F-doping, respectively, which may be due to (i) increased carrier concentration, (ii) larger grain size and (iii) preferred orientation. Beyond the above concentration the observed

Table 3
Minimum resistivity values of undoped and doped SnO_2 films on glass substrate (T_s = 400°C)

Films	Resistivity [Ω cm]
SnO_2 (undoped)	4×10^{-3}
SnO_2:Mo (6 at.%)	2×10^{-3}
SnO_2:Sb (1.5 at.%)	8×10^{-4}
SnO_2:F (4.5 at.%)	4×10^{-4}

increases in resistivity may be due to the increase in the contribution from ionised impurity scattering [5].

The variation of sheet resistance with thickness for optimum concentrations of the dopants is shown in Fig. 6.

3.4 Optical properties

The variation of the average optical transmission over the range 400–800 nm as a function of sheet resistance for undoped and doped films is shown in Fig. 7. The optical transmission is observed to decrease with decreasing sheet resistance in the case of both undoped and doped films. It is seen for all the films that the optical transmission drops off more rapidly at lower values of the sheet resistance. This is due to an increase in surface roughness of films having a low sheet resistance which have a proportionately higher thickness [1,26]. However, F-doped films are found to have a high optical transmission even at a low sheet resistance of 100 Ω/□.

The films are found to compare quite favourably in terms of electrical and optical properties with those prepared by other methods as shown in Table 4. The figure of merit ϕ_{TC} for the films has been calculated according to Haäcke's [28] relation $\phi_{TC} = T^{10}/R_s$ for transparent conducting films, where T is the transmission and R_s the sheet resistance.

3.5. Conclusions

Undoped and Mo-, Sb-, and F-doped SnO_2 films deposited by the Open Air Chemical Vapour Deposition (OACVD) technique have been investigated in detail. The films show a high degree of crystallinity along with the largest values of electrical conductivity and optical transmission when deposited at a substrate temperature of 400°C. X-ray diffractometric study suggests that Sb- and F-doped SnO_2 films show a preferred orientation along the (110) plane. The surface morphology study by scanning

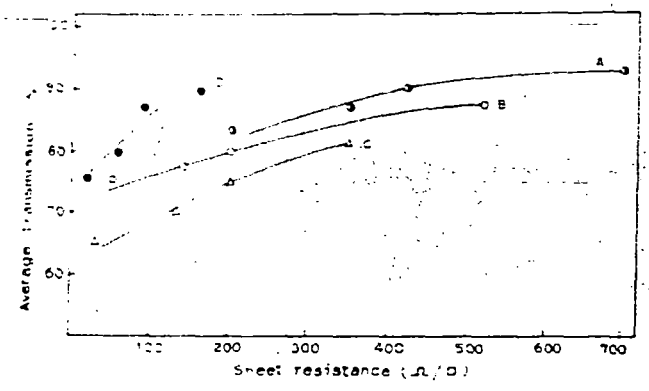

Fig. 7. The average optical transmission over 400–800 nm versus sheet resistance for undoped (curve A) and doped (curve B, SnO_2:Mo (6 at.%); curve C, SnO_2:Sb (1.5 at.%); curve D, SnO_2:F (4.5 at.%)) SnO_2 films prepared at a substrate temperature of 400°C.

Table 4
Comparison of the electrical and optical properties of tin dioxide films prepared by various workers

Material	Deposition technique	ρ	R_s	$T_a(\Delta\lambda)$	ϕ_{TC}
SnO_2	SP [27]	5×10^{-3}	83	85 (0.5–2)	2.40
	CVD [29]	7×10^{-3}	1200	93 (0.5–0.7)	0.42
	present work	4×10^{-3}	100	90 (0.4–0.8)	3.48
SnO_2:Sb	SP [1]	4.2×10^{-3}	28	87 (0.3–1)	9.40
	CVD [30]	2×10^{-3}	55	88 (0.4–0.7)	5.06
	present work	8×10^{-4}	20	75 (0.4–0.8)	2.82
SnO_2:F	SP [1]	4.6×10^{-3}	10	85 (0.4–1)	19.68
	CVD [13]	5×10^{-4}	20	90 (0.4–0.8)	17.43
	present work	4×10^{-4}	10	85 (0.4–0.8)	19.68
SnO_2:Mo	present work	2×10^{-3}	50	80 (0.4–0.8)	2.15

ρ = resistivity [Ω cm], R_s = sheet resistance [Ω □], $T_a(\Delta\lambda)$ = average optical transmission (wavelength range [%] (μm)), ϕ_{TC} = figure of merit [$\times 10^{-3}$ Ω^{-1}], CVD = chemical vapour deposition, SP = spray pyrolysis.

electron microscope suggests that for films deposited on glass substrates, the grain size increases in the case of Sb-doped and F-doped SnO_2 films but decreases for Mo-doped SnO_2 films. The grain size for undoped films on mica and aluminium sheet substrate is also larger than that for films deposited on glass substrates.

The lowest values of sheet resistance at a particular thickness are obtained for 6 at.% Mo-doped, 1.5 at.% Sb-doped and 4.5 at.% F-doped SnO_2 films on glass substrate. A typical value of resistivity of 4.5 at.% F-doped SnO_2 films is 4×10^{-4} Ω cm and that for 1.5 at.% Sb-doped SnO_2 is $\sim 8 \times 10^{-4}$ Ω cm.

The films compare quite well in terms of electrical conductivity and optical transmission with those obtained by other methods. The average optical transmission over the range of 400 to 800 nm is found to decrease as the sheet resistance decreases for Mo- and Sb-doped films. But for F-doped films, a negligible increase in transmission loss with decreasing sheet resistance is found to occur.

In conclusion, tin dioxide films having a sheet resistance of 10–1000 Ω/□ and an average optical transmission of 75–90% could routinely be obtained by this method. The merit of the present method is its extreme simplicity by which one can deposit useful tin dioxide films for device applications either on one side or both sides of a planar substrate or inside of a tube quite easily in any laboratory.

References

[1] K.L. Chopra, S. Major, D.K. Pandya, Thin Solid Films 102 (1983) 1–46.
[2] C.S. Rastomjee, R.S. Dale, R.J. Schaffer, F.H. Jones, R.G. Egdell, G.C. Georgiadis, M.J. Lee, T.J. Tate, L.L. Cao, Thin Solid Films 279 (1996) 98–105.
[3] I. Kocemba, T. Paryjczak, Thin Solid Films 272 (1996) 15–17.
[4] B.J. Hwang, K.L. Lee, Thin Solid Films 279 (1996) 236–241.

[5] E. Shanthi, V. Dutta, A. Banerjee, K.L. Chopra, J. Appl. Phys. 51 (12) (1980) 6243–6251.
[6] E. Shanthi, A. Banerjee, K.L. Chopra, Thin Solid Films 88 (1982) 93.
[7] G. Gordillo, L.C. Moreno, W. de la Cruz, P. Teheran, Thin Solid Films 252 (1994) 61–66.
[8] A.L. Unaogu, C.E. Okeke, Solar Energy Mater. 20 (1990) 29–36.
[9] H. Kim, H.A. Laitimen, J. Am. Ceram. Soc. 58 (1975) 23.
[10] E. Shanthi, A. Banerjee, V. Dutta, K.L. Chopra, Appl. Phys. 53 (1982) 1615.
[11] G. Maurodien, M. Gajardziska, Novkovski, Thin Solid Films 113 (1984) 93.
[12] J. Bruneaux, H. Cachet, M. Froment, A. Messad, Thin Solid Films 198 (1991) 129–142.
[13] J. Proscia, R.G. Gordon, Thin Solid Films 214 (1992) 175–187.
[14] Yan Dawei, Ma Xiaocui, Wang Zongchang, Wu Jam, Thin Solid Films 224 (1993) 257–262.
[15] A. Fujisawa, T. Nishino, Y. Hamakawa, Jpn. J. Appl. Phys. 27 (4) (1988) 552–555.
[16] M.R. Kadam, N. Vittal, R.N. Karekar, R.C. Aiyar, Thin Solid Films 187 (1990) 199.
[17] B.J. Baliga, S.K. Ggandi, J. Electrochem. Soc. 123 (1976) 941.
[18] J.P. Chatelon, C. Terner, E. Bernstein, R. Berjoan, J.A. Roger, Thin Solid Films 247 (1994) 162–168.
[19] C.J. Brinker, A.J. Hurd, P.R. Schunk, G.C. Frye, C.S. Ashley, J. Non-Cryst. Solids 147&148 (1992) 424–436.
[20] Y. Takahashi, Y. Wada, J. Electrochem. Soc. 137 (1990) 267.
[21] H. Demiryont, N. Tezey, Thin Solid Films 101 (1983) 345.
[22] A. Czapla, E. Kusior, M. Bucko, Thin Solid Films 182 (1989) 15.
[23] M.K. Karanjai, D. Dasgupta, J. Phys. D 21 (1988) 356–358.
[24] H. Dislich, E. Hyssmann, Thin solid films 77 (1980) 129–142.
[25] J.L. Vossen, in: G. Hass, M.H. Francombe, R.W. Hoffmann (Eds.), Physics of Thin Films, Vol. 9, Academic Press, New York, 1977, pp. 1–71.
[26] A. De, S. Ray, J. Phys. D 24 (1991) 719–726.
[27] J.C. Manifacier, L. Szepessy, J.F. Bresse, M. Perotin, R. Stuck, Mater. Res. Bull. 14 (1979) 163.
[28] G. Haacke, J. Appl. Phys. 47 (9) (1976) 4086–4089.
[29] J. Kane, H.P. Schweizer, W. Kern, J. Electrochem. Soc. 122 (1975) 1144.
[30] J. Kane, H.P. Schweizer, W. Kern, J. Electrochem. Soc. 123 (1976) 270.

ELSEVIER

Surface and Coatings Technology 102 (1998) 73–80

SURFACE & COATINGS TECHNOLOGY

Tin dioxide based transparent semiconducting films deposited by the dip-coating technique

Sekhar C. Ray, Malay K. Karanjai, Dhruba DasGupta *

Department of Physics, University of North Bengal, Siliguri, Darjeeling-734430, West Bengal, India

Received 29 April 1997; accepted 22 September 1997

Abstract

Undoped and F-doped transparent semiconducting films with tin dioxide as the active material have been prepared by a dip-coating technique. The film is formed in situ by the hydrolysis of stannous chloride which takes place when a substrate is withdrawn vertically from a methanol solution of $SnCl_2 \cdot 2H_2O$ and heat treated at a high temperature. F-doping is achieved by adding NH_4F to the starting solution. The maximum film thickness obtainable per dipping cycle is about 0.58 μm, but can be increased by multiple dipping. The films appear to be a mixed phase consisting of crystalline tin oxide over an amorphous background probably of Sn(OH)Cl. The film produced by a single dipping consists of a small number of isolated SnO_2 crystallites. But as the film thickness is increased these crystallites increase in number and finally merge into a continuous layer. A typical value of resistivity for F-doped films produced by this method is 2.4×10^{-2} Ω cm, with an average transmission of >85% at a thickness of 2.96 μm. © 1998 Elsevier Science S.A.

Keywords: Transparent semiconducting oxide; SnO_2-based thin films; Dip-coating technique

1. Introduction

Among transparent conducting oxide materials, tin dioxide films find wide use because of their excellent performance along with high mechanical, chemical and environmental stability and low cost. In recent years extensive studies have been carried out on these films, which are characterized by high electrical conductivity and high transparency in the visible region of the solar spectrum combined with a high reflectivity in the infrared (IR) region. Tin dioxide is a semiconductor with a wide band gap (3.5–4 eV) [1–3] having a refractive index of approximately 2.0 [3] and a tetragonal crystal structure. The material is used in a variety of display devices such as liquid crystal displays, electrochromic and electroluminescent cells and imaging tubes [4–6] such as photovoltaic devices.

A variety of techniques have been employed to deposit tin dioxide films. These include reactive sputtering [7], spray pyrolysis [8,9], "paste–heat" [10], chemical vapour deposition [11,12] and reactive evaporation [13].

The dip-coating technique is an extremely simple and low-cost method for the deposition of oxide thin films [14]. In this method, as in the related sol gel method [15,16], a metal oxide film is produced by hydrolysis of the corresponding metal alkoxide, nitrate or chloride on a substrate and subsequently heat treated at a high temperature. There are however, few reports in the literature on SnO_2 films prepared by this method, which tend to have a resistivity of at least an order of magnitude higher than those prepared by other techniques, such as chemical vapour deposition (CVD) [17]. This high value of resistivity, while not suitable for photovoltaic cells, would not be a problem for low current applications, such as liquid crystal displays. The present work describes the preparation of undoped and F-doped tin dioxide-based transparent semiconducting thin films by the dip-coating technique and results of study of their electrical and optical properties as well as surface morphology and crystal structure.

2. Experimental details

To prepare the films, the substrate is first dipped and then withdrawn vertically from a solution of

* Corresponding author

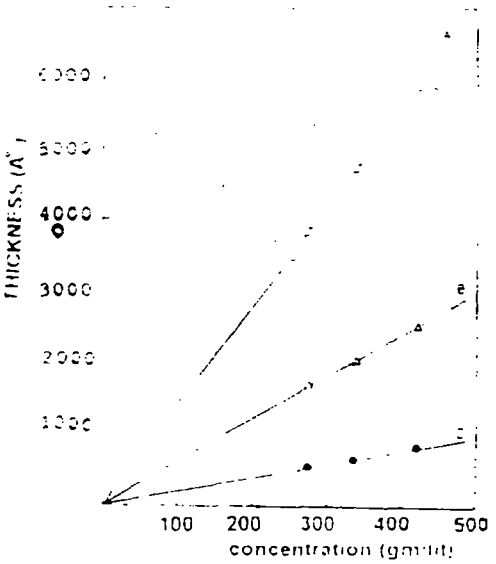

Fig. 1. Variation of thickness of films, deposited on glass substrates, with concentration of the starting solution [speed of withdrawal: A = 3 mm s, B = 1.3 mm s, C = 0.56 mm s].

$SnCl_2 \cdot 2H_2O$ in methanol at a controlled speed (1.33 mm s). The substrate together with its adhering liquid film is then transferred to a furnace kept at a high temperature and heat treated in air for 5 min. Details of the process are given elsewhere [18]. For doped film preparation, the requisite amount of ammonium fluoride is added to the starting solution.

Undoped and doped films were prepared for different heat-treatment temperatures. Variation of thickness with lifting speed and concentration was studied. Thicker films could be obtained by repeating the whole cycle (dip–withdrawal–heat treatment) a number of times.

Films were deposited on soda-glass microscope slides and mica sheets. The characterization was mostly done on those deposited on glass substrates.

The thickness of the deposited films was measured using the stylus method, while sheet resistance was measured by a standard four probe arrangement. Optical transmission as a function of wavelength was obtained by SHIMADZU UV-240 double-beam spectrophotometer. Surface morphology and X-ray diffractometric studies were carried out with a HITACHI S-530 scanning electron microscope and a PHILIPS diffractometer (model PW 1390) with CuK$_\alpha$ radiation.

3. Results

It was found that a heat-treatment temperature of 400–500 C was necessary to obtain films of useful quality in terms of low sheet resistance and high optical transmission. Within this temperature range there was no noticeable variation in the film properties. Results reported in this paper refer to films prepared at a heat-treatment temperature of 400 C.

4. Thickness

Figs. 1–3 show the variation of film thickness with speed of withdrawal, concentration and number of dippings, respectively. It is observed that the thickness

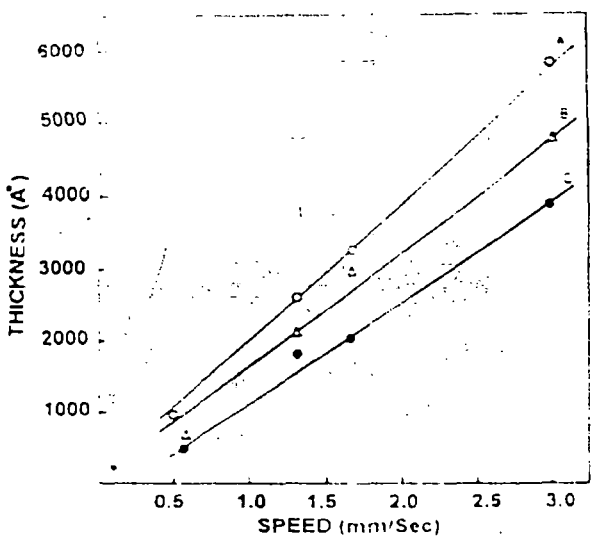

Fig. 2. Variation of thickness of films, deposited on glass substrates, with speed of withdrawal [concentration of the starting solution: A = 410 g l; B = 330 g l; C = 250 g l].

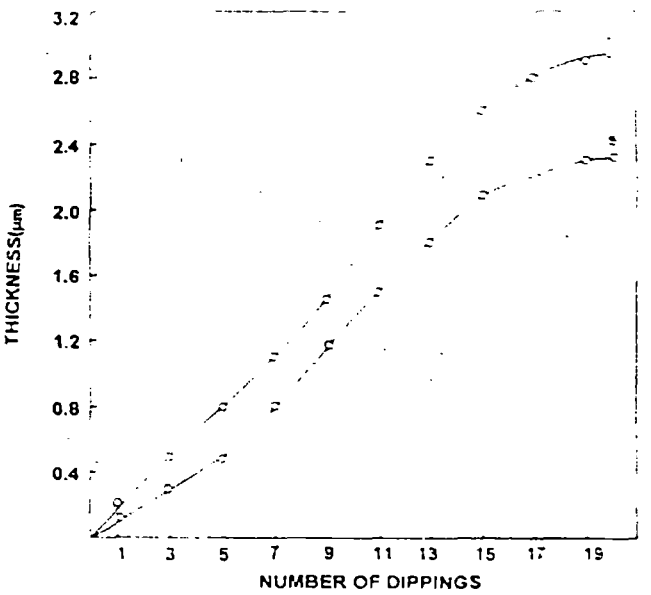

Fig. 3. Variation of thickness of films, deposited on glass substrates, with number of dippings at a speed of withdrawal 1.3 mm s [concentration of the starting solution: A = 330 g l, B = 250 g l].

of the deposited layer increases linearly up to 7–8 dippings, beyond which the rate of increase is slower.

5. X-ray diffractometric study

Fig. 4 shows the X-ray diffractograms of undoped films on glass substrate for five different numbers of dippings. It is evident from the diffractograms that crystallinity of the films increased with number of dippings up to a value of 20 dippings. Single dip films are predominantly amorphous.

Fig. 5 shows the X-ray diffractogram of a typical 10 dip film on mica substrate. The peaks are observed to be much sharper compared to those for films deposited on soda-glass substrates. The position of the peaks obtained on both glass and mica substrates are in conformity with the standard tetragonal crystal structure of SnO_2. Comparison with ASTM (I/I_0) data indicates that there is no significant preferential growth in any direction.

6. Electrical properties

Fig. 6 shows the decrease in sheet resistance of undoped and F-doped films (4.5 at.%) with thickness. The lowest values of sheet resistance, of undoped and 4.5 at.% F-doped films, are 300 Ω and 80 Ω, respectively, for a thickness of 2.96 μm which corresponds to resistivity values of 8.9×10^{-2} Ω cm and 2.4×10^{-2} Ω cm, respectively.

It was found that a film prepared by single dipping in a high concentration solution has a much higher value of sheet resistance compared to one having the same thickness but prepared by multiple dippings using a lower concentration dip solution. For example, at a thickness of 0.58 μm the sheet resistance of a single dip

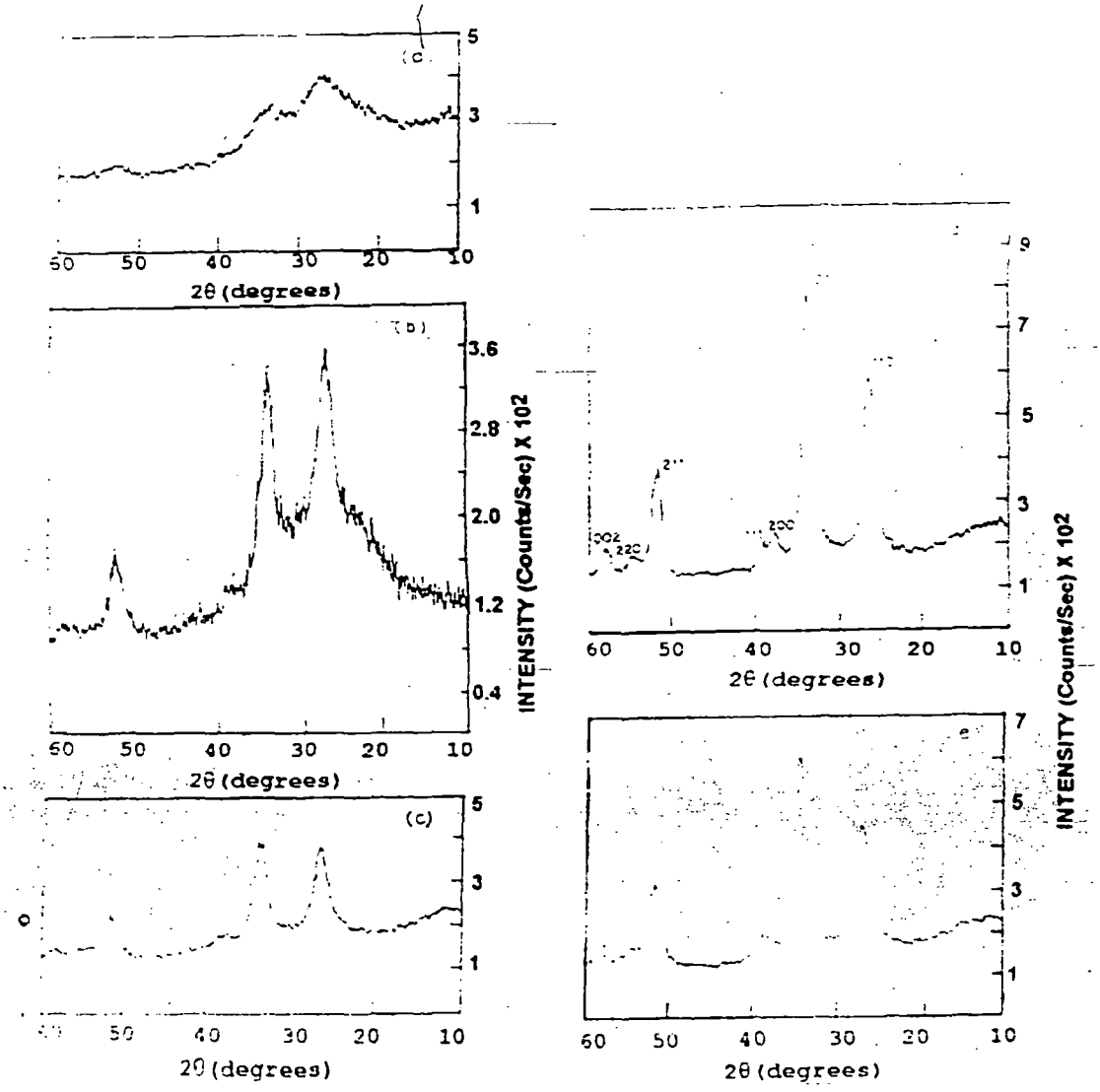

Fig. 4. X-ray diffractograms of dip coated undoped film on glass substrate: (a) 1st dip; (b) five dips; (c) ten dips; (d) twenty dips; (e) twenty five dips.

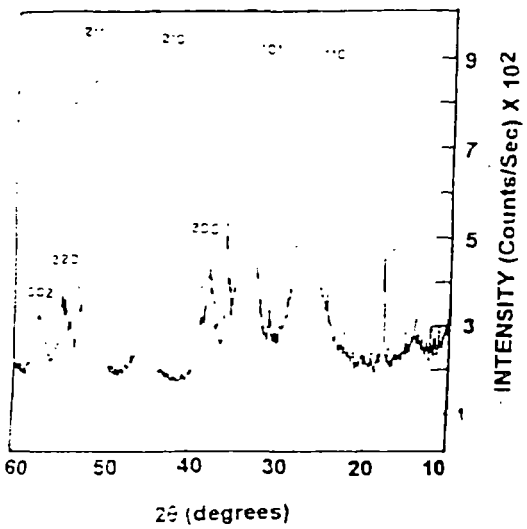

Fig. 5. X-ray diffractograms of a typical film on mica substrate (ten dips). Peaks which are unmarked do not correspond to SnO_2 and probably arise from the substrate itself.

film was $4 \cdot 10^4\ \Omega$, while that prepared by five dippings was $8 \cdot 10^3\ \Omega$. The possible reason may be that for single dipping, a number of loosely packed crystallites are formed, while for multi-dipping these crystallites formed at every deposition step tend to merge together and produce a continuous conducting path. Support for this argument is obtained from Fig. 6, where the sheet resistance of undoped films is seen to drop sharply at a thickness of about 1 μm. For F-doped films the drop occurs at a thickness of about 0.5 μm.

7. Surface morphology study by SEM

Fig. 7 shows the scanning electron micrographs of undoped and 4.5 at.% F-doped films. It is clear from the micrographs that for the undoped film, grain size increases up to 20 dippings. The initial layer (1st dip) films over an amorphous glass substrate is nearly amorphous which is evidenced from the XRD pattern also. Fig. 8 shows the surface morphologies of the films on mica. The grain size is considerably larger in the case of mica substrate than that on glass substrate (Fig. 7e). The much sharper XRD peaks observed in this case are also consistent with the larger grain size. It is possible that formation of bigger crystallites is facilitated by the single-crystal substrate, which is in contact with the growing film.

8. Optical properties

Films obtained by dip-coating technique are highly transparent. Fig. 9 shows the optical transmission *versus* wavelength curves for undoped and 4.5 at.% F-doped films with different sheet resistance values. It is seen that the optical transmission is reduced as a result of doping.

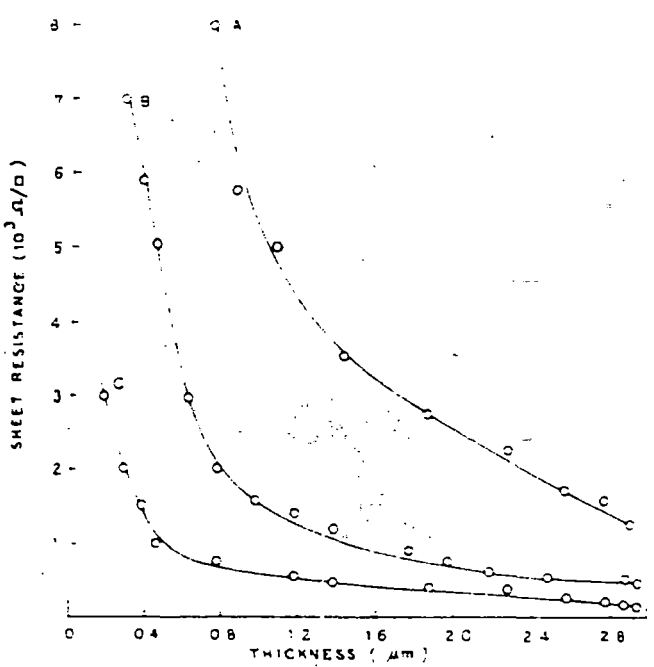

Fig. 6. Variation of sheet resistance of film deposited on glass substrates with thickness. Undoped: A = 250 g l; B = 330 g l. 4.5 at.% F-doped: C = 250 g l.

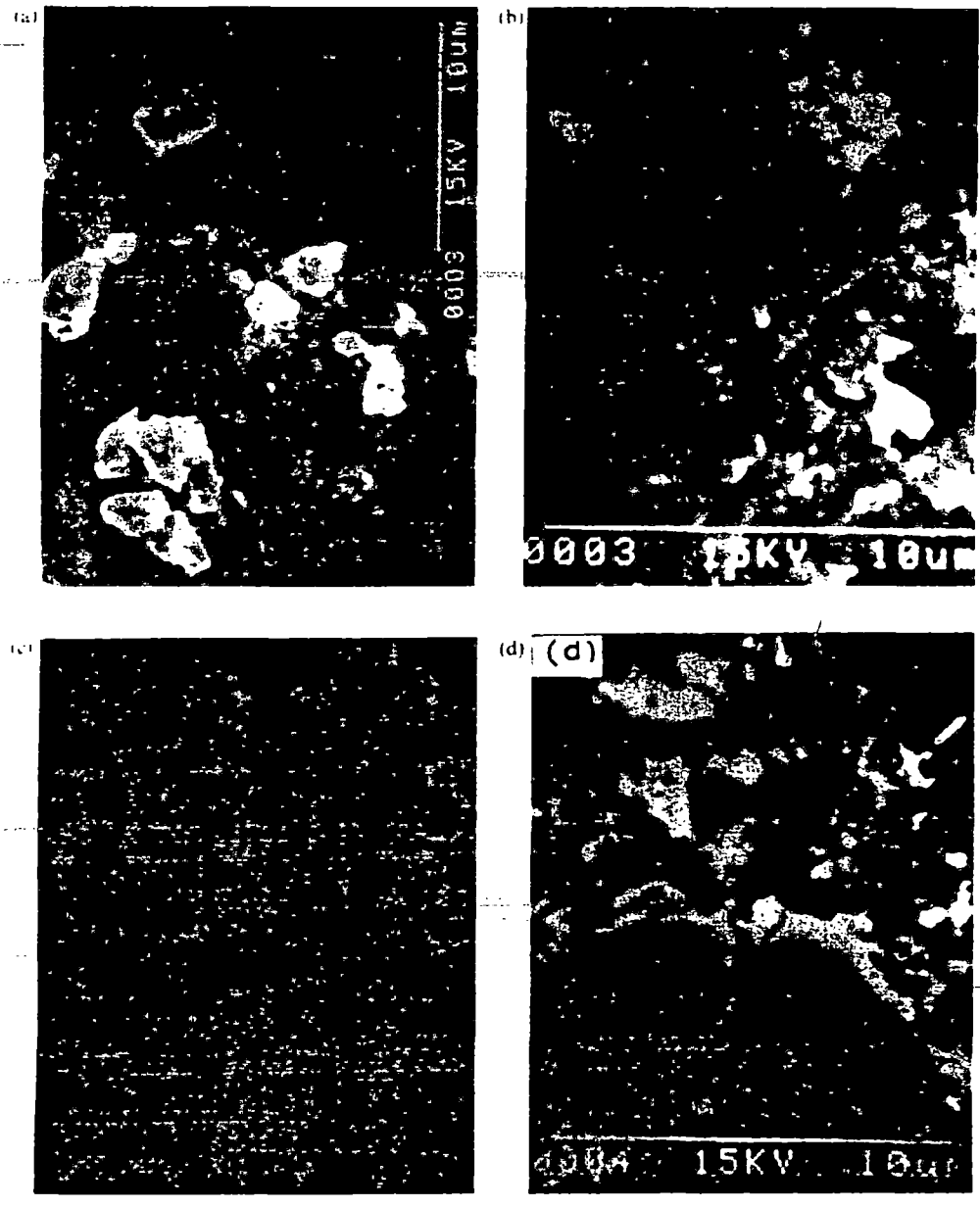

Fig. 7. Electron micrographs of undoped and doped films on glass substrate. Undoped: (a) 1st dip; (b) five dips; (c) ten dips; (d) fifteen dips; (e) twenty dips; (f) twenty five dips. 4.5 at.% F-doped film: (g) twenty dips.

A similar phenomenon has also been observed by Chopra et al. [4] and De et al. [19] and attributed by them to a high surface roughness of SnO_2 films having low sheet resistance compared to undoped ones. Average optical transmission 85–90% for undoped and 75–80% for F-doped films are obtained for a thickness of 2.96 μm over a range 400 to 900 nm.

9. Discussion

It is known [10,20] that $SnCl_2$ undergoes hydrolysis according to the equation

$$6SnCl_2 + H_2O \rightarrow 2SnCl_4 + 4Sn(OH)Cl \quad (1)$$

This reaction is relatively slow at room temperature, but is accelerated on heating. $SnCl_4$, in turn, readily hydrolyses to SnO_2 at a high temperature as given below

$$SnCl_4 + 2H_2O = SnO_2 + 4HCl \quad (2)$$

This forms the basis of preparation of conducting tin dioxide films by the paste–heat or OACVD methods [10,21]. In these methods, $SnCl_4$ produced from reaction (Eq. (1)) taking place in a separate area is allowed to hydrolyse on the substrate and yield SnO_2. In contrast, in the present method the Sn(OH)Cl also remains on the substrate and forms the amorphous matrix, while most of the $SnCl_4$ produced, escapes. A small fraction of this $SnCl_4$, however, is hydrolysed on the substrate

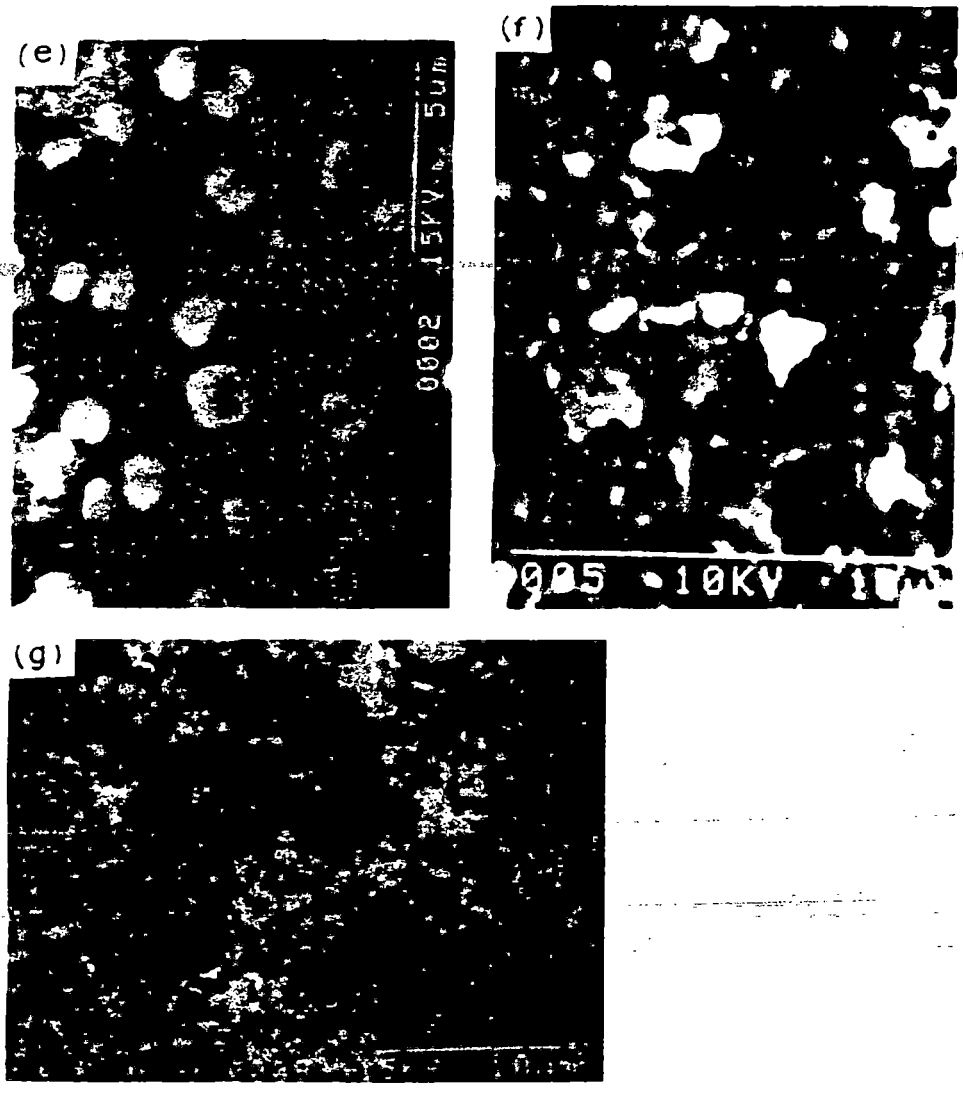

Fig. 7. (*continued*)

and produces small SnO_2 crystallites. Repeated dipping increases the number of these crystallites which form an interconnected network after about 15–20 dippings. This can be seen from the XRD spectra, the variation of sheet resistance with thickness and the SEM photographs. We see that the sharp drop in sheet resistance, appearance of sharp XRD peaks and merging of SnO_2 grains, all take place at a thickness of about 1 μm. However, even at this stage the proportion of the amorphous component is quite large, as shown by the high value of resistivity, viz. $2.4 \times 10^{-2}\,\Omega$ cm compared to $2.4 \times 10^{-4}\,\Omega$ cm for CVD SnO_2 films. It may be interesting to note that in the work of Gordillo et al. [22], also on spray-deposited SnO_2 films, a strong amorphous background is seen to be present in the XRD pattern when $SnCl_2$ was used as a starting material.

Although this amorphous component, most probably Sn(OH)Cl, is present in the films, it is highly transparent and leads to no significant drop in optical transmission. This component is responsible for making the resistivity about two orders of magnitude higher than that obtained for CVD films. However, the high optical transmittance makes these films suitable for those display applications where the current requirement is low, e.g. liquid crystal or electrochromic displays. In addition, the simplicity of the deposition method could make it attractive for enhancing the IR reflectivity at a low cost, e.g. in solar cookers.

The effectiveness of a transparent conducting film depends on its optical transmission as well as its sheet resistance. As already discussed, the high sheet resistance of the dip-coated films is, to a great extent, compensated for by their large optical transmittance. Haacke [23] has introduced a figure of merit for transparent conducting films defined by the relation $\varphi_{TC} = T^{10} R_S$, where T is the optical transmittance and R_S is the sheet resistance. This parameter can be used to evaluate the performance of a candidate material from its fundamental parame-

Fig. 8. Electron micrograph of undoped film on mica substrates (10 dips).

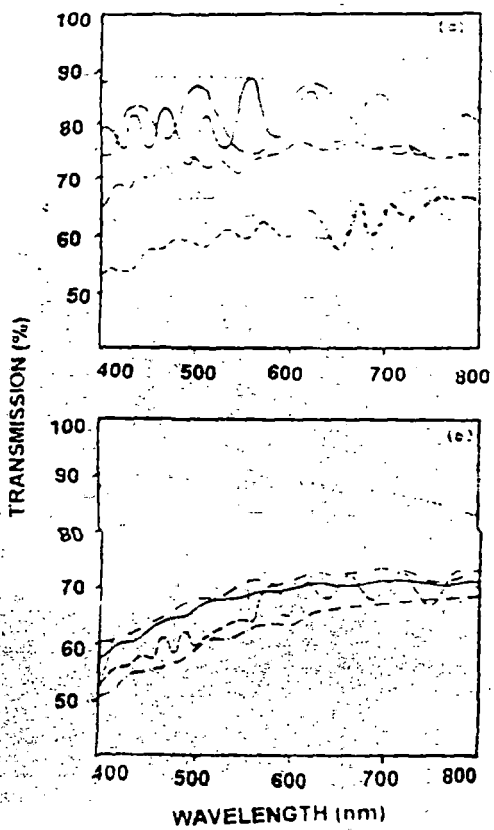

Fig. 9. Optical transmission *versus* wavelength for typical films of various sheet resistances. (a) Undoped: (.....), bare substrate; (——), 4000 Ω; (-.-.-.), 1250 Ω; (- - - -), 600 Ω; (), 250 Ω; (b) 4.5 at.% F-doped films: (.....), bare substrate; (——), 800 Ω; (), 500 Ω; (- - - -), 200 Ω; (-.-.-.), 90 Ω.

ters. A typical σ_{fc} value for our 4.5 at.% F-doped, dip-coated film is $2.5 \times 10^{-3}\ \Omega^{-1}$, which compares quite favourably with the value of $2.6 \times 10^{-3}\ \Omega^{-1}$ for CVD SnO_2 films [24,25].

10. Summary

It has been demonstrated that the dip-coating technique can be used to deposit transparent semiconducting films in a simple manner using $SnCl_2 \cdot 2H_2O$ as a starting material. The films contain crystalline SnO_2 in addition to an amorphous background, probably of Sn(OH)Cl. The resistivity of the films is somewhat higher compared to SnO_2 films prepared by CVD or spray pyrolysis. This is probably due to the presence of the amorphous constituent. However, the films are highly transparent and have a figure of merit comparable to that for conventionally-prepared SnO_2 films. The films would be potentially useful for low-current application such as display devices. The method is easily adaptable for deposition on large-area surfaces.

References

[1] J.C. Manifacier, L.D. Zepessy, J.F. Bresse, M. Perotin, Mater. Res. Bull. 14 (1979) 163.
[2] W. Spence, J. Appl. Phys. 38 (1967) 3767.
[3] Y.S. Hsu, S.K. Gandhi, J. Electrochem. Soc. II: Sol. State Sci. Technol. 127 (1980) 1592.
[4] K.L. Chopra, S. Major, D.K. Pandya, Thin Solid Films 102 (1983) 1.
[5] C.S. Rastomjee, R.S. Dale, R.J. Schaffer, P.H. Jones, R.G. Lodell, G.C. Georoiadis, M.J. Lee, T.J. Tate, L.L. Cao, Thin Solid Films 279 (1996) 98.
[6] J. Kocemba, T. Paryjczak, Thin Solid Films 272 (1996) 15.
[7] T. Matsuoka, J. Kuwata, M. Nishikawa, V. Fujita, T. Tohda, A. Abe, Jpn J. Appl. Phys. 27 (1988) 1088.
[8] E. Shanthi, V. Dutta, A. Banerjee, K.L. Chopra, J. Appl. Phys. 51 (1980) 6243.
[9] B.J. Baliga, S.K. Gandhi, J. Electrochem. Soc. 123 (1976) 941.
[10] M.K. Karanjai, D. DasGupta, J. Phys. D: Appl. Phys. 21 (1988) 356.
[11] T.P. Chow, M. Ehezzo, B.J. Baliga, J. Electrochem. Soc. 129 (1982) 1040.
[12] J.P. Upadhayay, S.R. Vishwakarma, H.C. Prasad, Thin Solid Films 169 (1989) 195.
[13] H. Demryont, N. Tezzy, Thin Solid Films 101 (1983) 345.
[14] H. Dislich, E. Hussmann, Thin Solid Films 77 (1981) 129.
[15] J.P. Chatelon, C. Terrier, E. Bernstein, R. Berjoan, J.A. Roger, Thin Solid Films 247 (1994) 162.
[16] C. Terrier, J.P. Chatelon, R. Berjoan, J.A. Roger, Thin Solid Films 263 (1995) 37.
[17] S. Sakka, J. Non-crystalline Sol. 73 (1985) 651.
[18] M.K. Karanjai, D. DasGupta, Thin Solid Films 155 (1987) 309.
[19] A. De, S. Ray, J. Phys. D: Appl. Phys. 24 (1991) 719.

[20] J.R. Partington, A Text Book of Inorganic Chemistry 6th edn. MacMillan, London, 1950, p. 829.
[21] S.C. Ray, M.K. Karanjai, D. DasGupta, Thin Solid Films 307 (1997) 221.
[22] G. Gordillo, L.C. Moreno, W. De la Cruz, P. Teheran, Thin Solid Films 252 (1994) 66.
[23] G. Hacke, J. Appl. Phys. [illegible] (1976) 4056.
[24] J. Kane, H.P. Schweizer, W. Kern, J. Electrochem. Soc. [illegible] (1975) 1144.
[25] J. Kane, H.P. Schweizer, W. Kern, J. Electrochem. Soc. [illegible] (1976) 270.

Reprints

ELSEVIER

Thin Solid Films 10619 (1998) xxx C

Thin Solid Films

Deposition and characterization of $Zn_xCd_{1-x}S$ thin films prepared by the dip technique

Sekhar C. Ray, Malay K. Karanjai, Dhruba DasGupta *

Department of Physics, University of North Bengal, Siliguri, Darjeeling-734430, West Bengal, India

Received 30 May 1997; accepted 16 October 1997

Abstract

$Zn_xCd_{1-x}S$ ($0 \le x \le 1$) thin films have been deposited by the dip technique on glass substrates. In this method, a clean substrate was dipped into an alcoholic solution of the corresponding nitrates and thiourea and then withdrawn vertically at a controlled speed, and finally baked in a furnace. X-ray diffractometric study suggests that for zinc atomic fraction $x \le 0.6$ films prepared at a baking temperature of 500°C are homogeneous with a hexagonal (wurtzite) structure. Increase in the proportion of zinc in the starting solution is found to produce a decrease in the lattice parameter. SEM studies reveal an increase in grain size with x up to a value of 0.6. For $x > 0.6$, the films appear to have an amorphous character, as no distinguishable peaks can be seen in the X-ray diffractograms. The SEM micrographs also do not show any clearly defined grains over this range. Values of bandgap obtained from optical absorption measurements as well as from spectral response of photoconductivity are in good agreement with each other and vary monotonically from 2.30 eV (CdS) to 2.69 eV ($Zn_{0.6}Cd_{0.4}S$) over the range $0 \le x \le 0.6$. © 1998 Elsevier Science S.A.

Keywords. Deposition process; Optical properties; Surface morphology; X-ray diffraction

1. Introduction

$Zn_xCd_{1-x}S$ thin films have been widely used as wide bandgap window material in heterojunction photovoltaic solar cells [1–5] and in photoconductive devices [6]. In solar cell systems, where CdS thin films have been proved to be useful, partial substitution of Zn for Cd increases the optical window of the heterojunction and also the diffusion potential [7]. Moreover, in heterojunction solar cells using $CuGaSe_2$, the use of $Zn_xCd_{1-x}S$ instead of CdS can lead to an increase in photocurrent by providing a match in the electron affinities of the two materials. This hexagonal $Zn_xCd_{1-x}S$ ternary compound is also potentially useful as a window material for the fabrication of *p–n* junctions without lattice mismatch in the devices based on quaternary materials like $CuIn_xGa_{1-x}Se_2$ [8] or $CuIn(S_zSe_{1-z})_2$ [9]. $Zn_xCd_{1-x}S$ thin films have been prepared by a variety of techniques, which include spray pyrolysis [7,10], ion beam deposition [11], molecular beam epitaxial growth [12], solution growth [13,14], and successive ionic layer absorption and reaction process [15].

The dip technique and the related sol–gel method have been traditionally used for the deposition of oxide thin films [16,17]. Usually, these involve the hydrolysis of the corresponding metal alkoxide, nitrate or chloride on a heated substrate. In a previous work [18], we reported a modification of the dip technique for the deposition of sulphide films. Here, the substrate is withdrawn from an alcoholic solution of the metal nitrate and thiourea, and transferred to a furnace maintained at a high temperature, where a chemical reaction takes place to yield the sulphide films.

As described in Ref. [18], attempts to produce $Cd_{0.8}Zn_{0.2}S$ films using a starting solution containing both cadmium and zinc nitrates resulted in the formation of a mixed phase material containing partially crystalline CdS and amorphous ZnS when prepared at a baking temperature of 400°C. It has been found that by increasing the baking temperature to 500°C homogeneous crystalline $Zn_xCd_{1-x}S$ films within the range $0 \le x \le 0.6$ could be produced. These shows continuous variation of lattice parameter and bandgap as a function of x. For $x > 0.6$, the films tend to develop an amorphous character. The bandgap varies monotonically from 2.3 eV (CdS) to 2.69 eV ($Zn_{0.6}Cd_{0.4}S$) over the range $0 \le x \le 0.6$. We describe in

* Corresponding author. Tel.: +91-353-450414; fax: +91-353-450546; e-mail: dhruba@nbu.ernet.in

PII S0040-6090(97)00932-2

this report the preparation of these films and their characterization by X-ray diffractometry, scanning electron microscopy, optical and photoconductivity measurements.

2. Experimental details

Three separate saturated solutions of cadmium nitrate [$Cd(NO_3)_2$, $4H_2O$], zinc nitrate [$Zn(NO_3)_2$, $6H_2O$] and thiourea with methanol as solvent were initially prepared. They were then mixed in requisite amounts to yield the starting solution for deposition by dipping. It was found that the mixing was best achieved without any precipitation taking place if the thiourea solution was divided into two parts which were mixed with the two nitrate solutions separately, and one of the mixtures then slowly added to the other.

Microscope glass slides, used as substrates, were cleaned by washing in detergent and chromic acid and finally degreased in acetone and methanol vapour.

In the film forming process, a clean substrate was dipped into the starting solution and then withdrawn vertically at a controlled speed, under atmospheric conditions, with the help of a pulley and geared motor, when a liquid film adhered to the substrate. The substrate together with the liquid film adhering to it was immediately transferred to a furnace for baking, when the chemicals reacted to form the desired solid film. It is found that films of a very high quality were obtainable when prepared at a baking temperature of 500°C. Thickness of the films could be increased by repeating the whole cycle (dip–withdrawal–bake) a number of times. Details are given in Ref. [18].

$Zn_xCd_{1-x}S$ films were deposited at 500°C for various concentrations of zinc from $x = 0$ to $x = 1$. The value of x was changed by changing the concentrations of Zn–nitrate and Cd–nitrate in the starting solution. The Zn/Cd ratio in the solid films was determined by Atomic Absorption Spectroscopy. The value of x was found to be essentially the same as the relative proportion of Zn atoms [Zn:(Zn + Cd)] in the starting solution. Film thickness was measured by stylus method. Characterization of the films was carried out by optical absorption, X-ray diffractometry, scanning electron microscopy and spectral response of photo conductivity measurements.

Optical properties were studied by Shimadzu UV-240 double-beam spectrophotometer. X-ray diffractometry and surface morphology studies were carried out by Philips diffractometer (model PW 1390) with CuK_α radiation (Ni-filter) at 1.54 Å and Hitachi S-530 scanning electron microscope, respectively. To determine the photo conductive (PC) spectral response, a PC cell was fabricated by depositing Ag-electrodes in the usual interdigitated pattern, which was subsequently placed at the detector position of a Spectromom 202 spectrophotometer, and the photo current measured as a function of wavelength. The area of the cell was about 1 cm^2.

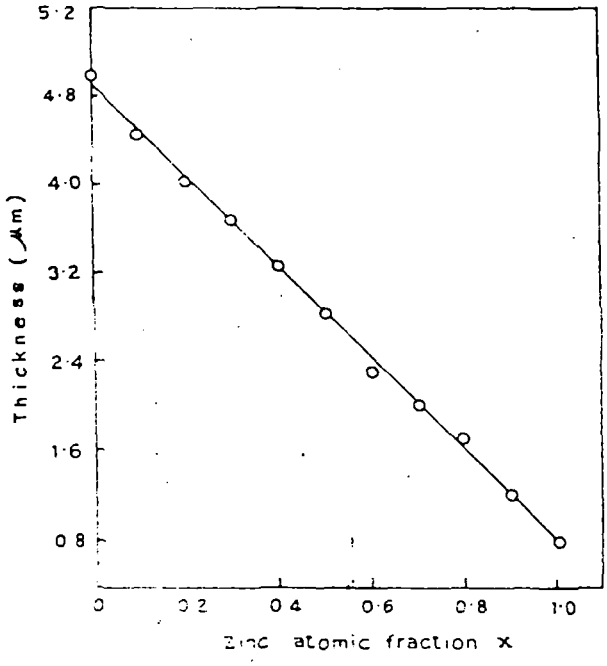

Fig. 1. Variation of thickness on zinc atomic fraction x of $Zn_xCd_{1-x}S$ thin films

3. Results and discussion

The $Zn_xCd_{1-x}S$ thin films were smooth, uniform, highly reflecting and strongly adherent to the substrate. Colour of the films was observed to change from yellow-orange to pale yellow with increase in zinc atomic fraction x. Zinc sulphide films ($x = 1$) were white in colour.

Films of different thicknesses were obtained by changing the lifting speed as well as increasing the number of dippings (dip–withdrawal–bake cycle). Smooth and uniform films could be obtained up to a maximum withdrawal speed of 1.33 mm/s. For higher speeds, the films tended to be non-uniform. At high withdrawal speeds, the liquid layer adhering to the substrate as it is pulled out is quite thick, and turbulence in this layer is also higher.

Results reported in this paper were obtained by measurements on films prepared by 10 dippings from a starting solution containing total 0.93 (Cd + Zn) mol/l and withdrawn at a speed of 1.33 mm/s.

3.1. Thickness

Fig. 1 shows the variation of the thickness of the film for different values of x, when the total number of (Cd + Zn) moles was kept constant in a given volume of the starting solution. Cd and Zn ratio in the solid films measured by Atomic Absorption Spectroscopy, agrees well with that in the starting solution for different concentrations. The thickness of the films is found to decrease linearly with the increase in zinc proportion.

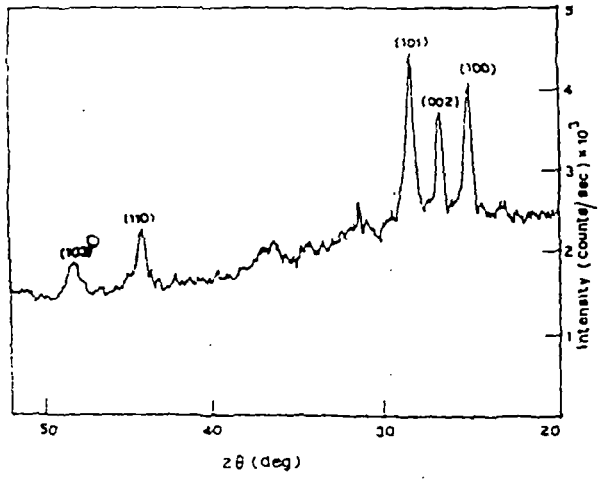

Fig. 2. X-ray diffractogram of a typical $Zn_xCd_{1-x}S$ thin film ($x = 0.4$).

3.2. X-ray diffractometric study

A typical XRD pattern for $Zn_xCd_{1-x}S$ (for $x = 0.4$) films is shown in Fig. 2. Comparison of the prominent peak positions (2θ-values) of the XRD spectra with the JCPDS data file for CdS [19] suggests that the $Zn_xCd_{1-x}S$ film deposited at a baking temperature of 500°C is hexagonal (wurtzite) in structure with the prominent X-ray diffraction peaks corresponding to (100), (002), (101), (110) and (103) planes.

It was observed that the diffraction angle (2θ) shifts to higher angles with increasing zinc atomic fraction x. The peaks, which are quite sharp up to $x = 0.4$, become weaker beyond this and no prominent peaks appear for $x > 0.6$, which means that in this range the films are mostly amorphous.

Fig. 3 shows the relationship between the lattice parameter and the zinc atomic fraction x over the range $0 \le x \le 0.6$. It is observed that the lattice constants decrease with increase in the proportion of Zn. This is consistent with the smaller size of the Zn atoms and also reflected in the decrease in thickness of the films with increasing x as described in Section 3.1. Similar results were obtained by Yamaguchi et. al [20]. The values of a and c for thin film prepared at $x = 0$ (pure CdS) are 4.13 Å and 6.73 Å, respectively. These values are in good agreement with the data for hexagonal CdS films from the JCPDS card [19].

3.3. Optical properties

The optical energy gap of the $Zn_xCd_{1-x}S$ thin film was estimated by measuring optical density (O.D.) of the films as a function of wavelength in the range 2.2 eV to 3.5 eV, from which absorption co-efficient (α) was obtained. Plots of $(\alpha h\nu)^2$ and $(\alpha h\nu)^{1/2}$ against $h\nu$ were made (Fig. 4). $(\alpha h\nu)^2$ vs. $h\nu$ plots yielded straight line over the range $0 \le x \le 0.6$. In contrast, for $x > 0.6$ straight lines were obtained when $(\alpha h\nu)^{1/2}$ was plotted against $h\nu$. This is indicative of the fact that the film are crystalline for $0 \le x \le 0.6$ and amorphous beyond this range.

Spectral response of photoconductivity curves are shown

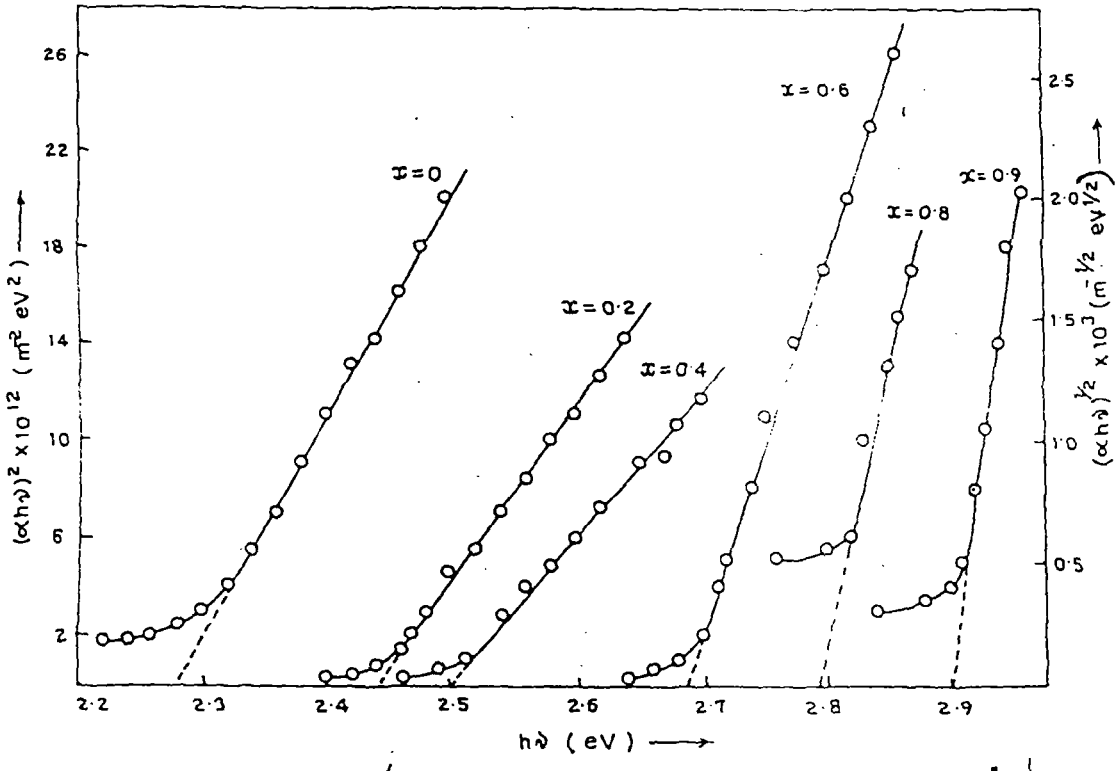

Fig. 4. The plots of $(\alpha h\nu)^2$ [for $0 \le x \le 0.6$] and $(\alpha h\nu)^{1/2}$ [for $x > 0.6$] against $h\nu$ of $Zn_xC_{1-x}S$ thin films

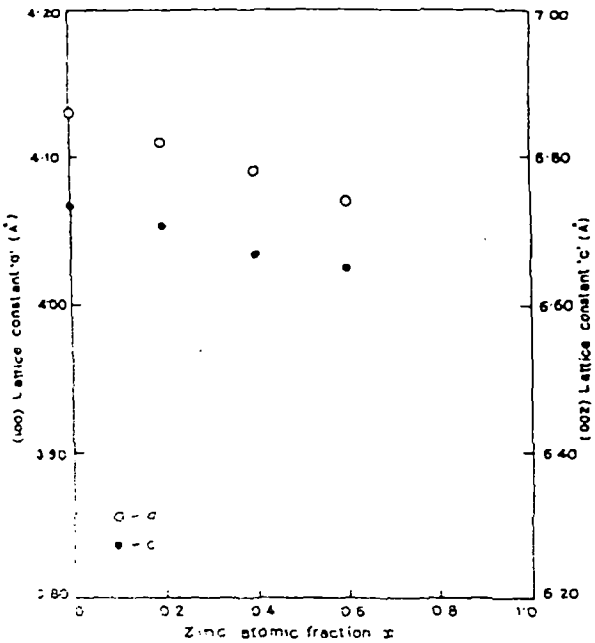

Fig. 3. The dependence of the lattice constants c and a on zinc atomic fraction x.

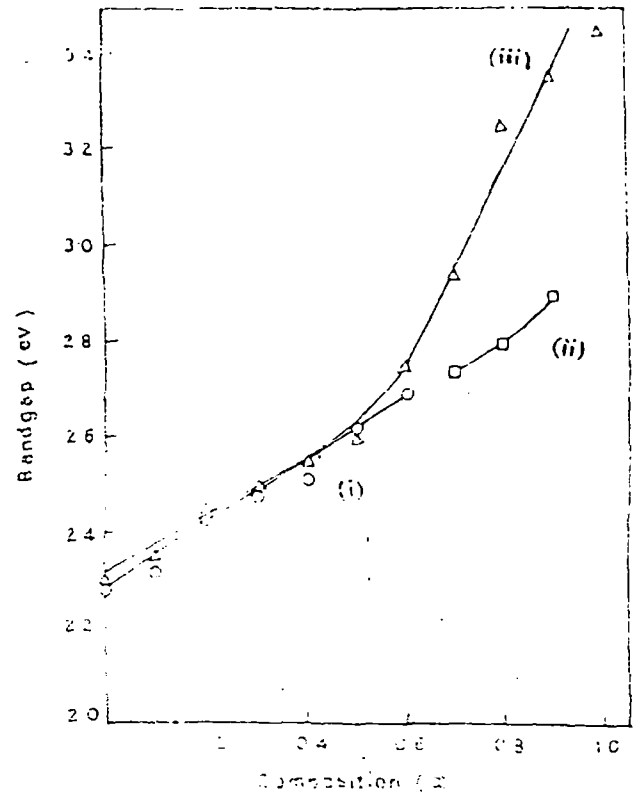

Fig. 6. Variation of (i) bandgap (○ ○ ○ ...) for $0 \le x \le 0.6$, (ii) optical bandgap (□ □ □ ...) for $x > 0.6$, and (iii) photon energy (Δ Δ Δ ...) with zinc atomic fraction x of $Zn_xCd_{1-x}S$ thin films.

in Fig. 5. The photocurrent values are normalized with the peak response for pure CdS taken as 1. No correction was made for the variation of intensity with wavelength of the tungsten filament source used in the spectrophotometer. With increasing x, position of the maximum moves from 540 nm for CdS to 360 nm for ZnS, corresponding to a shift in band gap from 2.3 eV to 3.4 eV. This continuous change in band gap with increasing proportion of zinc again confirms the formation of a solid solution.

Fig. 6 shows the variation with x of (i) bandgap for $0 \le x \le 0.6$, (ii) optical gap for $x > 0.6$, and (iii) the photon energy ($0 \le x \le 1$) at which peak response in photoconductivity is obtained. Curves (i) and (iii) agree quite closely in the range $0 \le x \lesssim 0.6$, where crystalline films

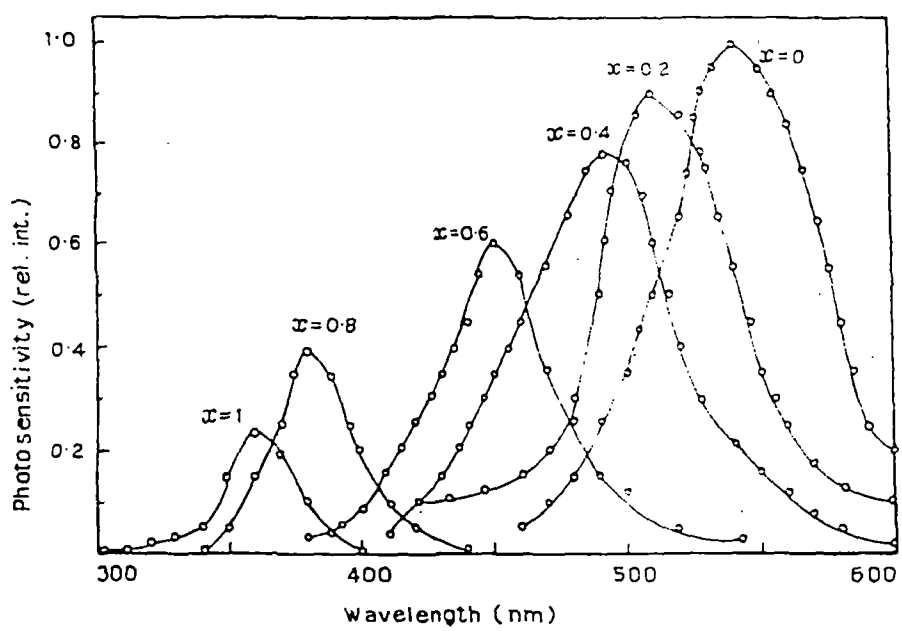

Fig. 5. The spectral response of photoconductivity curves of $Zn_xCd_{1-x}S$ thin films.

Ψ for peak photoconductive re

were obtained. The optical bandgaps for $x > 0.6$ are much less than that obtained from photoconductive measurements, which may be due to the amorphous nature of the films in that region.

According to H. Hill [21], the optical bandgap E_x of the $Zn_xCd_{1-x}S$ films can be expressed as:

$$E_{(x)} = E_{CdS} + (E_{ZnS} - E_{CdS} - b)x + bx^2$$

where b is the bowing parameter and x is Zn atomic fraction. The value of b for films is about 0.22 eV, estimated from curve fitting, with the values of optical bandgap in the range $0 \le x \le 0.6$. This value is in very close agreement with theory as obtained by Hill [21]. For $x > 0.6$, the value of b changes sharply to 0.07, again indicating a transition from crystalline to amorphous films.

3.4. Surface morphology

Fig. 7 shows the SEM micrographs of $Zn_xCd_{1-x}S$ th films for different values of zinc atomic fraction x. It evident from the micrographs that the grain size of the fil increases up to $x = 0.4$, beyond which a tendency reduction in crystallinity is observed. This is also ev denced in the XRD pattern, where sharp peaks are o served only over the range $0 \le x \le 0.4$.

4. Conclusion

Homogeneous and crystalline $Zn_xCd_{1-x}S$ thin film have been prepared successfully by the dip technique ov

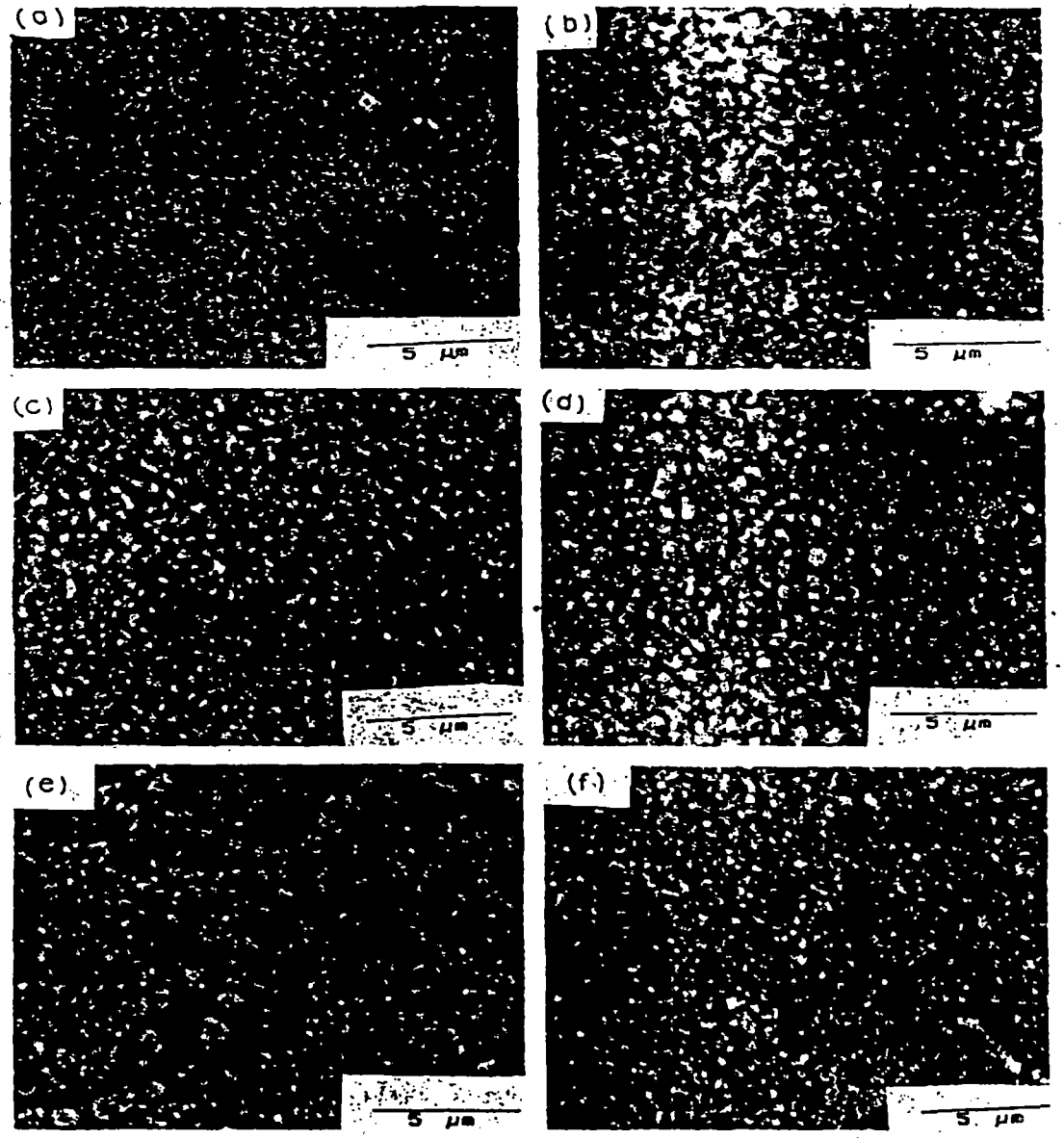

Fig. 7. The scanning electron micrographs of $Zn_xCd_{1-x}S$ thin films. (a) $x = 0$, (b) $x = 0.1$, (c) $x = 0.3$, (d) $x = 0.4$, (e) $x = 0.5$, (f) $x = 0.6$.

the range $0 \leq x \leq 0.6$ e films are hexagonal in structure, whose lattice parameters c and a are found to decrease with increase in x. An increase in x also produces a similar drop in the thickness of the film, when the total number of (Cd + Zn) moles in the starting solution is kept constant. This agrees well with the fact that the Zn atoms have a relatively smaller size compared to Cd atoms. The band gaps obtained from optical absorption and spectral response of photoconductivity measurements are in good agreement with each other and vary from 2.30 eV (CdS) to 2.69 eV ($Zn_{0.6}Cd_{0.4}S$), beyond which the bandgaps obtained from optical absorption measurements (optical gap) are much less than that obtained from photoconductive measurements. Surface morphology study by SEM as well as XRD data shows that good crystallinity is obtained up to a zinc atomic fraction of 0.4. For $x > 0.6$ the films appear to develop an amorphous character.

References

[1] K.T.R. Reddy, P.J. Reddy, J. Phys. D: 25 (1992) 1345.
[2] K.W. Mitchell, A.L. Fahrenbruch, R.H. Bube, J. Appl. Phys. 48 (1977) 4365.
[3] B.M. Basol, J. Appl. Phys. 55 (1984) 601.
[4] Y.K Jun, H.B Im, J Electrochem Soc.: Electrochem. Sci Techn 135 (1988) 1688
[5] H.S Kim, H.B Im, Thin Solid Films 214 (1992) 207
[6] J Torres, G Gordillo, Thin Solid Films 207 (1992) 231.
[7] T.A Chynoweth, R H Bube, J. Appl. Phys. 51 (1980) 1844
[8] T. Yamaguchi, J Matsufusa, A. Yoshida, Jpn J. Appl. Phys. (1992) L703
[9] T. Walter, M Ruckh, K O Velthaus, H.W. Schock, 1992, Proc. 11 EC Photovoltaic Solar Energy Conf., Montreux, p 124.
[10] A. Mzerd, D. Sayah, I.J. Saunders, B.K. Jones, Phys. Stat. Sol. 119 (1990) 487
[11] A. Kuroyanagi, Thin Solid Films 249 (1994) 91.
[12] T. Karasawa, K Ohkawa, T. Mitsuya, J. Appl. Phys. 69 (199 3226.
[13] Y.F. Nicolau, J.C. Menard, J. Cryst. Growth 92 (1988) 128.
[14] G.K. Padam, G L Malhotra, S.U M. Rao, J. Appl. Phys. 63 (198 770.
[15] Y.F Nicolau, M Dupuy, Electrochem. Soc 137 (1990) 2915.
[16] H. Schroeder, Oxide layers deposited from ...ic solutions, in: Hass, F Thun (Eds.), Physics of Thin Films, Vol. 5, Acaden Press, New York, pp 87–141, 1969.
[17] C. Terrier, J P. Chatelon, R. Berjoan, J.A. Roger, Thin Solid Fil 263 (1995) 37
[18] M.K. Karanjai, D Dasgupta, Thin Solid Films 155 (1987) 309.
[19] JCPDS, Swarthmore, PA, card no. 06-0314.
[20] T. Yamaguchi, Y Yamamoto, T. Tanaka, Y. Demizu, A. Yoshi Thin Solid Films 281–282 (1996) 375.
[21] H. Hill, J Phys C 7 (1974) 521.

140

PREPARATION AND STUDY OF MoS_2 THIN FILMS DEPOSITED B Y THE DIP TECHNIQUE

S.C.RAY, DEPARTMENT OF PHYSICS, UNIVERSITY OF NORTH BENGAL, SILIGURI DARJEELING - 734430, WEST BENGAL, INDIA AND
M.K.KARANJAI, DEPARTMENT OF PHYSICS, SILIGURI COLLEGE, SILIGURI, DARJEELING - 734401, WEST BENGAL, INDIA

Molybdenum sulphide (MoS_2) dichalcogenide thin film is a very promising semiconductor (bandgap 1.78 eV) for its various applications in solar cells, rechargeable batteries and as a solid lubricant for metallic and ceramic surfaces where hydrocarbon or other fluid-based lubricants are unsuitable, such as in high vacuum or high temperature applications MoS_2 thin films have been prepared by the dip technique In this technique, a clean glass substrate was dipped into the methanolic solution of ammonium molybdate and ammounium thiocyanate for half a min and then withdrawn vertically at a controlled speed, under atmospheric conditions, with the help of a pulley and geared motor, when a liquid film adhered to the substrate. The substrate together with the liquid film adhering to it was immediately transfered to a high temperature furnace for baking, where the chemicals reacted to form the desired solid film. Films are smooth, uniform and homogenious. X-ray diffractometric study suggests that, MoS_2 films deposited by the dip technique at a baking temperture of 300° C are amorphous in nature but those deposited at a higher baking temperatue of 360° C and 450°C are hexagonal in structure The optical bandgap (1 80 eV) calculated from the absorption measurement is quite comparable with the other reported value